DOCTOR OF PHILOSOPHY

Pyrolysis and gasification of biomass and acid hydrolysis residues

Manisha Patel

2013

Aston University

PYROLYSIS AND GASIFICATION OF BIOMASS AND ACID HYDROLYSIS RESIDUES

MANISHA PATEL

Doctor of Philosophy

Chemical Engineering

ASTON UNIVERSITY

June 2013

Aston University

Pyrolysis and Gasification of Biomass and Acid hydrolysis Residues

Manisha Patel

Doctor of Philosophy

2013

THESIS SUMMARY

This research was carried for an EC supported project that aimed to produce ethyl levulinate as a diesel miscible biofuel from biomass by acid hydrolysis. The objective of this research was to explore thermal conversion technologies to recover further diesel miscible biofuels and/or other valuable products from the remaining solid acid hydrolysis residues (AHR).

AHR consists of mainly lignin and humins and contains up to 80% of the original energy in the biomass. Fast pyrolysis and pyrolytic gasification of this low volatile content AHR was unsuccessful. However, successful air gasification of AHR gave a low heating value gas for use in engines for power or heat with the aim of producing all the utility requirements in any commercial implementation of the ethyl levulinate production process.

In addition, successful fast pyrolysis of the original biomass gave organic liquid yields of up to 63.9 wt.% (dry feed basis) comparable to results achieved using a standard hardwood. The fast pyrolysis liquid can be used as a fuel or upgraded to biofuels.

A novel molybdenum carbide catalyst was tested in fast pyrolysis to explore the potential for upgrading. Although there was no deoxygenation, some bio-oil properties were improved including viscosity, pH and homogeneity through decreasing sugars and increasing furanics and phenolics.

AHR gasification was explored in a batch gasifier with a comparison with the original biomass. Refractory and low volatile content AHR gave relatively low gas yields (74.21 wt.%), low tar yields (5.27 wt.%) and high solid yields (20.52 wt.%). Air gasification gave gas heating values of around 5MJ/NM^3, which is a typical value, but limitations of the equipment available restricted the extent of process and product analysis.

In order to improve robustness of AHR powder for screw feeding into gasifiers, a new densification technique was developed based on mixing powder with bio-oil and curing the mixture at 150°C to polymerise the bio-oil.

Keywords: Miscanthus, sugarcane bagasse, fast pyrolysis, catalytic pyrolysis, pelletisation

To my parents and bhai

ACKNOWLEDGEMENTS

Firstly, I would like to thank Prof. Tony Bridgwater who has been a pleasure to work with and without him; this PhD would not have been possible. I am truly grateful for his guidance, support and the things he has taught me over the last few years. I will never forget all he has done for me.

I would like to thank Prof. Victor Teixeira da Silva from UFRJ, in Brazil for the collaborative catalytic pyrolysis part of this work. Victor was a joy to work with and offered some valuable advice. Special thanks also to Richard Marsh at Cardiff University for providing access to a batch gasification unit. I would also like to thank Penny Challans and Angharad Beurle-Williams for support and making me feel welcome during my visit to Cardiff.

I would like to express special thanks to past and present members of the Bioenergy Research Group including Alejandro Alcala, Scott Banks, Ana Maria Cortes, Daniel Nowakowski, Javier Celaya, Sarah Alexander, Emma Wylde and Irene Watkinson for creating an enjoyable working environment. I am grateful to Surila Darbar who provided assistance with analytical equipment and Panos Doss for helping with the pelletisation work. Also, a word of thanks to Abba Kalgo, Antzela Fivga and Allan Harms for their help in the laboratory during the early stages of my PhD.

I wish to express my gratitude to Chris Mykoo for countless hours of fun, for being such a great listener and most of all, for making me smile when I felt down. I would also like to thank my close friend Sarah Carnell for all those trips out for 'Afternoon tea'. My other friends and extended family are thanked for several trips to Nandos and cocktail bars when I needed a break.

I am deeply grateful to my parents and my big brother, to whom I have also dedicated this thesis, for their endless support, love and encouragement. I would like to sincerely thank my mom who made my favourite meals and my dad who was always on standby in case I needed anything. I will always be grateful to my big brother, we have always been close and I always knew I could count on him for anything.

CONTENTS

LIST OF FIGURES

LIST OF TABLES

ABBREVIATIONS

AHR	Acid Hydrolysis Residue
ASTM	American Society for Testing and Materials
BERG	Bioenergy Research Group
BTG	Biomass Technology Group
CTC	Cane Technology Centre
Daf	Dry ash free
Dibanet	Development of Integrated Biomass Approaches Network
DMB	Diesel Miscible Biofuel
DTG	Differential Thermogravimetric
EC	European Commission
ER	Equivalence Ratio
ESP	Electrostatic Precipitator
GC	Gas Chromatography
GC-MS	Gas Chromatography- Mass Spectroscopy
GPC	Gel Permeation Chromatography
HHV	Higher Heating Value
PDI	Polydispersity Index
Py-GC-MS	Pyrolysis- Gas Chromatography- Mass Spectroscopy
SCBP	Sugarcane Bagasse Pellets
SEM	Scanning Electron Microscopy
TGA	Thermogravimetric Analysis
UL	University of Limerick

1 INTRODUCTION

Increasing worldwide energy demands have resulted in the increased dependency on fossil fuels such as coal, gas and crude oil. Significant interest in alternative sustainable solutions has been generated across the world to meet energy requirements and reduce carbon dioxide emissions. Biomass is recognised as a unique renewable energy resource that fixes atmospheric carbon dioxide. Biomass conversion processes and product upgrading technologies are extensively being developed to produce bioenergy and biofuels which could initially supplement and eventually replace fossil fuel derived energy and fuels [1].

1.1 Dibanet project overview

The research in this thesis was carried out for the European Commission sponsored Dibanet (Development of Integrated Biomass Approaches Network) project which primarily aimed to produce sustainable diesel miscible biofuels (DMB) from wastes and residues to improve renewability of transportation fuels by replacing diesel with biofuels. Agricultural residues such as sugarcane bagasse, which do not compete with food, can potentially be utilised more efficiently to create sustainable second generation biofuels. The project also aimed to increase collaboration between Europe and Latin America.

1.2 Dibanet scientific research objectives

The project co-ordinators of the Dibanet project focussed their efforts on the production of levulinic acid by acid hydrolysis of biomass. Levulinic acid was subsequently esterified with ethanol to produce ethyl levulinate for use as a diesel miscible biofuel. This acid hydrolysis process uses conditions which simulate the BioFine process and leaves a substantial amount of high lignin and humin content solid acid hydrolysis residue (AHR) [2]. AHR represents up to 80% of the original energy in the biomass and therefore is a potentially valuable feedstock for further processing.

One of the aims of the Dibanet project was to evaluate the potential for converting AHR into higher value products, such as a usable fuel for electricity generation and potentially DMB, by fast pyrolysis and gasification. Fast pyrolysis and gasification were considered as they are reported to produce high liquid and gas yields, respectively. However, further upgrading is required in both cases. Another aim was to integrate processes to make processes energetically self-sufficient by firstly utilising the AHR and then by thermally processing additional biomass if the energy from the AHR was insufficient. Therefore, both biomass and AHR were tested in this work. The overall process is shown in Figure 1.
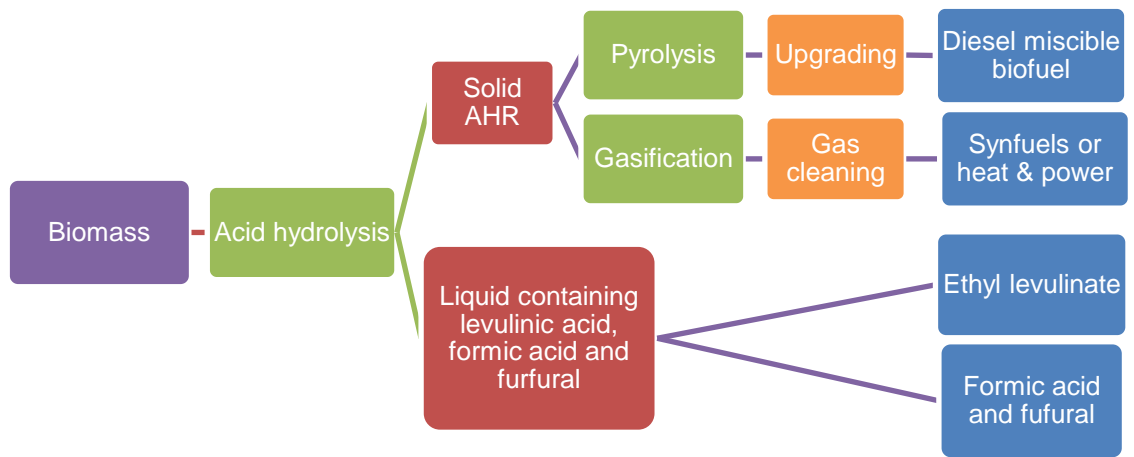
Figure 1: Overall Dibanet process (adapted from [3, 4])

1.3 Scientific research objectives

The overall objective of the research reported in this thesis was to explore the potential of producing DMB and/or bioenergy through pyrolysis and gasification of both AHR and biomass. Table 1 outlines the aims and objectives of this work and the approach adopted in order address these aims and objectives.

Table 1: Aims and objectives of this work

Aims and Objectives	Approach
Evaluate the composition and properties of biomass and AHR. Compare AHR with other lignin materials and investigate the effect of humins.	• Using literature • Scanning Electron Microscopy (SEM) • Proximate and ultimate analysis • Thermogravimetric analysis (TGA) • Bulk density testing • Melt testing and comparisons with Alcell lignin
Investigate fast pyrolysis of biomass and AHR in order to produce liquid bio-oil	• Using literature • By TGA • If results are promising from TGA, process AHR on a bench-scale fast pyrolysis rig
Compare miscanthus, miscanthus pellets, sugarcane bagasse, sugarcane bagasse pellets sugarcane trash. Test most promising feedstock on fast pyrolysis rigs at Aston University. Suggest methods to improve mass balances and compare product yields using different liquid collection systems.	• Prepare biomass according to required particle size • Test on a bench-scale fast pyrolysis rig by overcoming feeding and fluidisation problems. • Determine product yields from each feedstock. • Select most promising feedstock with highest organic liquid yield from smaller scale bench-scale processing. • Compare product yields and properties from this feedstock on 2 rigs with 3 liquid collection systems. • Compare this feedstock to beech wood.
Investigate the effect of molybdenum carbide on pyrolysis	• Investigate the effect of adding molybdenum carbide to a bench-scale fast pyrolysis unit. Analyse liquid product for water content, composition, viscosity, homogeneity and pH.
Understand the effect of process and feedstock variables on fast pyrolysis and gasification	• Using literature • Compare Dibanet feedstocks • Investigate the effect of temperature on fast pyrolysis.
Investigate gasification of AHR with biomass in order to produce a usable gas for heat and power or potentially synfuels	• Pyrolytic gasification • Air-blown gasification
Improve feeding and handling properties of AHR. Evaluate screw feeding, paste feeding and pelletisation of AHR. Investigate whether bio-oil can be used as a binder in pelletisation of AHR. If so, determine the minimum about of bio-oil required for successful pelletisation.	• Screw feed tests on bench-scale fast pyrolysis units • Past feeding with methanol • Pelletisation of AHR with water • Pelletisation of AHR with increasing concentrations of bio-oil

1.4   Structure of thesis

This thesis extends over twelve chapters and the structure is described below.

- Chapter one provides an overview and the detailed scientific research objectives of the Dibanet project. This chapter also outlines the structure of the thesis.

- Chapter two describes the biomass and acid hydrolysis residues tested in this work.

- Chapter three describes the characterisation techniques employed to analyse the biomass and acid hydrolysis residues tested in this work. Results are also presented and discussed.

- Chapter four describes and compares the available thermal conversion processes.

- Chapter five looks at the theory and literature review of fast pyrolysis and bio-oil upgrading.

- Chapter six describes and compares the fast pyrolysis of biomass in three sizes of fluidised beds using alternative liquid collection systems. Product analysis techniques used to analyse solid, liquid and gaseous products are also described. Careful mass balances were carried out, closures are reported and means of improvement are suggested.

- Chapter seven presents the effect of novel molybdenum carbide on pyrolysis of sugarcane bagasse using both Py-GC-MS and a fluidised bed.

- Chapter eight focuses on theory and literature review of gasification and gas upgrading.

- Chapter nine is the gasification section which compares pyrolytic gasification on a continuous unit at Aston University and air-blown gasification on a batch unit at Cardiff University. Limitations with the two gasification system are also reported. The effect of gasification temperature on product yields and composition from biomass and AHR is also compared.

- Chapter ten describes the methods used to overcome feeding problems of acid hydrolysis residue powder. It includes details of unsuccessful paste feeding tests and successful pelletisation tests using bio-oil.

- Chapter eleven recaps the interim conclusions presented at the end of each chapter.

- Chapter twelve makes recommendations for future research.

2   BIOMASS AND ACID HYDROLYSIS RESIDUES TYPES

The objective of this chapter is to examine the background of biomass, biomass components and the fifteen feedstocks tested in this work. Six biomass and nine acid hydrolysis residues (AHR) are also analysed and characterised by standard methods to identify a suitable thermal conversion process for the production of bioenergy and/or biofuels.

2.1   Biomass

Biomass includes agricultural and forestry wastes (wood chips, straw), industrial and consumer waste. It is a unique source of renewable energy as it produces fixed carbon from atmospheric CO_2 through photosynthesis. Also, woody biomass has a relatively low ash, sulphur and nitrogen content compared to coal. In this context, ash refers to the inorganic content after ashing or combustion and follows the conventional presentation of biomass characteristics. On the downside, large amounts of land are required for growing energy crops and there are cost issues with storage and transport of biomass. However, using waste and residues overcomes the land use issue. Fuel vs. food issues associated with first generation biomass are also overcome. Converting wastes and residues into a transportable liquid or gaseous fuel is a more acceptable way of producing second generation fuels and chemicals. For example, instead of using sugar to produce first generation bioethanol, waste sugarcane bagasse could be utilised to produce second generation biofuels which does not directly compete with food.

2.1.1   Biomass components

Biomass composition can vary depending on biomass type and origin. Land based biomass is lignocellulosic material made up of cellulose, hemicellulose and lignin. Biomass also contains small amounts of extractives and alkali metals in the form of ash, some of which are catalytically active. Biomass also contains moisture, nitrogen, phosphorus, chlorine and sulphur. Chlorine and sulphur are released as gas or are bound within the ash and in order to satisfy emission limits, chlorine and sulphur should be minimised. ECN have reported that the sulphur content in biomass range from 0.05 wt.% to more than 3 wt.%. Chlorine content of biomass is also reported to range from 0.01 wt.% to 2.4 wt.% on dry and ash free basis [5].

Figure 2 shows the main components present in biomass and shows approximate proportions of cellulose, hemi-cellulose and lignin as reported by Goyal et al. [6].
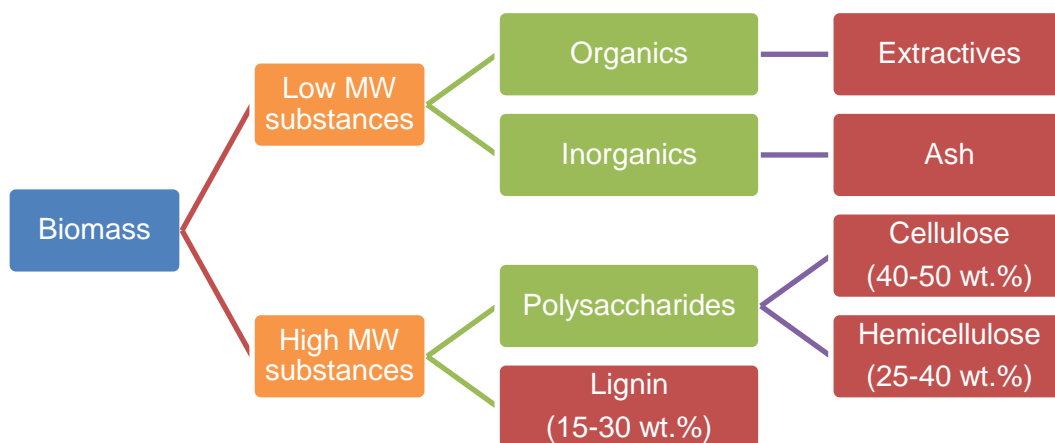
Figure 2: Biomass components (adapted from [7])

Extractives act as energy reserves and as defence against microbial and insect attack [7]. Examples include fats, waxes, alkaloids, proteins, phenolics, simple sugars, gums, resins, starches and essential oils [7]. Polar solvents (such as water, methylene chloride or alcohol) or nonpolar solvents (such as toluene or hexane) can be used to extract these extractives from biomass [7]. Acid hydrolysis uses water in the treatment process and therefore, water soluble extractives are removed from acid hydrolysis residues. Sugarcane is also washed with warm water in the sugar recovery process, therefore sugarcane bagasse is expected to be substantially water soluble extractive-free.

Biomass contains trace amounts of ash which consist of inorganic materials such as potassium, sodium, phosphorus, calcium and magnesium [7]. Ash is undesirable in fast pyrolysis because catalytically active alkali metals, present in the ash, are responsible for secondary cracking reactions which influence the decomposition products [8]. However, catalytically active ash cracks undesirable tars in gasification. Agricultural residues and grasses are reported to have higher ash content than wood [9] and ash analysis is carried out in section 3.1 to support this.

Cellulose consists of long polymer chains made up of D-glucose subunits, linked by b-1,4 glycosidic bonds. Cellulose gives biomass a tough fibrous nature and is made up of an arranged crystalline structure and non-arranged amorphous region [10]. Acid hydrolysis of biomass leads to oligomerisation of these long polymer chains resulting in the refractory humins found in AHR. Humins are described later in section 2.2.

Hemicellulose is made of short lateral polymer chains like five-carbon (pentoses), six carbon (hexoses) sugars and sugar acid. Hemicellulose can be more easily hydrolysed than cellulose and is stated to be the most thermal-chemical sensitive compared to cellulose and lignin. Hemicellulose acts as a connection

between cellulose and lignin and gives the biomass structure more rigidity [10], in other words, it holds the cellulose bundles together.

Lignin is an amorphous heteropolymer made up of phenylpropane units (p-coumaryl, coniferyl and sinapyl alcohol). Lignin is reported to contain nearly 60 wt.% carbon [11]. After cellulose and hemicellulose, lignin is one of nature's most abundant polymers [3]. It provides "*structural support, impermeability and resistance against microbial attack and oxidative stress*" [10]. Lignin is reported to be the most thermally resistant component in biomass and the method of lignin isolation has significant effect on its structure and thermal decomposition properties [12]. Lignin is widely available as a by-product from many processes such as second generation ethanol biorefineries. Dissolution of lignin into a solution, such as the Kraft pulping process or hydrolysis of cellulose and hemicellulose by acid, leaving lignin as an insoluble residue, are two of the methods of extracting lignin from lignocellulosic biomass [13].

The thermal degradation properties of biomass are strongly dependent on the lignocellulosic composition and catalytic activity of ash. Figure 3 shows the Differential thermogravimetric (DTG) profiles of biomass components. Xylan is representative of hemicellulose and is the least refractory of the biomass components as the maximum rate of devolatilisation is at approximately 300°C. The maximum rate of devolatilisation for cellulose is at approximately 350°C. It can be seen that the DTG profile for lignin is flatter indicating that lignin is more refractory than holocellulose and decomposes over a wider range of temperatures.

Aston University

Illustration removed for copyright restrictions

Figure 3 : DTG profiles of biomass components [14]

2.1.2 Biomass tested

Six biomass samples were analysed and processed in this work. Beech was used as a reference material early in this research when samples from the Dibanet project were not available. Miscanthus and miscanthus pellets were the primary European feedstock and sugarcane bagasse, sugarcane bagasse pellets and sugarcane trash were used as the Latin American feedstocks within the Dibanet project.

Beech wood, with a very low ash content, has extensive data available from other work so can be used for cross checking results and as a reference material. Beech was supplied by Rettenmeier based in Germany.

Miscanthus x Giganteus is a fast growing C_4 perennial woody type grass. Miscanthus has a low nutrient requirement and is harvested annually in March/April in Europe while the plant is senescent to reduce the ash and moisture contents and leaf to stem ratios. Miscanthus is an energy crop which is commercially grown to produce fuel. Yields of this energy crop are reported to range from 27 to 44 wet tonnes/ha/year in Europe [15]. Miscanthus (see Figure 4) was sourced from JHM Crops Ltd. (www.jhmcrops.ie), in Ireland. The miscanthus was chopped to 2cm, but not dried.

Pellets can be made from biomass to increase the bulk and energy density. Utilising pellets can increase throughputs in a continuous process and also allow more efficient and cost effective transport, handling and storage. Pellets are also more uniform and create less fines [16]. Miscanthus pellets with an 8mm diameter (see Figure 5) were supplied by Ignite Wood Fuels LTD, UK. Miscanthus pellets were ground for analysis and processing in this work. Explanations for grinding pellets can be found in section 3.3.

Figure 4: Chopped miscanthus (as received)

Figure 5: Miscanthus pellets (as received)

Sugarcane is a perennial C4 plant which is harvested annually between April and December (in Brazil). The main product of sugarcane is sucrose which can be used in the food industry or fermented to produce bio-ethanol. The stem of the sugarcane contains the largest quantity of sucrose and so is processed at the sugar mill soon after the sugarcane has been harvested. The residue from sugar recovery is a fibrous lignocellulosic residual waste called bagasse. In Brazil, 140kg of dry bagasse is produced per wet tonne of sugarcane processed [17]. Currently, the bagasse is recovered for use as a fuel in boilers to produce heat for the sugar mill. It is reported that these mills deliberately use inefficient burners to utilise the excessive waste and reduce the need for sending this waste to landfill [17, 18]. However, alternative, more efficient processes should be used to maximise the energy output from bagasse in order to reduce the reliance on fossil fuels for heat and power generation [17, 18].

Sugarcane bagasse (see Figure 6) was collected from storage piles at a sugar mill site in Brazil in August 2010 by members of Cane Technology Centre (CTC). The moisture content of the bagasse was between 50 and 60 wt.% and dried at room temperature for two weeks to avoid biological activity and degradation before being stored in boxes.

Sugarcane bagasse pellets (SCBP) were also used in this work to investigate the effect of densification on feeding ability and product yields. In order to make SCBP (shown in Figure 7), bagasse was dried in a flash drier to a moisture content of around 11 to 12 wt.%. The dryer promoted drying by direct contact between a hot exhaust gas (from a boiler) and bagasse. The continuous drying process used temperatures of approximately 280°C with a contact time of 3-4 seconds. The dried bagasse was then ground and pelletised in Brazil with no additives or steam. Pellet production is not standard practice at sugar mills in Brazil. However, CTC were involved in a small project testing SCBP and therefore a batch was sent to Aston University in April 2011 for thermal processing tests.

The bagasse drying temperature, similar to that of torrefaction (200 to 300 °C) leads to a loss of moisture and light organic materials. Torrefaction is a primary thermal process which occurs in an inert atmosphere between 200-300°C and can be applied to biomass to leave a dry, hydrophobic material with increased energy density [19]. Torrefaction of high moisture content sugarcane bagasse (50 and 60 wt.%) can also avoid biological degradation. Figure 7 shows the SCBP which are darker compared to loose bagasse. The hemicellulose and the fibrous structure of cellulose within biomass are destructed leaving a brittle and darkened material which can reduce milling costs, but can be friable during transport. Sugarcane bagasse pellets were ground prior to analysis and processing and explanations for grinding can be found in section 3.3.

| **Figure 6: Sugarcane bagasse (as received)** | **Figure 7: Sugarcane bagasse pellets (as received)** |

Sugarcane trash comprises the leaves and tops of sugarcane which are traditionally left on the sugarcane field and set on fire to facilitate sugarcane harvest. Due to pollution from burning of the cane fields [20], these manual harvesting techniques are being replaced by mechanical harvesting where a harvester cuts the crop at the base of the stalk, strips off the leaves and returns the leaves (trash) back to the field. There is currently a debate on whether trash should be left on fields to return the nutrients back to the soil or collected to produce bioenergy. It is reported that the same amount of trash is produced as bagasse. Therefore, 140kg of dry trash is produced per wet tonne of sugarcane processed [17]. Sugarcane trash (shown in Figure 8) was manually collected off the fields in Brazil by members of CTC in August 2010 and as with the bagasse, was dried at room temperature for two weeks and stored in boxes.

Figure 8: Sugarcane trash (as received)

2.2 Acid hydrolysis of biomass

Biomass can be pre-treated before it is thermally processed in order to break up the lignocellulosic structure. Acid hydrolysis has been extensively investigated to fractionate the lignocellulosic structure and release soluble sugar and other chemicals from biomass [21]. Acid treatment can also reduce the metal/ash content in biomass

and increases the yield of volatiles [22]. A reduction in ash content increases the organic liquid yield from fast pyrolysis by reducing catalytic cracking.

Both concentrated and dilute acid hydrolysis has been reported in the literature. Acid recovery issues and corrosion of acid hydrolysis equipment are limiting factors in concentrated acid hydrolysis. However, dilute acid hydrolysis has been well developed [23] where a dilute acid can be used as a liquid phase catalyst to pre-treat lignocellulosic materials. Sulphuric acid is commonly employed for acid hydrolysis [23-29] and has been used to manufacture furfural [21, 29]. However, other researchers have also investigated acid hydrolysis using hydrochloric [23, 30, 31], phosphoric [32, 33] and nitric acid [34]. Hydrochloric acid is viewed as unsuitable for pre-treating biomass as traces of chlorine can act as a catalyst and have undesirable effects in pyrolysis.

Part of the Dibanet project involved the production of levulinic acid by acid hydrolysis of biomass. Figure 9 outlines the overall acid hydrolysis process where biomass components are converted into water soluble chemicals containing a mixture of levulinic acid, formic acid and furfural. The composition of this mixture can be varied according to the process parameters employed.
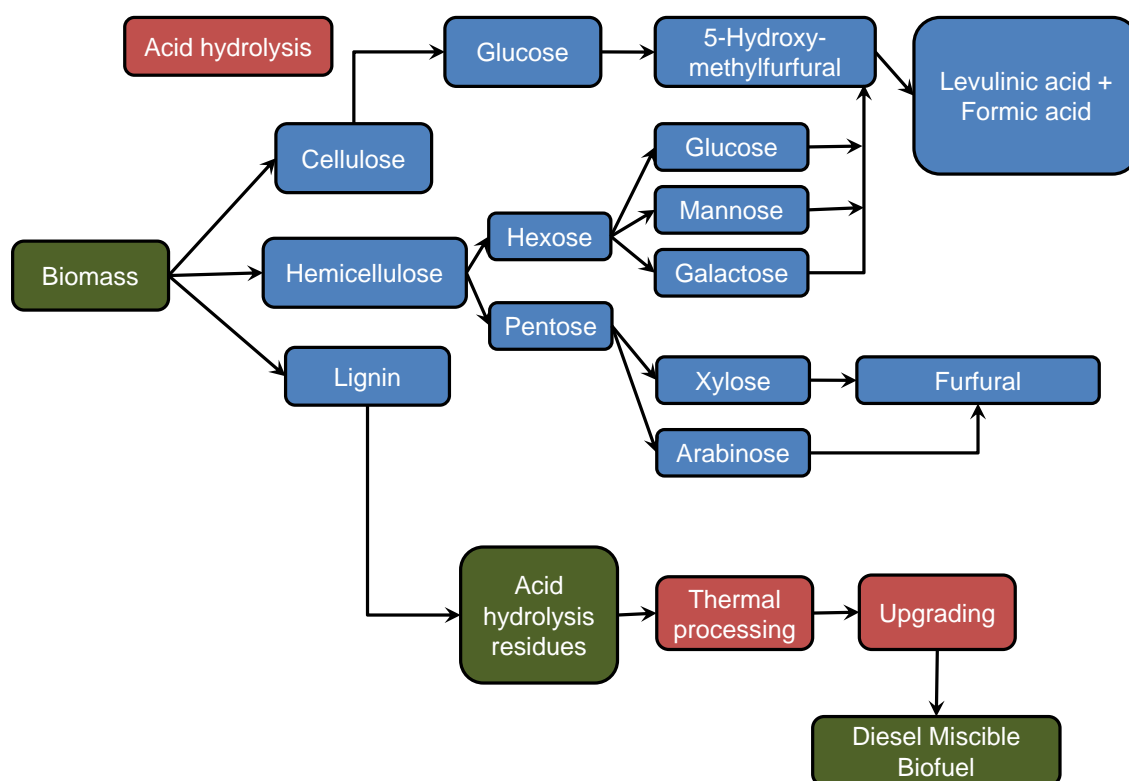
Figure 9: Overall acid hydrolysis process

2.2.1 Acid hydrolysis residues components

The remaining solid acid hydrolysis residues from the Dibanet project mainly consist of lignin and humins. Humins are carbonaceous dark coloured solids and are insoluble polymeric materials which are spherical in shape and have an aromatic

character [35] [3] [36]. Oligomerisation of the long cellulosic polymer chains results in the refractory and undesirable humins found in AHR. Humins are also reported to be derived from glucose and 5-Hydroxy-methylfurfural [36]. Therefore, the formation of humins is reported to limit levulinic acid yields [36]. Researchers at University of Limerick (UL) used sulphuric acid to hydrolyse miscanthus and sugarcane bagasse. However, sulphur in sulphuric acid can deactivate catalysts if they remain in AHR and so AHR were thoroughly washed with excessive amounts of water. These AHR were analysed and thermally processed in this work with the aim of producing biofuels or heat and power.

Figure 10 compares the DTG profiles of biomass components, miscanthus and an example of AHR. AHR is shown to decompose at even higher temperatures than lignin suggesting that the presence of humins makes AHR even more difficult to thermally decompose. Higher temperatures are required to break the strong bonds between lignin and humins.

Aston University

Illustration removed for copyright restrictions

Figure 10: DTG profiles of biomass components, biomass and AHR [37]

2.2.2   Acid hydrolysis residues tested

Three acid treated beech samples were produced at Aston University to simulate the acid hydrolysis process when AHR samples were not available from UL. Acid treatment conditions reported in literature were used as acid hydrolysis conditions were unknown at the beginning of the project. Six AHR were later provided by UL. Details of all nine AHR are shown in Table 2.

Table 2: Details of AHR

Feedstock	Conditions	Laboratory
AHR from beech	Single stage acid treated beech (1 wt.% H_2SO_4, 4h, 75°C)	Aston University
AHR from beech	Two-stage acid treated beech (1 wt.% H_2SO_4, 4h, 75°C) then (20 wt.% H_2SO_4, 4h, 75°C)	
AHR from beech	One-stage acid treated beech (20 wt.% H_2SO_4, 4h, 75°C)	
AHR from miscanthus	(5 wt.% H_2SO_4, 2h, 200°C)	University of Limerick
AHR from miscanthus	(1 wt.% H_2SO_4, 3h, 150°C)	
AHR from miscanthus	(1 wt.% H_2SO_4, 24h, 150°C)	
AHR from miscanthus	(1 wt.% H_2SO_4, 10 minutes, 200°C)	
AHR from miscanthus	(5 wt.% H_2SO_4, 1h, 175°C)	
AHR from sugarcane bagasse	(5 wt.% H_2SO_4, 1h, 175°C)	

Sulphuric acid is reported as the most widely used acid for pre-treatment of biomass [23-29] and was used for levulinic acid production at UL. Therefore, beech was subjected to mild acid hydrolysis, using sulphuric acid, to simulate the anticipated AHR from UL. These beech residues were then used for feeding tests on a continuous fluidised bed system to identify feeding problems that may occur with AHR from UL. The mass ratio of beech to sulphuric acid solution was 1:6 (mass basis). Acid concentration was varied to compare the effect of mild (1 wt.%) and strong (20 wt.%) acid treatment. Three experiments were carried out using approximately 200g of beech at the different acid concentrations as shown in Table 2. The particle size used was 355-500 µm to allow pneumatic feeding into a continuous fluidised bed system. The temperature of the solution was controlled at 75°C +/- 3°C and the system was maintained at atmospheric pressure. The acid hydrolysis treatment was run for four hours at 75°C.

Tests were conducted to compare the results of one and two stage strong acid hydrolysis. One stage acid hydrolysis involved treating the beech in one stage with 20 wt.% acid solution. However, two stage acid hydrolysis involved treating the beech with 1 wt.% acid solution and subsequently treating the remaining solid residue with 20 wt.% solution. The first stage was expected to break down the hemicellulose and the second stage to break down the cellulose, leaving a high lignin content residue analogous to residues from levulinic acid production. Figure 12 shows the AHR produced from ground beech using the most severe acid hydrolysis conditions (20 wt.% H_2SO_4, 4 hours, 75°C). Higher lignin and humin content samples are expected to be darker in colour, therefore as there was very little colour change after acid hydrolysis, it is expected that significant amounts holocellulose remained in the feedstock.

Figure 11: Untreated ground beech

Figure 12: AHR from ground beech: 20 wt.% H_2SO_4, 4 hours, 75°C

When the 8 litre acid hydrolysis batch reactor was up and running at UL, miscanthus and sugarcane bagasse (Figure 13) were hydrolysed in dilute sulphuric acid to maximise levulinic acid production. The effect of sulphuric acid concentration, reaction time and temperature were investigated by UL and the solid residues produced were sent to Aston University for analysis and thermal processing. The water soluble products, including the levulinic acid, from the biomass were collected as a liquid. The remaining solid AHR, with a moisture content of approximately 75 wt.%, was filtered and dried at 60°C for at least 12 hours to a moisture content of 6-8 wt.%. Six AHR were produced at UL using higher temperatures (up to 200°C) and pressures (up to 15bar), compared to Aston, allowing for lower acid concentrations (maximum of 5% H_2SO_4) which produced a solid AHR with significant amounts of holocellulose removed. Figure 14 shows an example of an AHR from sugarcane bagasse which is considerably darker than the untreated sugarcane bagasse. It is also much darker than the AHR produced from beech. This AHR looked similar to the other five AHR from levulinic acid production.

Figure 13: Untreated sugarcane bagasse (as received)

Figure 14: AHR from sugarcane bagasse: 5 wt.% H_2SO_4, 1hour, 175°C (as received)

AHR from miscanthus and sugarcane bagasse were brown non-homogeneous fine powders which crumbled easily. Feeding of this material into a pyrolysis or gasification reactor posed a challenge. The characteristics of the feedstocks described in this chapter can be found in chapter 3.

2.3 Interim conclusions

- Lignin is more refractory than hemicellulose and cellulose and so AHR is more refractory than whole lignocellulosic biomass.

- AHR mainly consists of humins and lignin.

- Humins are derived from cellulose.

- AHR is shown to decompose at even higher temperatures than lignin suggesting that the presence of humins makes AHR even more refractory.

- AHR produced from beech were insufficiently hydrolysed and did not simulate the anticipated AHR from UL.

- Feeding of powdered AHR into a thermal processing unit is likely to be problematic.

3 BIOMASS AND ACID HYDROLYSIS RESIDUE ANALYSIS

The objective of this chapter is to determine the lignocellulosic composition of the biomass and acid hydrolysis residues (AHR) tested in this work. Feedstocks are also characterised by scanning electron microscopy to compare the structure of the biomass with AHR. Proximate and elemental analysis is also presented to evaluate the usefulness of the feedstocks as a fuel for thermal processing. Differential thermogravimetric analysis is also an important factor to investigate feedstock thermal properties. Preparation methods used for the biomass and the most promising AHR reported by University of Limerick are subsequently reported.

Figure 15 shows the procedures employed at the beginning of this project to determine the lignocellulosic composition of biomass and AHR, but the analyses were unsuccessful because of separation problems due to the finely dispersed nature of the AHR. It can be seen that although holocellulose and lignin can be separated using the Klason lignin procedure, there is no analytical way of differentiating lignin and humins. The AHR powder dissolved in the filtrate so mass loss of feedstock was not realistic. Therefore, results reported in literature were used to compare the lignocellulosic composition of biomass with AHR.
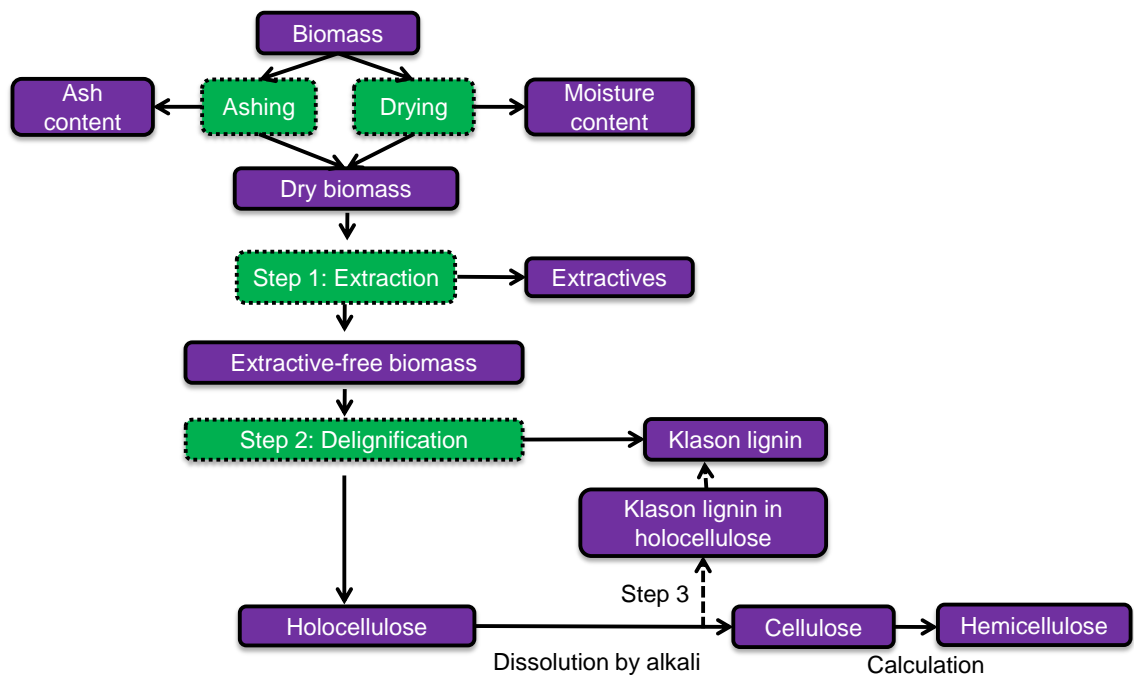
Figure 15: Lignocellulosic component analysis of biomass (adapted from [38])

Table 3 compares the reported lignocellulosic compositions of the feedstocks tested in this work. Melligan et al. report the Klason lignin content of AHR as high as 95.5 wt.% [2] and do not make any reference to humins which are expected to be present in AHR. However, Girisuta et al. reports that the acid insoluble solid AHR contain unhydrolysed lignin and humins [39] and state that humin content can be

estimated by assuming the lignin content from the original biomass. The calculations carried out to estimate the composition of the AHR can be found in section 3.2.

Table 3: Approximate lignocellulosic composition (wt.% dry basis) of tested feedstocks

Feedstock	Hemicellulose	Cellulose	Lignin
Beech [40, 41]	23.51-32.6	38.6-45.1	22.3-26.4
Miscanthus [2, 42, 43]	18-27	37-43	20-25
Sugarcane bagasse [44-46]	23-26	31-52	13-22
Sugarcane trash [47]	26-31	45-48	7-20
AHR [2]	0.1-0.2	0.36-15.4	95.5

Hemicellulose is the most reactive and unstable component of biomass. However, lignin is the least reactive [48]. For this reason, AHR with a significantly higher proportion of acid insoluble solids, reported as lignin, is expected to be less reactive and more refractory compared to whole biomass.

Figure 16 shows the SEM image for miscanthus and Figure 17 shows that the remaining structure of the AHR derived from miscanthus is still intact; however, the hemicellulose and cellulose have been removed leaving a very porous structure.
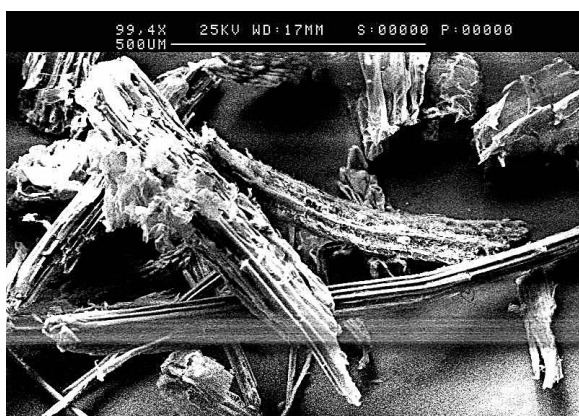
Figure 16: SEM of miscanthus   **Figure 17: SEM of AHR derived from miscanthus**
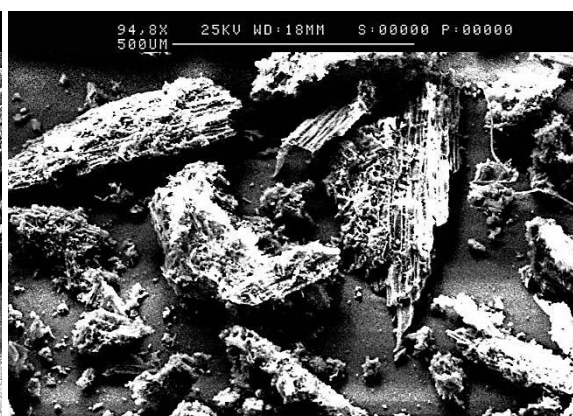
The structure of the ground SCBP in Figure 19 is more porous compared to the loose sugarcane bagasse in Figure 18 suggesting there was loss of material caused by the drying conditions during pelletisation. Figure 20 shows the SEM image for sugarcane trash which seems less fibrous than sugarcane bagasse. It is expected that the washing of sugarcane, in the sugar recovery process, partially destroys the sugarcane bagasse.
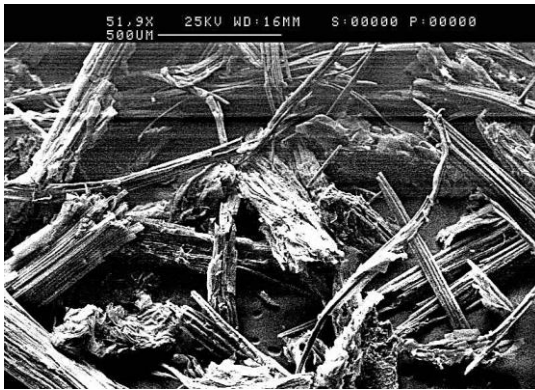
Figure 18: SEM of sugarcane bagasse
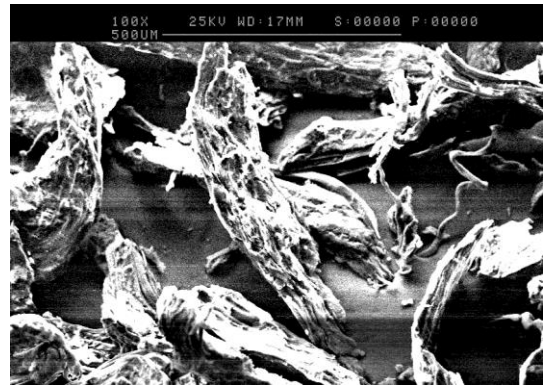
Figure 19: SEM of bagasse pellets
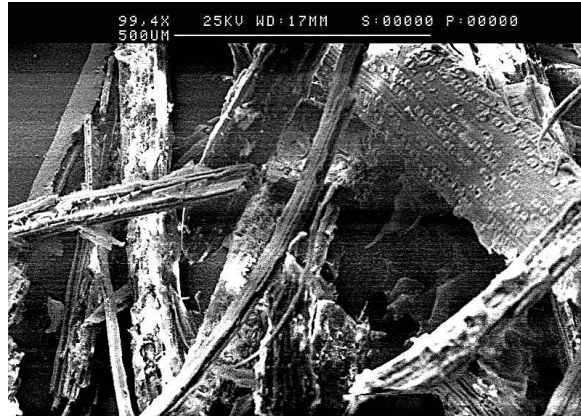
Figure 20: SEM of sugarcane trash

3.1 Proximate and ultimate analysis

Elemental analyses were carried out to calculate the higher heating value of each feedstock. Feedstocks were dried in an oven, to constant weight, before Carbon (C), Hydrogen (H) and Nitrogen (N) content analysis was carried out in duplicates using a Carlo-Erba 1108 elemental analyser by an external company (Medac Ltd.). Averages of values (+/- 0.30 wt.%) were used to calculate the higher heating value. The mean sulphur and chlorine content of the biomass tested in this work, according to the Phyllis 2 database [49], is presented in Table 4. Sulphur content of these feedstocks was below the detection level of the equipment used at Medac Ltd. Also, due to the number of samples and the availability of funding, chlorine analysis was not possible in this work.

Table 4: Sulphur and Chlorine content of biomass tested [49]

Ash content analyses of samples were carried out in triplicates using the "Standard Test Method for Ash in Biomass" (ASTM E1755). Averages of results were taken and the minimum and maximum values are shown as error bars in corresponding

figures. Equation 1 was subsequently used to calculate the higher heating value (HHV) from the elemental and ash data. Channiwala et al. report that this equation can be used to calculate the HHV of gases, liquids, biomass and residue derived fuels [50].

Equation 1: HHV Equation [50].

HHV = 0.3491C + 1.1783H + 0.1005S - 0.1034O - 0.0151N - 0.0211Ash (MJ/kg)

Table 5 shows the elemental analysis of all of the AHR derived from beech and the processing conditions are shown in brackets. The nitrogen and sulphur content of these feedstocks were below the equipment detection limit <0.10 wt.%. Oxygen was calculated by difference. The carbon and hydrogen content of the untreated beech were as expected and as reported in the literature by Bridgwater et al. [51] .The table shows that the carbon and hydrogen content increase with increasing acid concentration.

Table 5: Elemental analysis for beech (dry basis)

Sample (treatment conditions)	C (wt.%)	H (wt.%)	N (wt.%)	O* (wt.%)	S (wt.%)	Ash content (ASTM) (wt.%)	HHV (MJ/kg)
Beech	47.60	5.96	<0.10	45.62	<0.10	0.82	18.91
Single stage acid treated beech (1 wt.% H_2SO_4, 4h, 75°C)	48.04	6.09	<0.10	45.55	<0.10	0.33	19.22
Two-stage acid treated beech (1 wt.% H_2SO_4, 4h, 75°C) then (20 wt.% H_2SO_4, 4h, 75°C)	48.56	6.24	<0.10	45.13	<0.10	0.08	19.64
One-stage acid treated beech (20 wt.% H_2SO_4, 4h, 75°C)	48.51	6.26	<0.10	45.19	<0.10	0.05	19.63

*Oxygen by difference

As discussed earlier in section 2.2.1, depending on the severity of acid hydrolysis conditions, AHR produced at UL mainly consist of lignin and humins. Table 6 compares the carbon and hydrogen content of humins, ALM and Etek lignin and indicates that typical carbon content of humins and lignin is approximately 60 wt.% which is much higher than that of whole biomass [11]. Humins are also reported to be carbonaceous similar to that of lignin [19]. Therefore AHR containing a combination of humins and lignin, are expected to have a carbon content of approximately 60 wt.%.

Table 6: Elemental composition comparison of humins and lignin

	C (wt.%)	H (wt.%)
Humins [19]	61.2-63.1	4.2-4.5
ALM and Etek lignin [52]	51.33-63.81	5.7-7

An increase in carbon content is an indication of increased lignin and humin content. The carbon content of the AHR from beech was approximately 48 wt.% which was significantly lower than the carbon content of lignin and humins (60 wt.%) and more similar to the carbon content of biomass (47.6 wt.%). This suggested that there were still significant amounts of holocellulose remaining in these AHR. However, although these AHR were not sufficiently hydrolysed, the carbon content results indicated that increasing acid concentrations improved holocellulose removal. The table also shows the oxygen content reduced from 45.62 to 45.19 wt.% due to increasing carbon content in the AHR.

Figure 21 shows that acid hydrolysis can be used as a pre-treatment method to reduce the ash content of beech from 0.82 to 0.05 wt.%. One stage acid hydrolysis reduced the ash content to 0.05 wt.%, but two stage acid hydrolysis reduced the ash content to 0.08 wt.%. Therefore, one stage acid hydrolysis is preferred if the aim is to reduce ash content which is catalytically active and undesirable in processes such as fast pyrolysis.
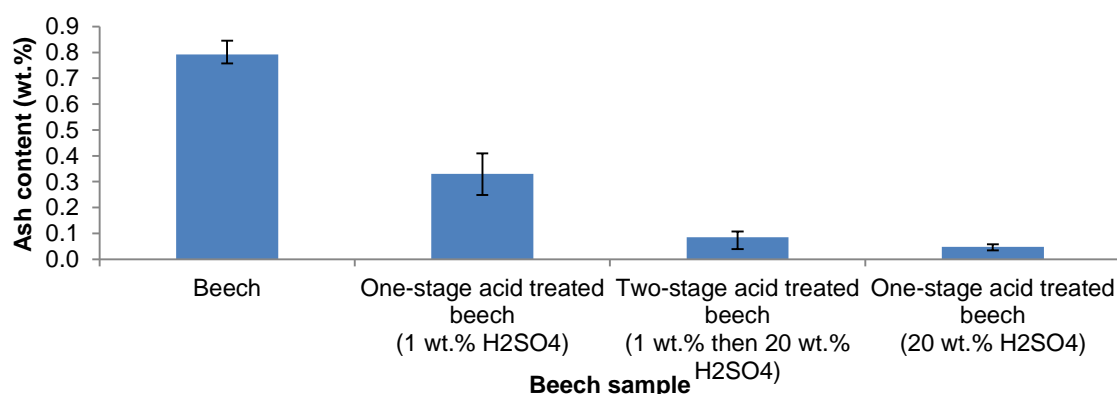
Figure 21: Ash content (wt.%) of beech and AHR derived from beech

The reported HHV value of cellulose and hemicelluloses is approximately 18.6MJ/kg. The reported HHV value of lignin ranges from 23.26 to 26.58MJ/kg [53]. The HHV of humins is unknown, but expected to be similar to that of lignin as both have similar carbon content. Therefore, feedstock HHV is expected to increase with increasing lignin and humin content. Heating value can be used as an indicator of the lignin and humin content of a feedstock. Figure 22 shows that the heating value of the AHR was greater than that of biomass and heating value increased with the severity of acid hydrolysis conditions as the carbon content increased. The calculated HHV increased from 18.91 to 19.64MJ/kg by increasing acid treatment from 1 wt.% to 20 wt.%. It is expected that the acid removed some holocellulose which increased the HHV.

Beech sample
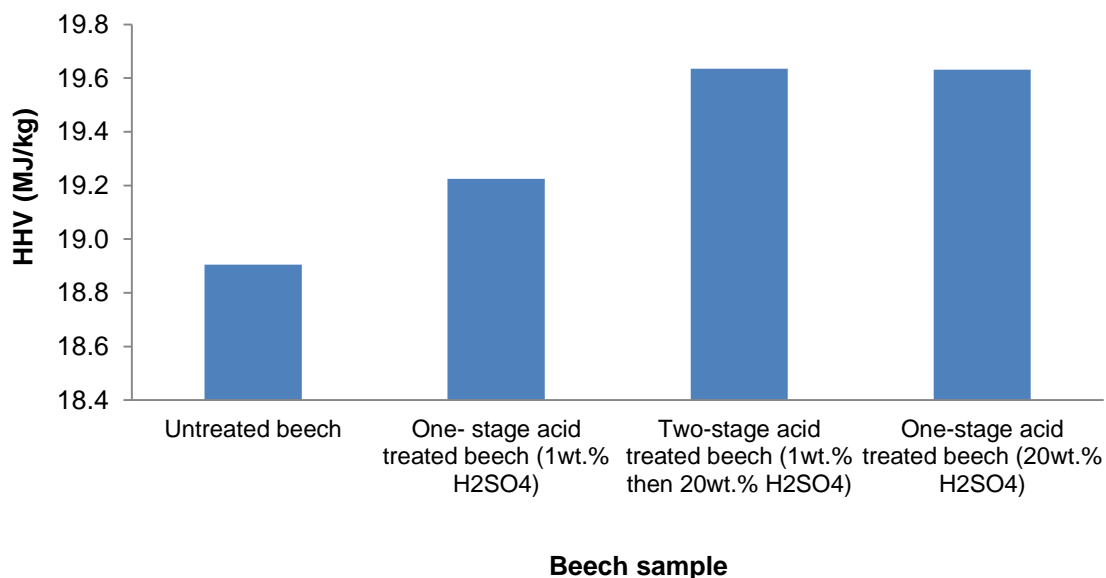
Figure 22: HHV (MJ/kg) of beech and AHR derived from beech

Table 7 summarises the elemental data for all eleven Dibanet feedstocks. As mentioned earlier, an increase in carbon content is an indication of increased lignin and humin content. The carbon content of the AHR from miscanthus (5 wt.% H_2SO_4, 1h, 175°C) was the highest 63.21 wt.% which was comparable to the carbon content of lignin and humins (60 wt.%). This suggested that this AHR had the most holocellulose removed and these acid hydrolysis conditions were expected to be the optimum for levulinic acid production. The same acid hydrolysis conditions were applied to sugarcane bagasse and the carbon content was 62.61 wt.% which was comparable to the carbon content of the AHR from miscanthus.

The sulphur content was below the analyser detection level (<0.10 wt.%) for beech samples and sulphur content reported in literature was also below the detection level. Therefore, sulphur content so was not measured (Nm) for all samples. However, as the AHR were hydrolysed with sulphuric acid, it was expected that sulphur would remain in the residues. Therefore, the sulphur content of the two residues from miscanthus and sugarcane bagasse (5 wt.% acid, 1h, 175°C) was later measured.

Although oxygen was calculated by difference in this work, sulphur and chlorine data from literature was reviewed and not expected to greatly impact the comparisons made using the oxygen data. The oxygen content of the AHR was consistently lower than biomass as holocellulose was removed. For example, the oxygen content of sugarcane bagasse was 45.88 wt.% compared to AHR from sugarcane bagasse (5 wt.% acid, 1h, 175°C) which was 26.07 wt.%. A lower oxygen content feedstock may be beneficial for producing a lower oxygen content bio-oil, but the high carbon content is expected to contribute to high char yields from fast pyrolysis.

Table 7: Elemental analysis of Dibanet samples (dry basis)

Sample (treatment conditions)	C (wt.%)	H (wt.%)	N (wt.%)	O* (wt.%)	S (wt.%)	Ash (wt.%)	HHV (MJ/kg)
Miscanthus	45.99	6.03	0.49	47.47	Nm	4.94	18.25
Miscanthus pellets	46.82	6.15	0.99	46.02	Nm	4.54	18.82
AHR from miscanthus (5 wt.% H_2SO_4, 2h, 200°C)	62.66	4.57	0	32.77	Nm	2.69	23.86
AHR from miscanthus (1 wt.% H_2SO_4, 3h, 150°C)	49.66	6.23	0.14	43.97	Nm	0.41	20.13
AHR from miscanthus (1 wt.% H_2SO_4, 24h, 150°C)	51.90	6.01	0.15	41.94	Nm	0.38	20.86
AHR from miscanthus (1 wt.% H_2SO_4, 10 minutes, 200°C)	61.78	5.31	0.515	32.40	Nm	0.93	24.46
AHR from miscanthus (5 wt.% H_2SO_4, 1h, 175°C)	63.21	5.01	0.44	29.26	0.16	1.93	24.91
Sugarcane bagasse	47.66	6.06	0.39	45.88	Nm	3.19	19.03
SCBP	43.47	5.66	0.20	44.69	0.27	5.71	17.12
AHR from sugarcane bagasse (5 wt.% H_2SO_4, 1h, 175°C)	62.61	5.00	0.15	26.07	0.18	6.00	24.94
Sugarcane Trash	45.24	5.88	0.685	48.17	Nm	6.03	17.72

*Oxygen by difference

Figure 23 shows the effect of acid hydrolysis on ash content. The error bars for ash content each of these feedstocks is also presented. The ash content of all the AHR were lower than miscanthus. There was little effect of increasing reaction time from 3 to 24 hours. However, the results showed that increasing the reaction temperature from 150 to 200°C increased the ash content from 0.38 wt.% to 0.93 wt.%.
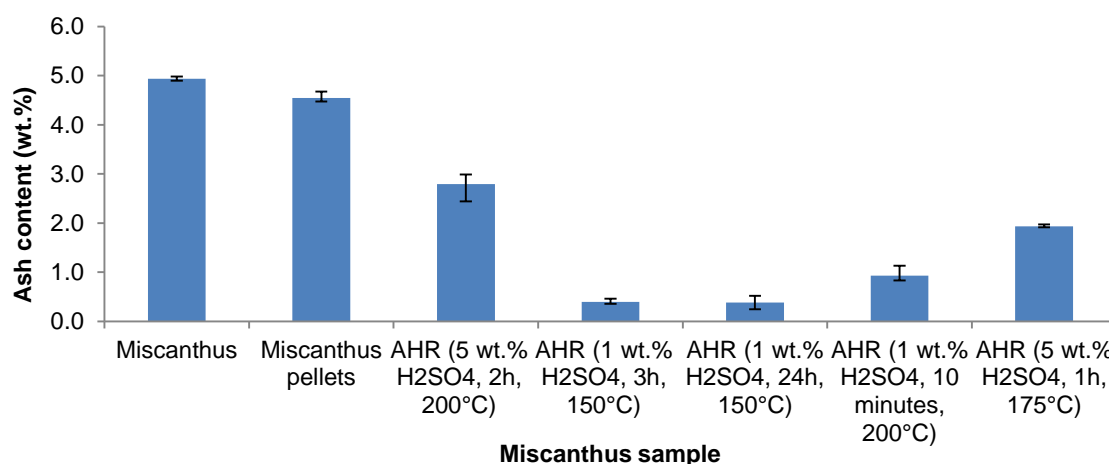
Figure 23: Ash content (wt.%) of miscanthus and AHR derived from miscanthus

Figure 24 shows that the ash content in SCBP was higher (5.71 wt.%) than in unpelletised bagasse (3.19 wt.%). This could be partly due to possible differences in biomass source, harvest times, soil contamination or due to the loss of organic materials from drying or pelletising. Also, storage and handling can affect the composition of biomass which could explain variances between batches. The ash content of sugarcane trash is higher than bagasse which is expected to be a result of soil contamination when the trash was left on the field before collection. The ash

content of the AHR from bagasse did not show a decrease in ash content, but this may be due to the variances between bagasse batches. Sugarcane bagasse samples analysed later in the project had an ash content of approximately 20wt.% which confirms that the ash content of sugarcane bagasse composition can vary significantly between batches depending on storage location and duration. It is likely that a batch of bagasse with significantly higher ash (>6 wt.%) was used to make these AHR samples.
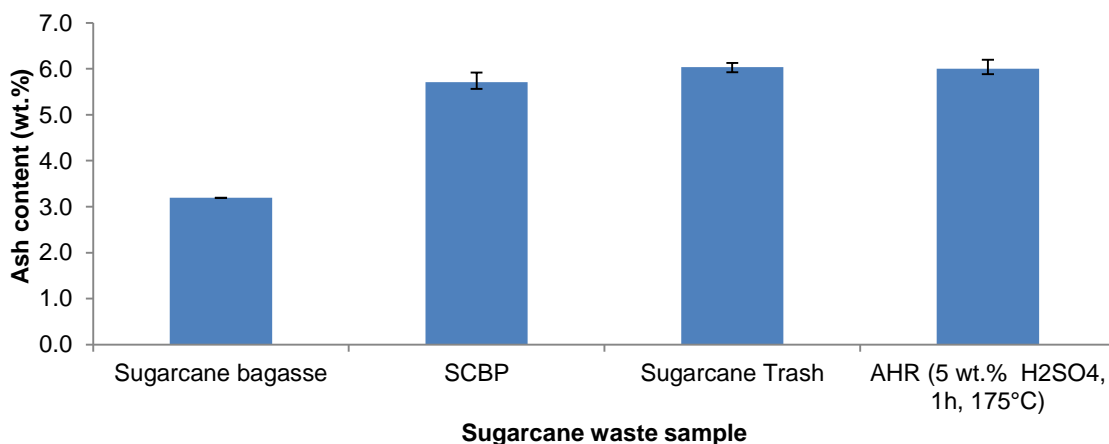
Figure 24: Ash content (wt.%) of sugarcane waste and AHR derived from sugarcane bagasse

Figure 25 shows the calculated HHV of miscanthus compared with AHR from miscanthus. As expected, increased severity of acid hydrolysis conditions increased the HHV of AHR due to an increased lignin and humins content which have a higher energy content (approximately 23.26 to 26.58 MJ/kg) [53] compared to holocellulose (18.6 MJ/kg) [53].
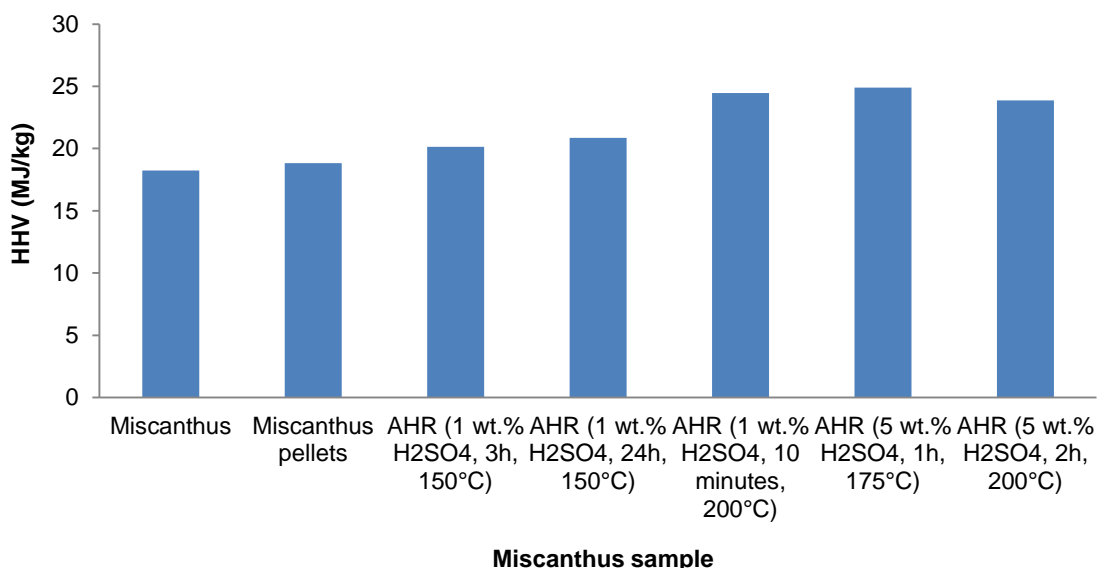
Figure 25: Calculated HHV (MJ/kg) of miscanthus and AHR derived from miscanthus

The calculated HHV of sugarcane bagasse was 19.03 MJ/kg compared to AHR from sugarcane bagasse which was 24.94 MJ/kg (Figure 26). This was also expected as lignin and humins content increased.

37
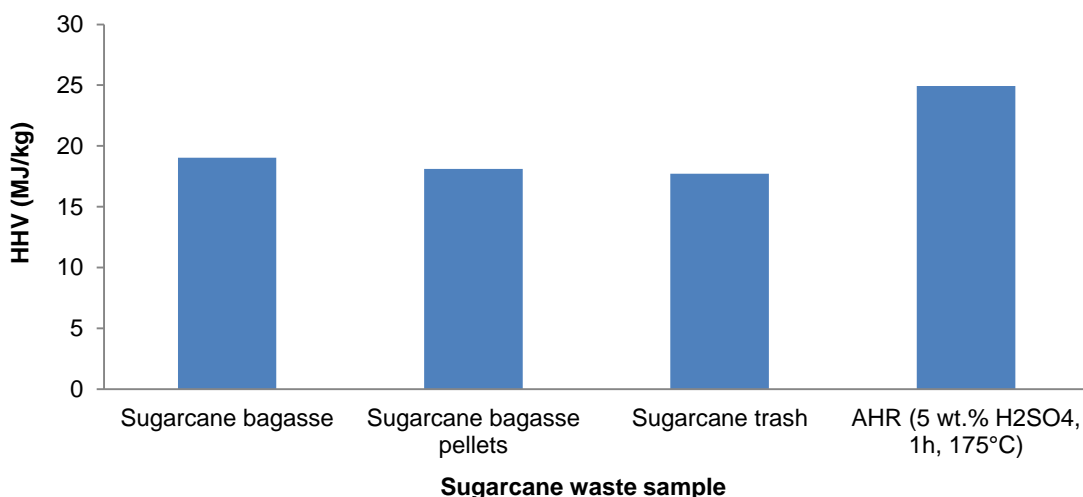
Figure 26: Calculated HHV (MJ/kg) of sugarcane waste and AHR derived from sugarcane bagasse

Proximate analysis was carried out using Thermogravimetric Analysis (TGA) where a feedstock was heated up to a specified temperature in a PerkinElmer Pyris 1 thermogravimetric analyser and the mass loss gravimetrically measured. This technique is not representative of a fast pyrolysis system as it has slower heating rates, longer hot vapour residence times and the flow regime is completely different from that of a fluidised bed. However, TGA is valuable as it can be used to show how samples might behave under slow pyrolysis conditions and to estimate the relative char yields during pyrolysis. TGA was used to determine the moisture content (physically bound water), volatiles (including reaction water), char, ash and fixed carbon content of each feedstock.

TGA uses only 4-5 mg of sample and large particles would not fit into the TGA crucibles so fifteen feedstocks of less than 0.25mm were analysed. Feedstock composition is reported to vary with different fractions of the crop [18]. Therefore, homogenous samples were tested in duplicate to check reproducibility and averages of reproducible results (+/- 1 wt.%) were used. TGA was carried out in two stages: Char was produced in stage 1 using a nitrogen flow. Total combustion of the remaining char was carried out in stage 2 to allow for the alternative determination of the ash content.

- Stage 1: TGA Pyrolysis was used with nitrogen to produce char up to a maximum temperature of 500°C. 4-5 mg of sample was pyrolysed with a heating rate of 5 °C min-1 and a hold time of 5 minutes.

- Stage 2: Slow combustion of char (from stage 1) to produce ash. TGA Combustion with air up to a maximum temperature of 575 °C, a heating rate of 2.5 °C min^{-1} and a hold time of 5 minutes.

Yields of volatiles and char from fast pyrolysis depend on the pre-treatment method [13]. Table 8 shows the TGA pyrolysis yields for the beech samples. The TGA

yields of beech closely resemble data reported in literature [51]. Acid-pretreatment can be used to increase volatile content by reducing ash content. As the ash content of these AHR was decreased, the volatile content of these AHR was higher (up to 88.65 wt.%) than for untreated beech (85.11 wt.%).

Table 8: TGA results of beech and AHR derived from beech (dry basis)

Sample (treatment conditions)	Volatiles (wt.%)	Char (wt.%)	Fixed carbon (wt.%)	Ash (wt.%)
Beech	85.11	14.89	13.06	1.83
Single stage acid treated beech (1 wt.% H_2SO_4, 4h, 75°C)	88.65	11.35	9.45	1.90
Two-stage acid treated beech (1 wt.% H_2SO_4, 4h, 75°C) then (20 wt.% H_2SO_4, 4h, 75°C)	87.36	12.64	10.43	2.22
One-stage acid treated beech (20 wt.% H_2SO_4, 4h, 75°C)	87.33	12.67	10.85	1.82

Table 9 shows the TGA results for all eleven Dibanet feedstocks. Acid hydrolysis of the sugarcane bagasse under severe conditions (5 wt.% acid, 1h, 175°C) reduced the volatile content from 82.40% to 36.17 wt.% as the acid removed a significant amount of holocellulose leaving a high lignin and humin content residue. TGA of the 5 wt.% acid, 1h, 175°C residue resulted in a very high char content (63.83 wt.%) suggesting that high lignin and humin content residues such as AHR would produce a high char yield under fast pyrolysis conditions. Milder acid hydrolysis conditions (i.e. 1 wt.% acid, 3h, 150°C and 1% acid, 24h, 150°C) which only partially hydrolysed the hemicellulose and cellulose were not acceptable conditions for maximising levulinic acid production. It should be noted that the volatile content of AHR from miscanthus (1 wt.% acid, 3h, 150°C) was 80.43 wt.% whereas the volatile content for miscanthus was 73.66 wt.%. This unexpected result may be due to the use of different batches and could not be confirmed as analysis of the miscanthus batch used for this set of acid hydrolysis tests was not possible. It is evident that acid hydrolysis of biomass significantly reduced the ash content i.e. reduced the ash content of miscanthus from 3.6 wt.% to as low as 0.73 wt.% with acid hydrolysis conditions of 1 wt.% H_2SO_4, 3h, 150°C.

Table 9: TGA results of Dibanet samples (dry basis)

Sample (treatment conditions)	Volatiles (wt.%)	Char (wt.%)	Fixed carbon (wt.%)	Ash (wt.%)
Miscanthus	73.66	26.34	22.74	3.60
Miscanthus pellets	74.05	25.95	21.59	4.36
AHR from miscanthus (5 wt.% H_2SO_4, 2h, 200°C)	38.05	61.95	58.50	3.45
AHR from miscanthus (1 wt.% H_2SO_4, 3h, 150°C)	80.43	19.57	18.84	0.73
AHR from miscanthus (1 wt.% H_2SO_4, 24h, 150°C)	73.70	26.30	24.96	1.33
AHR from miscanthus (1 wt.% H_2SO_4, 10 minutes, 200°C)	49.08	50.92	49.08	1.84
AHR from miscanthus (5 wt.% H_2SO_4, 1h, 175°C)	40.07	59.93	58.39	1.54
Sugarcane bagasse	82.40	17.60	14.78	2.82
SCBP	75.85	24.15	18.47	5.68
AHR from sugarcane bagasse (5 wt.% H_2SO_4, 1h, 175°C)	36.17	63.83	56.80	7.03
Sugarcane Trash	74.14	25.86	19.46	6.40

Earlier work carried out with beech showed that acid treatment could be used to reduce the ash content in biomass. However, the TGA results showed that acid hydrolysis of sugarcane bagasse increased the ash content from 2.82 wt.% to 7.03 wt.%. This is likely to be due to the variances between batches and/or possibly particle size distribution. The effect of particle size on ash content is discussed later in section 3.3. Also, as mentioned earlier, biomass composition can vary between batches, but analysis of the sugarcane bagasse batch used for these acid hydrolysis tests was not possible.

Table 10 compares the ash content results derived using the "Standard Test Method for Ash in Biomass" (ASTM E1755) and TGA. Although the same particle sizes were used, there is no visible trend. This is also expected to be a result of differences in batches and variances between heating rates and batch sizes.

Table 10: Comparison of ash content using the ASTM standard and TGA

Sample (treatment conditions)	Ash content (wt.%) using ASTM	Ash content (wt.%) using TGA
Miscanthus	4.94	3.60
Miscanthus pellets	4.54	4.36
AHR from miscanthus (5 wt.% H_2SO_4, 2h, 200°C)	2.69	3.45
AHR from miscanthus (1 wt.% H_2SO_4, 3h, 150°C)	0.41	0.73
AHR from miscanthus (1 wt.% H_2SO_4, 24h, 150°C)	0.38	1.33
AHR from miscanthus (1 wt.% H_2SO_4, 10 minutes, 200°C)	0.93	1.84
AHR from miscanthus (5 wt.% H_2SO_4, 1h, 175°C)	1.93	1.54
Sugarcane bagasse	3.19	2.82
SCBP	5.71	5.68
AHR from sugarcane bagasse (5 wt.% H_2SO_4, 1h, 175°C)	6.00	7.03
Sugarcane Trash	6.03	6.40

DTG results from the TGA were also used to investigate the thermal degradation behaviour of each feedstock under pyrolysis conditions. Figure 27 shows that the peak decomposition of beech samples occurs between 200°C and 500°C. The decomposition temperature ranges for biomass components are reported as follows: hemicellulose (150–350°C), cellulose (275–350°C) and lignin (250–500°C) [54]. However, Yang et al. report the decomposition of lignin to occur over a wider range of temperatures (150–900°C) [55]. The DTG profile for beech shows a shoulder at approximately 350°C which represents the decomposition of hemicellulose and initial decomposition of cellulose. The second step is the final decomposition of cellulose and decomposition of lignin. The peak decomposition temperature for 20 wt.% acid treated beech was lower (350°C) compared to beech (approximately 400°C) due to the higher volatile content and insufficiently hydrolysed AHR.
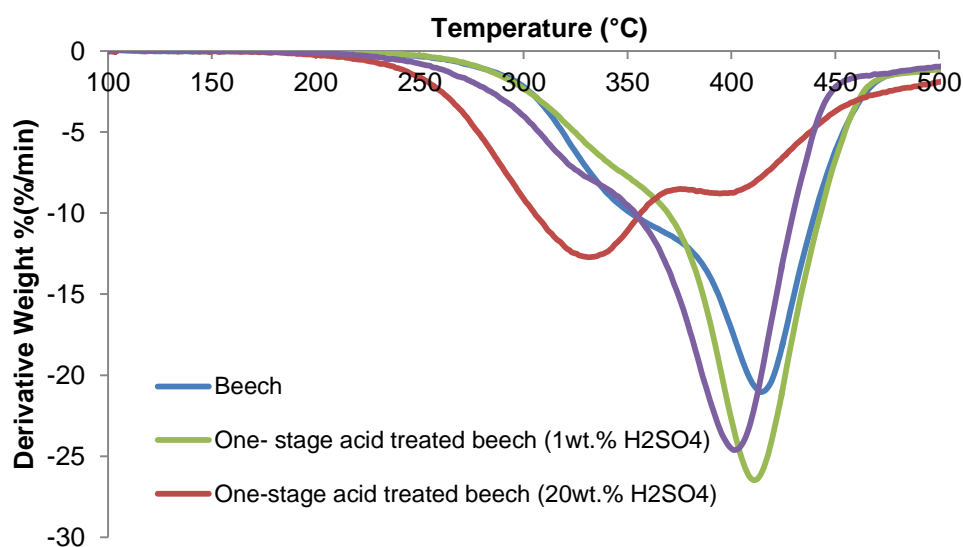
Figure 27: DTG profiles of beech and AHR derived from beech

Lignin is more refractory than holocellulose and therefore expected to shift DTG peaks towards higher temperatures. The thermal degradation behaviour of lignin is widely researched, but that of humins is poorly understood. However, as with lignin, humins are reported to shift DTG peaks towards higher temperatures [39]. Therefore AHR, which consist of a combination of lignin and humins, was expected to shift DTG peaks towards higher temperatures. Figure 28 shows the differential thermogravimetric (DTG) results comparing the thermal properties of miscanthus and AHR derived from miscanthus. The TGA results showed that decomposition of these samples occurred between 200°C and 500°C. The DTG profiles of the AHR from more severe acid hydrolysis conditions had flatter profiles which showed that the decomposition occurred over a wider range of temperatures and the sample decomposed more slowly due to higher lignin and humin content compared to lignocellulosic biomass. The DTG profiles indicate that thermal degradation properties of AHR are similar to those of lignin suggesting that thermal degradation properties of humins are similar to those of lignin. The DTG profiles of the two AHR produced with 1 wt.% H_2SO_4 acid, for 3 or 24 hours at 150°C showed that increasing the reaction time from 3 to 24 hours did not affect the thermochemical properties of the feedstock. University of Limerick reported that the acid hydrolysis conditions for four out of the five AHR derived from miscanthus were too mild and gave unacceptable levulinic acid yields so were not considered for thermal processing.
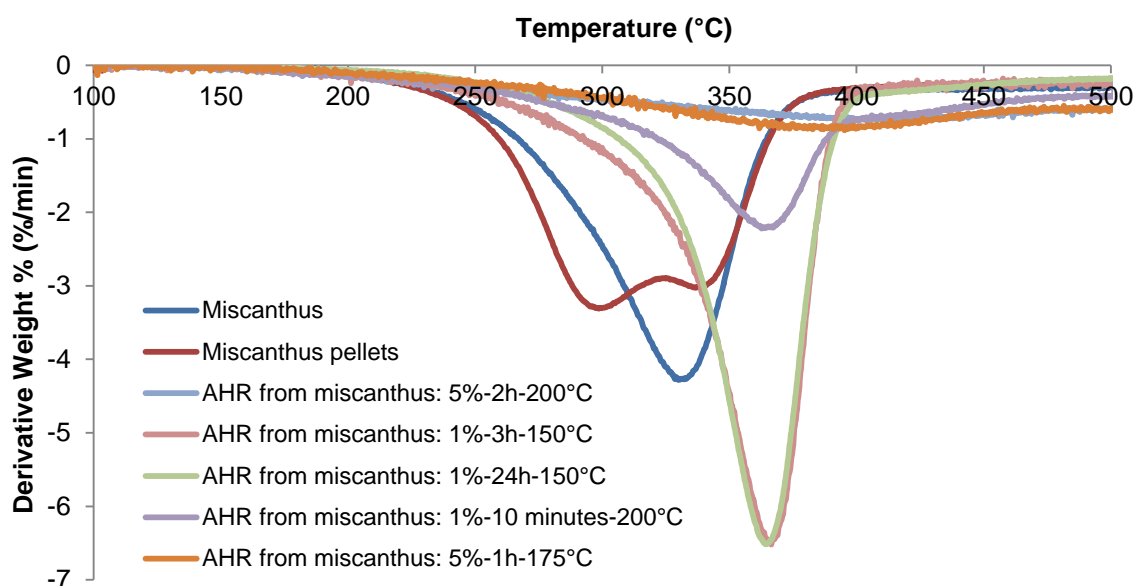
Figure 28: DTG profiles of miscanthus and AHR derived from miscanthus

The acid hydrolysis conditions reported by UL to maximise levulinic acid production, in a single stage acid hydrolysis process from miscanthus and sugarcane bagasse, were 5 wt.% H_2SO_4, for 1 hour at 175°C. These AHR were used for pyrolysis and gasification. Figure 29 shows the differential thermogravimetric (DTG) results comparing the thermal degradation properties of sugarcane bagasse, SCBP, AHR

derived from sugarcane bagasse and trash. The peak temperature for decomposition for sugarcane bagasse occurred at approximately 350°C compared to AHR which had a higher peak temperature range for decomposition.
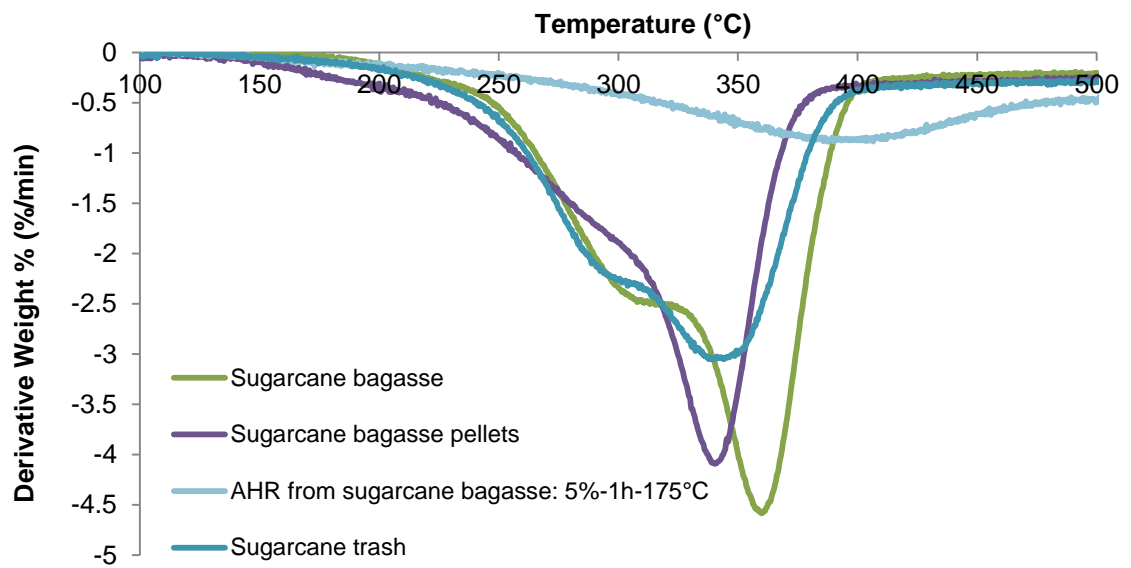
Figure 29: DTG profiles of sugarcane waste and AHR from sugarcane bagasse

Figure 30 compares the differential thermogravimetric (DTG) profiles of the AHR from miscanthus and sugarcane bagasse which were produced using the same acid hydrolysis conditions (5 wt.%-1hour-175°C). The profile shows that the degradation properties of the two AHR are very similar. The peak decomposition temperature was at approximately 400°C which is higher than lignocellulosic biomass due to the high lignin and humin content.
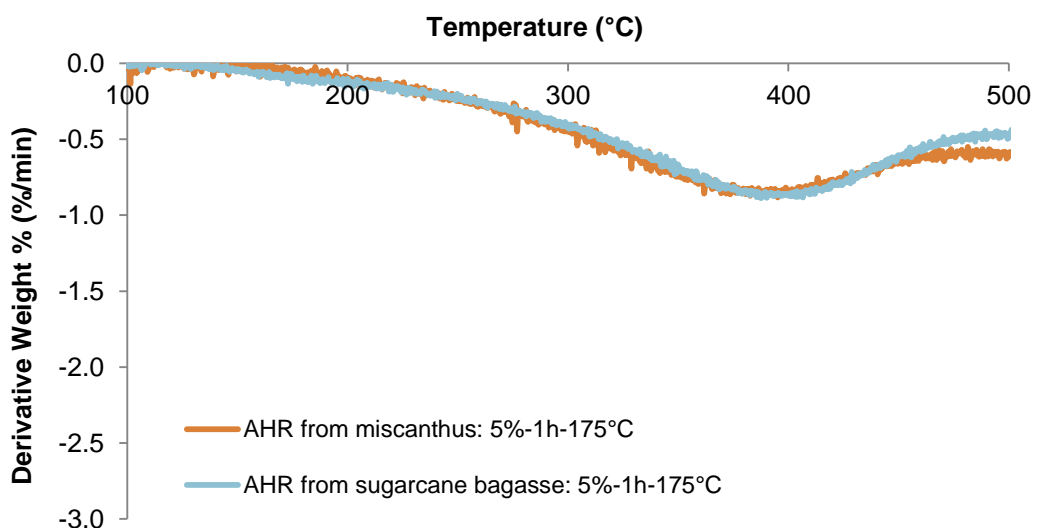
Figure 30: Comparing DTG profiles of AHR from miscanthus and sugarcane bagasse

3.2 Composition and energy content of agreed AHR

Melligan et al. [2] report the Klason lignin content of these AHR as high as 95.5 wt.% and do not discuss the humin content of the AHR. Girisuta et al. also report the acid insoluble lignin content as high as 91.18 wt.% [39]. Although the composition varies depending on acid hydrolysis conditions [39], the following example of mass balance calculations suggest that the remaining AHR cannot be 95.5 wt.% lignin. The AHR consists of lignin, humins, ash and moisture. Humins are unreacted cellulose and oligomerised cellulose which are insoluble in acid so also remain as a solid when determining the Klason lignin content. There are currently no known analytical techniques to differentiate humins and lignin other than by calculation. Therefore, the lignin and humin content in AHR were calculated as follows:

- Basis:
    - 100kg of biomass
    - AHR yield from biomass of 62 wt.% (varies depending on acid hydrolysis conditions) = 62kg of AHR [56]

- Assumptions:
    - AHR is composed of lignin, humins, ash and moisture only
    - Approximate lignin content of biomass is 21 wt.%
    - All Klason lignin (21kg) from original biomass (100kg) is associated with AHR

- Measurements:
    - Ash content of AHR is 6 wt.% (dry basis)
    - Moisture content of AHR is 5.6 wt.%

- Calculations:
    - 21kg lignin in 62kg of AHR
    - Ash in 62kg of AHR 0.06 x 62= 3.72kg
    - Moisture in 62kg of AHR 0.056 x 62= 3.47kg
    - Humins (balance) in 62kg of AHR = 62 - 21 – 3.47 – 3.72 = 33.81kg

This AHR (5 wt.%-1hour-175°C) contained ash (6 wt.%), moisture (5.6 wt.%), lignin (33.87 wt.%) and humins (54.53 wt.%). The humin content of the AHR was expected to be greater (54.53 wt.%) than the lignin content (33.87 wt.%) so AHR may not thermally decompose like other lignins.

The following calculations confirm that AHR represents a considerable proportion (up to 80%) of the original energy in the biomass.

- Basis:
  - 100kg of biomass
  - AHR yield from biomass of 62% (varies depending on acid hydrolysis conditions) = 62kg of AHR [56]
- Measurements:
  - HHV of sugarcane bagasse is 19MJ/kg
  - HHV of AHR from sugarcane bagasse is 24.94MJ/kg
- Calculations:
  - 100kg of sugarcane bagasse has 19 x 100 = 1900MJ
  - 62 wt.% of sugarcane bagasse is AHR so 62kg of AHR has 24.94 x 62 = 1546.28MJ
  - Energy in AHR from original energy in sugarcane bagasse = 1546.28/1900 x100 = 81.38%

The acid hydrolysis process results in a substantial amount (up to 62 wt.% on dry biomass basis) of solid AHR which can be separated by filtration from the water soluble stream [39]. AHR consists of mainly lignin and humins that represents approximately 80% of the original energy in the biomass and therefore were considered for thermal processing.

3.3 Sample preparation for analysis and thermal processing

All samples require preparation before thermal processing in order to maximise organic liquid yields from fast pyrolysis or gas yields from gasification. For example, moisture and ash content and particle size of the feedstock has a significant effect on pyrolysis and gasification. This is discussed in sections 5.3 and 8.3.

All feedstocks were oven dried at 105°C, before ash and elemental analysis was carried out. A Sartorius MA35 moisture analyser was used to determine the moisture content of all samples before thermal processing. Feedstocks with significantly high moisture content were oven dried before pyrolysis and gasification.

Biomass needs to be ground to ensure high heat transfer rates and minimise vapour diffusion through the catalytically active external char layer. Biomass was ground to the required particle size using a Heavy-Duty Cutting Mill, Type SM2000 supplied by Retsch Ltd. in Germany. As only a few milligrams (<5mg) of feedstock were required for analysis, samples were ground and sieved to less than 0.25mm. A stack of wire mesh sieves were used to vibrate and separate the different particle sizes. Particles larger than 0.25mm were retained at the top of the sieve shaker. These

were re-ground and sieved to obtain a homogeneous sample. Particle sizes greater than 1mm were not available in this batch of samples. However, larger particles would not be used in this processing work as these may cause blockages in the narrow pipes leading to the reactor. Figure 31 shows the effect of particle size on the ash content of miscanthus, sugarcane bagasse and trash. Sugarcane bagasse had the lowest ash content as sugar extraction in a sugar mill is carried out with water where some ash is likely to be removed. For all biomasses, increasing the particle size range of biomass from <0.25mm to 1mm reduced the ash content.
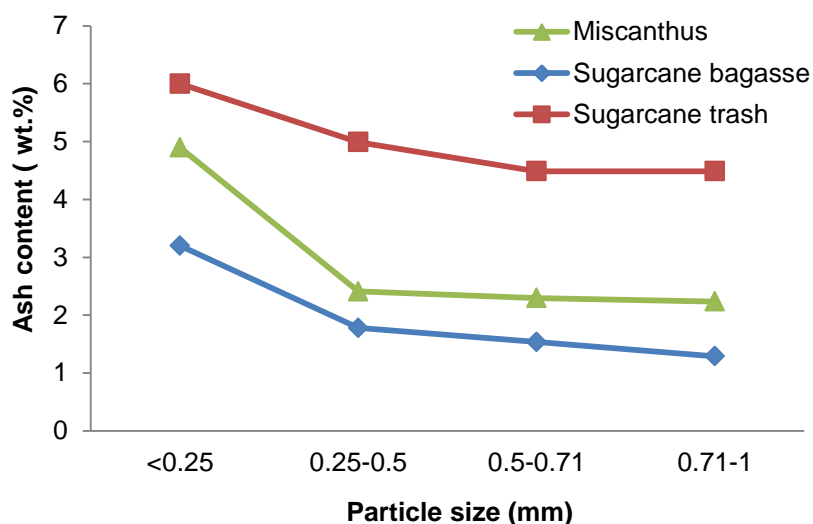
Figure 31: Effect of particle size on ash content (wt.%)

Bridgeman et al. also confirm that ash content was lower with larger particle sizes [57]. Milling and sieving could be used as a pre-treatment method to improve biomass quality for thermal processing [57]. Therefore, for a low ash feedstock, it was necessary to remove particles smaller than 0.25mm.

Determination of feedstock bulk density was important for fast pyrolysis processing in a fluidised bed reactor to ensure the bed material, such as sand, was retained in the reactor and the char was entrained out of the reactor. The bulk density of the feedstocks, char and sand were determined experimentally using a 500ml glass measuring cylinder as reported by Milligan [58]. The measuring cylinder was filled and tapped one hundred times to help settle the particles. Six measurements were carried out and averages were taken. Table 11 shows the bulk density of the ground and sieved feedstocks (according to feed requirements) that were considered for processing. As expected, sugarcane bagasse and trash had a low bulk density in comparison to bagasse pellets. Pelletising low bulk density feedstocks such as bagasse before grinding is important for processing in order to increase the throughput and improve feeding on the systems available in this work. There is a low throughput through narrow pipes if the biomass has a low bulk density.

46

Table 11: Bulk density of feedstocks, sand and char

Feedstock, sand and char	Bulk density (kg/m^3)
Miscanthus	274.77
Miscanthus pellets	357.41
Sugarcane bagasse	133.44
Ground SCBP	434.44
Sugarcane trash	159.68
AHR from miscanthus (5 wt.% acid, 1h, 175°C)	619.89
AHR from sugarcane bagasse (5 wt.% acid, 1h, 175°C)	684.88
Sand (355-500µm)	1598.95
Sand (500-600µm)	1638.30
Char (from ground SCBP)	313.48

Lignin is reported to have a low melting point (80-200°C) and the melt is very adhesive [59]. Therefore, a melt test was conducted to see if pre-pyrolysis of high lignin content AHR would occur and block in the existing feeding systems. Alcell lignin and AHR are all brown powders and look very similar. 1g of Alcell lignin and 1g of AHR from miscanthus (5 wt.% H_2SO_4, 1 hour at 175°C) were heated up from 200°C to 600°C at 100°C intervals. Figure 32 to Figure 36 depicts Alcell lignin and AHR after conducting melt tests at increasing temperatures. Alcell lignin melted at approximately 200°C and then became a crisp solid before reaching 600°C. However, the AHR did not melt; it remained solid and became ash even after the oven temperature reached 600°C.

The 300g/h reactor can be heated to a maximum of 650°C and the tip of the feeding screw is inside the reactor and heat can be conducted along the screw. However, there is a supply of nitrogen through the feeder via the screw which is at room temperature and also a water cooling pipe wrapped around the end of the screw to avoid pre-pyrolysis. Therefore, although the temperature along the screw has not been measured, it is assumed that the screw will not reach temperatures higher than 600°C and AHR will not melt in the casing of the screw before entering the 300g/h reactor.

Figure 32: Alcell lignin and AHR after melt test at 200°C

Figure 33: Alcell lignin and AHR after melt test at 300°C

Figure 34: Alcell lignin and AHR after melt test at 400°C

Figure 35: Alcell lignin and AHR after melt test at 500°C

Figure 36: AHR after melt test at 600°C

3.4 Interim conclusions

- The volatile content of miscanthus and sugarcane bagasse is between 73-83 wt.% suggesting fast pyrolysis of these feedstocks would give a high liquid yield.

- Sugarcane bagasse shows the highest volatile content of 82.40 wt.% so expected to give the highest organic liquid yields from fast pyrolysis.

- Sugarcane trash has the highest ash content 6.03 wt.% which is undesirable for fast pyrolysis as catalytically active ash can lead to secondary cracking of pyrolysis vapours.

- There is no difference in terms of thermochemical properties when increasing acid hydrolysis reaction time from 3 to 24 hours at 1% acid treatment.

- Acid hydrolysis of miscanthus or sugarcane bagasse at 5 wt.% H_2SO_4 for 1hour at 175°C was defined as the optimum conditions for maximum levulinic acid production by University of Limerick.

- The low volatile content (36-40 wt.%) of the AHR from miscanthus and sugarcane bagasse indicates AHR would give low liquid yields and high char yields from fast pyrolysis.

- AHR has a higher carbon content (62.6 wt.%) than biomass (47.6 wt.%) which is responsible for the high char yields from fast pyrolysis. Therefore, the focus for value added products from AHR is product gas using gasification.

- AHR from sugarcane bagasse (5 wt.% H_2SO_4, 1h, 175°C) has the highest HHV of 24.94MJ/kg which is an indication that it has the highest lignin and humin content.

- AHR has a higher ash content (6 wt.%) than SCBP (2.97 wt.%) so AHR is expected to yield higher solids in pyrolysis and gasification than SCBP. The higher ash content can also contribute to more secondary catalytic cracking reactions.

- AHR yield from biomass is 62 wt.% dry feed basis when the optimum acid hydrolysis conditions reported by UL are used.

- AHR represents approximately 80% of the original energy in the biomass.

- AHR, as received from University of Limerick, contains ash (6 wt.%), moisture (5.6 wt.%), lignin (33.9 wt.% estimated by calculation) and humins (54.53 wt.% by difference). The humin content of the AHR is greater (54.5 wt.%) than the lignin content (33.9 wt.%)

- DTG results showed that AHR is refractory and reacts more slowly than biomass.

- DTG profiles indicate that AHR decomposes slowly over a wide range of temperatures as with lignin. Therefore, humins are expected to be refractory like lignin.

- TGA pyrolysis of AHR yields low volatiles and high char so are not suitable for fast pyrolysis as low liquid yields and high char yields are expected. Slow pyrolysis of AHR is likely to be more suitable if maximising biochar is the objective (as carried out in part of the Dibanet project).

- The AHR does not melt at temperatures as high as 600°C and is more refractory compared to other high lignin materials due to the presence of humins. Therefore, AHR is not likely to melt in the pipework leading to the reactor thus avoiding blockages.

4   THERMAL CONVERSION PROCESSES SUMMARY

The objective of this chapter is to summarise and compare the thermal conversion processes currently available for the production of bioenergy and/or biofuels from biomass and AHR.

Biomass is a broadly distributed, low energy density and bulk density material which can be difficult and costly to transport and store. Figure 37 shows some of the thermal conversion processes that are currently being developed to process biomass. These include combustion, pyrolysis and gasification. The process conditions and main products are depicted.
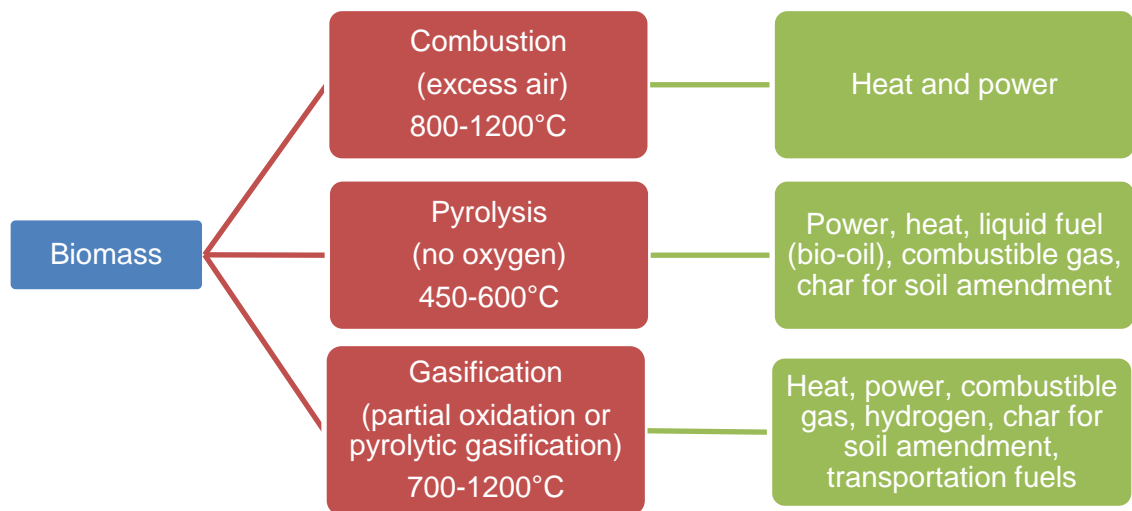
Figure 37: Biomass thermal conversion processes (derived from [6, 60, 61])

4.1   Combustion

Combustion is a straightforward exothermic process which uses oxygen or air to completely thermally decompose biomass to produce usable heat energy and ash. The thermal energy must be used immediately; the heat cannot be stored or transported like the liquid and gaseous products from pyrolysis or gasification. Combustion is the most widely used thermochemical process for conversion of biomass and is responsible for 97% of the world's energy production from biomass [62]. However, the efficiency of the process for direct heating is reported to range from 20 to 40% which is considerably low [62].

4.2   Pyrolysis

Pyrolysis occurs in the absence of oxygen to produce solid char, liquid and gases. The product yields are strongly dependent on the process conditions such as temperature, reactor type, vapour residence times, cooling and collection and these can be controlled to maximise the desired products. Table 12 shows the conditions and product composition (wt.%) for fast, intermediate and slow pyrolysis. These modes of pyrolysis vary in hot vapour residences times and temperature. Table 12 indicates that

low temperatures and long residence times increase the char yield, whereas higher temperatures with shorter residence times favours high liquid yields [63, 64]. Fast pyrolysis compared to intermediate and slow pyrolysis is ideal for liquid production as it produces up to 75 wt.% liquid product and only 12 wt.% char from wood on a dry feed basis. High liquid yields make fast pyrolysis an attractive process. However, liquid composition and quality vary between feedstocks and processing conditions.

Table 12: Typical product yields (dry wood basis) obtained by different pyrolysis modes [64]

Aston University

Illustration removed for copyright restrictions

4.3 Gasification

There are two modes of gasification which include pyrolytic gasification and oxidative gasification which are used to maximise gaseous products with a variety of uses such as power or electricity generation. Process heat for pyrolytic gasification is provided by combustion of recycled char and therefore reduces by-product yields. Product gases from pyrolytic gasification have a medium heating value (17-19 MJ/Nm^3) [65]. On the other hand, oxidative gasification uses air, oxygen or steam. The product gas from air-blown gasification is diluted with nitrogen so has lower energy content (4-7 MJ/Nm^3). However, product gas from oxygen or steam gasification has higher energy content (10-18 MJ/Nm^3). Table 13 compares the typical product yields from pyrolytic and oxidative gasification of wood. An oxidative gasification agent is required if gas yields are to be maximised. However, pyrolytic gasification can also be used to produce high yields (85 wt.%) of gas from wood, without the addition of an oxidant.

Table 13: Comparison of typical product yields (dry wood basis) from gasification [64, 66]

Mode	Conditions	Liquid (%)	Solid (%)	Gas (%)
Pyrolytic gasification	High temperature up to 900°C, short hot vapour residence time ~ 1 sec, recycled fluidising gas	5	10	85
Oxidative gasification	High temperature, long residence times, gasification agent (air, steam or O$_2$)	0	1-2	95-99 [67]

Table 14 summarises the advantages and disadvantages of combustion, fast pyrolysis and gasification.

Table 14: Advantages and disadvantages of combustion, fast pyrolysis and gasification [68, 69]

	Advantages	Disadvantages
Combustion	• Commercial • useful heat can be used directly to raise steam for power	• Emissions problems • Thermal energy must be used immediately • Heat cannot be stored • Volume of gas produced is high compared to gasification so larger gas cleaning equipment is required • Leaching property of bottom ash is considered to be hazardous
Fast pyrolysis	• Bio-oil can be stored & transported more easily than solid biomass and syngas. • Variety of products • Use as energy carrier or fuel for power, biofuels or chemicals • Bio-oil can be burned in a boiler • Bio-oil has a higher energy density than syngas • Potential integration in biorefinery • Lower operating temperature than gasification and combustion • Lower emissions	• Technology less developed than combustion and gasification • Reduced HHV compared to heavy oil • Upgrading required for use in engines and turbines • Immiscible with hydrocarbons • Long-term storage of corrosive bio-oil is difficult
Gasification	• Technology is at demonstration scale • Fuel flexible • Lower operating temperature than combustion so longer gasifier lifetimes • Lower emissions • Existing infrastructure using coal syngas can supplement it with biomass syngas • Volume of gas produced is low compared to combustion so smaller gas cleaning equipment is required • Char from low-temperature gasification can be used as activated carbon or soil amendment.	• Gas cleaning required and unproven • Costs associated with steam and oxygen • Complex operation as oxygen separation units are required for oxygen • Scaling unknown for biomass gasification • High ash feedstocks can result in agglomeration

Combustion converts biomass directly into heat energy and ash, whereas both fast pyrolysis and gasification deliberately limit conversion so that valuable intermediates can be recovered and further processed to produce valuable fuels such as clean syngas or upgraded bio-oil. Therefore, fast pyrolysis and gasification are investigated in this work. Table 15 compares fast pyrolysis and gasification. However, the theory and literature review of pyrolysis and gasification can be found in Chapter 5 and Chapter 8 respectively.

Table 15: Comparison of fast pyrolysis and gasification

	Fast pyrolysis	**Gasification**
Temperature (°C)	450-600	700-1200
Gasification agent	None	Oxygen free gasification agent, air, steam or oxygen
Pressure	Atmospheric	Atmospheric or pressurised
Residence time	Short (< 2 seconds)	Varies
Further processing	Bio-oil is immiscible with diesel so further catalytic upgrading is required	Gas cleaning and cracking of long chain hydrocarbons is required

5 THEORY AND LITERATURE REVIEW: FAST PYROLYSIS AND BIO-OIL UPGRADING

The objective of this chapter is to present the theory and review the literature to fast pyrolysis processing and product upgrading. Fast pyrolysis of the feedstocks within the Dibanet project is of particular interest and has been reviewed in this chapter. Bio-oil upgrading techniques are also reviewed to give an insight to the topic and provide a foundation for experimental work.

5.1 Background

Fast pyrolysis has been well established in large scale plants since the 1990s [70]. Bridgwater reports that the University of Waterloo is recognised for preliminary research into fast pyrolysis [71]. The technology is relative new and at an early stage of commercialisation compared to combustion and gasification, but there have been significant advances in this area around the world in the last 15 years. Ensyn Technologies, Dynamotive, KIT and BTG are some of the companies which are currently leading the development [9]. The most recent review of fast pyrolysis and product upgrading by Bridgwater [72] reports fast pyrolysis to be an attractive thermal conversion process for converting biomass into valuable transportable liquid [70]. Fast pyrolysis of biomass has the potential to produce high yields of liquid (up to 75 wt.% on dry feed basis) [73] with low production costs. It is also reported to be one of the most efficient biomass conversion processes and capable of competing with fossil fuels as energy fuels with high fuel-to-feed ratios can be produced [74].

Figure 38 shows the overall fast pyrolysis process.
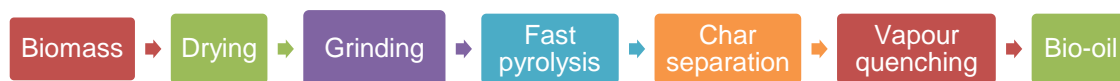
Figure 38: Fast pyrolysis process (adapted from [64])

Fast pyrolysis is a thermal decomposition process which takes place at atmospheric pressure in the absence of air and produces liquid bio-oil, char and non-condensable gases. Char and gases are by-products of fast pyrolysis. Bridgwater reports that some commercial fluidised bed processes recycle this char to provide heat for the fast pyrolysis process as char can have HHV of up to 23 MJ/kg. Non-condensable gases, mainly carbon dioxide, carbon monoxide, methane and C_2-C_4 hydrocarbons that are produced, can also be used for process heat. As a result, only flue gas and char remain as waste streams [72]. Some researchers use fast pyrolysis char for soil amendment and carbon sequestration studies which means that if char is not available for process heat for the fast pyrolysis process, energy would need to be provided from an external source such as fossil fuels.

The main product from fast pyrolysis of biomass is bio-oil which is a dark brown free flowing liquid consisting of mainly organics and water. Liquid bio-oil is easier to transport and store than solid biomass as well as having the potential to be used as a fuel or a base for chemical production [75]. The main components in bio-oil are acids, aldehydes, alcohols, sugars, esters, ketones, phenolics, oxygenates, hydrocarbons, and steroids [63]. Figure 39 shows the applications of bio-oil. Although many applications of bio-oil exist, the Dibanet project initially focused on using fast pyrolysis to produce a bio-oil which could subsequently be upgraded to transportation fuels.
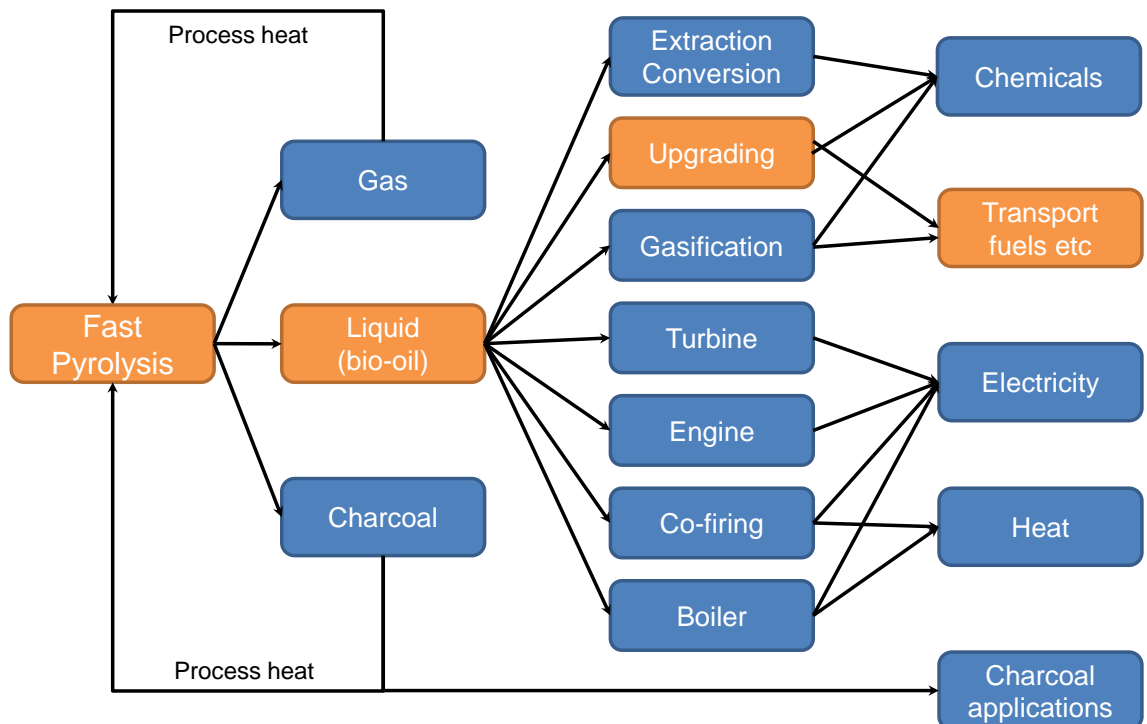
Figure 39: Applications of Bio-oil (adapted from [76])

Table 16 shows the unwanted characteristics of bio-oil. It also shows the problems that are caused and possible solutions to the problems.

Table 16: Unwanted characteristics of Bio-oil (adapted from [73, 77])

Characteristic	Cause	Problem	Solution
Acidity	• Organic acids from degradation	• Corrosion of pipe-work and vessels	• Adequate materials e.g. stainless steel or polyethylene/ polypropylene • Neutralization • Upgrading
High viscosity		• Handling • High pumping cost • Gives high pressure drop increasing equipment cost • Poor atomisation	• Add water or solvent
Instability, in-homogeneity and temperature sensitivity	• High water in the feed • High ash in feed • Poor char separation	• Inconsistency in handling, storage and processing • Phase separation, layering, poor mixing • Decomposition and gum formation • Viscosity increase over time from secondary reactions such as condensation	• Avoid contact with hot surfaces • Stabilisation or refining through catalytic treatment • Add water or solvent or diluents
Char and solids content	• Incomplete char separation	• Aging of oil • Sedimentation • Filter blockage • Catalyst blockage • Engine injector blockage • Alkali metal poisoning[73]	• Liquid filtration • Improved cyclones • Multiple cyclones • Hot gas filtration
Alkali metals	• Nearly all alkali metals report to char so not a big problem • High ash feed • Incomplete solids separation [73]	• Catalyst poisoning • Deposition of solids in combustion • Erosion and corrosion • Slag formation • Damage to turbines	• Biomass pre-treatment to remove ash • Hot gas filtration • Process oil • Modify application • Catalytic upgrading
Water content	• Pyrolysis reactions, • Water in the feed	• Complex effect on viscosity and stability: Increased water lowers heating value, density, stability, and increase pH. • Affects catalysts [73]	• Optimisation and control of water content according to application
Contaminants (chlorine, nitrogen, sulphur)	• Contaminants from biomass • High nitrogen feed	• Catalyst poisoning • NO_x in combustion	• Include suitable cleaning processes

Characteristic	Cause	Problem	Solution
	such as proteins in wastes		• Feed blending • Careful feed selection • Add NO_x removal in combustion applications
Very low miscibility with hydrocarbons	• Highly oxygenated product	• Immiscible with hydrocarbons so incorporation into a refinery is difficult	Upgrading by: • Hydrotreating • cracking with zeolites

Bio-oil has several undesirable characteristics compared to conventional diesel as shown in Table 17. The high oxygen content of bio-oil is what makes bio-oil oleophobic and immiscible with conventional hydrocarbon transport fuels and therefore deoxygenation is required before bio-oil can be used as a transportation fuel.

Table 17: Comparison of typical bio-oil and diesel characteristics (derived from [78, 79])

Physical Property	Bio-oil	Diesel	Comments
Water content (wt.%)	15–30	0.05	Water from: • original moisture in feedstock • dehydration reaction • storage Water reduces the heating value and reduces the viscosity [78].
Oxygen content (wt.%)	35-40	0	The high oxygen content leads to the lower energy density and immiscibility with hydrocarbon fuels [78].
Low pH	2.5	-	Large amounts of carboxylic acids, such as acetic and formic acids. Corrosive nature of bio-oil requires expensive material of construction [78].
Viscosity (@ 50°C) cP	40-100	4	Important for fuel injection system and combustion properties of fuel [78] [70].
HHV (MJ/kg)	16-19	45	Low HHV due to high oxygen content [70].
Ash content (wt.%)	0-0.2	0.01	Alkali metals in ash can cause erosion, corrosion problems [78] [70].

Figure 40 is a simplified flowchart of pyrolysis which depicts the fate of the biomass components. Some cellulose and lignin remain as char. Extractives, cellulose, hemicellulose and lignin decompose and collect as liquid which is a mixture of organics and water. Cellulose and hemicellulose contribute to the production of non-condensable gases. Finally, it can be seen that ash remains in the char.
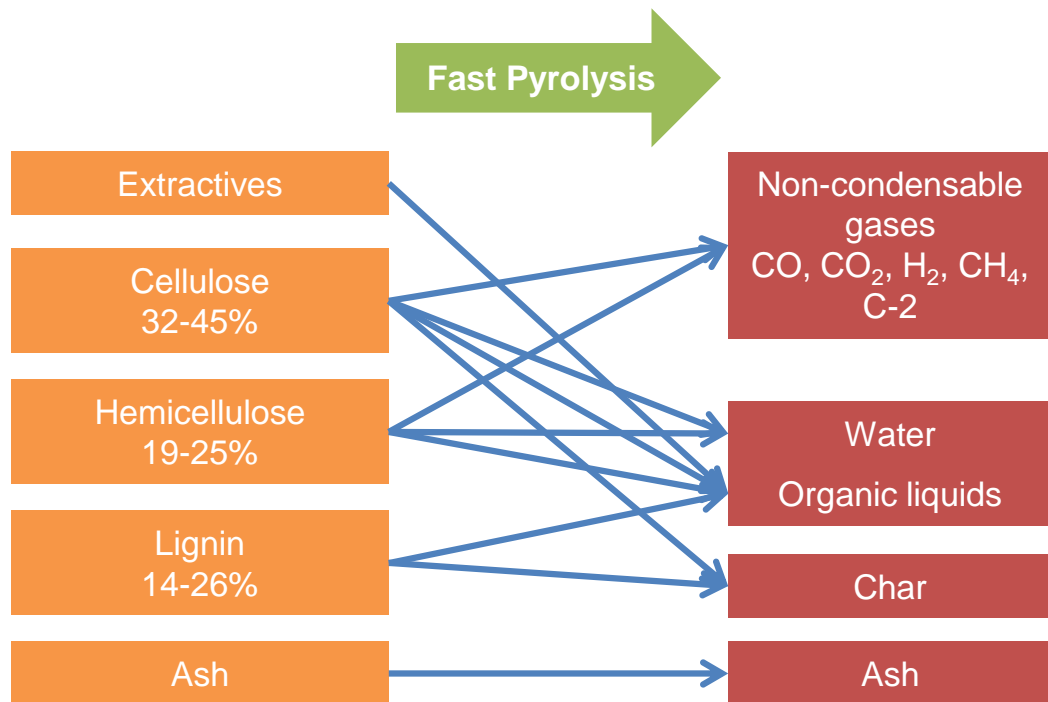
Figure 40: Biomass pyrolysis (adapted from [80])

Sannita et al. report that the behaviour of biomass is a result of a sum of the behaviour of the hemicellulose, cellulose and lignin [81]. However, the alkali metals present in ash are catalytically active which can also significantly affect the quality and quantity of bio-oil. The degradation products of hemicellulose, cellulose and lignin are shown in Figure 41 to Figure 43. Ketones, aldehydes, acids and furans are derived from hemicellulose and cellulose. Sugars are also derived from hemicellulose. Phenolics such as eugenol and vanillin are derived from lignin [52]. Acids, phenols and sugars are reported to contribute to the acidity of bio-oil [82].

Figure 41: Degradation products from hemicellulose [82]

Figure 42: Degradation products from cellulose [82]

Figure 43: Degradation products from lignin [82]

The main performance indicators for fast pyrolysis in this work are liquid yields and liquid heating value. Liquid oxygen content is also important as this determines the miscibility with hydrocarbons and the HHV. The water content also has significant effect on the performance as it directly affects the viscosity, pH, liquid HHV and can lead to undesired phase separation during storage and use.

5.2 Fast pyrolysis process variables

Bio-oil quality and quantity is dependent on process variables such as reactor type, heating rates, reaction temperature, hot vapour residence time, char removal and vapour quenching [63, 70]. There are several different types of pyrolysis reactors including fluidised bed (Figure 44), circulating fluidised bed/transported bed (Figure 45), rotating cone (Figure 46) and ablative pyrolysers (Figure 47).

Figure 44: Bubbling fluidised bed [83]

Figure 45: Circulating fluidised bed/transporting reactor [83]

Figure 46: Rotating cone pyrolyser [83]

Figure 47: Ablative pyrolyser [83]

Continuous bubbling fluidised bed pyrolysers are a popular fast pyrolysis reactor configuration as these provide good temperature control, high heat transfer rates, short residence time which produce up to 75 wt.% of bio-oil on a dry feed basis. These reactors are suitable for large scale operation as they are simple in construction and operation. Four bubbling fluidised bed pyrolysers are available at Aston University with biomass processing capacities of 100g/h, 300g/h, 1kg/h and 7kg/h. The advantages and disadvantages of these are stated in Table 18.

Table 18: Advantages and disadvantages of a fluid bed adapted from [84-88]

Advantages	Disadvantages
• Good gas-solid contact between particles • High heat transfer coefficients • Easy handling and transporting solids into and out of reactor. • Uniform temperature distribution (good T control) giving uniform quality of products • Good solid mixing in bed • Continuous operation • Can use wider particle size range • Suitable for large scale operation • Technology is well understood	• De-fluidisation due to agglomeration of solids • Erosion due to high velocities • Expensive solid separation • Solid entrainment • Channelling of gas phase • Lower conversion • Elutriation of fines can limit performance • Excessive gas by-passing possible

Fluidisation in a fast pyrolysis fluidised bed reactor is achieved by passing a fluidising gas, usually recycled non-condensable gases, upwards through a sand bed supported on a distributor plate. Particles with a lower density than the bulk density of the sand bed float and those heavier sink and remain in the reactor until they have been thermally processed [89].

The behaviour of a fluidised bed reactor is impacted by control parameters such as elevated temperatures and pressures and particle properties such as density, velocity, particle size. As fast pyrolysis is operated at atmospheric pressure, only the effect of temperature will be presented in this thesis. Temperature is inversely proportional to the gas, leading to changes in the fluidising behaviour. Increasing process temperature inside a fluidised bed reactor reduces the gas density. It is important to consider the hot/cold scaling criteria as the fluidisation behaviour changes with temperature. However, the most promising temperature reported to maximise organic liquid was used in this work, therefore effect of pyrolysis temperature on fluidisation behaviour was not monitored.

Particles with different sizes, shapes and densities behave differently in a fluidised bed reactor. The Geldart system is widely accepted for classification of particles with different sizes and densities. Figure 48 depicts Geldart's classification of powders which has become the standard to determine the types of gas fluidisation [90]. The bed particles in Group A exhibit expansion after minimum fluidisation. Gas bubbles appear at the minimum fluidisation velocity for Group B powders. Particles in group C classification are difficult to fluidise and stable spouted bed are formed with group D powders.

Illustration removed for copyright restrictions
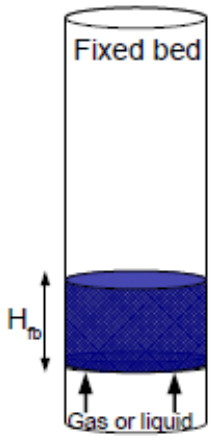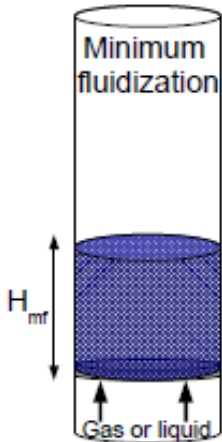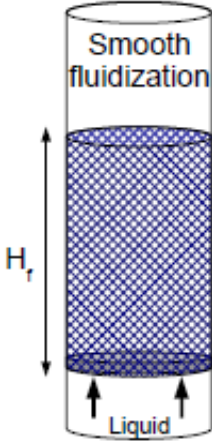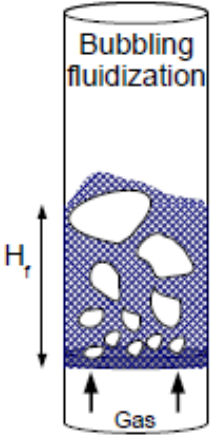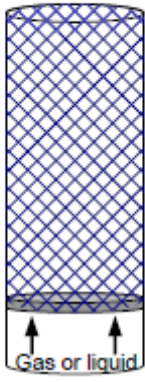
Figure 48: Geldart's classification of powders according to fluidisation properties [91]

In fast pyrolysis, it is necessary for the char particles to be ejected from the fluidised bed whilst the sand particles collapse back to ensure sufficient heat transfer [92]. Therefore, bed depth is an important design feature of a fluidised bed reactor with regards to residence time and solid char entrainment. Typically, fluidised bed reactor comprises a freeboard above the dense fluidised bed. The freeboard height is also important to ensure the heat transfer medium i.e. sand, does not get entrained. A larger bed depth can also increase the hot vapour residence time which can lead to undesirable secondary reactions.

Table 19 shows the fluidisation regimes as a result of increasing fluidising velocity. The fluidising velocity is related to the bed depth of a fluidising bed reactor. Bubbling fluidised bed reactors are operated at Aston University.

Table 19: Fluidisation regimes (adapted from [93])

Fixed bed	Minimum fluidization	Smooth fluidization	Bubbling fluidization
H_{fb} — Gas or liquid	H_{mf} — Gas or liquid	H_f — Liquid	H_f — Gas
Very low fluid flow rate is passed through the bed and the fluid moves through the voids created by the solid particles.	The fluid flow equals the weight of the particles.	Smoothly fluidized bed usually encountered when fluidising with a liquid.	Bubbling beds are of great importance due to its mixing capabilities.

Slugging (axial slugs)	Slugging (Flat slugs)	Turbulent fluidization	Lean phase fluidization with pneumatic transport
Gas	Flat slug — Gas	Gas	Gas or liquid
When bubbles occupy more than 50% of the tower diameter they are referred to as slugs. Bubbles coalesce to form an axial slug. Typical for smooth fine particles. Wall slugs form when the fine particles are rough.	Typical for large particles.	Irregularly shaped voids and clusters of particles move around in turbulent motions when the superficial gas velocity is increased pass the terminal velocity of the particles.	Particles are blown out of the tower to form the lean or dilute phase.

Gas to solid heat transfer from hot fluidising gas to biomass occurs by convection and the solid to solid heat transfer from fluidising medium to biomass occurs by conductive heat transfer [92] [94]. A review by Isahak et al. reports that higher heating rates favour liquid production whereas lower heating rates favour char production [95]. High heating rates as high as 1000°C/s are reported to minimise char yields and maximise liquid production [92, 96].

Fast pyrolysis processing temperatures can vary from 450-600°C. Figure 49 shows the effect of temperature on the product yields from fast pyrolysis depicted by Bridgwater where organic liquid yields are maximised between 500 and 520°C. The optimum temperature to maximise liquid yields from wood is reported to be around 500°C [64] [97]. Higher temperature pyrolysis (pyrolytic gasification) can be applied to biomass in order to increase the gas yield where the increased temperature allows additional shrinkage of the biomass particle. It can be seen in Figure 49 that increasing the reaction temperature increases the gas yield at the expense of the organic yield. A review by Akhtar et al. reports that increasing temperature to greater than 600°C reduces the organic liquid yield and reduces the char yield [96]. However, liquid yield decreases more than that of char [96]. This is also supported by Scott et al. who report that char decreases with increasing temperature to an almost constant value above 650°C where devolatisation is almost complete and shrinkage of char particles slows down [98].

Aston University

Illustration removed for copyright restrictions

Figure 49: Effect of temperature on product yields from fast pyrolysis of wood (wt.% on dry feed basis) [97]

The hot vapour residence time is the time taken for the hot pyrolysis vapours to be cooled, condensed and collected as liquid bio-oil. This is reported to have an impact on the product quality and yield. High temperatures and longer hot vapour residence times are known to lead to secondary vapour cracking reactions which have a negative impact on the organic liquid yield, but are suitable for producing oxygenate free bio-oil [96]. Shorter hot vapour residence times maximise liquid yields and minimise char and gas yields [99]. Hot vapour residence times of less than 2 seconds are reported to be the optimum for fast pyrolysis [64].

Almost all of the ash present in the original biomass is retained in the char. The alkali metals present in the ash are reported to be catalytically active [8, 9] and so char removal from the vapour stream is critical in order to salvage the organic liquid product. In a fluidised bed system, char is separated by ejection and entrainment and then by cyclones.

Quenching of vapours is usually achieved by direct contact of pyrolysis vapours with an immiscible quench liquid. Hot pyrolysis vapours need to be rapidly cooled and collected to avoid secondary cracking reactions which lead to a reduction in the organic yield and effect the composition of the liquid bio-oil.

5.3 Feedstock variables

Feedstock type, moisture, ash and particle size have a direct impact on fast pyrolysis product yields and quality. The lignocellulosic composition of biomass determines the bio-oil composition. For example, biomass containing significant amounts of lignin is reported to decompose more slowly and therefore form large quantities of char under fast pyrolysis conditions. Also, high cellulose and hemicellulose content is expected to give higher liquid yields than lignin [95].

High moisture content feedstocks slow down the rate of biomass heating [96]. During fast pyrolysis, feed moisture and water from dehydration reactions are collected with the liquid bio-oil which lowers the bio-oil heating value [96]. Oasmaa et al. also report that phase separation of the bio-oil is likely to occur when the water content is greater than 30 wt.% [100]. Feedstocks with a considerably low moisture content are likely to produce a very viscous bio-oil with poor flow properties which is also undesirable. Bridgwater recommends a moisture content of less than 10 wt.% to limit the water collected in the liquid product and reduce the potential of phase separation [8].

It is reported that the alkali metals present in ash are responsible for secondary catalytically cracking reactions which can lead to increased water and gas production at the expense of organic liquid [8, 9]. It is also reported that biomass with ash content

greater than 2.5% causes phase separation of the bio-oil [8] and biomass with an ash content less than 2.5% gives a more homogeneous bio-oil. Abdullah et al. also reports that an ash content of less than 3 wt.% (dry basis) is necessary to avoid bio-oil phase separation [101]. However, ash composition can also affect bio-oil quality. For example, a feedstock with 5 wt.% ash may contain a large amount of inactive components which do not lead to catalytic cracking or bio-oil phase separation. Therefore, ash compositional analysis would be required to support this claim. Bridgeman et al. reports that milling and sieving can be used as a pre-treatment method to reduce ash content of biomass as ash content is lower with larger particle sizes [57]. Low ash feed is necessary in order to reduce the catalytic activity, maximise liquid yields and optimise liquid quality. Biomass composition varies depending on production environment and crop management [47]. Therefore, it is also important to carefully manage the biomass during harvest and preparation as any soil deposits could increase the ash content of the feedstock.

Pyrolysis yields are a function of particle size and this conclusion is supported by the work carried out by Scott et al. [102]. Biomass needs to be ground to ensure high heat transfer rates and minimise vapour diffusion through the catalytically active external char layer. Biomass also has a low thermal conductivity, which means that smaller particles are required to achieve high heating rates and short residence times. Large particles would not sufficiently thermally decompose in the short solid residence times which could limit the organic liquid yields. On the other hand, Bridgeman et al. reports that ash content increases with smaller particles [57], therefore processing of the smaller fraction was avoided in this work. Also, small particles are likely to entrain out of fluidised bed fast pyrolysis reactors and end up in the liquid product before being thermally degraded. Bridgwater recommends the optimum particle size is usually less than 2-3mm [72] [103]. However, milling and sieving was required as a pre-treatment method to reduce the ash content of each feedstock tested in this work

Densification of biomass can increase the throughput on a continuous fast pyrolysis unit. However, char yields from higher density ground pellets is expected to be higher than the char yields from loose biomass [104] because there is reduced shrinkage during pyrolysis of pellets and unreacted carbon remains as char.

5.4 Fast pyrolysis of biomass

Fast pyrolysis of a variety of biomass types has received much attention and has been reported in literature. The focus of this work is the product yields derived from fast pyrolysis of the Dibanet feedstocks i.e. miscanthus, sugarcane waste and acid hydrolysis residues (AHR).

Published data for the fast pyrolysis of miscanthus is available for cross checking liquid bio-oil yields. The characteristics and kinetics of the pyrolysis of miscanthus have been analysed by thermogravimetric analysis by Jong et al. [105] and Jeguirim et al. [106]. Yorgun et al. used a fixed bed reactor for fast pyrolysis of miscanthus and found that the highest bio-oil yield of 23.92 wt.% (dry ash free basis) was obtained at 550°C at a heating rate of 50°C/min [107]. When a fixed bed batch reactor is used for fast pyrolysis and char is not removed from the reactor, pyrolysis vapours pass through the catalytically active char layer and organic liquid yields are lower than expected from a continuous system. Also, the low heating rate of 50°C/min increases the time taken to reach processing temperature, therefore the sample is thermally degraded during the heat up stage. The increased reaction time decreases the liquid bio-oil yield, increases the gas and solid yield as with slow pyrolysis. Therefore, fixed bed reactors are not entirely representative of continuous fast pyrolysis processes.

Fast pyrolysis of miscanthus was carried out in a 150g/h continuous fluidised bed reactor at Aston University by Hodgson et al. [108] who reported a maximum total liquid yield of 61.31 wt.% from miscanthus (dry feed basis). Kalgo [92] tested miscanthus whilst upgrading the feeding system on a 300g/h continuous fluidised bed reactor at Aston University and reported a total liquid yield of 59.29 wt.% (dry feed basis) at 493°C. Results reported by Kalgo complement the work carried out by Hodgson et al. In both systems, char was removed by cyclones and collected in a char pot which is likely to have limited secondary catalytic cracking reactions. Therefore, total liquid yields of approximately 60 wt.% can be expected on a dry miscanthus basis.

Fast pyrolysis of sugarcane bagasse and in particular sugarcane trash, reported in literature, is limited. Drummond et al. investigated fast pyrolysis between 400-700°C in a wire mesh reactor. The maximum liquid yield was reported to be 54.6 wt.% (dry feed basis) at 500°C with a heating rate of 1000°C/s [109]. Keown et al. reported fast pyrolysis of sugarcane bagasse and trash using a quartz fluidised-bed/fixed-bed reactor. The reactor was fluidised, but a quartz frit was fixed in the reactor freeboard to prevent char elutriation hence creating a thin char bed. The focus of this work was on alkali metals and bio-oil liquid yields were not reported in this paper [110]. Lancas et al. pyrolysed up to 1g of bagasse, but it was reported that controlling the heating rate and hold time at the peak temperature proved to be problematic [111]. Stubington et al. studied pyrolysis kinetics of bagasse at high heating rates (200-10000°C/s) [112]. Ounas et al. also looked at the pyrolysis kinetics of sugarcane bagasse using TGA [113]. Several other researchers have conducted TGA studies with sugarcane bagasse. Asadullah et al. reports processing bagasse in a batch fixed bed unit with

maximum liquid yields of 66 wt.% at 500°C [114]. Asadullah et al. simply state that this liquid yield is on a bagasse basis. They do not report whether this yield is on a dry or wet basis. Tsai et al. report 50 wt.% liquid yield using a fixed bed reactor. As mentioned earlier, fixed bed reactors can have negative effects on the organic liquid yield from fast pyrolysis [115]. If high heating rates are used with a very hot vapour residence time as in a Py-GC-MS, results can be comparable to those obtained on a continuous fast pyrolysis system. However, systems such as Py-GC-MS cannot be used to approximate fast pyrolysis product yields and is of limited value in this work.

Although, sugarcane bagasse is widely available as waste from sugar mills, pelletising of bagasse is not yet common practise. Erlich et al. reported pyrolysis of whole SCBP in a large thermogravimetric analyser and as expected, reported that higher density pellets underwent less shrinkage resulting in higher char yields from pyrolysis [104]. A fluidised bed system with char removal could be used to reduce the catalytic cracking activity of char associated with batch systems such as TGA. Successful fast pyrolysis of sugarcane bagasse, sugarcane trash or ground SCBP have not previously been reported using a laboratory-scale continuous fluidised bed reaction system.

5.5 Fast pyrolysis of AHR

To better understand thermal processing of high lignin and humin content AHR, it is important to review existing techniques for processing lignin and humins. Lignin is a source of aromatic hydrocarbons for biofuel and chemical production [13] and valuable phenolic compounds. The aim of lignin pyrolysis is to increase the yield of phenolics compounds [81]. However, the liquid product can contain a combination of light liquids such as water, methanol, formic acid and acetic acid, lignin oil i.e. neutral compounds such as hydrocarbons and ethers, monomeric phenols such as phenols, guaiacols, syringols and catechols. Also, oligomeric phenolics such as dimers, trimers and tetramers are formed.

Fahmi et al. report that pyrolysis of lignin tends to produce an inhomogeneous and unstable liquid with a majority of the heavier weight compounds found in bio-oil [22]. They summarise that lower lignin content biomass increases bio-oil stability by reducing the chances of phase separation [22]. It is also speculated by Ghetti et al. that lower lignin content biomass produces a lighter pyrolysis product which can be considered a better bio-oil for fuel [116].

Ghetti et al. report that TGA can be used to determine the lignin content of a sample. TGA results were shown to be correlated with the lignin content determined by standard methods such as the van Soest method. However, lignin content can vary

depending on how the lignin or insoluble residue was obtained. For example, Ghetti et al. presents Klason lignin data for miscanthus as 21-22 wt.%, but only 6.4 wt.% lignin using the Van Soest method [116]. TGA is not representative of a fast pyrolysis system as it has longer hot vapour residence times, the heating rates are much longer and the process is not continuous. However, TGA is of importance as the volatile content of a sample can be used as an indication of the yields of liquids and gases produced during pyrolysis.

Previous studies carried out at Aston University showed that mainly phenolics are observed at higher temperatures [13, 117]. Phenolics are lignin derived which indicates that high lignin content residues will decompose at higher temperatures. Liquid yields from fast pyrolysis of biomass are reported to be maximised at 500°C. However, the yield of phenolics is reported to peak at 600 °C [117]. For this reason, there is a possibility that the AHR will not sufficiently decompose at lower temperatures producing significant amounts of char instead of organic liquid. Higher temperatures are required to break the C-C bonds found in lignin [117]. Lignin is not soluble in water which makes lignin depolymerisation and processing very difficult [10, 52]. A maximum of 60% biomass conversion is reported even at temperatures as high as 800-900°C [96]. Studies carried out by Sannita et al. also report that approximately 30–50 wt.% of lignin is reported to result as char from fast pyrolysis [81]. Higher proportions of hemi-cellulose and cellulose are observed to produce more liquid and gaseous products [12, 95]. This implies that a high lignin content feedstock will have negative effects on the organic liquid yields and produce more char compared to whole lignocellulosic biomass.

Previous work on lignin pyrolysis has been carried out using micro-scale reactors i.e. grid reactor, a microwave reactor, Py-GC-MS, fluid bed and fast fluidised twin bed reactors [13]. This is due to feeding and blockage problems associated with low melting point lignin [52]. Nowakowski et al. managed to a feed a few grams of lignin, but reported a low melting point for lignin (<180°C) and also reported that lignin was difficult to process in a system designed for pyrolysis of whole lignocellulosic biomass [52]. Pre-pyrolysis occurred in the inlet to a fast pyrolysis system and led to blockages. ECN used a water cooled screw feeder and reported 2 hours of operation in a fluid bed reactor at 400°C, but insufficient thermal degradation and low liquid yields are expected at such low temperatures. Higher reactor temperatures are likely to give lower cooling effect. However, ECN do not report any pyrolysis results at higher temperatures. Although a water cooled screw feeding system may overcome the feeding problem [118], agglomeration in the fluid bed is likely to lead to defluidisation.

Pyrolysis of humins has not been reported in literature. Pyrolysis of AHR has also barely been reported in literature. Huang et al. studied the pyrolysis of AHR derived from acid hydrolysis of corncob and pinewood [119]. They reported lower organic liquid yields and higher char yields compared to whole biomass. Huang et al. also reported that char yield increased as the lignin content of the original residue increased [119]. It is possible that humins were present these AHR, but no reference to humins was made in this paper.

Girisuta et al., who are also members of the Dibanet project, report the effect of different acid hydrolysis conditions (acid concentration, temperature and reaction time) on AHR and pyrolysis products [39]. These are the same AHR which are characterised in Chapter 3. This paper reports that milder acid hydrolysis conditions produce an AHR with a higher holocellulosic content which is preferred for pyrolysis as higher organic liquid yields can be achieved. However, the aim of the Dibanet project was to maximise levulinic acid production from biomass which involved hydrolysing the holocellulosic components leaving a significantly high lignin and humin content AHR.

After reviewing the literature, it is expected that pyrolysis of AHR will produce a high char yield [39]. Girisuta et al. report catalytic pyrolysis to deoxygenate bio-oil, but as a result, this further reduced the organic liquid yield from AHR [39]. For this reason, it is likely that an alternative thermal conversion process such as gasification should be the focus for deriving value added bioenergy and/or biofuels from AHR.

5.6 Bio-oil upgrading

The purpose of upgrading in this work is to produce a bio-oil that is miscible with diesel over a sufficiently wide range of concentrations to make it a commercially attractive product. This will also result in an improvement of properties such as a heating value, oxygen content, water content, viscosity and acidity. It is reported that bio-oil requires full deoxygenation for it to be miscible with conventional diesel [76]. However, biodiesel with 10-11 wt.% oxygen is miscible with diesel in almost any proportion [120, 121] so the necessary extent of deoxygenation of bio-oil is yet to be determined. There are several upgrading techniques available which include hydrodeoxygenation, emulsification, esterification and catalytic cracking of pyrolysis products, which are summarised below.

Hydrodeoxygenation uses moderate temperatures (up to 400°C), hydrogen and high pressures (70-200bar). The high pressure and hydrogen requirement is expensive and therefore unattractive [8] [122] [78]. The undesired oxygen is removed as H_2O or CO_2 [78]. Conventionally, crude oil derived fractions are hydrotreated with sulphided $CoMo/Al_2O_3$ and $NiMo/Al_2O_3$, but this route has been discredited due to hydrolysis of

the alumina-silicate support [63, 78]. This method is under active commercial development [123], but catalyst deactivation from coking needs to be overcome due to the poor C:H ratio [72].

Emulsification is described as the simplest technique where the bio-oil is combined directly with diesel using a surfactant [78]. However, it is considered a short term approach [63] as there are economical and corrosion issues associated with this technique [78] [63]. Heating value and cetane numbers were also unsatisfactory [63].

Another recent technique is esterification which uses alcohol and acid catalysts to make esters. Water content of less than 5 wt.% has been reported using sulphuric acid [124]. The properties are improved compared with original bio-oil [125].

The advantage of catalytic cracking over hydrotreating is that no hydrogen or pressure is required and so operating costs are reduced. Although, coke formation leads to shorter catalyst lifetimes with both hydrotreating and catalytic cracking [125], the coking problem is more prevalent with cracking catalysts [8]. Catalytic cracking of pyrolysis vapours involves dehydration, decarboxylation and decarbonylation reactions [126] over catalysts to remove oxygen and improve thermal stability. Hydrocarbon molecules are reduced in chain length [127]. Oxygen is removed as H_2O (dehydration is the main route) [126], CO_2, and CO at 450 °C and atmospheric pressure [76, 78]. Catalytic cracking is a leading technique [78]. However, Guo et al. reported that finding a "catalyst with good performance of high conversion and little coking tendency is demanding much effort" [78]. Catalytic pyrolysis of pyrolysis vapours is preferred to bio-oil upgrading as re-heating of bio-oil can be prevented.

A catalyst accelerates a reaction without changing in chemical composition. However, catalysts can be deactivated by coke formation which then needs continuous regeneration. The problem of deactivation may be overcome by burning off the coke and char on the catalyst surface as in an FCC (fluid catalytic cracking) unit in a refinery [128] with continuous catalyst regeneration [76, 128, 129]. An ideal catalyst should have high strength, high porosity (increased active sites), low pressure drop, minimum pore diffusion resistance, thermal/hydrothermal stability, long lifetime, high activity and high selectivity [130].

Shape selective, acidic and highly active cracking catalysts have been used to reject oxygen as carbon dioxide and water and yield mainly aromatic hydrocarbons. However, oxygen removal results in a reduced organic liquid yield [8]. Some of the cracking catalysts currently being investigated are Zeolites (ZSM5) [131-135], mesoporous aluminosilicates [136], nanopowder metal oxides [137], precious materials (such as platinum) [138], MCM41 [139] and titania [140]. Adjaye and Bakhshi have

found HZSM-5 as the most effective catalyst [134] where oxygen is rejected as CO_2 [73]. However, these catalytic tests were carried out using re-vapourised bio-oil which is not representative of a whole raw bio-oil vapour stream. The main focus for catalytic pyrolysis currently involves modifying existing catalysts to overcome the coking problem [141]. Hydrotreating catalysts such as CoMo and NiMo have previously been tested under fast pyrolysis conditions [142]. However, molybdenum carbide which has also shown to be quite active in oxygen removal in hydrotreating has noble metal behaviour and is expected to function like precious metals but without the cost and therefore could replace the rare and expensive noble metals [122]. Integrated catalytic pyrolysis using molybdenum carbide has been not previously been reported in the literature and the effect of this catalyst on pyrolysis products is interesting.

Table 20 summarises the advantages and disadvantages of the bio-oil upgrading techniques.

Table 20: Advantages and disadvantages of bio-oil upgrading techniques (derived from [143])

Upgrading method	Advantages	Disadvantages
Hydrodeoxygenation	• Commercialised already	• High pressures requirements • High hydrogen requirements • High costs • High coking • Poor fuel quality obtained
Catalytic cracking	• Makes larger quantities of light products	• Complicated equipment required • Excessive cost • Catalyst deactivation • Reactor clogging
Esterification	• Simple • Low cost of solvents • Reduces bio-oil viscosity	• Mechanisms in adding solvent are not quite understood yet • Solvents required
Emulsification	• Simple • Less corrosive • Product is diesel miscible	• High energy requirements • Short term approach • Economical and corrosion issues • Surfactants required • Unsatisfactory heating value and cetane numbers

Catalytic cracking of pyrolysis vapours is currently in research stages. This upgrading technique seems promising and should be investigated further. There are several possible configurations of introducing catalyst to the existing fast pyrolysis process as shown in Figure 50.
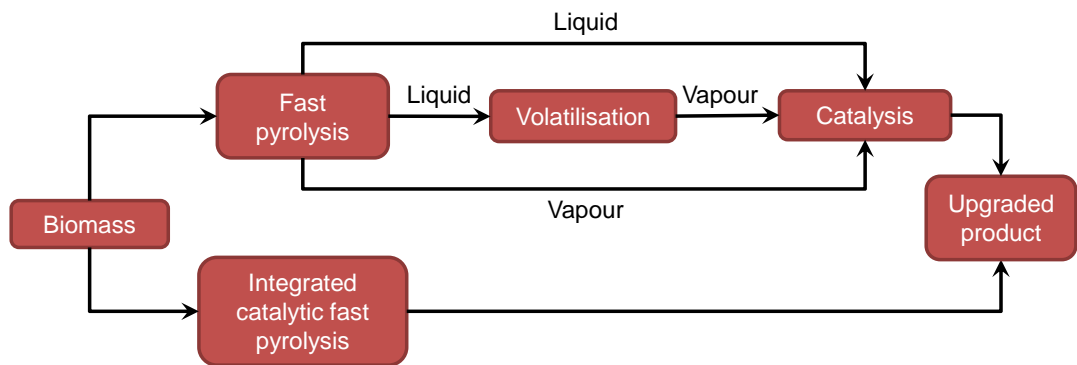
Figure 50: Catalytically cracking of fast pyrolysis products (adapted from [73])

Biomass naturally contains very catalytically active ash [72]. Direct contact of the alkali metals (present in the ash) with catalysts can be problematic, therefore reaction system configuration is critical. Integrated catalytic fast pyrolysis has been carried out by numerous researchers, but have had limited success due to catalyst coking. Incorporating catalysts into the pyrolysis reactor limits the process to a single temperature and also requires continuous catalyst regeneration due to the presence of char from pyrolysis [73]. CPERI (Greece) has used a circulating fluidised bed reactor using zeolites and mesoporous catalysts for upgrading [128], but there was incomplete deoxygenation [73]. Figure 51 shows configurations where the char particles produced from fast pyrolysis have direct contact with the catalyst using an integrated system. The char would deactivate the catalyst quickly and currently, it is difficult to regenerate catalysts. Burning off the char is an option, but this can also thermally degrade the catalyst. Also, as a result of the configurations in A and B, catalyst particles can end up in the bio-oil.
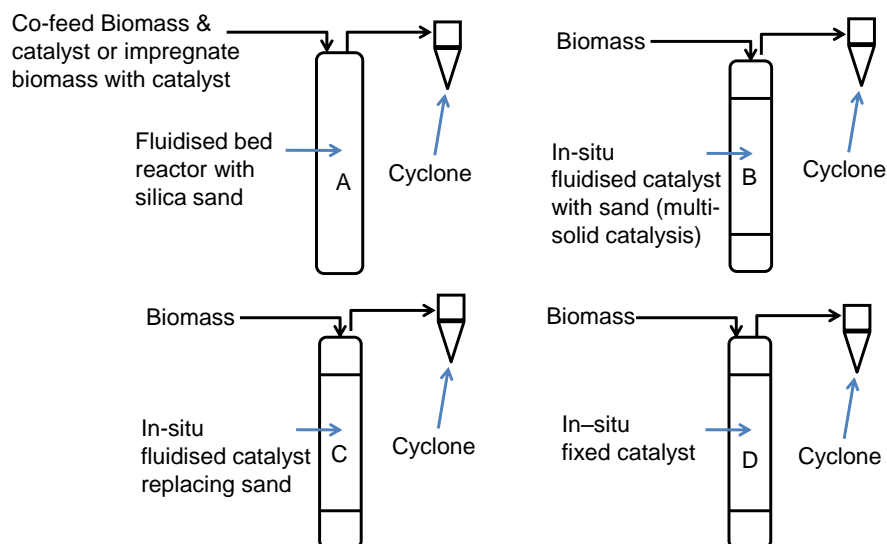
Figure 51: Integrated catalyst pyrolysis (adapted from [142])

Decoupled liquid bio-oil upgrading involves upgrading liquid bio-oil. It has been researched using zeolite catalysts at University of Pisa (Italy) in 2000 [126, 132] and at the University of the Basque Country (Spain) in 2004 [144, 145]. Another technique using catalysts to upgrade bio-oil has also been investigated by Adjaye and Bakhshi

[146]. It involves decoupled upgrading of revapourised bio-oil. However, condensing vapours from fast pyrolysis and then re-vapourising them not only requires a lot of energy, but is not efficient as no more than 50% of bio-oil can be vapourised [147]. Also, the revapourised oil is not representative of a whole raw bio-oil vapour stream.

Reviews by Bridgwater summarise the organisations which have carried out close coupled vapour upgrading [72] [73]. Figure 52 to Figure 54 shows a secondary close coupled catalytic reactor configuration in which the catalyst can be introduced after char separation. Promising catalysts, which are susceptible to coking, (such as zeolites) could be tested in a secondary close coupled catalytic reactor. It is also more flexible as the temperature of the close coupled reactor is independent of the fast pyrolysis temperature (450-600°C).
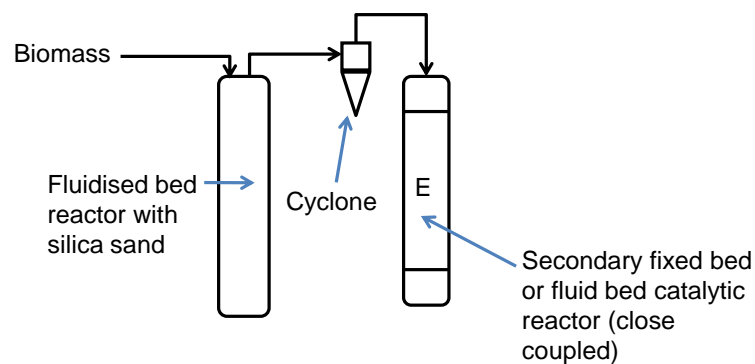
Figure 52: Close coupled secondary fixed bed catalytic reactor

Multiple or sequential reactors (see Figure 53) are also an option, but would increase the hot vapour residence time and may reduce the liquid yield and quality. Secondary reactors would need to be close coupled in order to keep the residence time low as in fast pyrolysis. The use of secondary reactors also leads to additional costs.
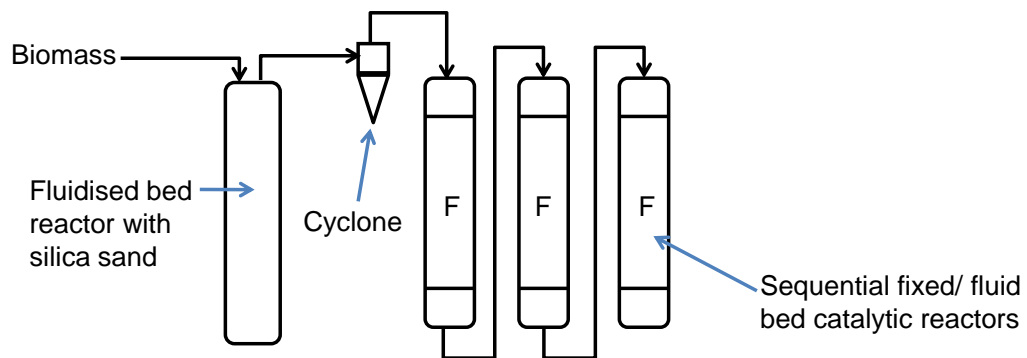
Figure 53: Sequential fixed bed catalytic reactors

Figure 54 shows catalysts replacing the fluidised bed material with an additional secondary close coupled catalytic reactor.
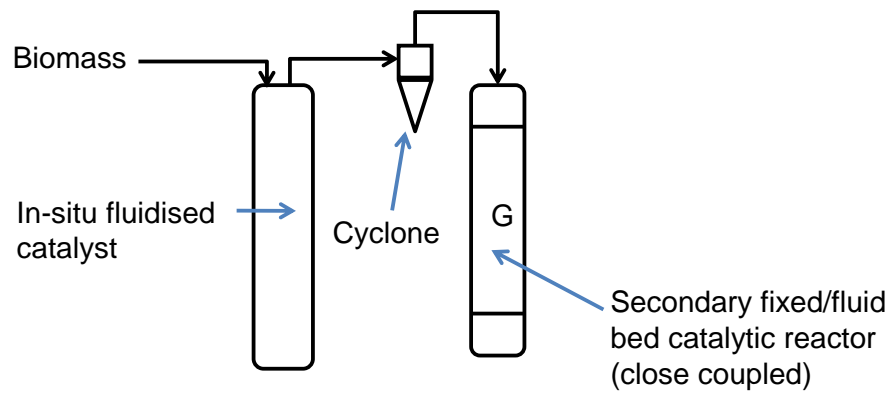
Figure 54: Sequential catalytic upgrading

Table 21 summarises the advantages and disadvantages of the various configurations of catalyst incorporation for catalysis of pyrolysis vapours.

Table 21: Advantages and disadvantages of various catalyst incorporations

Configuration		Advantages	Disadvantages
Integrated upgrading	Co-feed catalyst with biomass	Better contact between catalyst and reactants.	Limits the process to a single temperature and also requires continuous catalyst regeneration due to the presence of char from pyrolysis Catalyst particles can end up in the bio-oil
	Impregnate catalyst into biomass	Better contact between catalyst and reactants.	Limits the process to a single temperature and also requires continuous catalyst regeneration due to the presence of char from pyrolysis Catalyst particles can end up in the bio-oil
	In-situ catalysis with sand (multi-solid catalysis)	There is better temperature control within the reactor. Prevents cold and hotspots. Better heat transfer.	Limits the process to a single temperature and also requires continuous catalyst regeneration due to the presence of char from pyrolysis Catalyst need to be robust as sand could erode the catalyst
	In-situ catalysis replacing sand	The catalyst can also act as a heat carrier.	Limits the process to a single temperature and also requires continuous catalyst regeneration due to the presence of char from pyrolysis
	In-situ fixed bed catalysis	Better contact between catalyst and reactants.	Limits the process to a single temperature and also requires continuous catalyst regeneration due to the presence of char from pyrolysis Poor heat transfer
Close coupled upgrading	Secondary fixed bed catalysis	Can operate the catalysis at lower temperatures. Catalysts with various optimum temperatures can be used.	Increases the residence time and may reduce the liquid yield. Secondary reactors would need to be close coupled in order to keep the residence time low as in fast pyrolysis (<2 seconds). Additional reactors incur additional costs to the process.
	Secondary fluid bed catalysis	Can operate the catalysis at lower temperatures. Catalysts with various optimum temperatures can be used.	Increases the residence time and may reduce the liquid yield and quality. Secondary reactors would need to be close coupled in order to keep the residence time low as in fast pyrolysis (<2 seconds).Additional reactors incur additional costs to the process. Complex designs required compared to a fixed bed reactor.
Sequential	In-situ catalysis and close coupled upgrading	Multiple catalysts can be used to upgrade the bio-oil at different temperatures.	Coking of catalyst. Complex process with additional costs.

5.7 Interim conclusions

- Liquid yields from fast pyrolysis can be maximised with a reaction temperature of 500°C and hot vapour residence time of less than 2 seconds.

- Biomass with less than 10 wt.% moisture is recommended to limit the water collected in the liquid product and reduce the potential of phase separation.

- Removal of small particle sizes can lower feed ash content to reduce the catalytic activity, maximise liquid yields and optimise liquid quality.

- Maximum particle sizes of 2-3mm should be used to achieve high heating rates and short residence times.

- Fast pyrolysis of high bulk density feedstocks gives higher char yields than lower bulk density feedstocks.

- Total liquid yields of approximately 60 wt.% (dry feed basis) can be expected from miscanthus.

- Successful pyrolysis of sugarcane bagasse, sugarcane trash or ground SCBP has not been reported using a laboratory-scale continuous fluidised bed reaction system.

- Higher organic liquid yields can be achieved from fast pyrolysis of higher holocellulosic content feedstocks.

- Lignin has a low melting point (<180°C). The melting point of humins is unknown.

- Fast pyrolysis of lignin will produce an inhomogeneous and unstable liquid and a high char yield (approximately 30–50 wt.%).

- Fast pyrolysis of humins has not been reported in literature.

- Fast pyrolysis of AHR produces a lower organic liquid yield and higher char yield compared to whole lignocellulosic biomass.

- Currently bio-oils do not meet the requirements of a transportation fuel and so require deoxygenation before being accepted commercially.

- Catalytic pyrolysis of pyrolysis vapours seems a promising approach for deoxygenating bio-oil as long as catalyst deactivation can be overcome.

- Integrated catalytic pyrolysis using molybdenum carbide has been not been reported in the literature and the effect of this catalyst on pyrolysis products is interesting.

- The most promising catalytic upgrading technique would involve condensing the vapours after catalysis in order to avoid the need to re-vapourise the bio-oil. It is likely that catalytic pyrolysis will need to be carried out in multiple steps in order to satisfactorily upgrade the bio-oil.

6 FAST PYROLYSIS OF BIOMASS

The objective of this chapter is to describe all continuous fast pyrolysis rigs available at Aston University and detail product characterisation methods used for fast pyrolysis processing. One objective of this chapter was to screen feedstocks by comparing feedstock throughput, product yields and characteristics on the smaller bench-scale fast pyrolysis units, such as the 100g/h and 300g/h rigs. Product yields and characteristics using the interchangeable collection systems on the 300g/h rig were subsequently compared. Liquid collection systems with poor liquid recovery lead to poor mass balance closures and so methods in overcoming mass balance issues are discussed in detail. Product yields and characteristics obtained from the 300g/h and 1kg/h rigs using the highest liquid yielding feedstock were compared to investigate the scalability of the 300g/h rig. Finally, the promising feedstock was then compared with beech wood where liquid yields as high as 75% (dry feed basis) are reported [72].

6.1 Fast pyrolysis units

Four continuous fast pyrolysis units are available with a biomass processing capacity of 100g/h, 300g/h, 1kg/h and 7kg/h. The 100g/h and 300g/h rigs are set up on laboratory benches and have interchangeable liquid collection systems which are a glass collection and a quench collection system. The 1kg/h and 7kg/h are stand-alone units with quench collection systems which are more representative of the liquid collection systems used on a commercial scale. Table 22 shows the strengths and weaknesses of these fast pyrolysis reaction systems.

Table 22: Strengths and weaknesses of reaction systems available at BERG

Rig	Strengths	Weaknesses
100g/h	• Good mass balance as all equipment can be weighed when using the glass collection system including the reactor • Small sample sizes require little preparation • Easy to clean • Interchangeable collection systems	• Fibrous biomass cannot be pneumatically fed due to blockages • Limited processing capacity • Small volumes of bio-oil limiting analysis
300g/h	• Screw feeder to easily feed the biomass • Easy to clean • Interchangeable collection systems	• Limited processing capacity • Small volumes of bio-oil limiting analysis
1 kg/h	• Larger bio-oil samples • Long runs possible up to 8h • Hot vapour filter available	• Large quantities of feed which need preparation • Requires additional labour • Cleaning is more difficult
7 kg/h	• Larger bio-oil samples • Computer controlled • More representative of full scale plant	• Large quantities of feed which need preparation • Requires additional labour • Cleaning is more difficult

The larger 7kg/h system was not used in this work as large quantities of feed were not available from the Dibanet project. The methodology adopted for the 100g/h, 300g/h and 1kg/h continuous units are discussed in more detail in section 6.2.

6.2 Fast pyrolysis methodology

All fast pyrolysis experiments were carried out at approximately 500°C where liquid yields are reported to be maximised. A good mass balance is necessary to ensure all products are accounted for and losses are minimised. Therefore, a successful fast pyrolysis run was defined as having a mass balance of approximately 95 wt.%, 50 wt.% liquid yield from high ash feed and 65 wt.% liquid yield from low ash feed (on a dry feed basis). The experiments should also be run for one hour to ensure no agglomeration or blockages would occur. The reactor bed was considered successfully fluidised when there was very little char retained in the reactor at the end of an experiment.

6.2.1 100g/h

The 100g/h rig (as shown in Figure 55 and Figure 56) was developed using the Waterloo Fast Pyrolysis Process (WFPP) [71]. The 100g/h rig has biomass processing capacity of 100g/h. The 100g/h and 300g/h rigs have interchangeable collection systems. The glassware collection is most commonly used with the 100g/h rig as the lower volumes of liquid produced cannot be sufficiently quantified in a quench column. The quench column is discussed later in section 6.2.2.
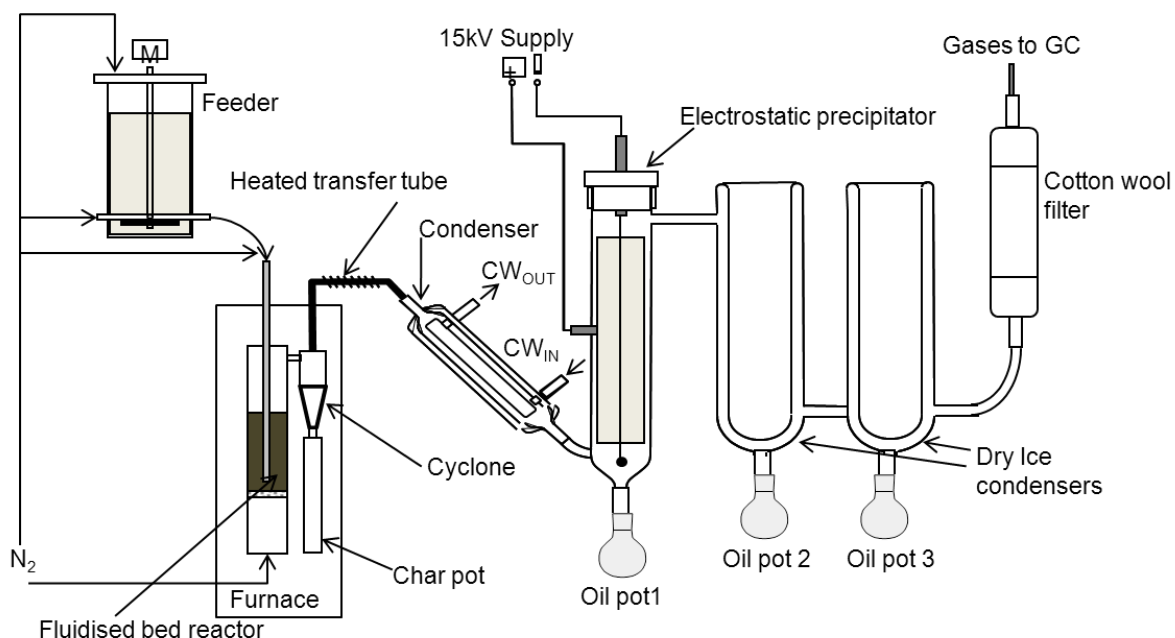
Figure 55: Flowsheet of 100g/h continuous fluid bed reaction system
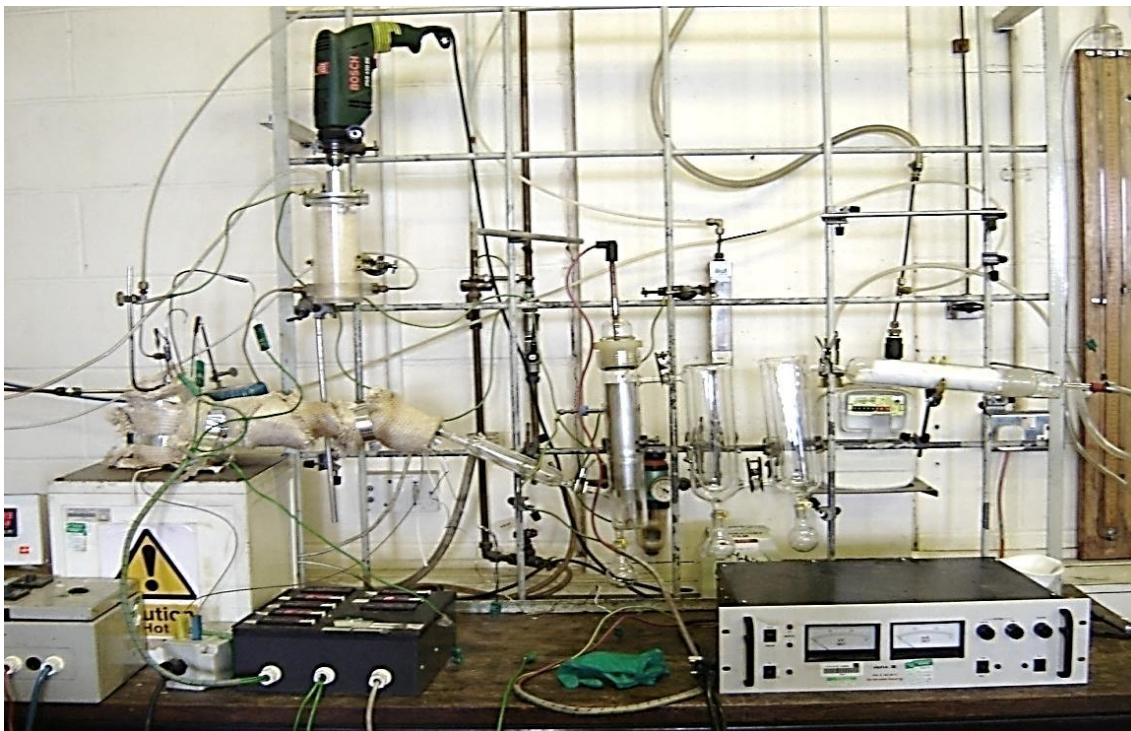
Figure 56: 100g/h continuous fluid bed reaction system

The pneumatic feeder used on the 100g/h rig consists of a clear Perspex tubular hopper, a stirrer and an entrainment tube. Pattiya [148] replaced the original feeding tube (2mm internal diameter) with a larger feeding tube (3.28mm internal diameter) to reduce blockages caused by needle-like or very fine biomass particles. The stirrer speed and nitrogen flow rates were set to control the biomass feed rate directly into the top of the reactor according to the biomass properties. Biomass particle sizes of 0.355-0.5mm could usually be successfully fed into this system.

The 100g/h reaction system consists of a 316 grade stainless steel bubbling fluidised bed reactor with a 260mm length and 40mm internal diameter [148]. Sand was used as the heat transfer medium. The fluidised bed and freeboard temperature were recorded. The cyclone is welded onto the reactor where char is separated and collected in a detachable char pot. The entire reaction system, cyclone and char pot are placed in an electrically heated furnace and insulated to regulate the temperature and minimise heat loss. A transfer tube from the cyclone to the liquid collection system was trace heated to around 450°C to ensure pyrolysis vapours did not cool in the pipes and create blockages. Also, temperatures higher than 500°C lead to secondary cracking reactions which significantly reduce the organic liquid yield.

An ideal collection system should condense pyrolysis vapours rapidly with no effect on the bio-oil composition. The glassware collection system gives a good mass balance of approximately 95 wt.% as all of the rig components, including the reaction system, can be weighed. Also, there is no contamination of products as no quench liquids are used. This collection system has a glass water condenser to condense

pyrolysis vapours, an electrostatic precipitator (voltage at 15 kV and current at 0.5 A) to collect aerosols, two dry ice-acetone condensers (with temperatures as low as -20°C) to condense the light liquid fractions. A cotton wool filter was used to improve the mass balance and avoid any carry over in the gas meter and MicroGC which followed. A negatively charged wire passing through the middle of the ESP charges the aerosols which are then deposited on the positively charged stainless steel plate. This collection system collects a fractionated liquid product. The deposits in the ESP and water condenser run as mobile liquid and collect in oil pot 1 which was referred to as bio-oil. There are two further collection pots which collects the secondary condensates. Some heavy organic liquid remain in the glass water condenser and on the walls of the ESP which reduce the HHV of the bio-oil collected in oil pot 1. Ethanol washings and subsequent rotary evaporation would recover deposits on the walls of the water condenser and ESP. This transparent glassware collection system was ideal to see when pyrolysis vapours had stopped and when all of the liquid has been recovered compared to stainless steel material of construction.

The 100g/h rig was used for fast pyrolysis of untreated beech and acid hydrolysis residues (AHR) from beech as AHR from levulinic acid production were not available in the early stages of the project. Untreated beech with a moisture content of 7.25 wt.% and an ash content of 0.78 wt.% was fast pyrolysed in the 100g/h reactor at approximately 500°C with a feeding rate of 66g/h. The experiment was run for 110 minutes.

The mass of char, liquid and gas were quantified to carry out a mass balance. The mass of char was the sum of the mass gain on the sand in the reactor, in the char pot, transition pipe and glass transition pipe. Fine char particles ended up in the liquid product as particles <10μm could not be efficiently removed from the vapour streams by the cyclone. The bio-oil solid content was measured to correctly quantify the char yield. Also, the presence of solids is reported to lead to aging of bio-oil, sedimentation, filter blockage, catalyst blockage and engine injector blockage [73]. Bio-oil solid content was determined by ethanol washings of the glass condenser and ESP and the filtering of the ethanol solution using vacuum filtration. The solid mass gain of the dried filter paper was taken as a portion of the total liquid collected in those rig components.

The mass of liquid was the sum of the mass gain on the water condenser, ESP, 2 dry ice condensers, 3 oil pots and cotton wool filter. The solid content measured from the ethanol washings of the ESP and water condenser was excluded. The water content of bio-oil has a complex effect on viscosity and stability. Increased water lowers HHV, density, stability and can also affect catalysts. However, water increases pH [73]. The total water content is also measured to complete mass balance calculations and

determine organic liquid and reaction water yields. Total water content of the liquid is a sum of the water in the feed and the reaction water. The total water minus the water in the feed is regarded as the reaction water. The total liquid minus the total water is the total organic liquid. A Mettler Toledo V20 volumetric Karl-Fisher titration system was used to determine the bio-oil and condensates water content. The system was calibrated using Hydranal water standard. Hydranal working medium K was used as the solvent and Hydranal Composite 5K as titrate. All Karl Fischer analysis was carried out in triplicate to check reproducibility.

The total volume of gas was measured by the gas meter and gas composition was analysed by the MicroGC. The mass of non-condensable gas, produced in the pyrolysis process, was subsequently calculated on a nitrogen-free basis. More details can be found later in section 6.2.4.

Equation 2 was then used to calculate the product recovery.

Equation 2: Calculating product recovery

$$\text{Recovery} = \frac{\text{Total mass out (solid, liquid and gas)}}{\text{Mass of feed in (dry feed basis)}} \times 100$$

Beech was successfully pyrolysed, but there were feeding problems with AHR using the pneumatic feeding system at the beginning of the project. The feeder tube and the sand fluid bed blocked within ten minutes. The blockage was expected to be due to agglomeration of char in the top of the feeding tube or the particles may have been too dry and static in the feeder. The two experiments did not run long enough and so very few results were recorded. Also, from previous experience [149], bagasse cannot be pneumatically fed into the 100g/h rig. It was concluded that the 100g/h rig would not be used for processing low bulk density, fibrous feedstocks such as sugarcane bagasse or AHR. These initial experiments were useful in training and feed testing various feedstocks. Feeding such feedstocks into the top a fluidised bed reactor can be problematic. Ideally, biomass should be fed directly into the fluidised bed for improved heat transfer and mixing to reduce agglomeration. Therefore, further fast pyrolysis work was carried out using the 300g/h rig.

6.2.2   300g/h rig

The 300g/h bubbling fluidised bed reaction system has the same fast pyrolysis principles as the 100g/h rig. However, this rig has an improved screw feeding system which can deliver more fibrous and difficult to feed biomass types into the side of the reactor and directly into the hot sand bed. The 300g/h system can run at approximately half of its biomass processing capacity and feed rates of approximately 200g/h have been achieved in this work. Throughput strongly depends on the biomass density as

narrow piping can limit the biomass feed rate. The feeding system consists of a tubular storage hopper, a K-Tron K-ML-KT20 gravimetric screw feeder and a water cooled fast screw. The water cooling helps minimise pre-pyrolysis in the screw casing therefore avoiding blockages. The fast screw speed needs to be carefully controlled so that biomass does not accumulate before entering the reactor.

The stainless steel tubular reactor has a 335mm length and 40mm internal diameter. A sintered Inconel distribution plate is situated 50mm from the reactor bottom with a 3mm thickness and an average pore size of 0.1mm [92]. A centred fluidising gas inlet at the reactor bottom allows an upward stream of pre-heated nitrogen through a fluidising sand bed. A Watlow Starflow circulation pre-heater (power of 800 W) pre-heats the fluidising nitrogen up to 650°C to keep the reactor bed temperature stable. Additional nitrogen enters the reactor at room temperature through the screw feeder to aid biomass feeding and prevent sand from the reactor bed flowing back through the screw. The nitrogen from the feeder and fluidising line combined is considered as the total nitrogen available for fluidising the reactor bed.

Two Watlow ceramic knuckle band heaters (800 W and 500 W respectively) are used to heat the reactor up to a maximum of 650°C. 150g of quartz sand was used as the fluidising medium with a typical particle size of 0.5-0.6mm. The reactor was thoroughly insulated to maintain a uniform temperature across the reactor and avoid hot or cold spots. Char is separated using a cyclone and collected in a char pot. An additional cyclone and char pot can be added to this reactor configuration if high ash feedstocks are being processed. However, one cyclone and char pot was sufficient in this work. Heating tapes were used to heat the transition pipe between the reactor and water condenser to ensure pyrolysis vapours did not cool in the pipes and create blockages.

K-type thermocouples were used to monitor the reactor bed, freeboard, heating tape and pre-heater temperatures. The pre-heater, reactor bed and trace heater temperatures were controlled by a Watlow temperature control unit. The pressure drop across the reactor bed and the pressure in the transition pipe were also monitored to identify blockages throughout each experiment. The fluidising gas and feeder gas were controlled and set depending on the nature of the feedstock. A high bulk density feedstock such as ground sugarcane bagasse pellets (SCBP) requires higher fluidising gas velocity (0.744m/s) compared to lower bulk density feedstocks such as sugarcane bagasse (0.507m/s). As discussed in section 3.3, feedstocks particle size in the range of 0.25 to 1mm was used. The cooling water flowrates for the fast screw and the water condenser were also controlled.

The liquid can either be collected by a glassware collection system or a quench column. These two systems are interchangeable on the bench scale rigs as shown in Figure 57. However, the quench collection system is usually only used with the 300g/h rig as the lower volumes of liquid produced from the 100g/h rig cannot be sufficiently quantified in a quench column.
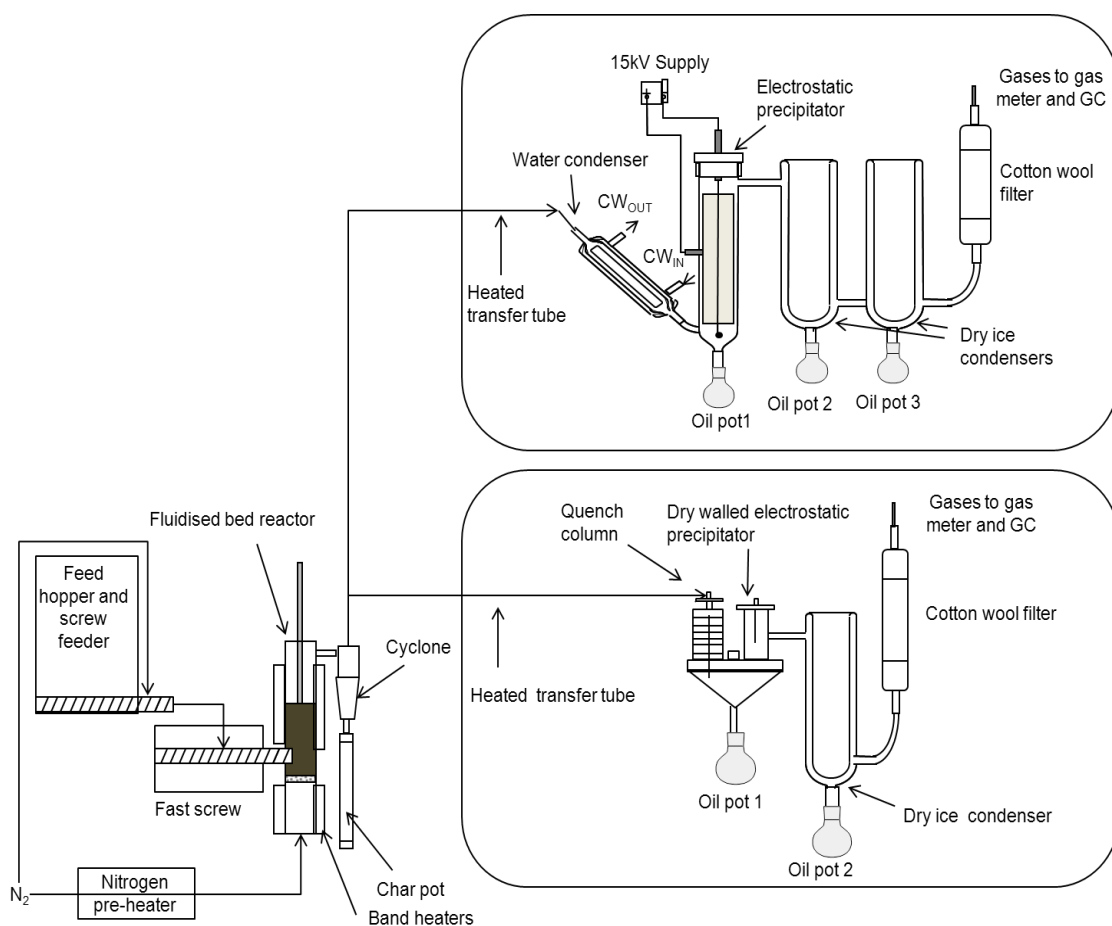
Figure 57: Flowsheet of the 300g/h rig with interchangeable collection systems

The glass collection system as detailed in section 6.2.1 was also used on the 300g/h rig. The set-up is shown in Figure 58.
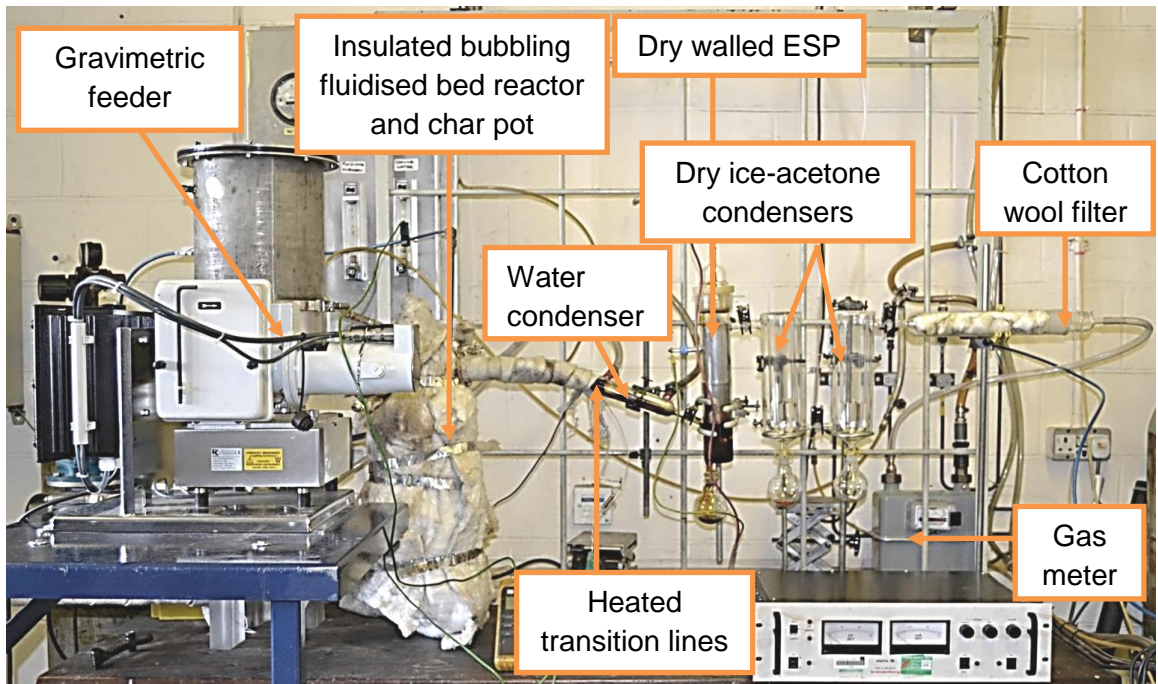
Figure 58: Glassware collection system

Screening was carried out using the 300g/h rig with glassware collection system to identify the most promising feedstock which would be processed using a quench column and then scaled up on the 1kg/h rig. Comparison tests were carried out with the quench collection system as it produces a whole bio-oil and is more representative of a commercial process. This set-up had a disc and doughnut quench column and a dry-walled electrostatic precipitator. Figure 59 shows the quench collection system where pyrolysis vapours have direct contact with Isopar to cool and collect as bio-oil. A cooling water jacket also enhances the cooling effect. More details about this particular quench column can be found in the work carried out by Kalgo [92].
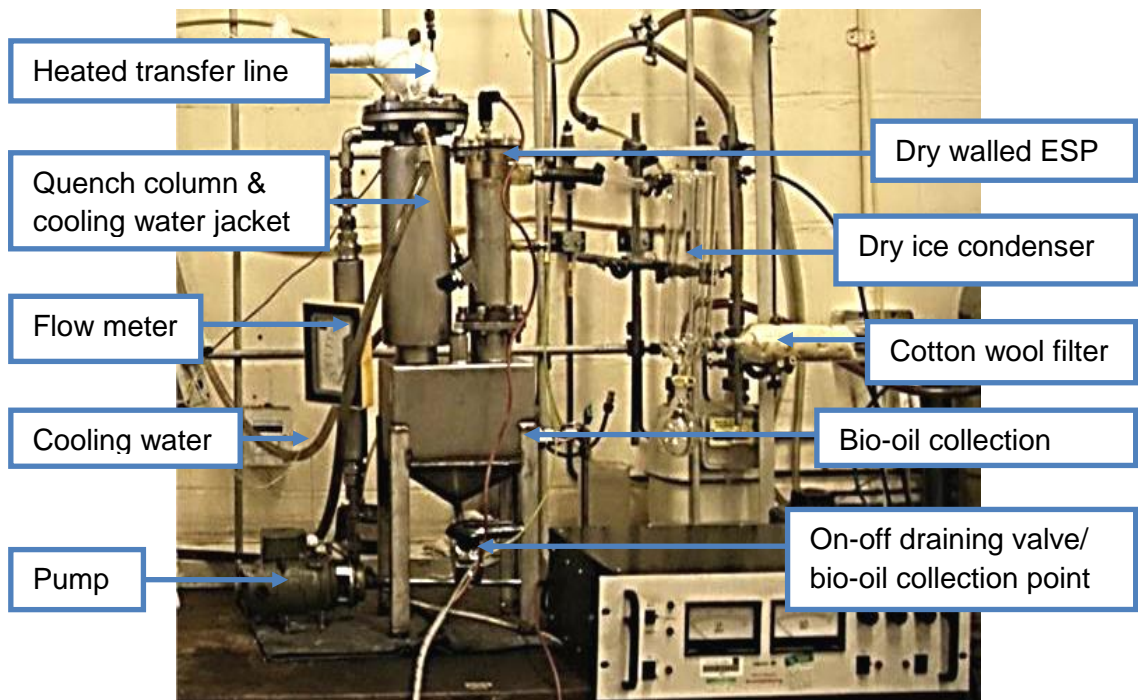
Figure 59: 300g/h rig with quench collection system

An ideal collection system should rapidly cool and condense pyrolysis vapours with no effect on the bio-oil composition and if a quench liquid is used, should be immiscible with bio-oil. Isopar V is a colourless liquid, supplied by Multisol Limited, consisting of saturated branched hydrocarbons with a boiling range between 270°C-320°C. Non-polar hydrocarbons such as Isopar are immiscible with polar water and bio-oil. For this reason, Isopar, which is a commercial name for isoparaffin, was used as a quench liquid. Li et al. [150] and experimentation carried out at Aston University showed that the use of Isopar as a quench liquid has little or no effect on the composition of bio-oil. Pyrolysis vapours enter the quench system through a transfer line which was heated to approximately 450°C to ensure the pyrolysis vapours did not cool prematurely leading to blockages. This also ensured that the entire product collected before the quench system was char. Approximately 2 litres of clean Isopar was filled in this quench column. There were 19 discs with 6 holes on each disc on the quench plates.

The Isopar and bio-oil mixture was collected in a bio-oil collection tank below the quench column and ESP. Higher density bio-oil (approximately 1.2kg/l) sank to the bottom of the tank while the lower density Isopar (0.819kg/l) floated on top of the bio-oil. Recycled Isopar was pumped around the quench column. The lighter fractions of phase separated bio-oil may float in the tank and enter the pump resulting in bio-oil deposits in the pipe work and on the pump impellor. Therefore, after each experiment, thorough cleaning with solvents such as ethanol was required to maintain the quench system.

The mass balance calculations for the 300g/h rig using the glassware collection system are similar to those for the 100g/h as mentioned in section 6.2.1. However, the 300g/h reactor cannot be physically weighed. Removing this reactor would require time-consuming disassembling of the reactor from the screw feeding system and removal of the two knuckle band heaters. Instead, the reactor contents were removed using a vacuum cleaner and the mass gain in the vacuum bag was associated with char and the 150g of sand. After feeding was stopped, the experiment was completed when there were no pyrolysis vapours visible in the collection system indicating that any mass gain in the reactor was due to char and not unpyrolysed biomass.

All of the quench system components cannot be disconnected and physically weighed which posed a challenge when trying to do a mass balance over the quench column. The quench system was also too heavy to physically carry and clean. The quench column was welded on top of the collection tank so could not be removed to be weighed. Only the ESP and the quench plates were detachable. The ESP is currently made of plastic, which over time, cracks after washing with organic solvents. The ESP

on this quench system cannot be made of glass as the fittings would crack the glass. There was approximately 40g of liquid holdup in the quench system when the pipework was disconnected and each component was carefully weighed. Modifications to the quench system were required to improve mass balances. The following problems with the quench exist and solutions have been given in Table 23.

Table 23: Proposed solutions to problems on the quench column

Problem	Possible solutions	Practicality
Estimating/reducing the severity of holdup on the quench column	The quench column is currently made of stainless steel which is not transparent so we cannot visually estimate the severity of the holdup. Using another transparent material such as plastic or glass is an option.	The bio-oil is dark and is expected to line the transparent material and create difficulties in seeing through the column after a run. Glass is also difficult to scale up and can break easily. Plastic can crack over time after washing with organic solvents.
	Unbolt the quench plates and weigh the plates before and after a run.	The bio-oil could spill when removing the plates so this needs to be done carefully.
	Reducing the number of quench plates or removing all of the quench plates	This can reduce the efficiency of quenching and lead to fouling
	Increasing the size of the holes will allow a longer run time as the increased free flowing area will slow down clogging.	This can reduce the efficiency of quenching
	Pumping Isopar at higher flow rate could prevent the settling of particles in the quench.	Too high flow rates of Isopar would flood the column.
	The current balance is not accurate enough. A balance to measure the quench system (up to 20kg) with 1g accuracy would be ideal.	The balance is very expensive.
	Load cells on the bench under the quench system would mean the quench would not need to be moved.	The load from the transition pipes is unknown; however, if build-up of char in the transition pipe is negligible then mass gain can be associated with the bio-oil produced in the quench system. This could be expensive.
	Pump ethanol through system after draining Isopar and bio-oil	Produces waste ethanol, but ethanol is used for cleaning anyway. Ethanol can be evaporated using rotary evaporation.
	Two sequential runs. The first run should fully load the quench plates with bio-oil and the holdup is expected to be small in the second run. The plan is to do one fast pyrolysis run for as long as possible, do a mass balance and empty char pot, repeat the run with same feedstock and	It is difficult to tell when the plates are fully loaded with bio-oil. The quench column still cannot be weighed accurately enough as it is not detachable.

Problem	Possible solutions	Practicality
	conditions, then do another mass balance.	
	Use a spray nozzle	Nozzles may block from fouling depending on feedstock.
Too heavy to physically carry the quench column	The quench column may be modified by adding a flange to the bottom of the column so the column can be removed for cleaning and weighing.	This is a good solution.
Isopar miscibility with catalytically upgraded products	Quench with bio-oil, but if using a viscous bio-oil (such as that from SCBP) then a better pump is required.	This requires bio-oil to already be produced.
Deposits on wall of ESP	A wet walled ESP would overcome deposits on the wall by a flow of Isopar down the ESP wall.	Problems with miscibility with catalytically upgraded products.
Mass balance < 95%	A longer run will improve the mass balance	This is a good solution. Increase the run time to 2 hours instead of 1 hour.

Pumping ethanol through the quench column was the most promising and practical technique to overcome the holdup problem and obtain a better mass balance closure. The ethanol dissolved the deposits on the walls, quench plates, in the pipe work and pump at the same time. Bio-oil deposits on the pump became sticky over time and caused the pump impellor to turn slower or not at all. Also, bio-oil build up in the pipe work led to blockages. Pumping ethanol for approximately 10 minutes at high flowrates was shown to effectively clean and maintain the quench system. The mass gain of ethanol washings was not measured as ethanol evaporated. Instead, rotary evaporation would ideally be used to speed up evaporation of ethanol and leave a bio-oil and Isopar residue which can be weighed.

6.2.3   1kg/h rig

The 1kg/h rig (see Figure 60 and Figure 61) consists of a tubular hopper connected to a K-Tron screw feeder. The metering screw speed can be set to determine the feed rate before commencing feeding. The 1kg/h rig has a stainless steel reactor with a total length of 1020mm. This length consists of the pre-heating zone at the bottom which heats the fluidising nitrogen before it enters the fluidised bed, the reaction zone in the middle and the disengagement zone at the top of the reaction system. The reaction zone internal diameter is 75mm. 35l/min of cold nitrogen was pre-heated and used to fluidise the larger sand particle size (0.6-0.71mm) in the reaction zone. The sand bed sits above a 4mm thick distribution plate which is situated 80mm above the pre-heated zone. The feed inlet is 100mm above the distribution plate and allows biomass to be fed directly into the hot sand bed. This rig has two cyclones and two char pots where most of the char is collected in char pot 1. The collection system consists of a quench column and a wet-walled electrostatic precipitator where 14 litres of Isopar is pumped around both liquid collection components. A cooling water jacket

on the quench column enhances the cooling effect. A wet walled electrostatic precipitator provides better collection than dry walled as Isopar is pumped through to remove and collect deposits on the ESP walls. The cotton wool filter was also combined with silica gel to absorb moisture from the product gas and also collect any residual tars in the gases.
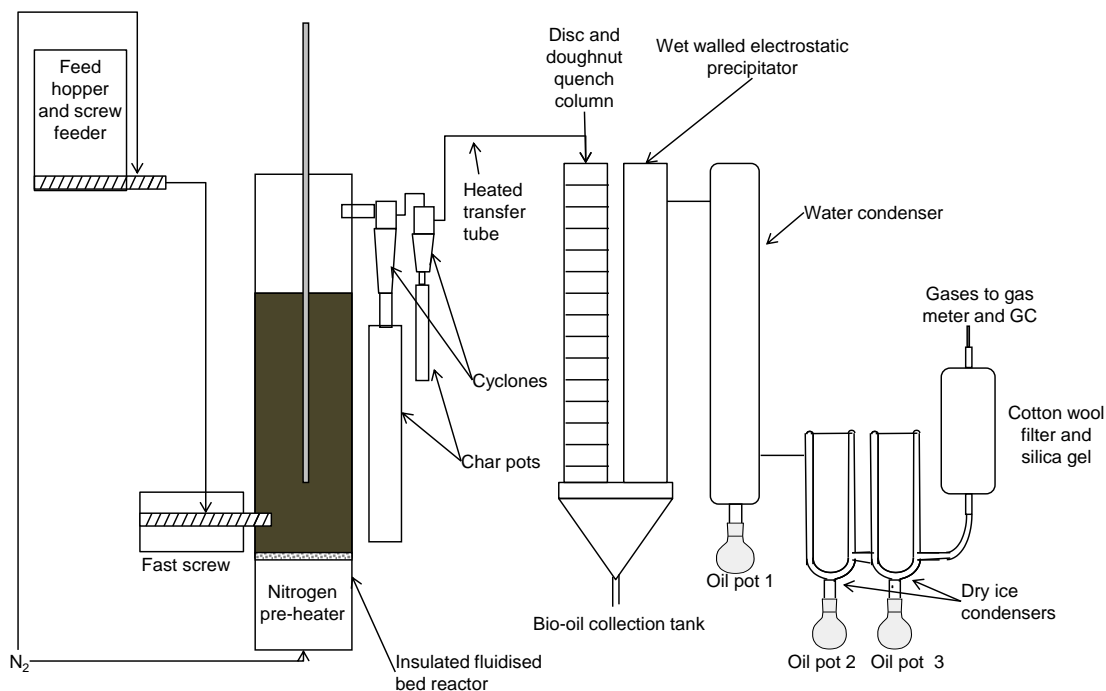
Figure 60: Flowsheet of the 1kg/h continuous fluidised bed reaction system

The difference in mass of biomass initially added to the hopper and removed post-run was used to cross check the feed rate and determine the mass of biomass fed. The larger rig components like the reactor, char pots, quench and ESP cannot be physically weighed. As with the 300g/h rig, sand was vacuumed out of the reactor and the mass gain of the vacuum bags was measured. Both char pots were emptied into bags and then weighed. The bio-oil and Isopar mixture was drained into a separation funnel, at the bottom of the bio-oil collection tank and then left to separate. The bio-oil was then drained into a bottle and weighed. The mass gain of the remaining glassware, cotton wool filter and silica gel were associated with liquid product and these were weighed and collected. Experiments on this rig showed a 5 wt.% increase in the mass balance closure when introducing silica gel to the collection system. Mass balances of approximately 95 wt.% were achievable on this larger scale rig when a low ash feedstock was used to produce a one-phase bio-oil. In the future, silica gel should also be added to the 300g/h rig after the cotton wool filter to further improve the mass balance to greater than 95 wt.%.
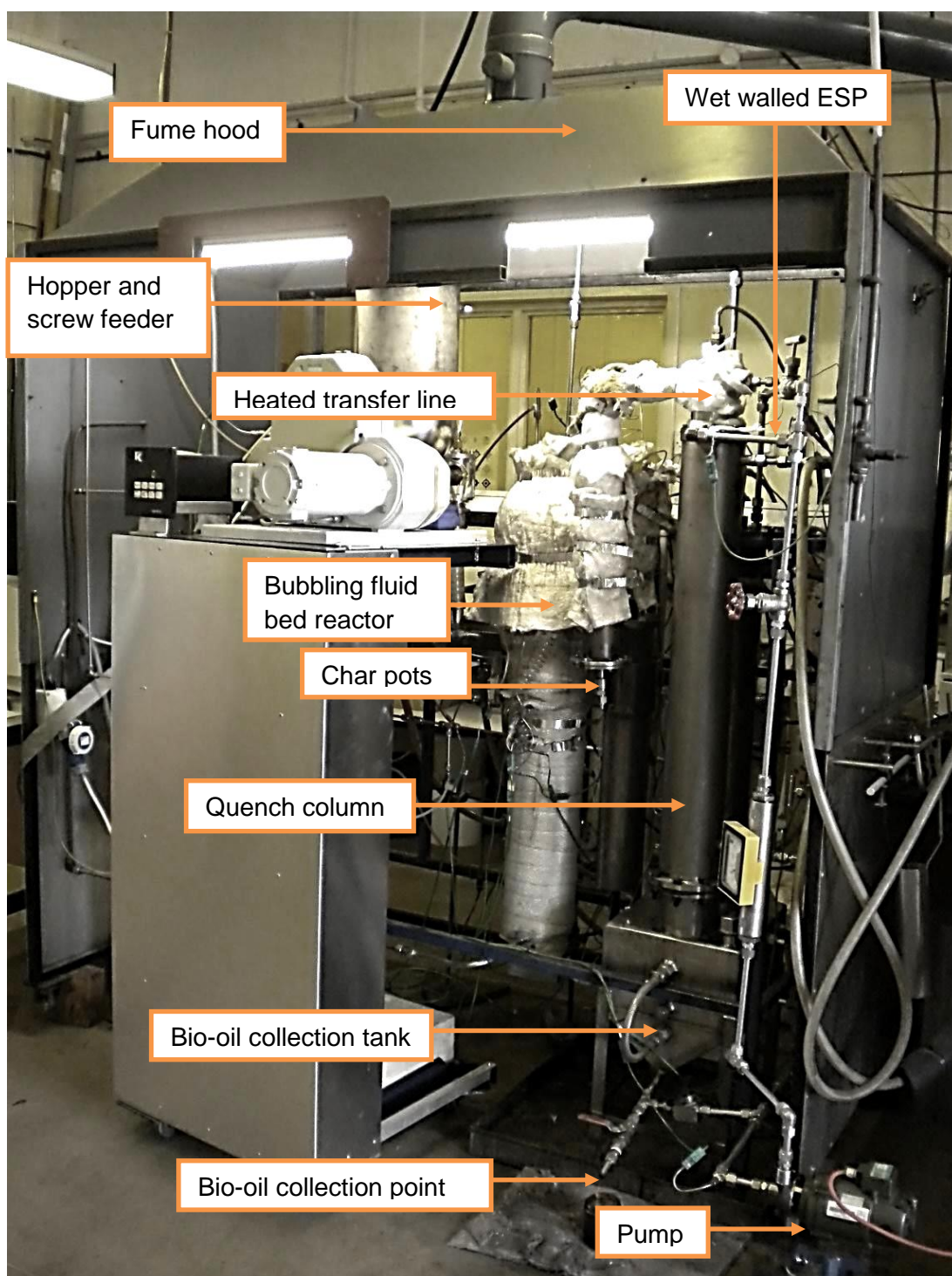
Figure 61: 1kg/h continuous fluidised bed reactor system

6.2.4 Product analysis

This section describes the techniques used to analyse bio-oil, char and gas properties from the feedstocks detailed in chapter 3. Due to bio-oil complexity, bio-oil analysis exemplifies a real challenge. The solid content and water content were critical to improve the accuracy of mass balances over the fast pyrolysis units and the methodology for these has previously been described in section 6.2.1. The main bio-oil was also analysed in terms of chemical composition, molecular weight distribution,

viscosity and elemental composition to calculate the HHV. pH of the main bio-oil and secondary condensates was also carried out.

Bio-oil chemical composition was analysed using a combined Varian 450-GC Gas chromatograph and Varian 220-MS Mass Spectrometer. A Varian VF-5ms (30m, 0.25mm id and 0.25µm df) capillary column was used. The GC oven temperature program was 45°C for 2.5 minutes with a heating rate of 5°C/minute up to 260°C. Hold time was 7.5 minutes. The bio-oil sample was diluted in ethanol in 1:5 (m/m) ratio and 1 µL of this mixture was used for the GC separation. The mass spectra for separated compounds were obtained in the molecular mass range m/z=15-650. The chemicals were identified using the NIST 98 MS library. This technique was valuable in identifying some of the chemicals present in the bio-oil. However, as only 1 µL of mixture is injected into this system, it was difficult to identify all of the chemicals present. Also, the NIST 98 MS library can limit data value as specific peaks can be identified as many alternative chemicals or not at all. Preliminary tests carried out in this work also showed that trace amounts of quench liquid can significantly affect the results from this technique. Centrifuging bio-oil samples was necessary to aid Isopar separation in some cases. However, this could affect the composition of the bio-oil sample being analysed as higher molecular weight compounds were likely to collect at the bottom of the tube leaving a non-representative sample for analysis. Relative quantification using the peak areas was employed in this work, but the accuracy of this data is questionable. Ideally, GC-MS-FID should be used for chemical quantification within the bio-oil. However, this would require an extensive study involving the calibration of model compounds which was not possible in this work.

Gel permeation chromatography was used to determine the molecular weight distribution of compounds in bio-oil. Bio-oil was characterised by a variety of definitions for molecular weight as shown below:

- Mp –Molecular weight at highest peak
- Mn-Number average molecular weight
- Mw-Weight average molecular weight
- Mz-Size average molecular weight

This technique was used to measure homogeneity of bio-oil. Polydipersity Index (PDI =Mw/Mn) is a measure of molecular homogeneity and indicates the distribution of molecular weights. PDI is always greater 1. Higher PDI values indicate a lower molecular homogeneity [92]. A PL-GPC 50 from polymer laboratories, UK, with a refractive index (RI) detector was used. It has a PLgel 3µm MIXED-E column, 300x7.5mm which operates at 40 ºC. Calibration of the GPC system was carried out using polystyrene calibration standards for a molecular weight range between 105 and

19880g/mol. The bio-oil was diluted in HPLC-grade tetrahydrofuran (THF) in 1:20(m/m) ratio. It was then filtered using a millipore Puradisc 25TF filter (0.1μm pore size) to remove solids which could cause blockages in the system. A PL-AS RT autosampler was used to inject the sample into the column. However, as only a small sample mixture is injected into this system, it is difficult to obtain a representative sample of the whole bio-oil. Averages of duplicates were used to maximise the value of this analysis.

Bio-oil viscosity is directly related to the water content of bio-oil. Viscous liquids are difficult to handle, give poor atomisation, can result in high pumping costs and give high pressure drop increasing equipment cost [73]. A Brookfield (Viscometer model DV-II+pro) rotational type viscometer was used to measure the bio-oil viscosity at 40°C. A minimum of 6.7ml of bio-oil was required to carry out viscosity analysis using this system so viscosity analysis could not be carried out for all experiments as insufficient quantities of bio-oil were produced.

The acidity of bio-oil is an undesirable characteristic as it can lead to corrosion of pipe-work and vessels. The pH of all liquid samples was measured using a Sartorius PB-11 pH meter. pH buffers supplied by Sartorius were used to calibrate the meter to pH 2, 4 and 7. pH measurements were triplicated to check reproducibility.

Bio-oil and char HHV can be calculated from the elemental composition and ash content or measured using a bomb calorimeter. Bio-oil and char elemental composition was analysed by Medac Ltd. as described earlier in section 3.1. Bio-oil ash content was not measured, but was expected to be around <0.2 wt.% [79] as most ash is associated with the char [76] and collected separately in char pots. Char composition and HHV is important as it can either be recycled for heat in a commercial fast pyrolysis process or recovered for biochar applications [72]. The ash content of char was measured using the ASTM ashing method described in section 3.1.

Non-condensable gases were passed through a gas meter to measure the volumetric flow rate (m^3/h). A sample was then injected every three minutes into an online Varian MicroGC cp 4900 gas chromatograph with a thermal conductivity detector (TCD) to analyse the gas composition. The system was calibrated with standard composition gas mixtures. The GC system is equipped with 2 columns. Column A detects hydrogen, oxygen, nitrogen, methane and carbon monoxide. Column B detects nitrogen, methane, carbon dioxide, ethane, propene, propane and n-butane.

The mass of non-condensable gas, produced in the pyrolysis process, was calculated on a nitrogen-free basis. Low heating value non-condensable gases mainly consist of carbon monoxide and carbon dioxide and are commercially used for process heat and fluidisation. The carbon monoxide is oxidised to carbon dioxide and therefore,

the fluidising gas is mainly carbon dioxide. Inert nitrogen was used for these tests to reduce the expense of recycling and compression of the non-condensable product gases.

6.3   Fast pyrolysis results and discussion

This section discusses the results obtained from biomass fast pyrolysis. The results aim to identify the most promising feedstock and rig setup for further processing. Table 24 shows a summary of the fast pyrolysis tests completed using the 100g/h, 300g/h and 1kg/h rigs. Several tests were carried out in the early stages of this project which were unsuccessful due to feeding and fluidisation problems. These problems are summarised in Table 24.

Figure 62 shows char in the glass transition pipe and water condenser. Adjustment of fluidisation gas velocity was necessary to ensure the char was collected in char pots and not blown into the liquid collection system. Figure 63 shows the three phase bio-oil produced from fast pyrolysis of miscanthus in test 7 as a result of the char being blown out of the reactor and collected in the glass transition pipe. Cold fluidisation tests were necessary to determine the fluidising gas velocity required to fluidise the sand, retain the unpyrolysed biomass and entrain the char.

Figure 62: Char in the end of the glass transition pipe

Figure 63: Phase separation in the main oil collection pot

Table 24: Test summary for fast pyrolysis of biomass

Test Ref No.	Date	Rig configuration	Feedstock	Problems/successful	Solution/conclusion
1	15/10/2009	100g/h & glassware	Beech	Successful run	N/A
2	17/11/2009		1% H_2SO_4 Acid Beech	Feeding problems. Feeder tube and the sand fluidised bed blocked within ten minutes. The blockage is expected to be due to agglomeration of char in the top part of the feeding tube	Acid treated feedstocks could not be fed pneumatically into the top of a fluidised bed reactor. Feeding acid treated residues directly into a sand bed may be more promising.
3	25/11/2009		1% H_2SO_4 Acid Beech		
4	07/12/2010	300g/h & quench	Miscanthus	Successful run	N/A
5	24/01/2011	300g/h & glassware	Miscanthus	Gas leaks from glass joints leading to poor mass balance	Use supports, clamps and grease to secure connections
6	21/02/2011		Miscanthus	Poor mass balance due to poor product recovery method.	Use a more powerful vacuum cleaner to remove content of the reactor. Use a torch to physically check that the reactor is clean before and after each experiment.
7	04/03/2011		Miscanthus	Phase separated bio-oil (see Figure 63). Some sand and char remained in reactor which required more effective cleaning for a better mass balance.	
8	10/03/2011		Sugarcane bagasse	Feed backing up at entrance to high speed feed screw (see Figure 64 and Figure 65). No vapours were visible in the ESP indicating that feeding had stopped. Pressure drop increase in the reactor indicating there was a blockage in the reactor due to agglomeration of char.	Increase the speed of high speed feeding screw to ensure all feed is delivered to the reactor and does not back up.
9	22/03/2011		Sugarcane bagasse	ESP failure	Replace ESP wire.
10	06/04/2011		Sugarcane trash	Blockage in pipework (see Figure 66) due to poorly wrapped trace heaters leading to condensation of pyrolysis products.	Wrap trace heaters adequately to cover all metal pipework so that products do not condense before glass collection system.
11	19/04/2011		Sugarcane trash	Feed backed up into the feeding pipe and char retained in reactor due to low	Increase fluidisation gas velocity and sand particle

Test Ref No.	Date	Rig configuration	Feedstock	Problems/successful	Solution/conclusion
				fluidisation gas velocity (see Figure 67).	size so sand retains in the reactor, but char is entrained. This also breaks up agglomerates.
12	05/05/2011		Sugarcane bagasse pellets	Char retained in reactor, agglomerates too big to leave the reactor (see Figure 67).	Increase fluidisation gas velocity and sand particle size so sand retains in the reactor, but char is entrained. This also breaks up agglomerates.
13	24/05/2011		Sugarcane bagasse	Pressure increase to above the maximum of pressure indicator.	Replace pressure indicator to one with higher readings.
14	02/06/2011		Sugarcane bagasse	Successful run	N/A
15	07/06/2011		Miscanthus	Successful run	N/A
16	09/06/2011		Sugarcane trash	Successful run	N/A
17	14/06/11		Sugarcane bagasse pellets	Successful run	N/A
18	15/08/2011	300g/h & quench	Sugarcane bagasse pellets	Successful run.	N/A
19	24/08/2011		Miscanthus pellets	Successful run	N/A
20	23/07/2012	300g/h & glassware	Sugarcane bagasse pellets	To check reproducibility of fast pyrolysis runs. Results were comparable so successful.	N/A
21	06/03/2012	1kg/h & quench	Sugarcane bagasse pellets	Successful run	N/A
22	04/10/2012	1kg/h & quench	Beech	Successful run	N/A

Figure 64 and Figure 65 shows sugarcane bagasse backing up in the vertical feeding tube between the metering screw and the high speed feed screw in test 8. This was a result of a slow screw speed restricting the biomass feed rate into the reactor.
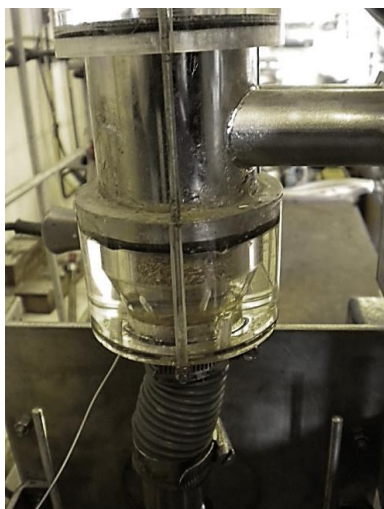
Figure 64: Feed backing up in the clear chamber of the feeder

Figure 65: Feed backing up in the vertical feeding tube between the metering screw and the high speed feed screw in test 8.

A blockage (see Figure 66) occurred in the narrow pipework downstream of the reactor in test 10 as the trace heating was wrapped poorly allowing pyrolysis vapours to condense prematurely.

Blockage in the cyclone pipe work
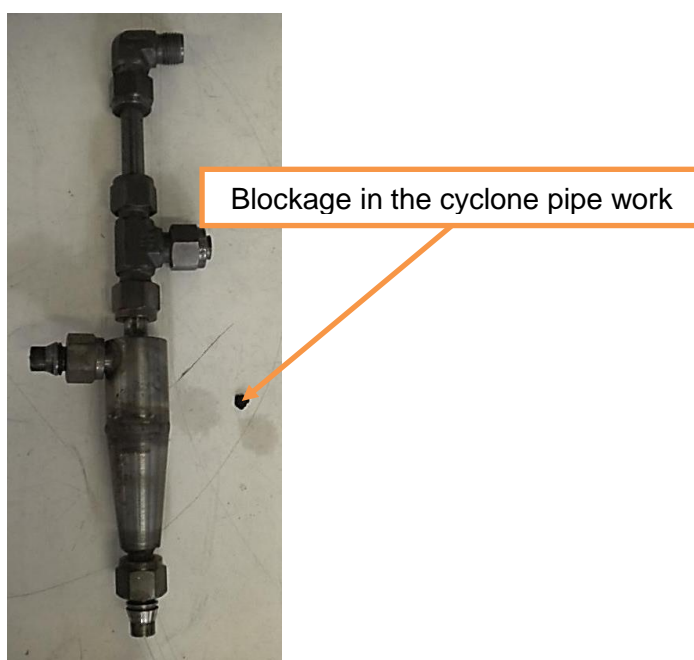
Figure 66: Second cyclone with char blocking the pipe work

There was char build up in the reactor in the form of agglomerates after tests 11 (sugar cane trash) and 12 (ground bagasse pellets) which could not be entrained out of the reactor as detailed in Table 24. Alkali metals present in char can act as a catalyst and crack pyrolysis vapours [8] and as a result, increase the bio-oil water content and increase the gas yields. Figure 68 shows an example of high water content phase-

separated bio-oil collected in the main bio-oil pot as a result of the char agglomerate being retained in the reactor (Figure 67). The advantage of using the glassware system on the 300g/h rig is that the bio-oil is visible as it is being collected. A high water content bio-oil from a standard low ash content feedstock such as sugarcane bagasse is an indication that the char has been retained in the reactor leading to secondary catalytic cracking of the pyrolysis vapours.

Figure 67: Example of char retained in the reactor
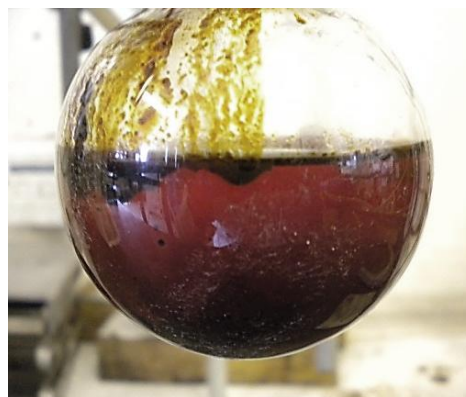
Figure 68: Example of high water content phase-separated bio-oil

Adjusting the fluidising velocity may help to break up the char agglomerates and aid char entrainment out of the reactor. Overloading of the char pot was not the issue as the char pot was empty. The main reason for char build up in the reactor is believed to be due to the nature of the feedstock that produced a char that agglomerated in the freeboard of the reactor. Tests 16 and 17 used the same feed materials, but with an adjusted fluidising velocity (see Table 25) which resulted in successful pyrolysis of sugarcane trash and SCBP.

Table 25: Fluidising velocities for Test 11, 16, 12 and 17

Test reference number	11	16	12	17
Test summary	Char retained; unsuccessful	Char entrained; successful	Char retained; unsuccessful	Char entrained; successful
Feedstock	Sugarcane trash	Sugarcane trash	Sugarcane bagasse pellets	Sugarcane bagasse pellets
Fluidising N_2 velocity (m/s)	0.068	0.406	0.744	0.507
N_2 velocity through feeder (m/s)	0.575	0.203	0.101	0.237
Total N_2 velocity (m/s)	0.643	0.609	0.845	0.744

Large agglomerates in the reactor cannot fit through the narrow pipework leading to the cyclone and so char is retained in the reactor. Increasing the fluidising gas velocity reduced the formation of agglomerates allowing char particles to be entrained out of the reactor. The effect of hot vapour residence time is unknown, but is not believed to be significant as this would only vary slightly to maintain suitable fluidising conditions. Table 26 presents the operating conditions used for the successful fast pyrolysis tests carried out in this work.

Table 26: Fast pyrolysis operating conditions for successful tests

Reactor and collection system configuration	100 g/h reactor with glassware	300 g/h reactor with glassware					300 g/h reactor with quench column		1 kg/h reactor with quench column	
Sand particle size range (mm)	0.355-0.5	0.5-0.6					0.355-0.5	0.5-0.6	0.6-0.71	0.6-0.71
Feedstock particle size range (mm)	0.355-0.5	0.250-1					0.250-1	0.250-1	0.250-1	0.250-1
Fast screw speed (rpm)	N/A	110					100	110		
Run time (min)	110	60					85	60	80	80
Test Ref. No	1	14	15	16	17	19	4	18	21	22
Feedstock	Beech	Sugarcane bagasse	Miscanthus	Sugarcane trash	Sugarcane bagasse pellets	Miscanthus pellets	Miscanthus	Sugarcane bagasse pellets	Sugarcane bagasse pellets	Beech
Biomass feed rate (g/h)	66	51.49	103.07	55.54	207.72	155.37	145.47	213.41	748.76	903.75
Fluidising N_2 velocity (m/s)	0.23	0.338	0.406	0.406	0.507	0.507	0.474	0.507	1.184	1.184
N_2 velocity through feeder (m/s)	0.006	0.169	0.203	0.203	0.237	0.271	0.371	0.237	0.575	0.575
Total N_2 velocity (m/s)	0.236	0.507	0.609	0.609	0.744	0.778	0.845	0.744	1.759	1.759
Average pyrolysis T (^{o}C)	500	485	493.9	512	493	525	470	503	512	510
Pyrolysis T (^{o}C) range	Not recorded	480-500	490-509	509-519	506-525	518-532	460-480	492-513	506-525	Not recorded
ΔP across reactor (bar)	Not recorded	0.04	0.06-0.07	0.07-0.09	0.16	0.14-0.16	Not recorded	0.14-0.16	Not recorded	Not recorded

6.3.1   100g/h rig

Fast pyrolysis of beech was useful in initial training and for cross checking results with those already obtained by previous members of the research group. Table 27 shows the mass balance summary for beech fast pyrolysis using the 100g/h rig. High mass balance closures (>95 wt.%) are expected from the 100g/h rig as all rig components, including the reactor, could be weighed. This mass balance closure (90.91 wt.%) was lower than expected. The gas and char yields are comparable to beech fast pyrolysis carried out by other members of BERG on the larger 1kg/h rig. The total liquid yield (70.85 wt.% dry feed basis) was lower than expected and there were no visible leakages so the poor mass balance closure was likely to be due to poor liquid recovery. Due to limitations in the availability of the equipment and feedstocks, no other repetitions were made using beech on the 100g/h rig.

Table 27: Mass balance summary from fast pyrolysis of beech using 100g/h rig (dry feed basis)

Product	
Feed moisture (wt.% wet feed basis)	7.25
Feed ash (wt.% dry feed basis)	0.78
Average bed T (°C)	500
Run time (minutes)	110
Feed rate (g/h)	66
Char (wt.% dry feed basis)	15.47
Total liquid (wt.%)	70.85
Organic liquid (wt.% dry feed basis)	60.19
Total water (wt.%)	10.66
Water in the feed (wt.%)	7.82
Reaction water (wt.% dry feed basis)	2.84
Average water content of main bio-oil from oil pot 1 (wt.%)	0.45
Average water content of condensates from oil pots 2 and 3 (wt.%)	57.35
Gas (wt.% dry feed basis)	12.41
H_2	0.09
CO	5.27
Methane	0.63
CO_2	6.03
Ethene	0.15
Ethane	0.08
Propene	0.11
Propane	0.02
n-Butane	0.02
Total product out (g)	110.94
Total feed in (g)	121.15
Recovery (wt.% dry feed basis)	90.91

24 compounds identified in the bio-oil by GC-MS analysis can be found in Appendix 1. As expected, the bio-oil contains oxygenates with high molecular weight compounds consisting of acids, alcohols, phenolics, esters and ketones.

Table 28 shows the bio-oil molecular weight distribution produced from beech collected in oil pot 1 on the 100g/h rig. The PDI is 1.74. Bio-oil homogeneity is reported

to increase as the PDI is closer to 1. It is expected that this data has a close correlation with the viscosity of the bio-oil. However, as there was an insufficient volume of bio-oil collected in this experiment, viscosity analysis could not be carried out. Also, it should be noted that the glassware collection system collects fractionated liquid with high water content (57.35 wt.%) secondary condensates in oil pot 2 and 3. The main bio-oil from this glassware collection system is likely to be more viscous and with a higher PDI compared to bio-oil collected using an improved quenching system. In order to carry out viscosity analysis a longer run time or a larger processing unit would be required.

Table 28: Molecular weight distribution of main bio-oil from beech on the 100g/h rig

	Beech
Mp	137
Mn	311
Mw	542
Mz	716
PDI	**1.74**

The pH of the main bio-oil produced from beech was 2.97 and this is less acidic than reported by Bridgwater (approximately 2.5) [79]. The pH of the secondary condensates was 2.47. This system collects a fractionated liquid product compared to a quench system; the secondary condensates contain significant amounts of water, but also expected to contain light organics such as acids, which would lower the acidity.

Table 29 shows the elemental analysis, ash content and calculated HHV for the bio-oil and char from beech. The bio-oil oxygen content is 38.25 wt.% which is within the range reported in literature (35-40 wt.%) [79]. In order to be miscible with diesel, bio-oil oxygen content needs to be reduced using a bio-oil upgrading technique. Bio-oil has a HHV of 16-19MJ/kg when the water content is 15-30% [79]. However, this bio-oil HHV is higher (23 MJ/kg) due to the lower water content obtained from the fractionated liquid when using a glassware collection system. It was strongly believed that the measured water content of the main bio-oil (0.45 wt.%) was incorrect and as water content analysis was repeated, the problem is likely to lie with the calibration of the Karl Fischer unit. The calibration was corrected for all future Karl Fischer analysis.

Table 29: Analysis of bio-oil and char from beech

	Bio-oil from beech	Char from Beech
C (wt.%)	55.24	82.88
H (wt.%)	6.52	1.9
N (wt.%)	<0.10	0.32
O* (wt.%)	38.25	14.89
S (wt.%)	Nm	0
Ash (wt.%)	<0.02	3.38
HHV (MJ/kg)	23	29.63

*Oxygen by difference

6.3.2   300g/h rig

This section presents and discusses the results from screening feedstocks using the 300g/h rig. Mass balances are compared to identify the feedstock which yields highest organic liquid. The glassware and quench collection systems are then compared to see whether the glassware system, which collects a fractionated liquid product, can be used to give realistic product yields and bio-oil composition results.

Table 30 shows the mass balance summaries of successful fast pyrolysis experiments on the 300g/h rig using the glassware collection system. Fast pyrolysis of sugarcane trash produces the highest yield of char (24.25 wt.%) as it has a higher ash content (4.44 wt.%) than the other feedstocks. The char yield from loose sugarcane bagasse is 14.84 wt.% whereas the char yield from ground SCBP is 17.32 wt.%. The char yield from higher density ground pellets is expected to be higher than the char yield from loose biomass as there is reduced shrinkage during pyrolysis of pellets [104]. The pyrolysis temperature was lower (493°C) for loose miscanthus than for ground miscanthus pellets (525°C). Lower pyrolysis temperatures also reduce the shrinkage of the biomass particles leaving a higher char yield. This explains why the char yields from loose miscanthus is as high as 17.56 wt.% when it is expected to be less than the char yield from ground miscanthus pellets (17.79 wt.%). Fast pyrolysis of miscanthus gave total liquid yields of 63.12 wt.% (on a dry feed basis) which are comparable to the results obtained by Hodgson et al. [108] and Kalgo [92]. Ground SCBP was the most promising feedstock for further processing as it gave the highest organic liquid yield (60.4 wt.%), highest throughput (207.72g/h) and reliable screw feeding.

Table 30: Mass balance summaries for the 300g/h rig and glassware collection system

Feedstock	Miscanthus	Miscanthus pellets	Sugarcane bagasse	Bagasse pellets	Sugarcane trash
Feed moisture (wt.% wet feed basis)	9.26	9.97	9.95	9.62	11.35
Feed ash (wt.% dry feed basis)	1.87	3.50	1.05	2.97	4.44
Average pyrolysis T(°C)	493	525	485	493	512
Feed rate (g/h)	103.07	155.37	51.49	207.72	55.54
Char (wt.% dry feed basis)	17.56	17.79	14.84	17.32	24.25
Total liquid (wt.%)	63.12	71.14	72.96	73.14	57.15
Organic liquid (wt.% dry feed basis)	39.83	53.96	60.39	60.45	42.49
Total water content (wt.%)	23.28	17.19	12.57	12.69	14.67
Average water content of main bio-oil from oil pot 1(wt.%)	34.57	10.15	11.92	7.27	17.52
Average water content of condensates from oil pots 2 and 3 (wt.%)	63.29	65.85	61.52	51.93	62.22
Phase separation	NO	NO	NO	NO	NO
Water in the feed (wt.%)	10.20	11.07	11.05	10.64	12.80
Reaction water (wt.% dry feed basis)	13.08	6.12	1.52	2.05	1.86
Gas (wt.% dry feed basis)	23.64	15.83	20.45	14.01	24.86
H_2	0.05	0.04	0.07	0.04	0.07
CO	7.15	4.69	5.86	4.73	6.37
Methane	0.93	0.59	0.77	0.54	0.90
CO_2	10.51	5.94	5.57	5.27	7.86
Ethene	0.70	0.61	1.07	0.52	1.25
Ethane	0.76	0.66	1.28	0.48	1.33
Propene	0.97	0.89	1.51	0.67	1.84
Propane	1.25	1.18	2.14	0.84	2.57
n-Butane	1.33	1.25	2.19	0.90	2.68
Total product out (g)	97.56	146.56	50.19	196.14	52.32
Total feed in (g)	103.07	155.37	51.49	207.72	55.54
Recovery (wt.% dry feed basis)	94.11	93.70	97.20	93.83	93.46

Bio-oil, a brown viscous liquid, contains low and high molecular weight compounds. Figure 76 shows an example of the fractionated bio-oil collected in the 3 oil pots from the glassware liquid collection system.

Figure 69: Bio-oil collected in oil pot 1, 2 and 3

There were no distinct aqueous phases in the main oil pot suggesting that the reactor was successfully fluidised and the contact time between the pyrolysis vapours and the catalytically active char were minimised. Bio-oil typically has an average water content of 15-35 wt.% [79]. The results show that bio-oil water content ranged from 7.27-34.57% as the glassware collection system collected a fractionated liquid product and the water content reported by Bridgwater is based on using a more effective liquid collection system such as a quench system. Phase separation is reported to occur when water content is higher than 30 wt.% [151]. However, no phase separation was observed in the bio-oil from miscanthus where the water content was high as 34.57 wt.%. Viscous organics were collected on the walls of the ESP and oil pot as shown in Figure 70 to Figure 73. High water content secondary condensates ranging from 51.93-65.85% were collected in oil pots 2 and 3. The secondary condensates collected in oil pot 2 were combined with oil pot 3 as initial experiments showed that the water content of these were very similar.

Figure 70: Bio-oil from miscanthus

Figure 71: Bio-oil from sugarcane bagasse

Figure 72: Bio-oil from sugarcane trash

Figure 73: Bio-oil from sugarcane bagasse pellets

The compounds identified in the bio-oil produced from miscanthus, miscanthus pellets, sugarcane bagasse, SCBP and sugarcane trash can be found in Appendix 1. As expected, similar compounds were identified in both feedstocks. Degradation of hemicellulose, cellulose and lignin produce a liquid bio-oil consisting of acids, aldehydes, alcohols, sugars, esters, ketones, furans, phenolics, oxygenates and hydrocarbons. GC-MS analysis shows the presence of acids, furans and phenolics. The presence of organic acids such as acetic acid contributes to the low pH of bio-oil. Appendix 1 also shows the compounds identified in the bio-oil from sugarcane bagasse, SCBP and sugarcane trash.

Table 31 shows the PDI for the bio-oil from feedstocks used in this study. PDI values range from 1.59 for miscanthus to 1.74 for miscanthus pellets. Homogeneity increases when PDI values are closer to 1. Therefore, these results indicate that

homogeneity of bio-oil from miscanthus was greater than that of miscanthus pellets. The same trend can be seen with sugarcane bagasse and SCBP. Homogeneity of bio-oil from loose biomass is fractionally better than from pellets.

Table 31: Molecular weight distribution of feedstocks

Feedstock	Miscanthus	Miscanthus pellets	Sugarcane bagasse	SCBP	Sugarcane trash
Mp	139.5	153	133	113	136
Mn	150	171	149	145	140
Mw	238.5	298	243	240	233
Mz	426.5	538	408.5	416	425
PDI	1.59	1.74	1.63	1.66	1.66

At least 6.7ml of bio-oil is required to carry out viscosity measurements using the viscometer detailed in section 6.2.4. The viscosity of the bio-oil from all of the feedstock could not be measured as sufficient volumes of bio-oil were not produced. However, as the feed rate of SCBP was considerably higher than the other feedstocks, more bio-oil was produced in one hour allowing for viscosity analysis of this bio-oil. The viscosity of bio-oil is reported to be 40-100cPA at 50°C [79]. However, bio-oil from SCBP was very viscous (2780cP at 40°C) and did not flow due to such low water content (7.27 wt.%). This is because the glassware collection system collects a fractionated liquid product where a significant amount of water is collected separately in oil pots 2 and 3. On the other hand, a quench collection system collects the liquid products more effectively producing a bio-oil which has a higher water content and improved flow properties.

Figure 74 shows the pH of the main bio-oil and condensates produced on the 300g/h with a glassware collection system. These results show that pH of the main bio-oil range from 2.53 for trash to 3.30 for miscanthus. The pH of the condensates is consistently lower i.e. more acidic for all feedstocks. This is associated with the lighter acidic compounds which are collected in the secondary oil pots.
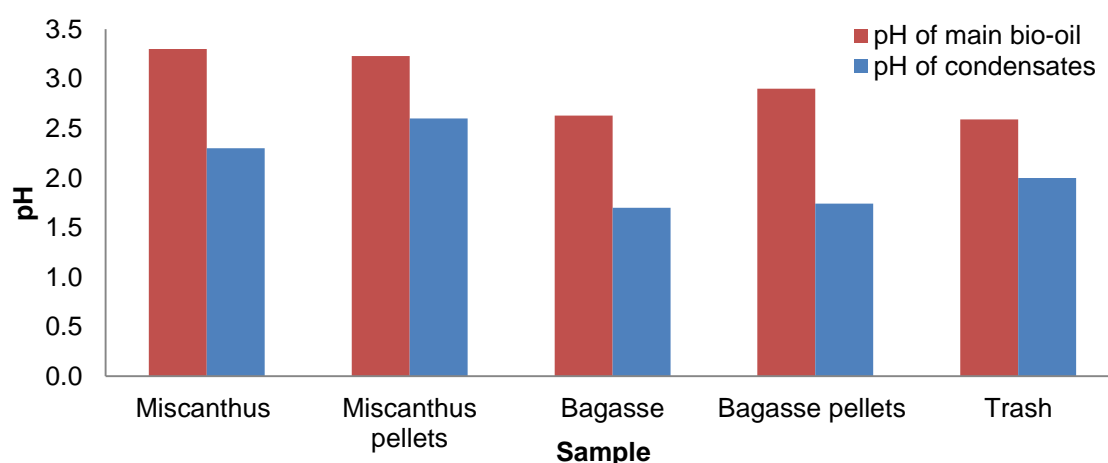
Figure 74: pH comparison of main bio-oil and condensates on the 300g/h rig and glassware collection system

Table 32 shows the elemental analysis, ash content and calculated HHV of bio-oil from each feedstock. The oxygen content ranges from 40-50 wt.% which is only slightly higher than what is expected (35-40 wt.%) [79]. A bio-oil HHV of 16-19MJ/kg is expected when the water content is 15-30% [79]. However, the HHV is higher (up to 22.48MJ/kg) due to the lower water content bio-oil collected using the glassware collection system.

Table 32: Analysis of bio-oil from feedstocks

Feedstock	Miscanthus	Miscanthus pellets	Sugarcane bagasse	SCBP	Sugarcane trash
C (wt.%)	46.57	51.95	46.48	51.99	42.5
H (wt.%)	8.85	7.12	8.06	7.25	7.92
N (wt.%)	<0.10	1.16	<0.10	<0.10	<0.10
O* (wt.%)	44.58	39.77	45.46	40.76	49.59
S (wt.%)	Nm	0	Nm	Nm	Nm
Ash (wt.%)	Nm	Nm	Nm	Nm	Nm
HHV (MJ/kg)	22.08	22.4	21.02	22.48	19.04

*Oxygen by difference

Table 33 shows the elemental analysis, ash content and calculated HHV for the char produced from each feedstock. The ash from the original biomass is associated with the char. Therefore, as trash has the highest ash content, the ash content of char from trash is higher (32.95 wt.%) compared with the other feedstocks. The HHV of the char ranges from 20.28 to 26.42 MJ/kg. The HHV of miscanthus char (26.42 MJ/kg) is higher than expected as the unreacted carbon is significantly higher (69.98 wt.%) than for the other feedstocks (55.44 to 60.67 wt.%).

Table 33: Analysis of char from feedstocks

Feedstock	Miscanthus	Miscanthus pellets	Sugarcane bagasse	SCBP	Sugarcane trash
C (wt.%)	69.98	60.67	59.52	55.44	57.42
H (wt.%)	3.04	2.76	2.65	2.52	2.77
N (wt.%)	0.6	1.14	0.6	0.61	0.73
O* (wt.%)	12.43	6.46	19.41	13.97	6.135
S (wt.%)	Nm	Nm	Nm	Nm	Nm
Ash (wt.%)	13.95	28.98	17.83	27.47	32.95
HHV (MJ/kg)	26.42	23.13	21.5	20.28	21.97

*Oxygen by difference

The feedstocks were screened using the glassware collection system and the most promising feedstock was selected for further processing based on the highest organic liquid production and throughput. Table 34 shows that ground SCBP was the most promising feedstock as it produced 60.45 wt.% organic liquid (dry feed basis) with a feed rate of 207.72g/h. The bio-oil oxygen content from this feedstock was one of the lowest (40.76 wt.%) which is more suited for catalytic upgrading to further deoxygenate the bio-oil. The bio-oil HHV was also the highest (22.48MJ/kg).

Table 34: Screening summary of feedstocks

Feedstock	Miscanthus	Miscanthus pellets	Sugarcane bagasse	Bagasse pellets	Sugarcane trash
Feed rate (g/h)	103.07	155.37	51.49	207.72	55.54
Organic liquid yield (wt.% dry feed basis)	39.83	53.96	60.39	60.45	42.49
Bio-oil oxygen content (wt.% dry feed basis)	44.58	39.77	45.46	40.76	49.59
Bio-oil HHV (MJ/kg)	22.08	22.40	21.02	22.48	19.04

Fast pyrolysis using the glassware collection system on the 300g/h rig was repeated to check reproducibility of results and run for 90 minutes to produce sufficient quantities of bio-oil for viscosity analysis. Due to availability of time and feedstocks, a repeat was only carried out using the most promising feedstock; ground SCBP. It can be seen that the results were comparable. Results from fast pyrolysis of miscanthus were also comparable to those obtained by previous researchers.

Table 35: Reproducibility results for ground SCBP

Run number	Run 1	Run 2
Feed moisture (wt.% wet feed basis)	9.62	
Feed ash (wt.% dry feed basis)	2.97	
Average pyrolysis T(°C)	493	501
Feed rate (g/h)	207.72	134.86
Run time (minutes)	60	90
Char (wt.% dry feed basis)	17.32	18.41
Total liquid (wt.%)	73.14	72.20
Organic liquid (wt.% dry feed basis)	60.45	59.54
Total water content (wt.%)	12.69	12.67
Average water content of main bio-oil (wt.%)	7.27	3.65
Average water content of condensates (wt.%)	51.93	50.96
Water in the feed (wt.%)	10.64	10.64
Reaction water (wt.% dry feed basis)	2.05	2.03
Gas (wt.% dry feed basis)	14.01	13.72
H_2	0.04	0.04
CO	4.73	4.63
Methane	0.54	0.53
CO_2	5.27	5.16
Ethene	0.52	0.51
Ethane	0.48	0.47
Propene	0.67	0.66
Propane	0.84	0.83
n-Butane	0.90	0.89
Total product out (g)	196.14	190.75
Total feed in (g)	207.72	202.29
Recovery (wt.% dry feed basis)	93.83	93.69

The bio-oil produced from ground SCBP, using the glassware and quench collection system, was compared to investigate the effect of collection system on the product yields and composition of the organic liquid. Table 36 compares the mass balances for fast pyrolysis of miscanthus and ground SCBP using the two collection systems. Miscanthus was processed earlier in the project using the prior liquid recovery

technique when SCBP were not available; hence the mass balance was only 91.01 wt.%. The ethanol washing recovery technique was used on the quench with ground SCBP which gave an improved mass balance (93.46 wt.%). This was similar to the mass balance closure for the glassware system (93.83 wt.%).

Table 36: Comparing mass balance summaries for fast pyrolysis of miscanthus and SCBP on the 300g/h rig (dry feed basis)

Feedstock	Miscanthus with glassware	Miscanthus with quench	Ground SCBP with glassware	Ground SCBP with quench
Feed moisture (wt.% wet feed basis)	9.26	12.00	9.62	9.62
Feed ash (wt.% dry feed basis)	1.87	1.87	2.97	2.97
Average pyrolysis T(°C)	493	470	493	503
Feed rate (g/h)	103.07	177.23	207.72	213.41
Run time (minutes)	60	60	60	60
Char (wt.% dry feed basis)	17.56	22.56	17.32	18.31
Total liquid (wt.%)	63.12	66.65	73.14	75.00
Organic liquid (wt.% dry feed basis)	39.83	28.61	60.45	63.38
Total water content (wt.%)	23.28	38.04	12.69	11.62
Average water content of main bio-oil (wt.%)	34.57	54.88	7.27	12.61
Average water content of condensates (wt.%)	63.29	89.24	51.93	72.22
Water in the feed (wt.%)	10.20	13.64	10.64	10.64
Reaction water (wt.% dry feed basis)	13.08	24.40	2.05	0.98
Gas (wt.% dry feed basis)	23.64	15.4	14.01	10.79
H_2	0.05	0.03	0.04	0.0
CO	7.15	4.74	4.73	3.09
Methane	0.93	0.61	0.54	0.40
CO_2	10.51	7.24	5.27	3.87
Ethene	0.70	0.35	0.52	0.46
Ethane	0.76	0.37	0.48	0.48
Propene	0.97	0.87	0.67	0.65
Propane	1.25	0.62	0.84	0.89
n-Butane	1.33	0.61	0.90	0.93
Total product out (g)	97.56	231.22	196.14	200.80
Total feed in (g)	103.07	251.08	207.72	213.41
Recovery (wt.% dry feed basis)	94.11	91.01	93.83	93.46

The important result here is the total organic liquid yield. It is evident that the quench cools and collects organic liquid (63.38 wt.%) more effectively than the glassware system (60.45 wt.%). However, the total water content is comparable for both as the feed moisture and the reaction conditions were very similar so the reaction water produced should be similar. As expected, the average water content of the main bio-oil is higher using a quench system (12.61 wt.%) compared to the glassware system (7.27 wt.%) as the rapid cooling effect of the quench column is able to collect

more of the condensable products more effectively. There is less gas measured with the quench (10.79 wt.%) than the glassware (14.01 wt.%) suggesting that the glassware system still allows some condensable gases or water vapour to escape with the non-condensable gas stream. The char yields for both are comparable (17.32 wt.% and 18.31 wt.%) as the reaction temperatures were very similar (493°C and 503°C) leading to similar level of biomass shrinkage. The temperature for the miscanthus run with quench was lower (470°C) than with glassware (493°C) confirming that reduced temperatures reduce particle shrinkage and explains why the char yield from the miscanthus run with quench (22.56 wt.%) was significantly higher than glassware (17.56 wt.%).

Figure 75 and Figure 76 show the heavy organic deposits on the ESP from both liquid collection systems which reduce the HHV of the mobile phase bio-oil. A wet walled ESP would overcome this problem with the quench system as Isopar would clean the ESP and collect the organic deposits in the collection tank.
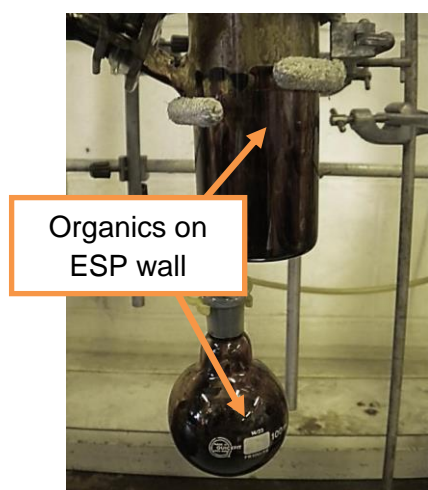
Figure 75: Organics on wall of ESP and main oil pot on the glassware collection system
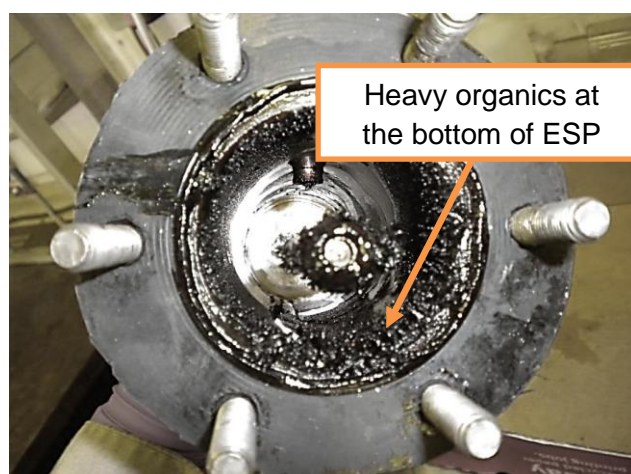
Figure 76: Deposits on the bottom of the ESP on the quench column

Clean Isopar is a clear liquid, however, it can be seen in Figure 77 that used Isopar is a yellow colour. This is expected to be due to the miscibility of some chemicals in bio-oil with Isopar. When re-using the Isopar, no further discolouration is observed. Therefore, it is expected that this Isopar is saturated and should no longer be miscible with any chemicals in bio-oil. Compositional analysis of the Isopar would be required to confirm this.
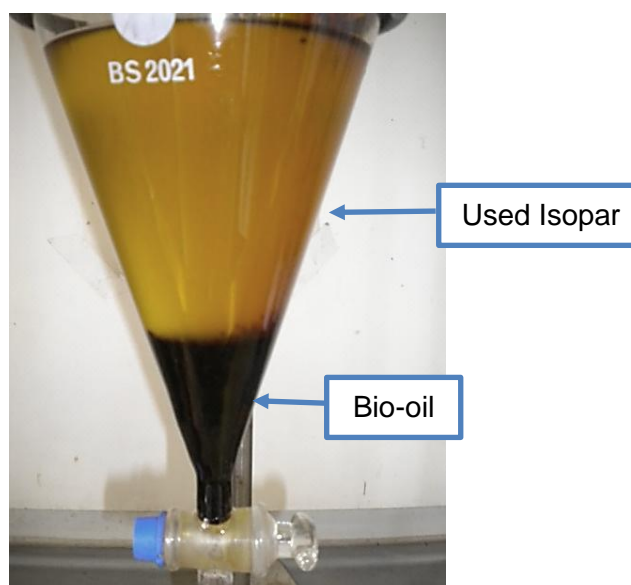
Figure 77: Phase separated Isopar and bio-oil from quench column

High oxygen content bio-oil requires deoxygenation for miscibility with diesel. ZSM-5 based cracking catalysts are expected to deoxygenate the bio-oil and reduce its polarity. Some compounds in deoxygenated bio-oil could become miscible with hydrocarbons like Isopar which could make separation and analysis, of the deoxygenated bio-oil and Isopar mixture, difficult. The quench column has a cooling water jacket to enhance the cooling effect. However, the cooling water alone, without quench liquid would lead to fouling from inefficient quenching of pyrolysis vapours. Though, if upgraded bio-oil only consists of aromatics hydrocarbons such as benzene and toluene, water could be used as the quench liquid as water is immiscible with aromatic hydrocarbons so separation of water from the products would not be an issue. Table 37 summarises the advantages and disadvantages of the glassware and quench collection system.

Table 37: Advantages and disadvantages of the collection systems

Collection system	Advantages	Disadvantages
Glassware	• Good mass balance • No issues with miscibility of quench liquid • No contamination with Isopar • It is obvious when glass is clean	• Fractionated liquid product • Cannot be scaled up
Quench column	• Whole bio-oil • More representative of real bio-oil and can be scaled up • High water content reduces the viscosity of main bio-oil	• Isopar is likely to be miscible with catalytic upgraded products. • Liquid holdup problems • Difficult to tell when the stainless steel is clean. • Weighing problems • Difficult to determine the solid content of an Isopar and bio-oil mixture using method described in section 6.2.1.

Increased water content improves the flow properties of the bio-oil as the viscosity is reduced. The quench column is easy to scale up and produces a more representative whole bio-oil compared to glassware. An ethanol washing method has been proposed and demonstrated to improve the mass balance using the quench column. However, commercially, a wet walled ESP would be used which would reduce the need for ethanol washings. Also, Isopar would be expensive to use as a quench liquid so bio-oil could be used as an alternative quench liquid.

6.3.3 1kg/h rig

Ground SCBP cannot be pneumatically fed into the 100g/h so no results are available from this rig. Ground SCBP were fast pyrolysed on the 300g/h rig with both liquid collection systems and then scaled up on the 1kg/h rig. Table 38 shows the results from these experiments which include details of the feed and the fast pyrolysis products. The quench system collects more liquid bio-oil and less gas compared to the glassware collection system. The total liquid yield from the quench and 300g/h is 75 wt.% compared to 80.21 wt.% for the 1kg/h. As collection of condensed pyrolysis vapours is improved, the average water content of the main bio-oil increases. The mass balance closure was improved with the 1kg/h rig as there was a longer processing time (80 minutes instead of 60 minutes), the ESP was pumped with Isopar and silica gel was added to the process to collect additional moisture and light tars. Also, as the 1kg/h is a larger system and the feed input is much higher, an inaccuracy of a few grams does not significantly affect the mass balance as with the 300g/h rig.

Table 38: Comparing fast pyrolysis product yields from SCBP on three rigs

Rig and collection system	300g/h with glassware and dry walled ESP	300g/h with quench and dry walled ESP	1kg/h with quench and wet walled ESP
Feed moisture (wt.% wet feed basis)	9.62		
Feed ash (wt.% dry feed basis)	2.97		
Average pyrolysis T(°C)	493	503	512
Feed rate (g/h)	207.72	213.41	748.76
Run time (minutes)	60	60	80
Char (wt.% dry feed basis)	17.32	18.31	14.83
Total liquid (wt.%)	73.14	75.00	80.21
Organic liquid (wt.% dry feed basis)	60.45	63.38	63.87
Total water content (wt.%)	12.69	11.62	16.34
Average water content of main bio-oil (wt.%)	7.27	12.61	18.09
Average water content of condensates (wt.%)	51.93	72.22	68.03
Water in the feed (wt.%)	10.64	10.64	10.64
Reaction water (wt.% dry feed basis)	2.05	0.98	5.70
Gas (wt.% dry feed basis)	14.01	10.79	11.69
H_2	0.04	0.03	0.04
CO	4.73	3.09	3.72
Methane	0.54	0.40	0.42
CO_2	5.27	3.87	4.83
Ethene	0.52	0.46	0.39
Ethane	0.48	0.48	0.39
Propene	0.67	0.65	0.53
Propane	0.84	0.89	0.65
n-Butane	0.90	0.93	0.72
Total product out (g)	196.14	200.80	963.03
Total feed in (g)	207.72	213.41	998.35
Recovery (wt.% dry feed basis)	93.83	93.46	96.09

Bio-oil is immiscible with saturated Isopar and due to differences in density, the Isopar floats on top of bio-oil. However, according to tests carried out using the GC-MS, some Isopar still remains in the bio-oil and can cause disturbances in the baseline of the chromatogram. Centrifuging the bio-oil sample for approximately five minutes helped remove the Isopar traces and gave better GC-MS chromatograms for compound identification. These chromatograms and identified compounds are shown in Appendix 1. As expected, the identified compounds from the three rig configurations are similar. The peak area % are summarised by group and are shown in Figure 78. Although the same products are produced from fast pyrolysis, the product distribution of the main bio-oil varies depending on how effectively the pyrolysis vapours are cooled and collected. A quench system allows more effective liquid collection as a whole bio-oil.
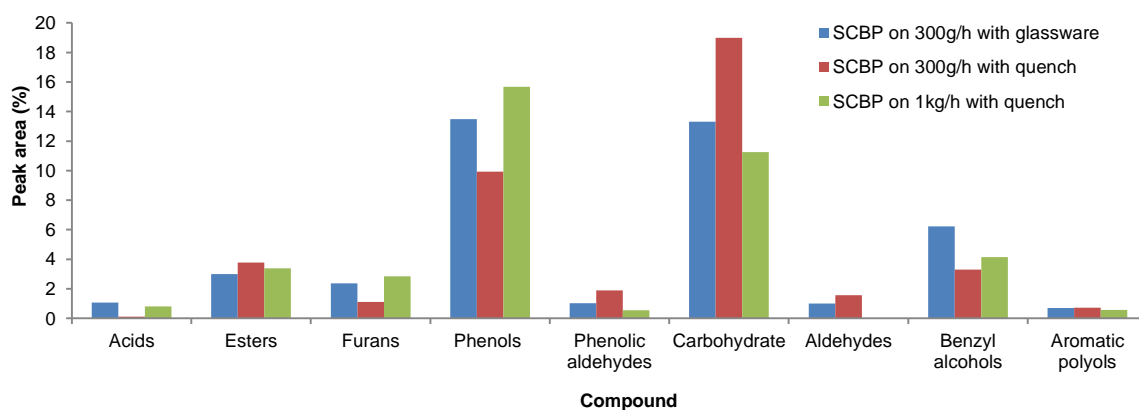
Figure 78: Effect of rig configuration on product distribution

Table 39 shows the PDI for the bio-oil from the three rig configurations used in this study. PDI values range from 1.39 for 1kg/h rig with quench to 1.66 for 300g/h rig with glassware. This data has a close correlation with the viscosity of the bio-oil. The results indicate that there is increased molecular homogeneity when using a quench column instead of the glassware collection system. The homogeneity of the bio-oil also improves when using a wet walled ESP on the 1kg/h rig instead of a dry walled ESP on the 300g/h rig.

Table 39: Molecular weight distribution of main bio-oil from SCBP

Rig and collection system	300g/h rig with glassware	300g/h rig with quench	1kg/h rig with quench
Mp	113	129	258
Mn	145	174	375
Mw	240	272	521
Mz	416	420.5	667
PDI	1.66	1.56	1.39

The viscosity of bio-oil is reported to be 40-100cPA at 50°C [4]. As mentioned earlier, the bio-oil from SCBP was very viscous (2780cP at 40°C) and did not flow due to such low water content (7.27%). To utilise this feedstock, its flow properties need to be improved. Using the quench column on the 300g/h decreased the viscosity to 158-160cP at 40°C, but the viscosity was further decreased to 39.24cP by using the 1kg/h rig. The viscosity reduction is directly related to the increased water content. The bio-oil water content from the 1kg/h rig was 18.09% which is the most commercially representative system.

Figure 79 shows the pH of the main bio-oil and secondary condensates produced on the 3 different rig set ups. As mentioned earlier, Bridgwater [4] reports that the pH of bio-oil is approximately 2.5. These results show a range of pH for the main bio-oil from 2.46 to 2.90. The acidity of the main bio-oil increased with improved collection system as the lighter compounds such as acids are cooled and collected in the main bio-oil rather than in secondary oil pots. The secondary condensates are

consistently more acidic for all rigs. However, the acidity of the secondary condensates decreased with improved collection systems as more acidic compounds were collected in the main bio-oil.
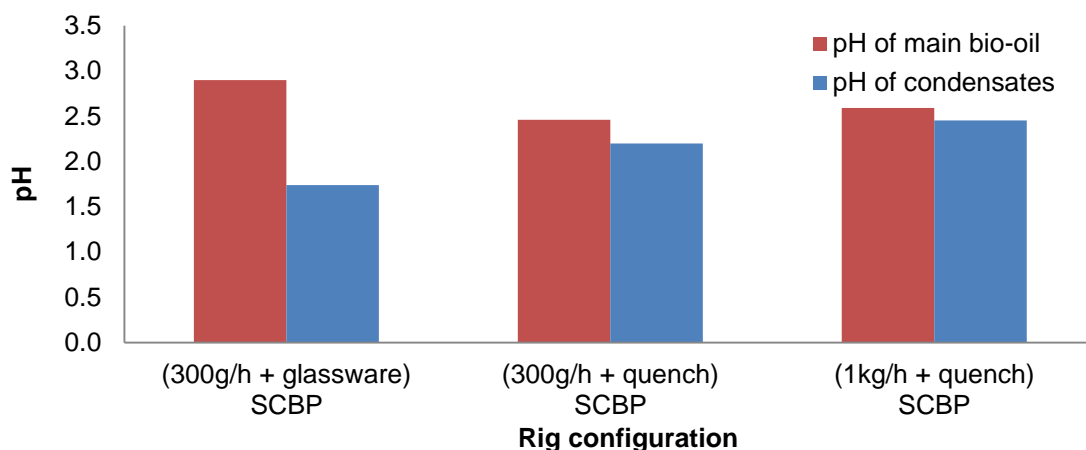
Figure 79: pH comparison of main bio-oil and condensates from 3 different rig set ups

Table 40 compares the water content of the main bio-oil compared with the viscosity. As expected, viscosity decreases with increasing water content as a result of improved liquid collection systems.

Table 40: Water content and viscosity of main bio-oil from SCBP

Rig and collection system	300g/h rig with glassware	300g/h rig with quench	1kg/h rig with quench
Average water content of main bio-oil (wt.%)	7.27	12.61	18.09
Viscosity of main bio-oil (cP at 40°C)	2780	158-160	39.24

Table 41 shows the elemental analysis, ash content and calculated HHV for the bio-oil from SCBP produced using the 3 different rig set-ups. The oxygen content ranges from 40-50 wt.% which is slightly higher than expected, but as expected the oxygen content of the bio-oil increased with increased water content from the quench system. The HHV decreases with improved liquid collection from 22.48 to 19.52 MJ/kg as there was increased water content. However, this reduces the viscosity and improves flow properties.

Table 41: Analysis of bio-oil from SCBP

Rig and collection system	300g/h rig with glassware	300g/h rig with quench	1kg/h rig with quench
C (wt.%)	51.99	47.66	43.35
H (wt.%)	7.25	7.39	7.98
N (wt.%)	<0.10	0.205	0.23
O* (wt.%)	40.76	44.75	48.45
S (wt.%)	Nm	Nm	Nm
Ash (wt.%)	Nm	Nm	Nm
HHV (MJ/kg)	22.48	20.72	19.52

*Oxygen by difference

115

Table 42 shows the elemental analysis, ash content and calculated HHV for the char from SCBP produced using the 3 different rig setups. The char is not expected to vary significantly with rigs. The feedstock particle size and temperature is most likely to determine the level of shrinkage and carbon conversion of the particle.

Table 42: Analysis of char from SCBP

Rig and collection system	300g/h rig with glassware	300g/h rig with quench	1kg/h rig with quench
C (wt.%)	55.44	51.54	54.92
H (wt.%)	2.52	2.53	2.68
N (wt.%)	0.61	0.73	0.45
O* (wt.%)	13.97	16.82	16.83
S (wt.%)	Nm	Nm	Nm
Ash (wt.%)	27.47	28.39	25.13
HHV (MJ/kg)	20.28	18.62	20.05

*Oxygen by difference

Wood such as beech is considered an ideal feedstock for maximum organic liquid yields from fast pyrolysis. Therefore, fast pyrolysis was carried out on the 1kg/h rig with beech as a standard. These results were subsequently compared with ground SCBP (0.25-1mm) to investigate whether ground SCBP are as promising as beech for fast pyrolysis and how the results obtained in this work compared to those achieved commercially. Nitrogen was used to fluidise the bed in this work. However, commercially, non-condensable gases are cleaned and compressed for use as the fluidising gas [103]. Table 43 compares the product yields of SCBP and beech obtained in this work. The results are also compared with wood (average fast pyrolysis results of Brockville poplar, white spruce and red maple) where the non-condensable gases were used for fluidisation instead of nitrogen. It can be seen that the organic liquid derived is 60.64 wt.% from beech, 63.87 wt.% from SCBP and 65.8 wt.% from wood reported in literature. Therefore, the results obtained in this work on the 1kg/h rig are comparable to those obtained commercially and confirms that SCBP can match the organic liquid yields derived from wood.

Table 43: Comparison of product yields from fast pyrolysis of SCBP, beech and wood

Feedstock	SCBP	Beech	Averages reported from wood* [103]
Feed moisture (wt.% wet feed basis)	9.62	12.08	6.03
Feed ash (wt.% dry feed basis)	2.97	0.82	
Average pyrolysis T(°C)	512	510	504
Fluidising gas	N_2	N_2	Non-condensable gases
Feed rate (g/h)	748.76	903.75	2000
Run time (minutes)	80	80	-
Char (wt.% dry feed basis)	14.83	14.35	14.15
Total liquid (wt.%)	80.21	81.36	
Organic liquid (wt.% dry feed basis)	63.87	60.64	65.8
Total water content (wt.%)	16.34	20.72	-
Average water content of main bio-oil (wt.%)	18.09	22.77	-
Average water content of condensates (wt.%)	68.03	69.83	-
Water in the feed (wt.%)	10.64	13.74	-
Reaction water (wt.% dry feed basis)	5.70	6.97	10.4
Gas (wt.% dry feed basis)	11.69	10.53	9.7
H_2	0.04	0.02	0.02
CO	3.72	3.39	4.2
Methane	0.42	0.81	0.4
CO_2	4.83	4.27	4.7
Ethene	0.39	0.31	0.17
Ethane	0.39	0.45	-
Propene	0.53	0.54	-
Propane	0.65	0.74	-
n-Butane	0.72	0.01	-
Total product out (g)	963.03	1125.54	-
Total feed in (g)	998.35	1205.00	-
Recovery (wt.% dry feed basis)	96.09	92.50	100

*Brockville poplar, white spruce and red maple

6.4   Interim conclusions

- The 100g/h rig can be used to screen feedstocks when there is limited availability of feedstocks. The 100g/h rig pneumatic feeding system cannot be used to feed fibrous feedstocks such as sugarcane bagasse and fine powder feedstocks such as AHR into the top of the fluidised bed reactor due to blockages in the feeder tube and the fluidised bed.

- Screw feeding biomass through a water cooled screw into the side of the reactor is more versatile and reliable than feeding into the top of a fluidised bed reactor. Therefore, the 300g/h rig with a screw feeding system is a suitable size system which can be used to screen feedstocks without the need for significant amounts of sample preparation or rig cleaning.

- Ground SCBP was the most promising feedstock producing 60.45 wt.% organic liquid on a dry feed basis from fast pyrolysis on the 300g/h rig with the glassware collection system. The bio-oil oxygen content from ground SCBP was one of the lowest (40.76 wt.%) which is more suited for catalytic upgrading to further

deoxygenate the bio-oil. The bio-oil HHV was also the highest (22.48MJ/kg). There were no problems with screw feeding ground sugarcane bagasse pellets. Densified material such as ground sugarcane bagasse pellets is preferred to loose sugarcane bagasse for more reliable feeding and improved biomass throughputs (207.72g/h).

- Using the glassware collection system ensures a good mass balance closure of approximately 95%. Ethanol washing of the quench system on the 300g/h rig, after an experiment, has been demonstrated to improve the mass balance using the quench column.

- The mass balance closure on the 1kg/h rig was improved by around 5% with the addition of silica gel which recovers more light tars and moisture.

- The quench column is easy to scale up and produces a more representative whole bio-oil compared to the glassware collection system.

- The 1kg/h rig is more representative of a commercial fast pyrolysis unit as it produces a whole bio-oil with reduced viscosity and improved flow properties. However, the smaller scale 300g/h rig can be used with the glassware collection system to approximate the product yields expected from larger scale fast pyrolysis processing.

- The 300g/h rig with glassware collection system is the most suitable for catalytic pyrolysis tests as there are no issues of miscibility or contamination of upgraded liquid products with quench liquids.

7   CATALYTIC PYROLYSIS OF BIOMASS

The objective of this chapter is to assess whether a novel supported molybdenum carbide catalyst, (20 wt.% Mo_2C/Al_2O_3), which has a noble metal behaviour, [152] but without the scarcity and cost issues of noble metals, can potentially be used to improve some of the physical properties of bio-oil under fast pyrolysis conditions. Noble metals are widely researched for hydrotreating [153]. However, the advantage of using catalytic fast pyrolysis rather than hydrotreating is that hydrogen and high pressures are not required. Bio-oil has some unattractive properties which mean that it usually requires upgrading before it can be used for direct use in heat and power applications. Bio-oil upgrading usually aims to improve properties such as a heating value, oxygen content, water content, viscosity and pH.

7.1   Methodology

Ground SCBP were used for catalytic fast pyrolysis experiments as high organic yields can be achieved from fast pyrolysis of this feedstock. The 20 wt.% Mo_2C/Al_2O_3 catalyst was prepared within COPPE at Universidade Federal do Rio de Janeiro (UFRJ) in Brazil. Transition metal carbides have a pyrophoric nature and if the sample was removed from the reactor after the carburization procedure it would ignite completely oxidising the carbidic phase. Therefore, the catalyst was stored in i-octane to allow its transportation and loading into the fluidised bed reactor without carbide oxidation. Mo_2C/Al_2O_3 was removed from the storage bottle, i-octane was drained and mixed with the sand used as the heat carrier in the fluidised bed in different proportions (0 wt.%, 12 wt.%, 25 wt.% and 50 wt.%) to investigate the effect of this catalyst on the pyrolysis products.

7.1.1   Py-GC-MS

Py-GC-MS is a micro-scale analytical pyrolysis technique where a pyroprobe is used to thermally degrade a few milligrams of sample while gas chromatography and mass spectroscopy are used to identify and quantify the compounds present in the degradation products. Although this system can be used to identify chemicals present in the pyrolysis vapours, it cannot be used to indicate the solid, gas and liquid yields which are an important factor defining the applicability of fast pyrolysis to a particular feedstock. Initial screening tests were carried out on a Py-GC-MS to investigate the activity of Mo_2C/Al_2O_3 before scaling up on the 300g/h continuous laboratory scale reactor.

A Perkin Elmer CDS 5000 Series Pyroprobe (model 5200) close coupled with a Perkin Elmer Clarus 680 Gas Chromatograph and a Clarus 600S Mass Spectrometer was used for this work. The temperature and heating rates are important to simulate

fast pyrolysis; the temperature was set at 500°C and the heating rate at 500ºC/s. The hold time was 30 seconds. Approximately 2mg of ground SCBP (particle size <0.25mm) was placed in a quartz filler rod. The column for the gas chromatograph was an Elite 1701, 30m length, 0.25 mm i.d., 0.25 µm film thickness. Helium was used as a carrier gas with a split ratio of 1:125. The GC oven programme operated at 50 ºC for 2 minutes and then the temperature was ramped up to 280 ºC at a rate of 5 ºC/min. The hold time was 7 minutes. The injector and detector temperatures were set to operate at 300 ºC. The peaks from these experiments were identified using a NIST98 mass spectra database. The experiment was repeated with a 1:1 mass ratio of molybdenum carbide to SCBP.

7.1.2 Catalytic fast pyrolysis on the 300g/h fluidised bed system

The primary objective of this work was to evaluate the influence and viability of replacing different proportions (0 wt.%, 12 wt.%, 25 wt.%, and 50 wt.%) of a 20 wt.% Mo_2C/Al_2O_3 catalyst directly into a fast pyrolysis fluidised bed reactor. A detailed description of the 300 g/h continuous screw fed fluidised bed fast pyrolysis system and glassware collection system that was used in these experiments can be found in section 6.2.2.

The reactor contains 150 g of sand as the fluidising medium and was replaced with different proportions of catalyst (0 wt.%, 12 wt.%, 25 wt.%, and 50 wt.%). Molybdenum carbide can potentially be used in hydrotreating with hydrogen and pressure. Due to safety reasons, hydrogen could not be added to the existing fast pyrolysis fluidised bed reactor so it was not possible to test molybdenum carbide under hydrotreating conditions in the absence of pressure. Catalytic fast pyrolysis could only be conducted using conventional nitrogen as a fluidising and carrier gas.

The bulk density of the sand, catalyst, feedstock and char was determined to ensure correct fluidisation of the bed material and ensure that sand and catalysts were retained in the reactor and the char was entrained out of the reactor. The bulk density of the ground SCBP, char, catalyst and sand were determined experimentally using the method detailed in section 3.3. The nitrogen flow required to efficiently fluidise the reactor bed was subsequently determined.

Bio-oil characterisation was carried out using the methods detailed in section 6.2.4. This included determining the bio-oil solid content, water content, pH, elemental analysis, viscosity and molecular weight distribution. Compounds present in the bio-oil were also identified by GC-MS.

7.2 Results and discussion

Table 44 shows that the bulk density of the sand, catalyst and ground SCBP is much higher than that of the char. Fluidisation velocity was successfully controlled to entrain char, but retain the sand, catalyst and unpyrolysed ground SCBP in the fluidised bed reactor.

Table 44: Sand, catalyst, feedstock and char bulk densities

	Bulk density (kg/m^3)
Sand (0.5-0.6mm)	1638.30
Catalyst Mo$_2$C (~ 0.6mm)	638.09
Ground SCBP (0.25-1mm)	1086.10
Char from fast pyrolysis of ground SCBP	313.48

7.2.1 Py-GC-MS

The chromatograms from the Py-GC-MS experiments which indicate that the catalyst has significant effect on the product composition at 500°C can be found in Appendix 2. Figure 80 summarises the peak area % of product groups obtained from fast pyrolysis of SCBP with and without catalyst. It can be seen that acids, ketones, esters and furanics increase while phenolics, phenolic aldehydes and carbohydrates decrease.
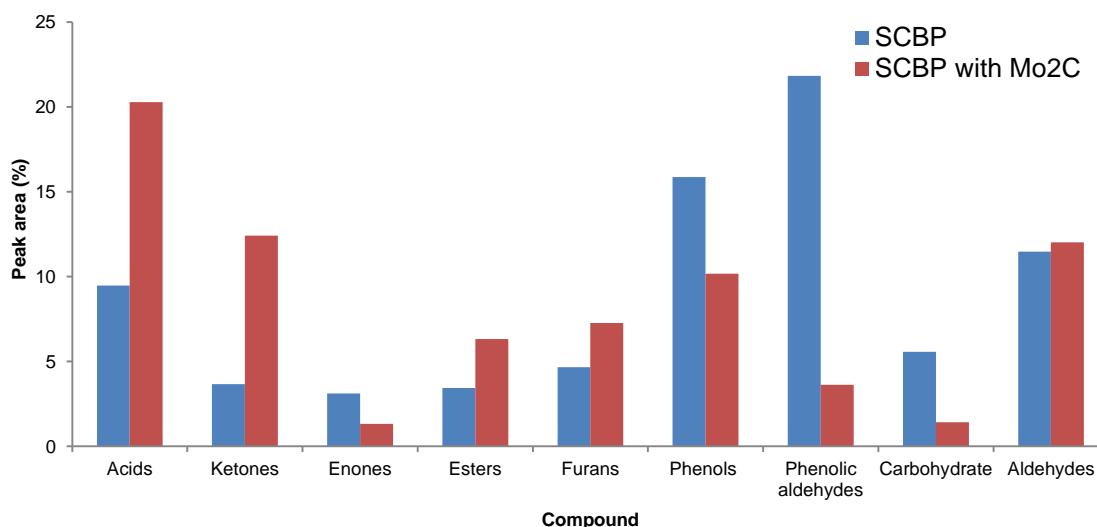
Figure 80: Variation of the pyrolysis product composition with addition of catalyst

The compounds identified and calculated peak areas are shown in Appendix 2. It should also be noted that using peak areas to quantify products is not ideal as only small sample is analysed so not all compounds are identifiable. Although all of the products in the pyrolysis vapour stream are detected, the product distribution obtained from Py-GC-MS cannot be used to predict the products and quantities obtained on large scale systems as the liquid collection system has a significant effect on the liquid product composition. For example, on both the 300g/h and 1kg/h rig, pyrolysis vapours are fractionated as main bio-oil and secondary condensates are collected separately.

Also, the catalyst and biomass interactions in a Py-GC-MS system are not representative of the interactions occurring in a fluidised bed reactor. Py-GC-MS can be used to carry out a significant number of valuable comparative tests. However, Py-GC-MS results are of limited value in this work as they cannot give estimations on product yields produced from fast pyrolysis.

7.2.2 Catalytic fast pyrolysis on the 300g/h fluidised bed system

Table 45 shows char, liquid and gas product yields from the pyrolysis of ground SCBP using increasing proportions of molybdenum carbide catalyst. All mass balance closures are greater than 90 wt.%.

Table 45: Catalytic pyrolysis of ground SCBP at 500°C

Weight % of Mo_2C catalyst	0 wt.%	12 wt.%	25 wt.%	50 wt.%
Feed moisture (wt.% wet feed basis)	9.62			
Feed ash (wt.% dry feed basis)	2.97			
Char (wt.% dry feed basis)	17.32	16.49	28.82	27.13
Total liquid (wt.%)	73.14	66.41	60.70	61.71
Organic liquid (wt.% dry feed basis)	60.45	49.45	43.33	39.30
Total water content (wt.%)	12.69	16.96	17.37	22.41
Reaction water (wt.% dry feed basis)	2.05	6.34	6.75	11.79
Water in the feed (wt.%)	10.64	10.62	10.62	10.62
Bio-oil water content from oil pot 1	7.30	18.50	24.20	33.80
Condensates water content from oil pots 2 and 3	51.90	61.70	64.70	66.10
Phase separation	NO	NO	NO	NO
Gas (wt.% dry feed basis)	14.01	20.14	19.63	14.47
H_2	0.04	0.21	0.34	0.10
CO	4.73	7.87	6.55	5.27
Methane	0.54	0.75	0.68	0.53
CO_2	5.27	7.27	7.19	4.84
Ethene	0.52	0.65	0.68	0.50
Ethane	0.48	0.54	0.65	0.51
Propene	0.67	0.81	0.99	0.77
Propane	0.84	0.90	1.13	0.90
n-Butane	0.90	1.14	1.43	1.06
Total product out (g)	196.14	171.77	144.57	185.69
Total feed in (g)	207.72	184.42	146.51	198.84
Recovery (wt.% dry feed basis)	93.83	92.41	98.53	92.69

Figure 81 shows that by increasing the amount of molybdenum carbide in the reactor from 0% to 50% reduced the organic liquid yield from 60.45 wt.% to 39.30 wt.% and increased the total water content from 12.69 wt.% to 22.41 wt.%. The decrease in organic yield was probably due to catalytic cracking of the vapours and the increase in water was likely to be associated with deoxygenation. Bio-oil needs to be deoxygenated for miscibility with diesel. Catalytic pyrolysis is expected to increase the water formed during dehydration reactions, but the more favourable hydrocarbons produced are likely to phase separate from water. However, the organic liquid produced in this work is miscible with the aqueous liquid and therefore indirectly increases the overall oxygen content of the bio-oil with increasing catalyst

concentration. Oasmaa et al. report that phase separation of the bio-oil is likely to occur when the water content is greater than 30 wt.% [100]. However, when using 50 wt.% molybdenum carbide, the water content of the bio-oil was 33.80 wt.% (dry feed basis) and no phase separation was observed.
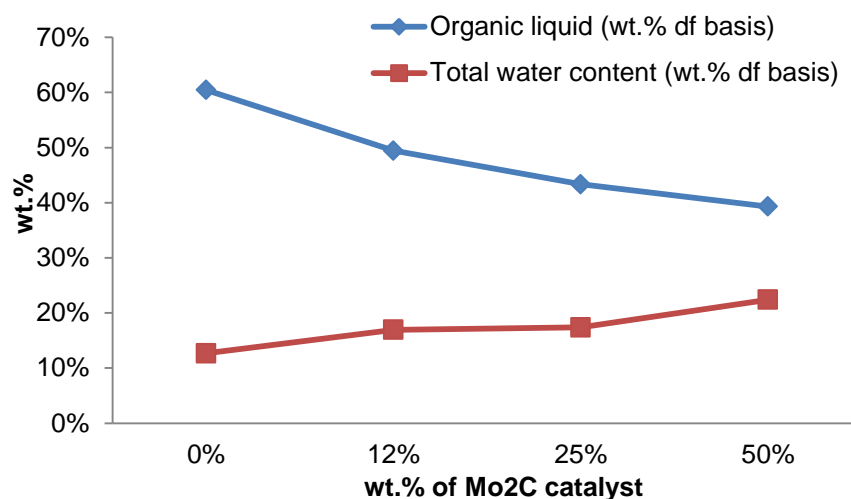
Figure 81: Effect of catalyst concentration on organic and water content

Table 46 shows a substantial reduction in bio-oil viscosity from 2780 to 8.2cP at 40°C with increasing molybdenum carbide concentration. This reduction in viscosity can be partly attributed to the increased water content, suggesting that the presence of molybdenum carbide in the fluidised bed promotes oxygen removal mainly by water formation and not by decarbonylation and/or decarboxylation as reported for other catalysts [154].

Table 46: Viscosity and pH analysis of bio-oil and secondary condensates from catalytic pyrolysis of SCBP with Mo2C

Catalyst concentration	Bio-oil viscosity (cP) @ 40 ^{o}C	Bio-oil pH	Condensates pH
Sand (0 wt.% Mo_2C)	2780	2.71	1.82
12 wt.% Mo_2C	71.5	2.82	1.6
25 wt.% Mo_2C	19.7	2.49	2.15
50 wt.% Mo_2C	8.2	2.49	2.43

Table 47 shows the elemental analysis and calculated bio-oil HHV obtained using increasing catalyst concentrations. The ash content of the bio-oil was not measured and is expected to be near to zero as most ash is associated with the char [103]. Oxygen is calculated by difference. The oxygen content ranges from 40-50 wt.% which is as expected. The HHV ranges from 19.18MJ/kg with 25 wt.% catalyst concentration to 22.48MJ/kg with no catalyst. The HHV is associated with the oxygen content as a result of the water content of the bio-oil. In the conditions used in fast pyrolysis and with the absence of hydrogen and pressure, Mo_2C/Al_2O_3 does not produce deoxygenated bio-oil therefore is not miscible with diesel.

Table 47: Elemental analysis of bio-oil from catalytic pyrolysis of SCBP with Mo$_2$C

Catalyst concentration	C (wt.%)	H (wt.%)	N (wt.%)	O* (wt.%)	S (wt.%)	Ash (wt.%)	HHV (MJ/kg)
Sand (0 wt.% Mo$_2$C)	51.99	7.25	<0.10	40.76	Nm	Nm	22.48
12 wt.% Mo$_2$C	47.99	7.64	0.34	44.025	Nm	Nm	21.20
25 wt.% Mo$_2$C	44.24	7.39	0.40	47.98	Nm	Nm	19.18
50 wt.% Mo$_2$C	48.12	7.83	0.25	43.81	Nm	Nm	21.29

*Oxygen by difference

Figure 82 shows the effect of catalyst concentration on bio-oil composition identified by GC-MS analysis. The figure shows a distinct reduction in the levoglucosan peak at approximately 25 minutes.
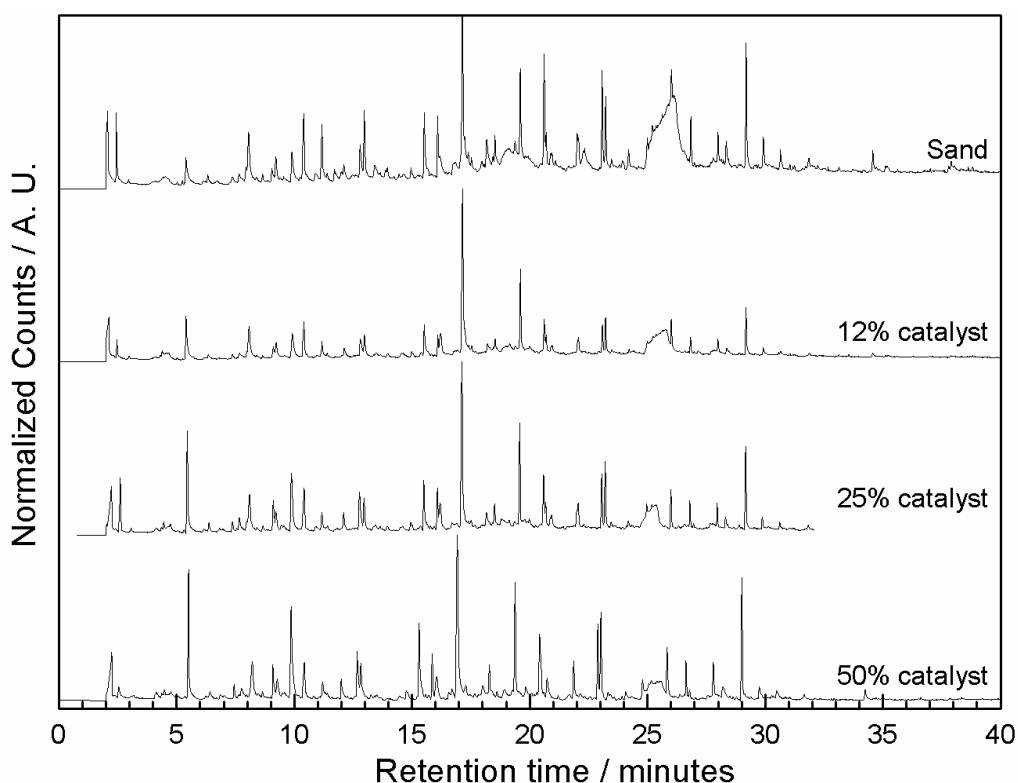
Figure 82: Effect of catalyst concentration on bio-oil composition

Figure 83 shows that while there was a decrease in the yield of sugars (mainly levoglucosan) from 7.15 wt.% to 2.16 wt.% an increase of furans from 1.48 wt.% to 2.43 wt.% and increase in phenols from 3.97 wt.% to 6.51 wt.% occurred. The increase in furanics has been related to the decrease of the levoglucosan [155]. The increase in phenolics can be attributed to a catalytic breakdown of the lignin by the molybdenum carbide.
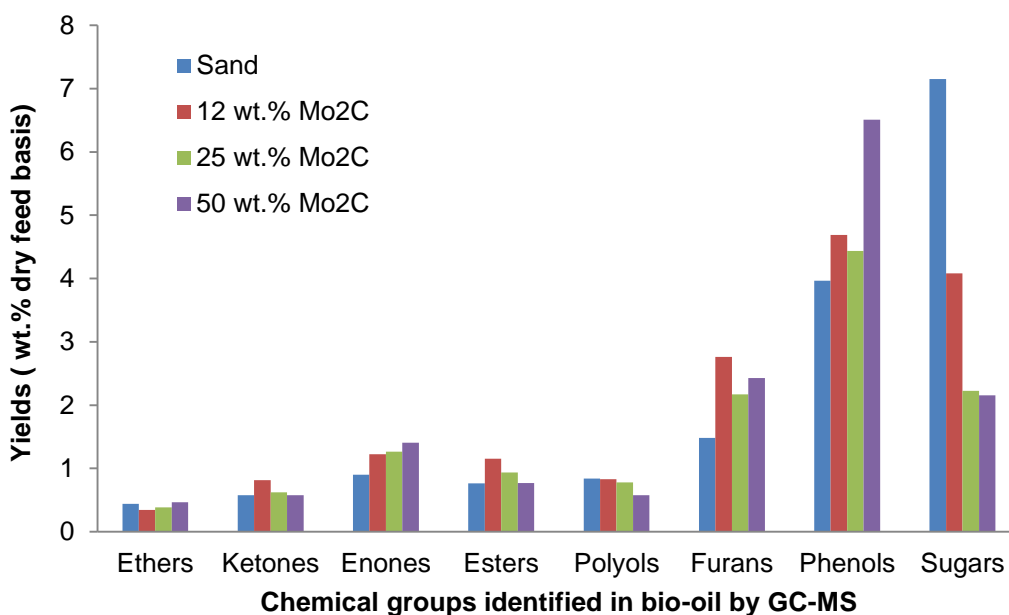
Figure 83: Variation of the bio-oil composition as a function of catalyst amount

Bio-oil molecular weight distribution can be analysed using gel permeation chromatography as described in section 6.2.4. Higher Polydispersity Index (PDI) values indicate a lower molecular homogeneity [92]. Table 48 shows the PDI for the bio-oil from SCBP with increasing concentrations of Mo_2C catalyst. PDI values range from 1.66 for no catalyst to 1.41 for 12, 25 and 50 wt.% catalyst. The results indicate that there is improved molecular homogeneity when introducing Mo_2C catalyst to the fast pyrolysis process, however the homogeneity stabilises above 12 wt.% catalyst concentration.

Table 48: GPC data of bio-oil from catalytic pyrolysis of SCBP with Mo_2C

Catalyst concentration	Mn	Mp	Mw	Mz	PDI
Sand (0 wt.% Mo_2C)	145	113	240	416	1.66
12 wt.% Mo_2C	255	233	359	476	1.41
25 wt.% Mo_2C	238	230	335	455	1.41
50 wt.% Mo_2C	216	164	305	415	1.41

7.3 Interim conclusions

- Py-GC-MS can be used to investigate catalyst effect on product composition to a certain extent. However, Py-GC-MS is of limited value in this work as the results cannot give estimations on product yields produced from fast pyrolysis. Also, the product distribution obtained from Py-GC-MS cannot be used to predict the products and quantities expected on large scale systems as the liquid collection system has shown to have a significant effect on the liquid product composition. It should also be noted that using peak areas to quantify products is not ideal as only small sample is analysed so not all compounds are identifiable.

- The 300g/h rig is a suitable size system which can be used to screen feedstocks and catalysts to give acceptable mass balance closures of approximately 95%

and realistic product yields believed to be representative of those achievable on a larger and/or commercial scale. The glassware collection system is more suited for catalytic pyrolysis as there are no problems of miscibility with hydrocarbons in upgraded bio-oil.

- Direct addition of Mo_2C/Al_2O_3 into a fast pyrolysis fluidised bed reactor does not deoxygenate bio-oil, but reduces the organic content and increases the water content of the liquid product. Mo_2C/Al_2O_3 improves the viscosity and homogeneity of bio-oil which is important if liquid bio-oil is to be further upgraded as the lower viscosity can facilitate the flow in a hydrotreater operated in trickle-bed regime.

- An increased concentration of molybdenum carbide reduces the concentration of sugars (levoglucosan) and increases the concentration of furanics and phenolics for production of speciality chemicals.

8 THEORY AND LITERATURE REVIEW: GASIFICATION AND GAS UPGRADING

The objective of this chapter is to present the theory and literature review of gasification and gas upgrading. Gasification of the feedstocks described in Chapter 2 is of particular interest in this work for the production of bioenergy and/or biofuels.

8.1 Background

Biomass gasification has been practised for decades with the aim of converting solid carbonaceous feedstocks into a combustible product gas at elevated temperatures. Figure 84 shows the overall gasification process from biomass or residues to fuels, heat and power. A solid residue (containing unreacted carbon and ash) and tars are produced as by-products from gasification. The undesirable tars are removed by gas cleaning techniques discussed later in section 8.6.

| Biomass or residues | Gasification → | Product gas | Gas cleaning → | Fuels or heat & power |

Figure 84: Biomass gasification process

Gasification typically includes a drying, pyrolysis, combustion and gasification stage [156] [157].

1. Drying: moisture is removed which may be used in later reactions
2. Pyrolysis: release of volatiles to produce char, tar and gas in the absence of oxygen.
3. Combustion: partial oxidation of volatiles and char with air/oxygen/steam.
4. Gasification: partial oxidation of char, tars and pyrolysis gases.

Gasification can be pyrolytic or oxidative and these differ in the way process heat is provided to the gasifier to produce a gaseous energy carrier in the form of a product gas. Heat from an external source/combustion of by-products can aid pyrolytic gasification which reduces by-product yields. On the other hand, heat from partial oxidation of the feedstock, using air, steam or oxygen or a mixture of these, can aid oxidative gasification.

Figure 85 shows the energy flow in and out of a gasifier. External energy is initially supplied to the gasifier for the drying and pyrolysis steps. Energy is also added to the system in the form of feed and gasification agent. The energy from the

exothermic combustion step subsequently provides sufficient energy to initiate the final gasification step.
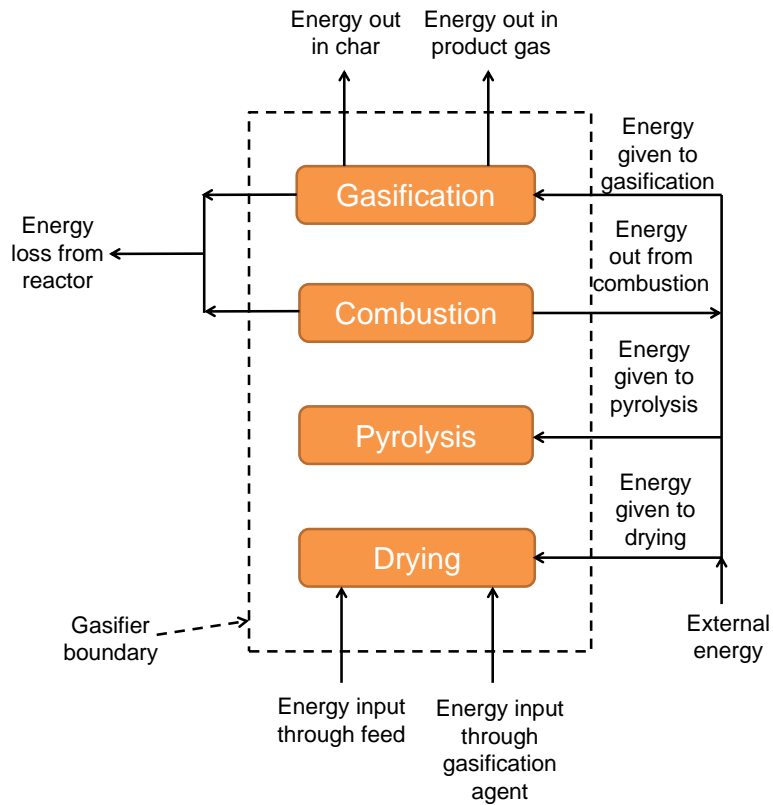
Figure 85: Energy flow in and out of a gasifier (adapted from [156])

The gasifier performance indicators used in this work are gas yields, gas HHV, carbon conversion efficiency and cold gas efficiency. The typical product yields from gasification of wood can be found earlier in Table 13. Oxidative gasification produces the highest gas yields (95-99%) [67]. However, pyrolytic gasification can also be used to produce high yields (85 wt.%) of gas from wood, without the addition of an oxidant. Gas yields are strongly dependent on various process and feedstock variables which are discussed in sections 8.2 and 8.3.

High yields of low energy content gas (<4 MJ/Nm^3) can be obtained from gasification, but such gas is not suitable for the production of biofuels. Therefore, there is a trade-off between gas yields and gas quality. Gas application needs to be specified in order to identify the gas quality required from gasification. Figure 86 shows the applications of gaseous products from gasification.
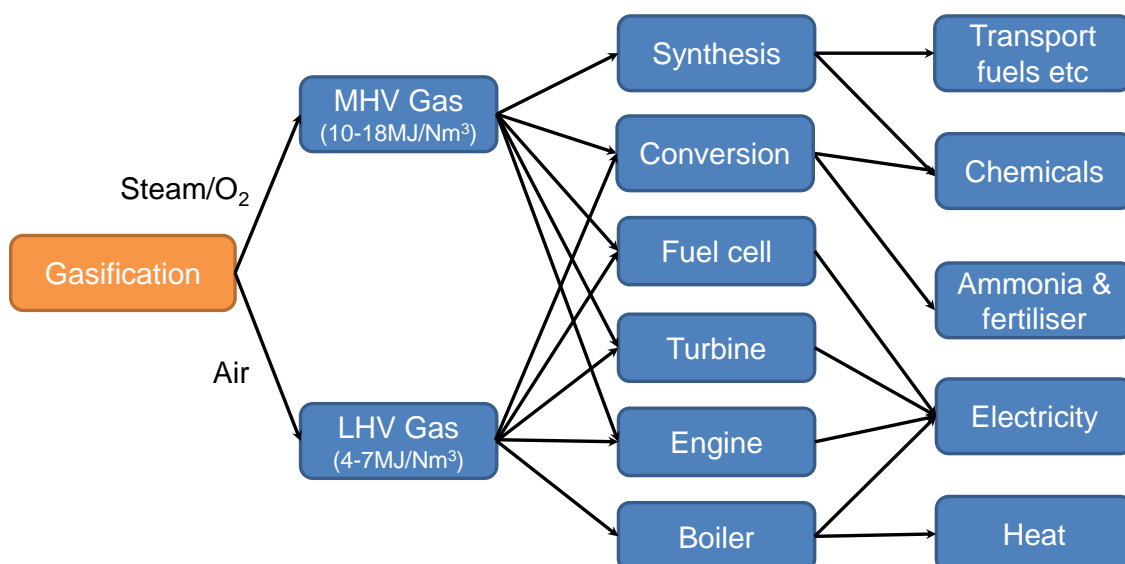
Figure 86: Applications of product gas from gasification (adapted from [66])

Product gas from gasification can either be a fuel gas or syngas (synthesis gas). Fuel gas is a low energy content gas from air-blown gasification usually containing CO, H_2, CO_2, CH_4 and small amounts of hydrocarbons such as ethene, ethane, propene, propane and water. As air is used, the combustible gas components in fuel gas are diluted with nitrogen which significantly lowers the gas HHV (4-7 MJ/Nm^3). Fuel gas is suitable for boilers, engines and turbine operation to ultimately produce heat or electricity, but cannot be transported through dedicated pipelines [158]. Fuel gas can be used in diesel or gasoline engines with minor modifications [69]. However, it can also be used as a synthesis gas in the production of chemicals such as ammonia or methanol. Syngas (synthesis gas) is a better quality medium energy content gas (10-18 MJ/Nm^3) from oxygen blown or steam gasification containing mainly CO and H_2 [159]. Syngas is more suited for transportation through dedicated pipelines [158]. Cleaned syngas could be used to produce fuels (e.g. ethanol, methanol, naptha, hydrogen, gasoline and diesel) or chemicals (e.g. acetic acid, dimethyl ether, and ammonia) [68, 122]. Pyrolytic gasification, without an oxidant, can also produce gases with medium heating value (17-19 MJ/Nm^3) [65].

Carbon conversion efficiency indicates the amount of carbon in the feed that was successfully converted into a carbon bearing gas such as CO, CO_2 and CH_4. Typical carbon conversion from fixed bed and entrained flow gasification can be as high as 99% [160]. However, carbon conversion of only 97% can be achieved in existing fluidised bed processes [160] due to the entrainment of fine char particles and temperature limits. The use of pressurised gasification has been reported to increase the carbon conversion efficiencies of fluidised bed gasifiers to 99% [160]. Although high conversion of biomass into gas is reported, conversion is limited as once char particles

continue to shrink, the resultant dust is entrained into the gas stream [67]. Higher conversion efficiencies can be achieved by combustion of the tars and solids.
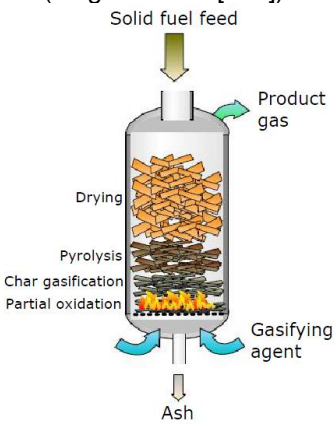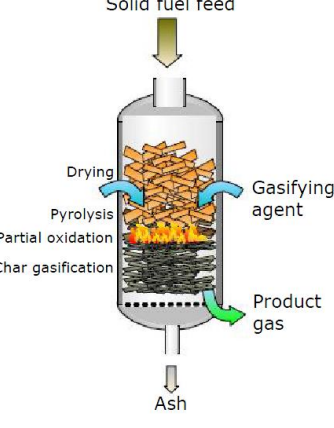
Cold gas efficiency can be used to determine the energy available in the product gas as a ratio of the energy in the original feed. Cold gas efficiencies of approximately 80% are achievable in fixed bed and entrained flow gasifiers [156, 161]. The other 20% is recoverable sensible heat, heat loss and energy remaining in tars and unreacted solids. In the case of fluidised beds, cold gas efficiencies of 89% can be achieved [156]. Work carried out by Cao et al. report cold gas efficiencies as low as 39-59% from air-blown gasification [162].
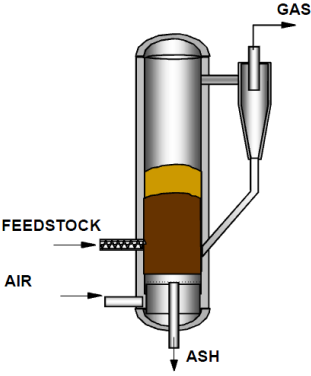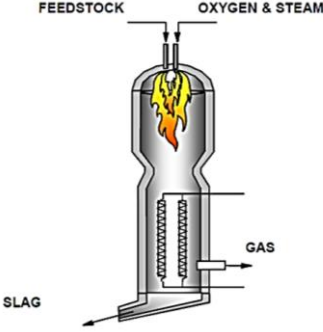
8.2 Gasification process variables

Pereira et al. has recently extensively reviewed the gasification technologies currently available for converting biomass into product gas. It is also broadly agreed that the quantity and quality of the product gas is influenced by process variables such as gasifier type, pressure, gasification agent, temperature, equivalence ratio and feedstock variables such as biomass type and particle size [163]. Catalyst addition is also viewed as necessary to optimise the gasification process and this is discussed later in section 8.6.

A suitable continuous gasifier is not available at Aston University for gasification of AHR. However, gasifier selection is critical and should be matched to feed characteristics and application. Gasifier classification is based according to their gas-solid contacting mode [156] and the three main gasifier designs are fixed bed, fluidised bed and entrained flow. The gasification medium conveys feed through fluidised beds and entrained flow gasifiers. However, the feed is added through the top and is supported on a grate in fixed bed gasifiers [156]. Table 49 shows the advantages and disadvantages of these gasifier designs.

Table 49: Advantages and disadvantages of various gasifiers (derived from [156, 164-167])

Type of reactor; Gasification agent; T(°C)	Advantages	Disadvantages
Fixed bed updraft (counter current flow); Air; 700-900°C (diagram from [168]) Solid fuel feed Product gas Drying Pyrolysis Char gasification Partial oxidation Gasifying agent Ash	• Good thermal efficiency • Easy control of temperature • Simple construction, Inexpensive • Suitable for feed with high ash (up to 25 wt.%), high moisture (up to 60%) • Small pressure drop • Low gas exit temperature (200-400°C) • High carbon conversion, low ash carry over • Can be operated under pressure	• Product gas is diluted with nitrogen • Very high tar content gas (30-150g/Nm^3) • Limited to 10MWth fuel input • Limited to approx. 60t/d each unit • Poor mixing • Poor heat transfer • Not feasible for small particles • Bridging or channelling of feed possible • Ash fusion/clinkering on grate • Potential channelling
Fixed bed downdraft (co-current flow); Air; 700-1200°C (diagram from [168]) Solid fuel feed Drying Pyrolysis Partial oxidation Char gasification Gasifying agent Product gas Ash	• Low tar content gas (0.015-3.0g/Nm^3) • Simple construction, Inexpensive • High carbon conversion, low ash carry over • Quick response to load changes	• Product gas is diluted with nitrogen • Not feasible for small particles • Moisture (25 wt.% max.) and ash content (6 wt.% max) of feedstock is very critical • Poor mixing • Poor heat transfer • High gas exit temperature (700°C) • Limitation on scaling up (<5MW$_{th}$) • Limited to <6t/d each unit • Requires multiple units for even small applications • Design tends to be tall • Bridging or channeling of feed possible • Ash fusion/clinkering on grate

Type of reactor; Gasification agent; T(°C)	Advantages	Disadvantages
Fluidised bed (Circulating or bubbling); Air or steam; <900°C (diagram from [169])	• Good temperature control • Bed material acts as a heat carrier or catalyst • Flexible feed type, feed rate, particle size, moisture and ash content • High throughput • Can be operated under pressure • CFB can process approx. 500t/d	• Medium tar content • Lower thermal efficiencies • Erosion and corrosion problems • Particle entrainment • Large pressure drop • High gas exit temperature • Carbon loss with ash • Operating temperature limited by ash clinkering • BFB limited to approx. 200t/d • Limited experience with biomass
Entrained flow; A mixture of oxygen and steam; >1200°C (diagram from [169])	• Can process fine particles-flexible to feedstock • Low methane gas and low tar content • low residence time • High temperatures above melting point of ash decomposing all tar. • High carbon conversion • Can be built as small as required • No size limits • Extensive experience with coal and some with biomass	• Very complex operation • High oxygen requirements • Gas cooling required due to very high gas exit temperature • High temperatures require special materials of construction • Ash slagging • Grinding biomass is expensive

The flow of gasification agent can be either updraft or downdraft. In an updraft gasifier, the gas is cooled through the drying zone at the top. However, in a downdraft gasifier the hot product gas passes through a hot char bed [62]. Therefore, the temperature of the exit gas from a downdraft gasifier is much higher (700°C) than for an updraft gasifier (200-400°C). In a downdraft gasifier, the product gas passes through a hot char bed which cracks tars and acts as a filter. Although downdraft gasifiers produce a relatively clean gas, they are not suitable for processing fine particles such as AHR or for large scale processing.

The main focus for large scale demonstration and commercial biomass gasification plants has been on fluidised beds rather than fixed beds due to the scalability and feed properties requirement [158]. Carbon conversion is an issue with fluidised beds due to the entrainment of fine char particles and temperature limits. A tall

freeboard could overcome this problem, but as there are cost issues with this option, most fluidised bed gasifiers return entrained char back to the gasifier using a cyclone and recycle system [156].

An entrained flow gasifier requires fine particles for complete conversion in the very short reaction times. This may be suitable for processing AHR powder, but there are high costs associated with the high oxygen requirements and high temperature resistant materials of construction. Raw gas cooling is also a problem with entrained flow gasifiers as the hot product gas requires the use of downstream heat exchangers or water quench. However, these heat exchangers recover the heat and produce superheated steam for gasification [156]. A larger reactor length is required for an entrained flow gasifier as the relatively slow char gasification reactions require longer reaction times for complete carbon conversion [156].

Table 50 shows the typical gas compositions from the different gasifier types identified above. Tar formation from a downdraft gasifier is reported to be higher (10-150 g/Nm^3)than that for an updraft gasifier (0.01-6 g/Nm^3) in Table 50. However in reality, there are fewer tars from downdraft gasification as the product gas passes through a hot char bed which cracks tars and acts as a filter. The LHV reported in this table are also dependent on other process variables such as pressure, gasification agent, temperature and equivalence ratio. These are discussed in sections 8.2.

Table 50: Typical gas composition from different gasifier types [62]

Figure 87 shows the status of the gasification technologies based on technology strength and market attractiveness. It can be seen that fluidised bed gasifier design are the most promising and one of the most popular gasifiers [156] compared to fixed bed and entrained bed gasifiers. Fluidised beds are preferred due to the scalability and flexibility in feed properties requirement [158].

TECHNOLOGY STRENGTH
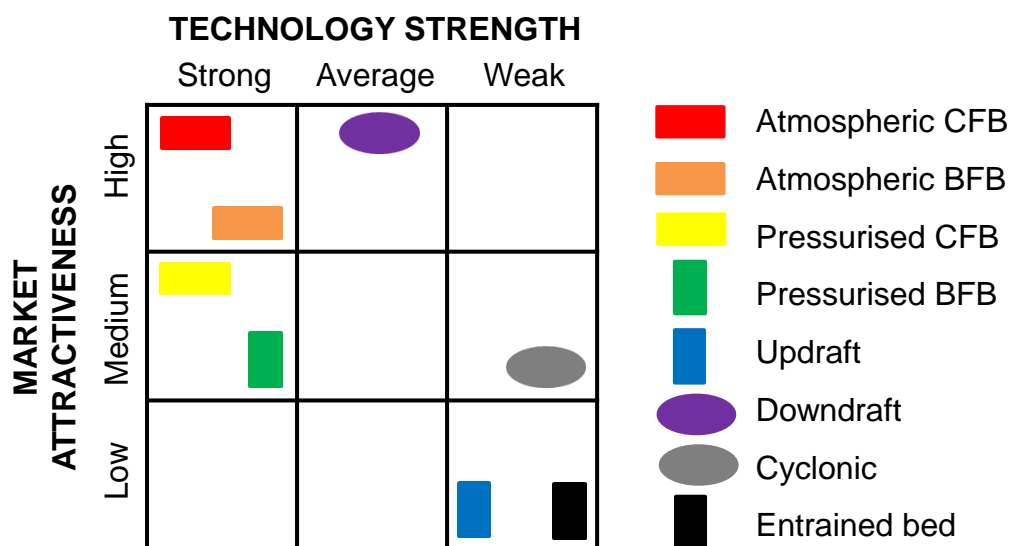
Figure 87: Status of gasification technologies (redrawn from [170])

In pressurised gasification, the oxidising agent is pressurised prior to entering the gasifier to minimise the need for costly gas compression post-gasification. On the other hand, a gasifier can be operated at atmospheric pressure, but gas compression is required for use in turbines [65]. An economic evaluation of this trade-off is required to compare high pressure gasification with atmospheric gasification and subsequent gas compression.

Biomass is more reactive than some coal and biomass can be gasified without requiring high pressures. Pressurised gasification is reported to be most advantageous for unreactive materials such as some coal [158]. AHR is more refractory than biomass similar to some coal and so pressurised gasification may offer considerable performance advantages for AHR gasification. Also, pressurised gasifiers have a smaller volume allowing higher processing rates compared to atmospheric gasifiers. However, pressurising a gasifier is not reported to have significant effects on gas composition and heating value [158]. Figure 87 also shows that gasifiers operated at atmospheric pressure are more commercially attractive compared to pressurised gasifiers. This is mainly due to the high capital cost associated with higher equipment and construction costs for pressurised gasification [158].

Table 51 shows the typical gas compositions and gas HHV expected from biomass gasification using various gasification agents.

Table 51: Typical gas compositions from biomass [158, 159, 164, 171, 172]

Gasification agent: Temperature range (°C)	Gas yields (vol.%)							HHV (MJ/Nm^3)
	H$_2$	CO	CO$_2$	CH$_4$	C$_{2+}$	N$_2$	H$_2$O	
Air: 780-830	5-16	10-22	9-19	2-6	0-3	42-62	11-34	4-7
Steam: 750-780	38-56	17-32	13-17	7-12	2	0	52-60	10-18
Steam and oxygen: 785-830	14-32	43-52	14-36	6-8	3-4	0	38-61	10-18

Air is the simplest gasification agent and air-blown gasification has been researched widely. However, the use of air results in a low energy density gas (4-7 MJ/Nm^3) as fuel gas is diluted with nitrogen. The presence of nitrogen increases the volume output of gases which requires larger gas cleaning equipment. If the product gas needs to be nitrogen free, air should not be used [164]. Using oxygen or steam can increase the HHV to approximately 10-18 MJ/Nm^3 [158]. Steam should be used as a gasification agent if the focus is to make hydrogen [156]. Some of the steam requirements can be provided from dehydration of the feedstock. Oxygen and steam could be used in this work to produce syngas and ultimately synfuels as the Dibanet project aims to product diesel miscible biofuels. However, air gasification is more widely used as the costs associated with oxygen and steam production can be avoided. Biomass gasifiers are usually operated below the ash fusion point. However, if temperatures are too high due to the exothermic nature of air/oxygen gasification, steam can be added to lower the temperature of the gasifier as the reaction between steam and char is endothermic [159].

Temperature controls the chemical equilibrium and kinetics of gasification which determines the gas composition, product yields and overall gasifier performance [173]. Table 52 shows the series of complex and competing reactions that take place during gasification which are used in analysis of the gasification test results.

Table 52: Gasification reactions [16, 157]

Gasification reactions		ΔH(kJ/mol)	
Partial or complete oxidation	$C +1/2O_2 \rightarrow CO$	-111	Exothermic
	$CO +1/2O_2 \rightarrow CO_2$	-283	Exothermic
	$H_2 + 1/2O_2 \rightarrow H_2O$	-242	Exothermic
Boudouard reaction	$C + CO_2 \rightarrow 2CO$	+172	Endothermic
Water gas reaction	$C + H_2O \rightarrow CO + H_2$	+131	Endothermic
Methanation reaction	$C + 2H_2 \rightarrow CH_4$	- 75	Exothermic
Water gas shift reaction	$CO + H_2O \rightarrow CO_2 + H_2$	- 41	Exothermic
Methane steam reforming reaction	$CH_4 + H_2O \rightarrow CO + 3H_2$	+206	Endothermic

Higher gasifier temperatures above 800°C favour the endothermic water gas reaction and result in an increased carbon monoxide concentration [69, 157]. Lower gasification temperatures between 650 and 800°C favour water gas shift reactions

which result in increased hydrogen concentration [69]. The heat for the endothermic reactions can be supplied by partial or complete oxidation of char where the combustion products can also acts as gasification agents. The water gas shift reaction helps establish chemical equilibrium in the final gasification step to balance the carbon monoxide, steam, carbon dioxide and hydrogen in the gasifier. Figure 88 shows the reaction mechanism for biomass as depicted by Ahmed et al [174]. The routes favoured by high heating rates and high reactor temperatures are shown as dotted lines [174].

Aston University

Illustration removed for copyright restrictions

Figure 88: Reaction mechanism of biomass gasification [174]

The equivalence ratio (ER) also referred to as the "*air factor*" is defined as the ratio of the actual air–fuel ratio to the stoichiometric air–fuel ratio and is a major contributor to the performance of a gasifier [156]. It determines the flow rate of oxygen required to partially oxidise a feedstock based on the carbon content of the feedstock. Theoretically, the ER for combustion must be 1 for the complete combustion of a feedstock to carbon dioxide and water. However, in most practical combustion applications, ER is greater than 1 [175] [176] as some energy from the exothermic reaction is lost and therefore, not available for the reaction. For air gasification, a ratio of oxygen to biomass is typically between 0.2 and 0.5 [156, 175]. Larger gasifiers can operate at lower ER due to reduced heat loss. The carbon conversion efficiency is reported to reach a maximum with increasing ER and then decline as the addition of

more oxygen favours the production of carbon dioxide and water [156]. The ER for pyrolysis, in absence of oxygen, is zero and leads to high tar yields therefore, lower ER give higher tar yields. When the ER is too low (<0.2), there is incomplete gasification, i.e. the char is not fully gasified where tar and char yields increase and gas yields decrease [175]. Updraft gasifiers have higher tar content gas due to the lower ER. Although increasing the ER increases the carbon conversion i.e. increasing gas yields [175], ER above 0.5 moves towards combustion [156] increasing the concentration of carbon dioxide and hence lowering the gas HHV [3][62]. The higher the ER the higher the exothermicity of the reaction and reaction temperature [175]. Therefore, the ER and reaction temperature are strongly dependant on one another.

The carbon boundary point is defined as the temperature or equivalence ratio where all solid carbon is theoretically converted to gas [159, 177] and the optimum point of operation for an air-blown gasifier [159, 177]. This is the maximum value for process efficiency which also fits the maximum H_2 and CO concentrations [178]. As more oxygen is added to the gasifier, the process moves from gasification to combustion so the reactor temperature increases and more gases with lower heating value (CO_2) are produced. Therefore, there is a trade-off between equivalence ratios and temperature increase [178] i.e. the temperature is dependent on the exact amount of oxygen added to achieve complete gasification [179] and as long as solid carbon is available, the product gas exergy increases with addition of air [176]. However, in practice, factors such as residence time and gas-solid contacting methods also play an important role in attainment of equilibrium [175]. The gasifier should be operating at the carbon boundary at steady state so there is no production or consumption of char. At the carbon boundary, the gasifier is at equilibrium where the rate of char production from pyrolysis zone is the same as the rate of char gasification in the gasification zone. By increasing the ER in a downdraft gasifier, the thickness of the char bed can be reduced as the addition of oxygen can increase the rate of char gasification in the gasification zone and vice versa [67].

8.3   Feedstock variables

It is important to understand feedstock behaviour for successful gasification. Almost all biomass types can be gasified, but as high volatile content feedstocks produce high tar yields [69], a lower volatile content feedstock is likely to be more suitable for engine applications.

High moisture content feedstocks reduce gasifier thermal efficiency [159, 180] as energy is required to evaporate the water before gasification can take place. However, some of the steam requirement for steam gasification can come from

dehydration of high moisture content feedstocks. The optimum water content of biomass for gasification is reported to be between 10% and 30% [69, 181, 182].

Gasification temperatures are usually higher than the melting point of ash which can lead to slagging and blockages. The melting point of the ash is dependent on the mineral composition [69]. A feedstock with less than 5% ash is recommended for gasification to avoid sintering [166]. The ash content of a sample also indicates the quantity of solid residues left after the volatiles and fixed carbon have been gasified [166]. However, ash can catalytically crack tars which is beneficial for gasification.

Larger particle sizes require longer reaction times for complete gasification [69]. The feed particle size must meet the requirements of the gasifier used. For example, a downdraft gasifier cannot process small particle sizes whereas other gasifier designs such as fluidised bed gasifiers are more flexible in feedstock specification tolerance. Grinding fibrous biomass into fine particles, for use in an entrained flow gasifier is difficult and costly. However, AHR is a powder (as received) which is more suited for feeding into an entrained flow gasifier.

Densification of biomass such as pelletisation can increase the throughput on a continuous gasifier. Pellets also have higher energy content per unit volume [69]. However, thermal processing of high bulk density feedstocks such as pellets or ground pellets yields more unreacted solids when compared to low bulk density feedstocks [104] due to incomplete carbon conversion in the short reaction times.

8.4 Gasification of biomass

Ahmed et al. reports steam gasification of sugarcane bagasse. A fixed amount of sample (15g) was introduced into an atmospheric pressure batch reactor with a continuous flow of steam. Reactor temperatures were increased from 800 to 1000°C and results showed that CO increased at the expense of CO_2 with increasing temperature [174]. Gomez et al. [183] performed gasification in a fluidised bed with sugarcane bagasse and trash. Feeding of these low bulk density feedstocks was reported to be problematic; therefore, sugarcane bagasse pellets (SCBP) were tested at 672°C to 774°C. The feed rate could not be reduced so an air factor greater than 0.22 could not be tested [183]. De Filippis [184] found that feeding fibrous bagasse proved to be problematic. Therefore, they studied gasification of SCBP in a two-stage unit. Stage one was reported to be working as an updraft gasifier and stage two was a fixed bed reforming reactor with alumina or nickel on alumina catalysts. Oxygen and steam was used as the gasification agent and complete gasification of SCBP was reported with no unreacted carbon or tar remaining. It is difficult to understand the effect of this updraft gasifier on SCBP and the effect of these catalysts as there was no

standard test reported for comparison, all experiments were carried out with catalysts. Erlich et al. reported that char from pellets compared to loose bagasse was less reactive during steam gasification [185]. Erlich recommended that the char gasification zone in the gasifier needed to be longer for densified material to avoid excessive unconverted char in the solid residue [185]. Therefore, it is expected that high char yielding feedstocks are expected to require longer reaction times in order to reduce the unconverted carbon in the residual ash. Gabra et al. used ground bagasse pellets in a cyclone gasifier, but experienced feeding problems [186]. Jorapur et al. report using a scraper drag-out conveyor and hopper for successfully feeding sugarcane bagasse and trash into a downdraft gasifier with a product gas HHV of 3.56-4.82MJ/Nm^3 [187]. The remaining char yield from this system was reported to be approximately 24 wt.% (dry feed basis) which is significantly high with a low carbon conversion efficiency. Sugarcane bagasse is likely to cause feeding problems, therefore it is important to utilise densified sugarcane bagasse. The use of densified material such as ground pellets will increase biomass throughput, but the remaining solid yield is likely to be marginally higher.

8.5 Gasification of AHR

Literature is widely available on biomass gasification, but as with pyrolysis very limited literature is available on AHR gasification. Huang et al. reports the pyrolysis of acid hydrolysis residues from pinewood and corncob which produces high char yields. The resultant char is subsequently gasified. The paper concludes that steam gasification at high temperatures and longer residence times is desirable [119] to convert the char produced from AHR to gas. There is no literature reporting the gasification of AHR in a single step. AHR mainly consists of humins and lignin, but there is no literature reporting gasification of humins. However, refractory biomass components such as lignin is reported to be difficult to gasify and requires gasification temperatures of approximately 900°C similar to that of coal [156, 188]. As refractory feedstocks such as coal can be gasified in existing gasifiers, it is expected that higher temperatures present with gasification are sufficient to convert the high quantities of carbon present in the AHR to gas.

8.6 Gas upgrading

Although biomass gasification can be used to produce high yields of product gas, the costs associated with drying biomass and secondary or auxiliary equipment to produce clean gas are some of the challenges that hinder biomass gasification commercialisation. Gas upgrading involves the removal of contaminants by catalytic, thermal and/or physical means. Removal of the contaminants identified in Table 53 can help prevent erosion and corrosion of the downstream equipment [172].

Table 53: Contaminants present in product gas (derived from [171, 189])

Contaminant	Problem	Cleaning method
Nitrogen (e.g. NH_3, HCN)	NO_x formation	Scrubbing
Particulates (e.g. bed material, ash, char)	Erosion of metal components and environmental pollution	Cyclone, filtration, scrubbing
Tars (e.g. refractory aromatics, heavy hydrocarbons)	Block filters and valves, deposits, difficult to burn	Physical (e.g. electrostatic precipitation, scrubbing), catalytic (e.g. dolomite or nickel-based catalysts) or thermal tar removal.
Alkali metals (e.g. Na, K)	Hot corrosion of metal, NO_x pollution	Cooling, adsorption, temperature control, filtration
Sulphur (e.g. H_2S)	Emissions and acid corrosion of metals	Dolomite scrubbing
Chlorine (HCl)	Corrosion	Wet scrubbing

Tar production can be limited by controlling temperature, gasification agent, equivalence ratio and residence time. However, not all of the liquid product can be converted due to the limitations with the reactor and of the reactions taking place [158]. Tars are undesirable from gasification as they can cause catalyst deactivation and may condense in pipework at reduced temperatures leading to operation interruption in engines and turbines [159, 163]. Tar can be removed inside the gasifier or as a secondary step. Secondary upgrading has proven to be effective, but in-situ tar removal is also being researched. Table 54 compares the compounds found in the tar product from fast pyrolysis and gasification.

Aston University

Illustration removed for copyright restrictions

Tar yields decrease with increasing temperature due to thermal cracking [43, 190, 191]. However, different trends are observed by Meng et al. [192] where tar content was higher at higher temperatures. This suggests that parameters, other than temperature, also affect tar yields.

Catalysts for gasification should remove tars, reform methane, resist deactivation, be easily regenerated, cheap and attrition resistant/robust so they can be used in fluidised bed gasifiers [122]. Tar analysis is crucial before a suitable cracking catalyst can be selected.

Fluidised bed gasifiers can use inert silica sand as bed material. However, bed material that can simultaneously act as a heat carrier and as a catalyst to crack tars are an attractive option [156]. According to the review by Pereira et al, naturally occurring catalysts (dolomite and olivine), nickel-based catalysts and alkali metals (KOH,K_2CO_3, $KHCO_3$, Na_2CO_3, $CaCO_3$, C_sCO3, KCl,$ZnCl_2$ and NaCl) have been evaluated for upgrading the product gas from gasification [163]. Alumina and activated carbon have also been evaluated [193]. The use of activated carbon resulted in decreased total tar production by 2.5 times and increased hydrogen production by a factor of 2 when compared with dolomite [163]. Table 55 summarises the advantages and disadvantages of the catalysts currently being used for tar removal. Combining existing catalysts seems a promising approach to combat tars from the gas stream in gasification e.g. dolomite as a catalyst support for nickel [122] or nickel impregnated olivine as nickel is active for steam reforming [156].

Table 55: Reported advantages and disadvantages of catalysts used for tar removal [163] [194] [156, 195]

Catalysts	Advantages	Disadvantages
Dolomite	• Easily available • Inexpensive • Disposable • Effective in reducing tars • Effective for cracking heavy hydrocarbons	• Deactivation due to quick calcination in gasifier • Soft and fragile material that erodes easily, generating a raw gas with a high particulate content
Olivine	• Mechanically stronger than dolomite • 4 to 6 times fewer particulates gas than dolomite • addition of NiO to the olivine catalyst was efficient for reducing tar • Fe content of olivine is catalytically active for tar reforming • A 10 wt.% Fe/olivine catalyst reduced naphthalene and toluene by 48% and 59%	• 1.40 times less effective for in-bed tar removal than raw dolomite
Nickel-based catalysts	• Effective in reducing tars and nitrogeneous compounds such as ammonia • Increased H_2 production (Ni/MCM-41 catalyst with steam increased H_2 production from 30.1 to 50.6 vol.% when Ni loading was increased from 5 to 40 wt.%).	• Expensive • Easily deactivated • Poisonous at high temperature

Gas can also be cleaned using dry (before gas cooling) or wet (after gas cooling) cleaning methods as shown in Table 56. Hot gas cleaning could improve energy efficiency and reduce operating costs. On the other hand, cooled gas cleaning creates water residue which needs further treatment before disposal and loss of overall

thermal efficiency [163, 171]. Alternative combinations of these methods are also reported in the literature.

Table 56: Typical equipment for gas cleaning [163, 171]

Dry (hot) gas cleaning	Wet (cooled) gas cleaning
• Cyclones • Filters (baffle, bag, ceramic, fabric/tube, sand bed and candle) • Adsorbers • Rotating particle separators (RPS) • Electrostatic precipitators (ESP)	• Scrubbers • Spray towers • Wet electro- static precipitators • Wet cyclones

8.7 Interim conclusions

- The components in fuel gas from air-blown gasification are diluted with nitrogen which significantly lowers the gas HHV (4-7 MJ/Nm^3). Fuel gas is suitable for boilers, engines and turbine operation to ultimately produce heat or electricity. Syngas (synthesis gas) is a better quality medium energy content gas (10-18 MJ/Nm^3) from oxygen blown or steam gasification. However, air gasification is the simplest and avoids high costs associated with oxygen and steam production.

- Pyrolytic gasification, without an oxidant, can also produce a lower gas yield with medium heating value (17-19 MJ/Nm^3).

- Fluidised beds are preferred to fixed beds due to the scalability and feed properties requirement. Entrained flow gasifiers may be suitable for processing fine AHR powder, but there are high costs associated with the high oxygen requirements and high temperature resistant materials of construction.

- Pressurised gasification is suitable for refractory feeds such as coal, but the higher equipment and construction costs associated with pressurised gasification makes it unattractive.

- The optimum water content of biomass for gasification is reported to be between 10% and 30%. High moisture in feedstocks can aid steam gasification.

- A feedstock with less than 5% ash is recommended for gasification, but ash is beneficial for gasification as they crack tars.

- High char yielding feedstocks are expected to require longer reaction times in order to reduce the unconverted carbon in the residual ash.

- Densified sugarcane bagasse will help overcome feeding problems and increase biomass throughput, but the remaining solid yield is likely to be marginally higher.

- Refractory biomass components such as lignin are reported to be difficult to gasify and require gasification temperatures of approximately 900°C similar to that of coal. Humins are refractory like lignin, so AHR are also expected to require gasification temperatures of approximately 900°C.

142

- There is no literature reporting the gasification of AHR in a single gasification step.

- Gasification is a well-established technology where tar removal seems critical to enable this technology to be commercialised. Thermal cracking could be used, but the use of catalyst could reduce the process operating temperature and the need for downstream physical gas cleaning. Combining existing catalysts seems a promising approach to combat tars from the gas stream in gasification e.g. dolomite as a catalyst support for nickel or nickel impregnated olivine.

9 GASIFICATION OF BIOMASS AND ACID HYDROLYSIS RESIDUES

The objective of this chapter is to compare the product yields obtained from gasification of standard ground SCBP with high lignin and humin content AHR (produced from sugarcane bagasse). These experiments help to evaluate product yields, carbon conversion and gas compositions as a function of reactor type, temperature, gasification agent and reaction times.

9.1 Gasification methodology

Gasification tests were carried out using a fluidised bed and a fixed bed batch system. These are discussed in more detail below.

9.1.1 Continuous fluidised bed gasification

The 300g/h fluidised bed reaction system which was previously used for fast pyrolysis experiments was also used for these tests to compare pyrolytic gasification of SCBP and AHR. Extensive details of the 300g/h rig can be found in section 6.2.2. Pyrolytic gasification of biomass is expected to give gas yields of up to 85 wt.% on a dry feed basis [66]. Nitrogen was used to fluidise the sand bed and used as the carrier gas. No other gasification agents were used for these pyrolytic gasification tests.

Increasing pyrolysis temperature allows additional shrinkage of the biomass particle and higher conversions to gas and as a result, increases the gas yields from biomass [97]. As temperatures above 650°C were not possible using the existing heaters on the 300g/h rig, the effect of increasing operating temperatures from 500 to 650°C at 50°C intervals was investigated. Commercial gasifiers are usually operated at much higher temperatures, however, the char yields obtained at 650°C would indicate the char yields expected at higher temperatures (>650°C) as char yields are reported to stabilise above this temperature [98].

Air-blown gasification using the existing 300g/h fluidised bed reaction system was not possible as the high temperatures resulting from the exothermic reactions could damage the band heaters used for the reactor. Also, designing and developing a continuous gasifier can be time consuming and very expensive, therefore not possible in the time available within the Dibanet project. Air-blown gasification tests could not be carried out on an existing large scale continuous fluidised bed gasifier due to the limited availability of AHR. Instead, air-blown gasification was carried out in a batch system at Cardiff University which was previously used for gasification experiments.

144

9.1.2 Batch gasification

Ground SCBP and AHR were gasified in a batch reactor. Batch systems are not representative of continuous systems as the reaction time, which has a significant effect on product yields, is set by the operator. Gas yields obtained from both batch and continuous pyrolytic gasification were compared to investigate the reliability of the results from the batch systems. The results obtained from the batch system would be of limited value if this comparison was not made. It was expected that this batch system would imitate higher temperature slow pyrolysis when using nitrogen due to the longer reaction time.

Figure 89 shows the horizontal tube furnace used for batch gasification experiments. A custom-made stainless steel pipe with a heated length of 330mm and an internal diameter of 30mm was used. A stainless steel boat (330mm x 20mm x 10mm) was used to load 3g of sample into the furnace. Preliminary tests showed that larger quantities of sample (>3g) led to excessive gas and tar production and an increase in pressure in the glassware collection system. The maximum temperature of the furnace was 1000°C. However, the initial reactor temperature, before loading the boat, was measured with a thermocouple and found to be 50°C lower than the furnace set point for all experiments. Batch pyrolytic gasification experiments were carried out when the initial reactor temperature was at 650°C for direct comparison of product yields with the continuous pyrolytic gasification. A temperature gradient throughout the sample was expected which was difficult to measure using a thermocouple (i.e. the surface of the sample in contact with the boat would heat up faster than the particles at the centre). Also, a relatively small sample size was used to ensure this temperature difference was kept to a minimum.
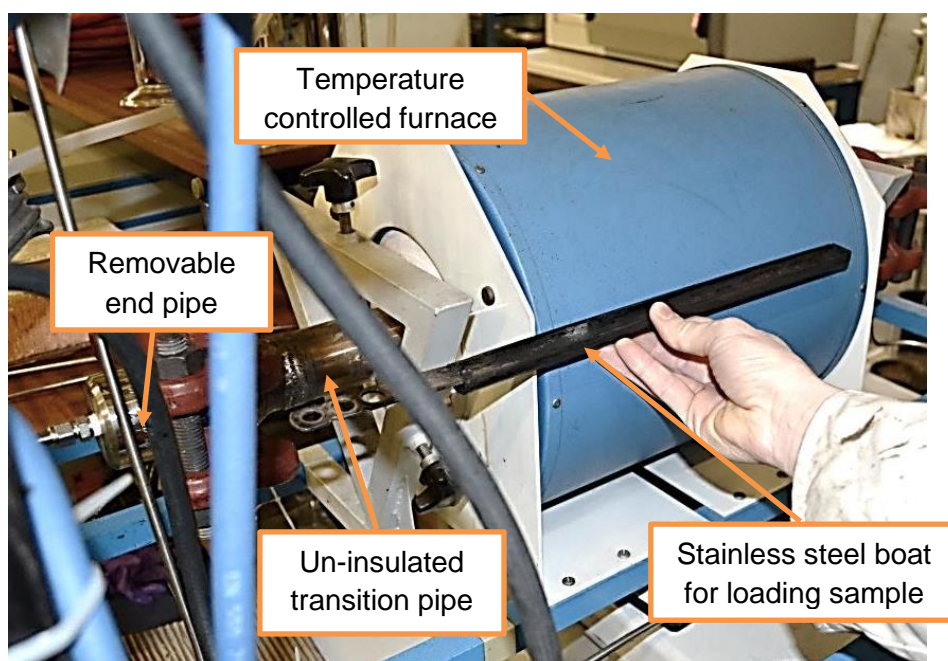
Figure 90 shows a flowsheet of the gasification rig set up.
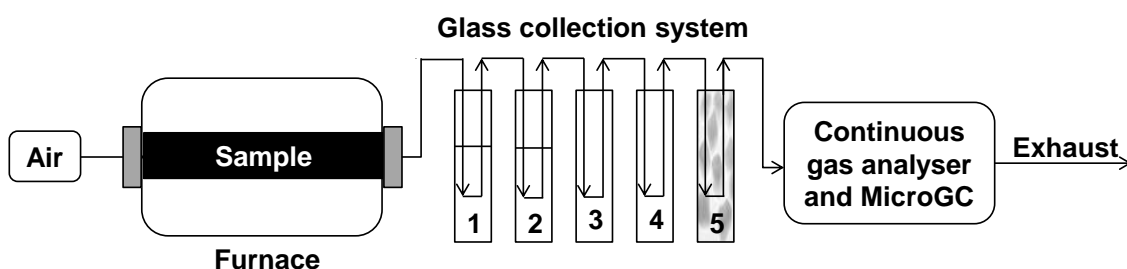
Figure 90: Batch system set up for gasification

Figure 91 and Figure 92 shows the metal to metal seal at the end of the reactor. Once the reactor had reached the initial reaction temperature, the end pipe was unbolted, the boat was loaded into the reactor and the end pipe was quickly put together to minimise losses. The timer and gasification agent was started as soon as the boat was loaded into the reactor. Gas leak tests were carried out to minimise losses and CO monitors were used for safety.
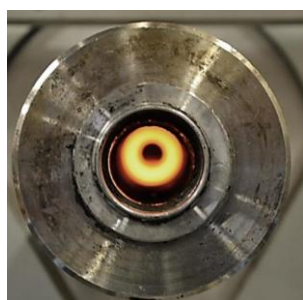
Figure 91: End of reactor

Figure 92: Removable reactor end pipe

The mass of remaining solid residue was determined by mass gain on the stainless steel boat. After the experiment was complete, the feed gas was turned off and the sample was quickly removed from the furnace before a stainless steel plank was set on top of the boat to reduce further oxidation. Ideally, to avoid further oxidation and mass loss of the sample, the boat should be cooled in nitrogen in the furnace before weighing. However, this was not possible using the existing rig set-up.

Tar was defined as the liquid product, containing organic liquid and water, collected after the oxidation reaction took place in the reactor. Figure 93 shows the glassware collection system on this rig which was used to scrub the tars and moisture out of the gas before it was analysed using a continuous gas analyser and MicroGC. Five dreschel glass bottles were used. Bottles 1 and 2 which contained approximately 150ml of iso-propanol acted as simple scrubbers which collected organic liquid (tars) and some of the water. Bottle 3 and 4 contained silica gel which absorbed moisture and also aided tar removal by impingement coalescence. Bottle 5 was a check bottle

containing a cotton wool filter which indicated, by colour change, whether the exit gas was almost tar free.
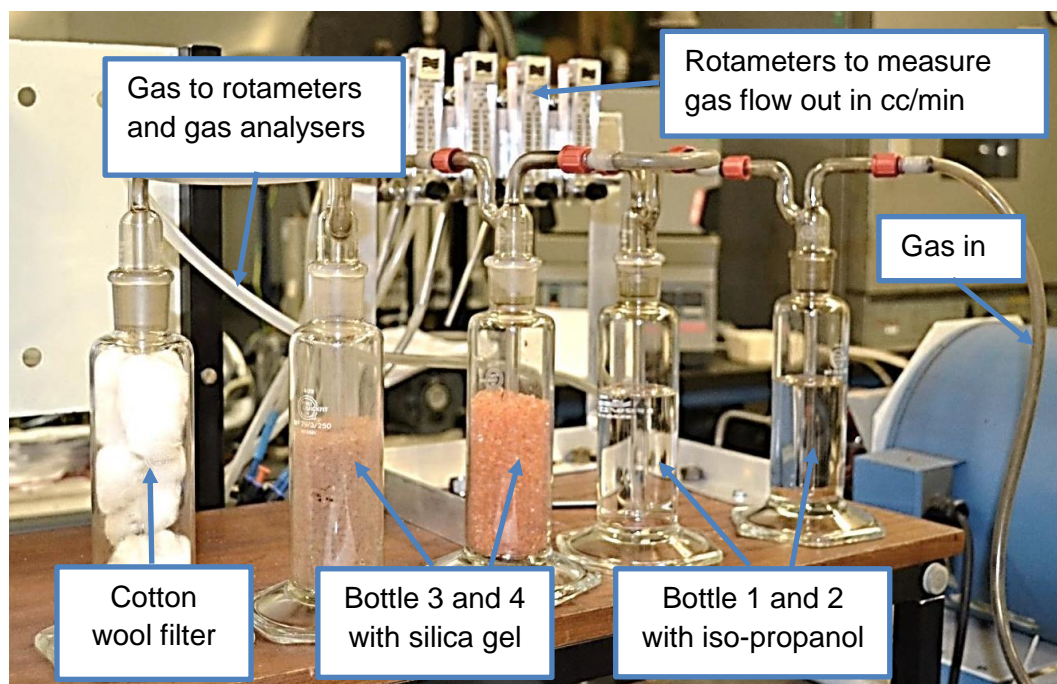
Figure 93: Liquid collection system

Iso-propanol has a boiling point of 82.5°C which meant that iso-propanol could evaporate when product gas entered the glassware collection system. The mass loss due to evaporation over the entire collection system was shown to be negligible over the time taken for each experiment. This was validated by an experiment conducted with an empty furnace at the highest temperature (950°C). The mass loss in bottle 1 and 2 was collected in bottle 3 and bottle 4 with the silica gel. This varied slightly with the furnace temperature. However, Table 57 shows that the evaporated iso-propanol, from tests carried out at the highest initial reactor temperature (950°C), was collected in the silica gel bottles.

Table 57: Measuring mass loss due to evaporation of iso-propanol at 950°C

Collection system component	Mass gain (g)
Bottle 1: Iso-propanol	-1.63
Bottle 2: Iso-propanol	-0.22
Bottle 3: silica gel	1.84
Bottle 4: silica gel	0.01
Total mass loss	0.00

As the reactor tube was fixed inside the furnace, any tar deposits inside the reactor could not be weighed which could affect the overall mass balance. Also, the entire reaction system could not be weighed to determine the mass gain due to its size and weight. Weighing the filtering components and piping was the best way to determine the tar yields. The tars were low in viscosity i.e. high water content, so most of the tar was cooled and collected within the piping and first 2 bottles. The mass of the

tar collected in the 5 filtering bottles and pipes was weighed and use to calculate tar yield.

A Rosemount NGA 2000 continuous gas analyser was used to measure the volume percentage of carbon monoxide, carbon dioxide and oxygen in the product gas. Readings were manually taken from the continuous analyser every 15 seconds until the sample had been completely gasified. Also, a Varian CP-4900 MicroGC was used to determine the composition of gases every 3 minutes. The gases detected were carbon monoxide, carbon dioxide, methane and hydrogen. The solid and tars were carefully collected and weighed whilst accounting for any possible losses. Errors with the gas measuring equipment and limitations of the gas analysers resulted in poor mass balance closures and so gas yields were determined by balance.

The effect of initial reactor temperature on reaction time, product yields and gas composition was investigated using air. Oxygen gasification was not possible for safety reasons and steam was not available. Experiments were carried out with SCBP and AHR when the initial reactor temperature was at 650, 750, 850 and 950°C. Each test was also repeated at least once to check reproducibility. The exit gas temperature was much lower than the reactor temperature as there was approximately 180mm of un-insulated exhaust pipe at the outlet of the furnace which allowed the exit gas temperature to drop before entering the glassware collection system. Several experiments were carried out to measure the temperature at the bottom of the exhaust pipe and results indicated that the temperature of the exit gas was between 40°C and 60°C. The thermocouple was removed for future experiments to avoid leaks and tar deposits. Therefore, the temperature increase caused by the exothermic reaction could not be measured as deposits on the thermocouple led to an error in the temperature reading, but is expected to be higher with higher oxygen concentrations.

The carbon content of the AHR was greater (64.6 wt.%) than SCBP (46.6 wt.%). This suggests that more oxygen was necessary for sufficient carbon conversion of the AHR to carbon monoxide compared to SCBP at the same initial reactor temperature. In continuous gasification processes, air flow rate (l/min) is determined by calculating the equivalence ratio and gasifiers are operated at the carbon boundary. However, batch systems cannot be operated at the carbon boundary. The glassware collection system coped best with air flows of 1l/min and so rotameters were used to flow 1l/min of air over 3g of sample. It was necessary to fix the reaction time as excess air flow would lead to increased production of carbon dioxide and water, at the expense of carbon monoxide and hydrogen and as a result, reduce the gas HHV. Therefore, the determination of the optimum operating conditions for this system was required and

tested in this work. Equivalence ratios were calculated after the experiments were carried out and some notes can be found in Appendix 3.

9.2 Gasification results and discussion

9.2.1 Summary of gasification experiments

Table 58 summarises the gasification tests carried out. The results of SCBP at 500°C were taken from section 0 and used to show the effect of increasing temperature on product yields with continuous pyrolytic gasification. Both feedstocks were subsequently gasified with nitrogen in a batch system to investigate the effects of reaction times. The addition of air to the batch system was expected to further increase gas yields by increasing the carbon conversion.

Table 58: Gasification test summary

Gasification mode	Feedstock and Temperature	Summary
Continuous pyrolytic	AHR at 500	Unsuccessful, AHR feeding problems
	SCBP at 600	Successful
	SCBP at 650	Successful
	SCBP at 550	Successful
	AHR at 650	Successful, pelletisation to produce a more robust sample is required
Batch pyrolytic	SCBP and AHR at 650°C	To compare with continuous pyrolytic gasification
Batch air-blown	SCBP and AHR at 650°C, 750°C, 850°C and 950°C (duplicates)	To compare feedstocks and test effect of temperature

9.2.2 Continuous pyrolytic gasification

Ground SCBP were screw fed into a continuous fluidised bed reactor with little difficulty. However, as the acid hydrolysis process destructs the biomass structure, AHR was received as a powder. The powder nature of AHR posed a challenge in screw feeding and such fine particles were prematurely entrained out of the fluidised bed reactor before being thermally processed. Pelletisation using water is conventionally used to strengthen inter-particle bonding and promote adhesion between biomass particles. Therefore, 20 wt.% water was added to AHR and densified using an agricultural pelletiser. The pellets were then ground and sieved to 0.25 to 1mm for direct comparison with ground SCBP which were of the same particle size range. The average moisture content of the ground AHR pellets was 16.61 wt.% due to the addition of water. Water present in feedstock is reported to beneficial as it can aid steam gasification to increase the hydrogen content of the product gas. The bulk density was measured using the same method detailed in section 3.3. The bulk density of the ground AHR pellets was 684.88kg/m^3 compared to the untreated bagasse which was 133.44kg/m^3. The ground pellets were screw fed into the reactor, but crumbled

back into a powder, by the screw, before entering the reactor. The high nitrogen flow prematurely entrained unreacted AHR out of the reactor and into the glassware collection system (electrostatic precipitator and bio-oil collection pot) as shown in Figure 94.

Figure 94: AHR blown out of reactor into the ESP

These AHR pellets were of insufficient mechanical strength to withstand crumbling by the feed screw. It is expected to be due to the hydrophobic and refractory nature of AHR. A cold fluidisation test was carried out using the AHR to determine the flow rates of nitrogen necessary to temporarily combat this fluidisation problem. Table 59 shows the changes made to the pyrolytic gasification experiment in order to successfully screw feed the AHR into the reactor. As this was only a temporary measure, an alternative more suitable densification method was required to strengthen the material for screw feeding into commercial fluidised bed gasifiers. Densification and improving feeding properties of AHR is addressed in more detail in Chapter 10.

Table 59: Changes to experiment to overcome AHR feeding problems

Process condition	Unsuccessful experiment with AHR	Successful experiment with AHR	Reason for change
Total nitrogen flow through reactor (l/min)	22	11-12	To retain AHR in the reactor and not blow it out into collection system before being processed
Sand particle size range (mm)	0.5-0.6	0.355-0.5	To allow for a fluidised bed using lower nitrogen flowrates
Fast screw speed (rpm)	110	60-80	To avoid excessive crushing of the ground pellets back into powder by the screw
Approximate feed rate (g/h)	200g/h	80g/h	To avoid feed backing up the feed system as the feed is delivered slower into the reactor.

The gas composition is crucial to estimate product gas HHV and the application of the gas is necessary to determine the required gas HHV. The HHV of hydrogen is 12.75MJ/Nm^3 and of carbon monoxide is 12.63MJ/Nm^3. Therefore, a hydrogen and carbon monoxide rich syngas is of interest if a medium energy content gas is required. Hydrogen concentrations were low as nitrogen was used as the gasification agent instead of steam. The key product gases from pyrolytic gasification were carbon monoxide and carbon dioxide. Figure 95 shows that gas production is increased from pyrolytic gasification of SCBP with increasing temperature.
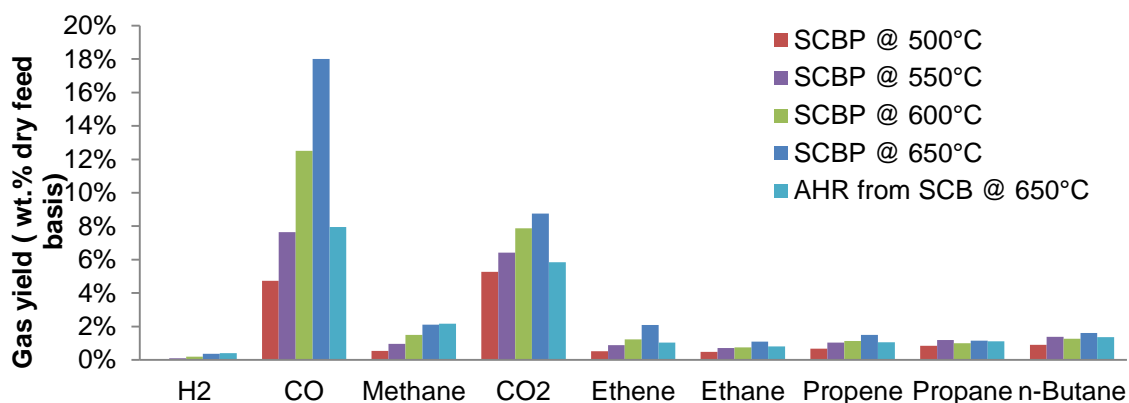
Permanent Gas

Figure 95: Gas yields from pyrolytic gasification of SCBP and AHR up to 650°C

The series of complex and competing reactions that take place during gasification can be found in earlier Table 52. Higher gasifier temperatures favour the products from the endothermic reactions i.e. increasing the CO concentration [157]. Therefore, CO production increases with temperature and the CO: CO_2 ratio is also expected to increase.

Carbon dioxide is of less importance if the gas is not going to be utilised immediately. Figure 96 to Figure 98 show the ratios of the product gas and the effect of temperature on the ratio. H_2/CO_2 and CO/CO_2 ratio increases with temperature which contributes to the enhancement in product gas quality. Figure 96 to Figure 98 show the H_2/CO, H_2/CO_2 and CO/CO_2 ratios increase with increasing temperature for SCBP. AHR gives higher H_2/CO and H_2/CO_2 ratios compared to SCBP at 650°C, but lower CO/CO_2 ratios.
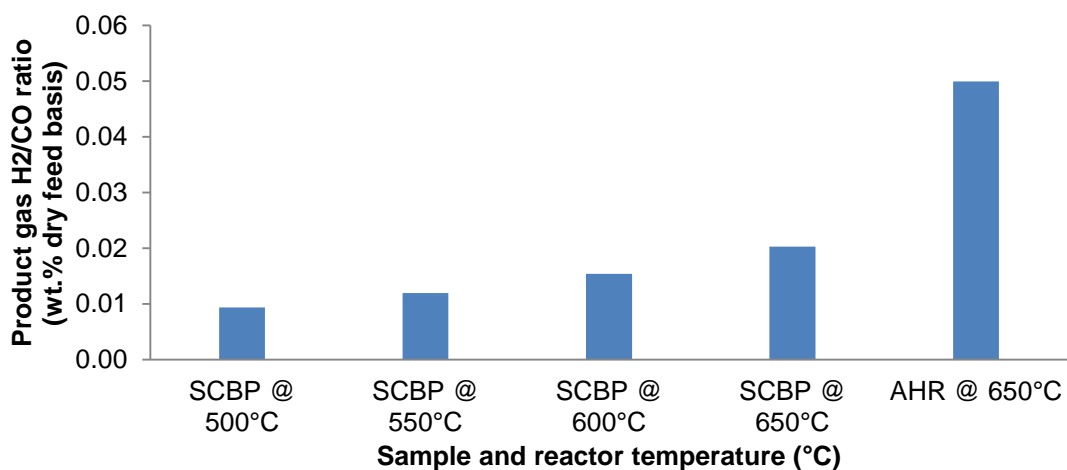
Figure 96: H$_2$/CO ratios of gaseous products
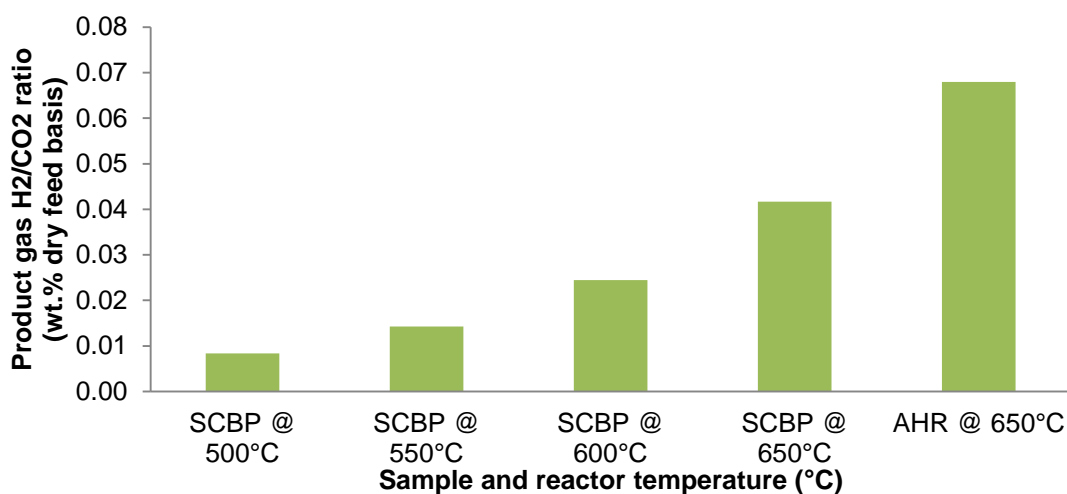
Figure 97: H$_2$/CO$_2$ ratios of gaseous products
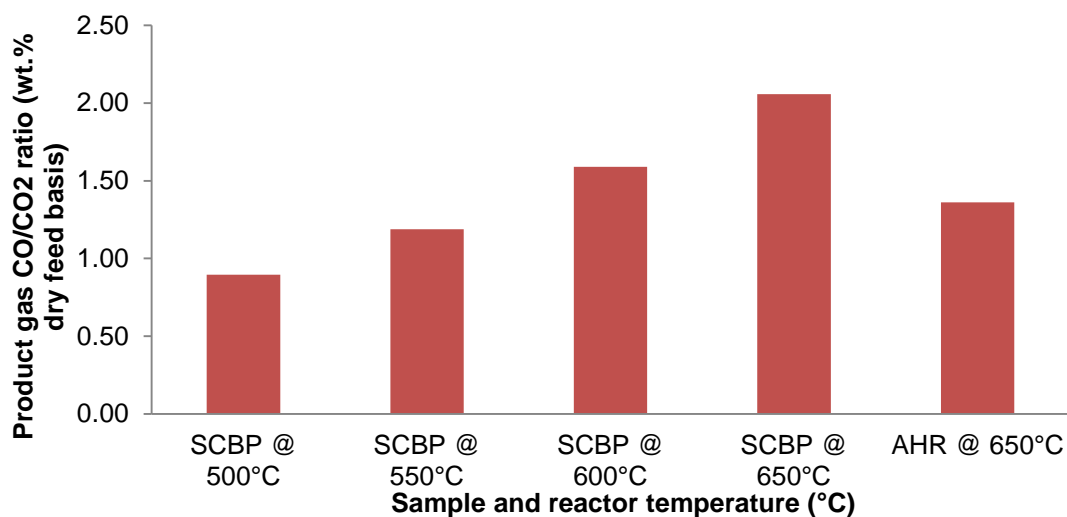
Figure 98: CO/CO$_2$ ratios of gaseous products

The mass balances (on dry feed basis) are shown in Table 60. The reactor could not be operated above 650°C. Increasing the temperature from 500 to 650°C for SCBP reduced the organic liquid yields from 60.45 wt.% to 39.78 wt.% and as a result, gas yields increased from 14.01 wt.% to 36.65 wt.%. The char yield decreased from 17.32 wt.% and then stabilised at approximately 14 wt.% at 550°C. Scott et al. report

that the shrinkage of char slows down at 650°C and the char content stabilises above this temperature [98].

Table 60: Mass balances for pyrolytic gasification of SCB pellets and AHR

Processing T (°C)	500°C	550°C	600°C	650°C	650°C
Feedstock		Ground SCBP			AHR from SCB
Feed moisture (wt.% wet feed basis)		9.62%			16.61%
Char (wt.% dry feed basis)	17.32	14.40	14.90	14.26	43.18
Total liquid (wt.%)	73.14	72.40	62.73	53.51	43.34
Organic liquid (wt.%)	60.45	58.97	49.74	39.78	23.17
Total water content (wt.%)	12.69	13.43	12.99	13.73	23.72
Gas (wt.%)	14.01	20.32	27.41	36.65	23.78
H_2	0.04	0.09	0.19	0.36	0.40
CO	4.73	7.64	12.51	18.00	7.95
Methane	0.54	0.96	1.49	2.10	2.16
CO_2	5.27	6.42	7.87	8.75	5.84
Ethene	0.52	0.89	1.23	2.09	1.04
Ethane	0.48	0.72	0.75	1.09	0.81
Propene	0.67	1.04	1.12	1.49	1.05
Propane	0.84	1.18	0.99	1.16	1.11
n-Butane	0.90	1.38	1.25	1.60	1.35
Total product out (g)	196.14	143.52	167.19	141.38	68.75
Total feed in (g)	207.72	148.25	176.09	149.79	82.39
Recovery (wt.% dry feed basis)	93.83	96.47	94.41	93.79	94.63

Figure 99 shows the gas, organic liquid and char yields (on a dry feed basis) from SCBP and AHR. The solid lines show an extrapolation of expected product yields by increasing temperature above 650°C. According to the extrapolation, gas yields as high as 85 wt.% can be expected from SCBP which is comparable to gas yields reported from biomass in literature. The X points mark the product yields obtained from AHR at 650°C. Pyrolytic gasification of AHR at 650°C gives a lower gas yield compared to SCBP. There is a low organic liquid yield (23.17 wt.%) from AHR compared to SCBP (39.78 wt.%). The experimental results and extrapolation indicate that pyrolysis vapours which usually cool, condense and collect as organic liquid, are cracked into permanent gases when increasing the temperature. The char yield decreased with increasing temperature and then stabilised at approximately 550°C. Work carried out by Scott et al. agrees with this and reports that char yields decreased with increasing temperature to an almost constant value above 650°C where devolatisation was almost complete [98]. For this reason, the char yield from AHR is expected to be approximately 40 wt.% at temperatures higher than 650°C.
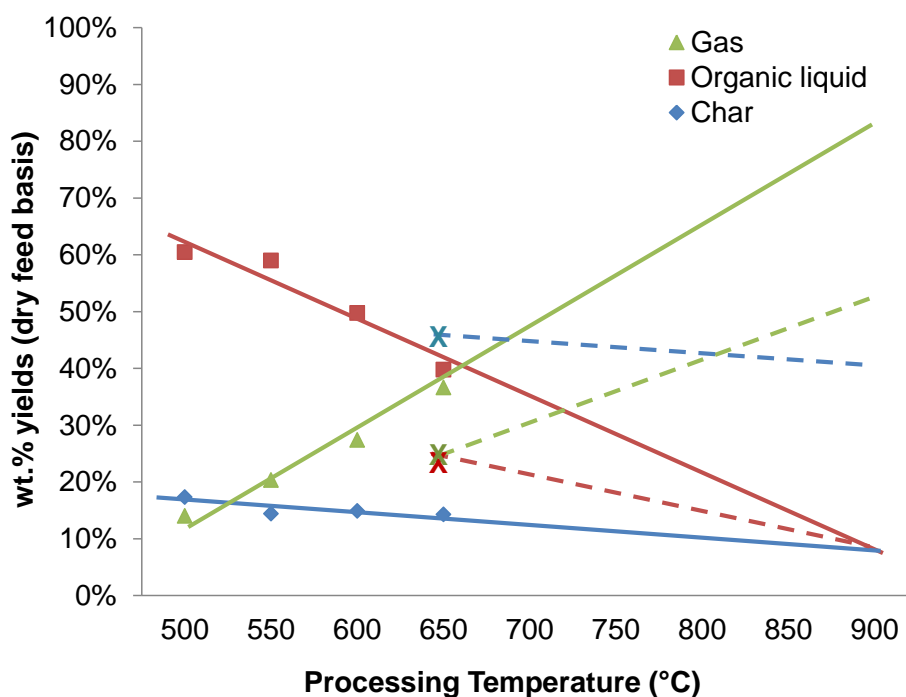
Figure 99: Product yields from pyrolytic gasification of SCB and AHR

Results show that, by simply increasing the pyrolysis temperature, without the addition of an oxidant, did not improve the gas yields significantly from AHR. The char yields are expected to stabilise at approximately 40 wt.% above 650°C and gas yields are expected to reach approximately 50 wt.% leaving low organic liquid yields (<10 wt.%) from pyrolytic gasification of AHR. Pyrolytic gasification thermally cracks the pyrolysis vapours and contributes to the production of permanent gases. Permanent gas production by secondary cracking is limited if there is a low amount of volatiles present for the production of pyrolysis vapours. Therefore, gas yields from pyrolytic gasification of low volatile content AHR is limited. Oxidative gasification of AHR was expected to be more promising as the presence of steam, oxygen or air could gasify the refractory carbon.

9.2.3 Comparison of batch and continuous pyrolytic gasification

Comparisons of the batch and continuous systems were made at 650°C as temperatures above 650°C were not possible using the continuous system. Figure 100 and Figure 101 compare the product yields from pyrolytic gasification on a continuous and batch system at 650°C using the SCBP and AHR respectively. A continuous system has a residence time of a few seconds whereas a batch system can have a relatively longer residence time which needs to be set by the operator. As expected, the longer residence time in the batch system gives a higher char yield and lower tar yield compared to the continuous system for both feedstocks. The solid yield increased from 36.58 wt.% to 50.40 wt.% and the tar yields decreased from 43.34 wt.% to 26.64

wt.% for AHR. The gas yields were marginally higher using the batch system for both feedstocks.
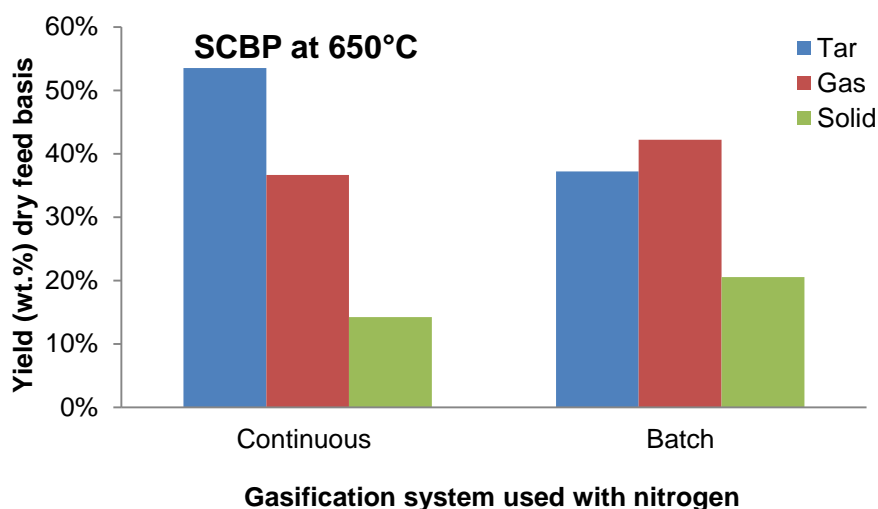
Figure 100: Comparison of product yields from SCBP using continuous and batch gasifiers
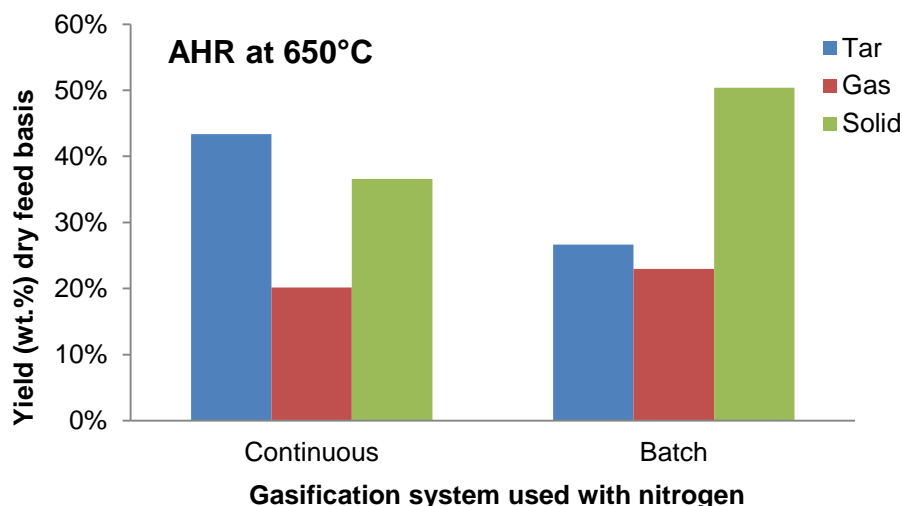
Figure 101: Comparison of product yields from AHR using continuous and batch gasifiers

9.2.4 Comparison of batch pyrolytic and air-blown gasification

Figure 102 and Figure 103 compare the product yields from pyrolytic and air-blown gasification with a batch reaction system at 650°C using the SCBP and AHR respectively. The introduction of air to the batch system at 650°C shows a decrease in tar and char yields and an increase in gas yields. This is as expected as the presence of oxygen converts additional carbon to carbon-bearing gases. However, it should be noted that introducing air into a gasification system leads to a higher yield of low energy content gas as the product gas is diluted with nitrogen.
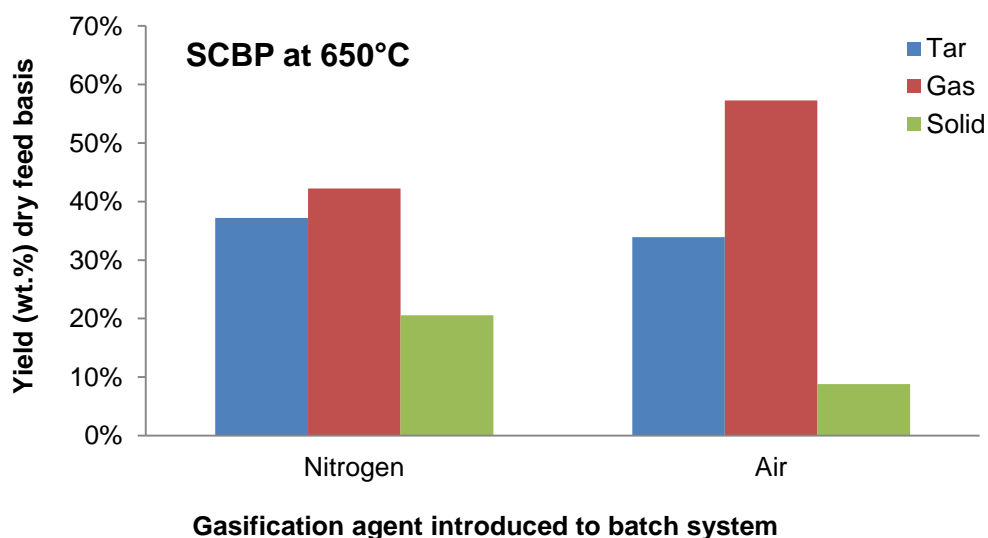
Figure 102: Effect of air addition on product yields from batch gasification using SCBP
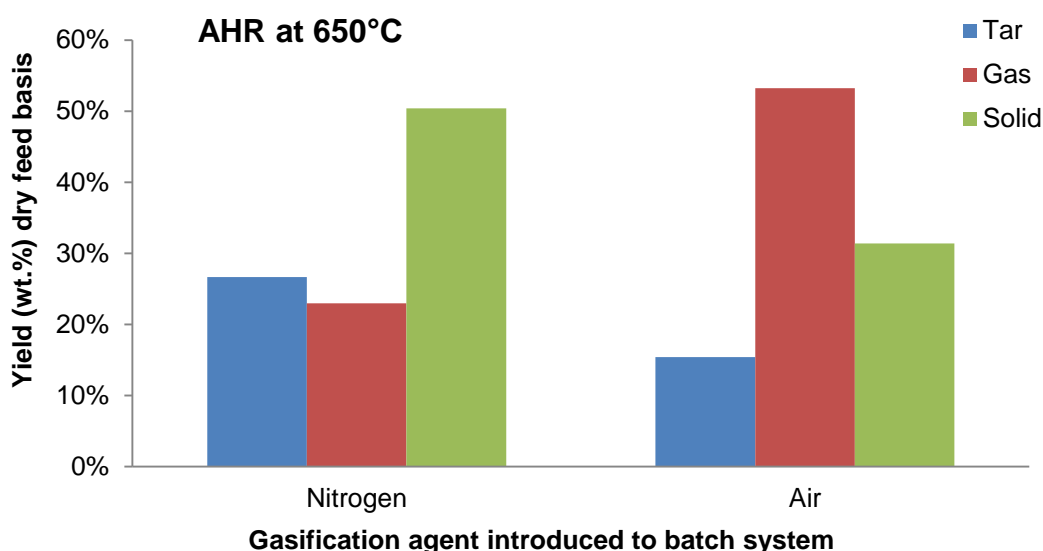
Figure 103: Effect of air addition on product yields from batch gasification using AHR

9.2.5 Batch air-blown gasification

Due to the limitations of this batch gasifier, the reaction time was determined by the production of CO. For initial experiments, once the CO concentration of the product gas had reached almost zero, the experiment was stopped to avoid addition of excessive oxygen leading to production of carbon dioxide. Stopping the experiments at this point meant that the concentration of CO_2 was much higher than CO limiting the gas HHV. Also the maximum H_2 and CO concentrations are reported to be the optimum point for an air-blown gasifier [178] where gas HHV can potentially be maximised. Therefore, the end of gasification and optimum point for gasification using this batch system, was defined as the point where the CO level started to drop as shown in Figure 104. Addition of oxygen beyond this point favoured the production of

undesirable carbon dioxide. In typical gasification, this point would not be the end of gasification as CO_2 can be converted to CO by the Boudouard reaction (C + CO_2 → 2CO).
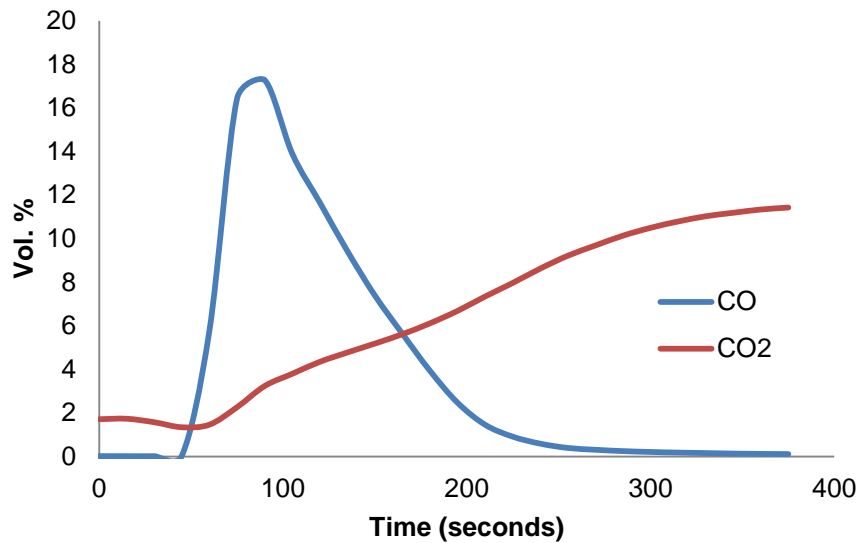
Figure 104: Changing concentration of CO and CO_2 from AHR

Figure 105 shows the effect of initial reactor temperature on the time taken for CO to peak i.e. the effect of temperature on reaction time. As expected, CO peaked quicker at higher temperatures, showing that rates of reaction increased as temperature increased. Also, AHR reacted more slowly compared to SCBP, confirming that AHR was more refractory and less reactive at lower temperatures.
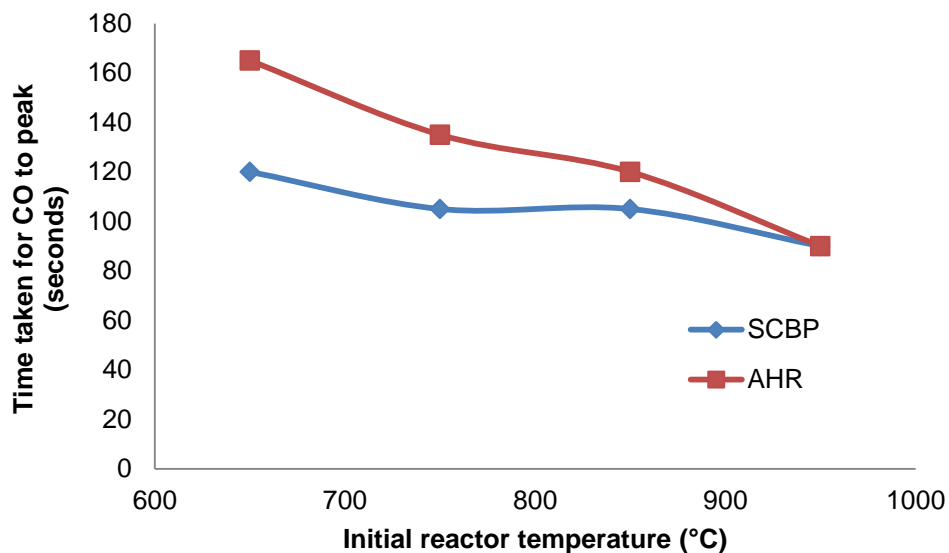
Figure 105: Effect of initial reactor temperature on time taken for CO to peak

The equation shown in Appendix 3 was used to calculate the product gas HHV. The product gas composition was calculated on an oxygen-free basis which disregarded any unreacted oxygen in the product stream. The effect of temperature on the product gas HHV can be seen in Figure 106. The HHV increased with temperature as the product gas concentration in nitrogen increased. The gas HHV produced at

950°C was 7.28MJ/Nm^3 for SCBP which was higher than expected on commercial gasifiers which could be a result of the high hydrogen content shown later in Figure 108. The gas HHV was 5.78MJ/Nm^3 for AHR which is expected from air-blown gasification [159] and suitable for boiler and engine applications [196].
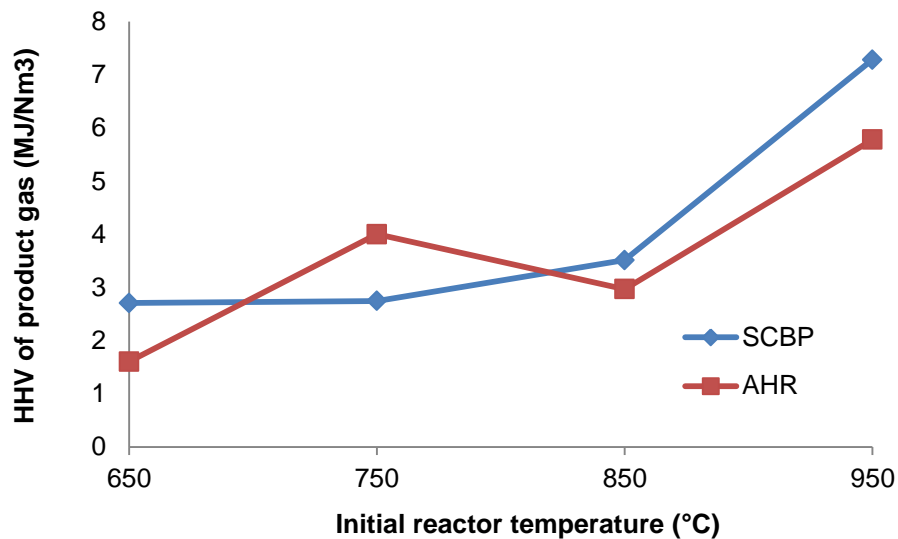
Figure 106: Effect of initial reactor temperature on the HHV of oxygen-free product gas

The equivalence ratio determines the flow rate of oxygen required to partially oxidise a feedstock based on the carbon content of the feedstock. Figure 107 shows the effect of temperature on equivalence ratios. The peak at 850°C for SCBP can be explained by the partial combustion as there was a delay in removing the sample from the reactor. These results are in agreement with literature which reports that the equivalence ratio of biomass is between 0.2 and 0.5. ER above 0.5 significantly reduces the product gas quality and thermal efficiency [175]. The equivalence ratios for SCBP are consistently higher than for AHR suggesting that the reaction time was limited for AHR as the CO concentration began to drop before sufficient quantities of air was added. As this gasification system was a batch system, the equivalence ratio was calculated after the experiment was carried out. A fixed amount of feed in the reactor was flushed with continuous air flow. The experiment was stopped when the CO concentration started to decrease and carbon dioxide started to increase. As the flow of air over the sample increased, the increased equivalence ratio would move the process from gasification towards combustion i.e. ER slowly increasing to 1. As the ER increased, the sample would be combusted and the reactor temperature would increase. There is a trade-off between equivalence ratios and temperature increase [178] i.e. the temperature is dependent on the exact amount of oxygen added to achieve complete gasification [179]. Therefore, the monitoring of gasifier temperature profile was important, but was not possible in this work.
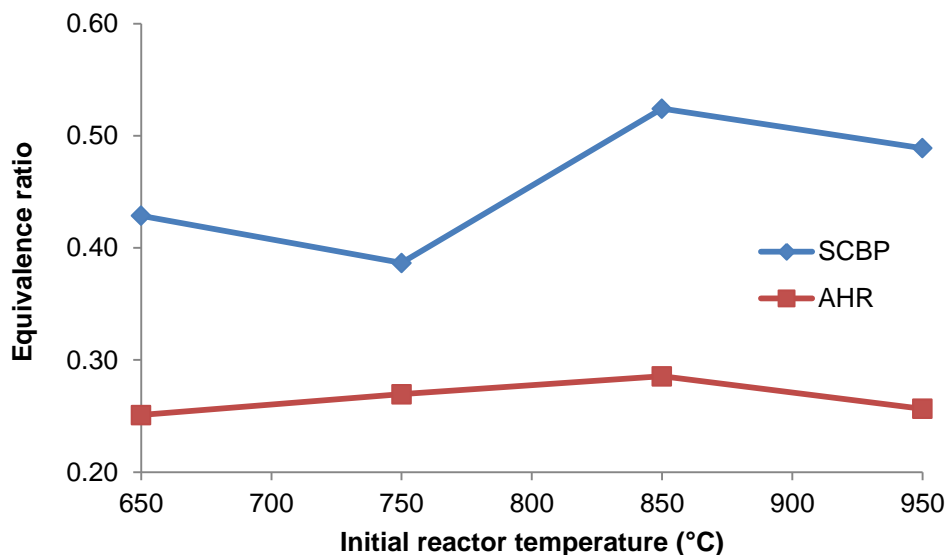
Figure 107: Effect of temperature on equivalence ratios

Figure 108 and Figure 109 show the gas composition (oxygen-free) produced from batch air-blown gasification of SCBP and AHR respectively. Nitrogen concentration was calculated by difference and compared with GC data. The graphs show the increasing gas concentrations with increasing initial reactor temperature for both SCBP and AHR respectively. CO is the dominant product gas, therefore, these samples were gasified and not combusted. SCBP has been partially combusted at 850°C as there was a delay in stopping air flow. This also explains the reduced HHV in Figure 106 and lower solid yield in Figure 110.
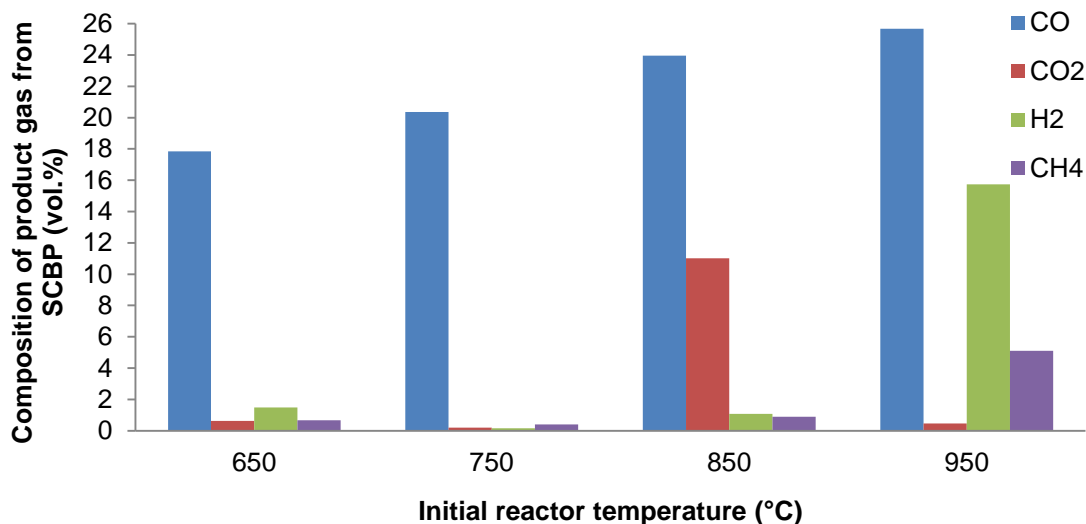
Figure 108: Composition of product gas from SCBP (vol.%)
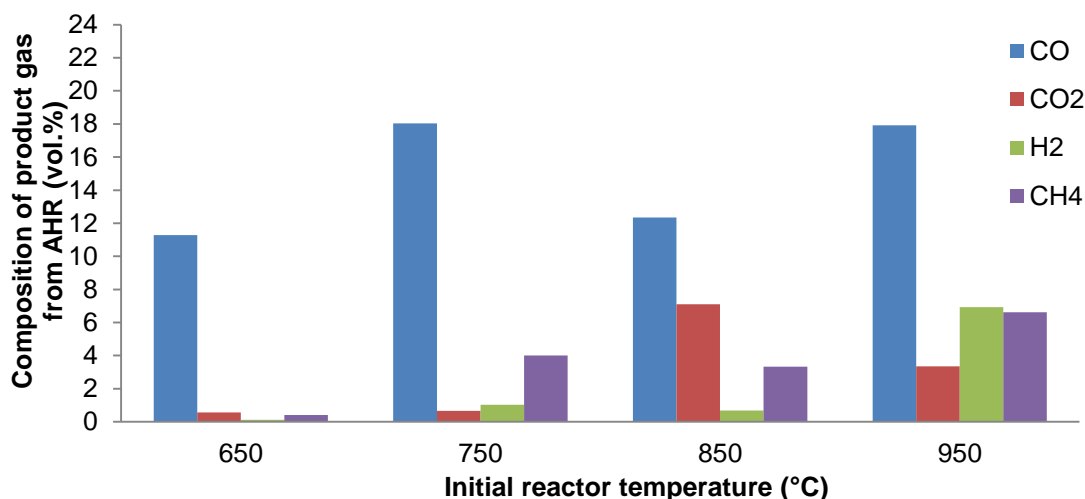
Figure 109: Composition of product gas from AHR (vol.%)

Batch systems, like the one used in this work, would not be used for gasification commercially. However, it was important to compare the results obtained in this work, with commercial gasification data. Table 50 presented earlier provides a comparison of gas compositions from various gasifiers. An entrained flow gasifier will give higher concentration of hydrogen and carbon monoxide, with lower dilution with nitrogen as enriched air is usually used as the gasification agent. Therefore, an entrained flow gasifier will give higher heating values compared to fixed bed gasifiers. Also, as AHR has a moisture content of approximately 70 wt.% when it leave the acid hydrolysis process, it may be possible to process the slurry using an entrained flow gasifier. However, there is very complex operation with intensive gas cooling and requirements for high oxygen and high temperature resistant material of construction. Slurry-fed gasifiers also require additional reactor volume to evaporate the water mixed with the feedstock [182]. Therefore, an air-blown fluidised bed gasifier may be more suitable for processing AHR.

Product gas composition and HHV from a commercial fixed bed downdraft gasifier and a fluidised bed gasifier are shown to be similar in Table 50. Therefore, data from commercial downdraft gasifiers in Table 61 was used as an indication of gas composition and HHV expected from an air-blown fluidised bed gasifier. Table 61 compares the gas composition from wood obtained from literature with the SCBP at 950°C on the batch system. The table also compares the gas composition from carbonaceous charcoal from literature with carbonaceous AHR at 950°C. Product gas consists of nitrogen and gasification products from air-blown gasification. The nitrogen content is usually around 50-54vol.% [159] of product gas for biomass and 55-65vol.% for charcoal [197] at temperatures of approximately 950°C. The results from the batch gasification at 950°C also reflect this. The product gas from SCBP consists of approximately 50vol% of gasification products and the product gas from AHR consists

160

of approximately 35vol% of gasification products. The remainder of the gas is nitrogen which significantly lowers the product gas HHV.

Table 61: Comparison of gas composition (vol%) with commercial fixed bed downdraft gasifiers

Gas component	Gas composition from wood from literature [197]	SCBP at 950°C	Gas composition from charcoal from literature [197]	AHR at 950°C
CO	17-22	25.67	28-32	17.91
CO_2	9-15	0.47	1-3	3.36
H_2	12-20	15.74	4-10	6.92
CH_4	2-3	5.11	0-2	6.62
N_2	50-54	53.00	55-65	65.19
HHV (MJ/Nm^3)	5-5.9	7.28	4.5-5.6	5.78

In this batch system, there is a trade-off between residence time, temperature and equivalence ratio which need to be controlled in order to optimise energy output. The feed quantity is fixed and the initial reactor temperature and air flow is set. The reaction time is dependent on the temperature and the air flow is stopped at maximum CO concentration which was defined as the end of gasification using this batch system. This point also reflected the maximum H_2 concentration which Pellegrini et al. report is the maximum value for process efficiency [178].

Solid residue samples, consisting of unreacted carbon and ash, were collected and weighed in order to calculate the solid yield (wt.%) at the end of the experiment. High ash content samples produce higher solid residue yields from gasification even after complete carbon conversion. AHR have a higher ash content (6 wt.%) compared to SCBP (2.97 wt.%) so even after complete carbon conversion, the solid yield from AHR would be greater than SCBP. AHR also has a higher fixed carbon content (56.80 wt.%) compared to SCBP (18.47 wt.%) suggesting that AHR would leave a higher solid residue compared to SCBP under the same processing conditions. Figure 110 shows that increasing the temperature from 650 to 950°C reduces the solid residue yield from 8.83 wt.% to 5.16 wt.% for SCBP and from 31.39 wt.% to 20.52 wt.% for AHR. The solid residue yield for SCBP at 850°C is lower than expected as there was a delay in removing the sample from the reactor.
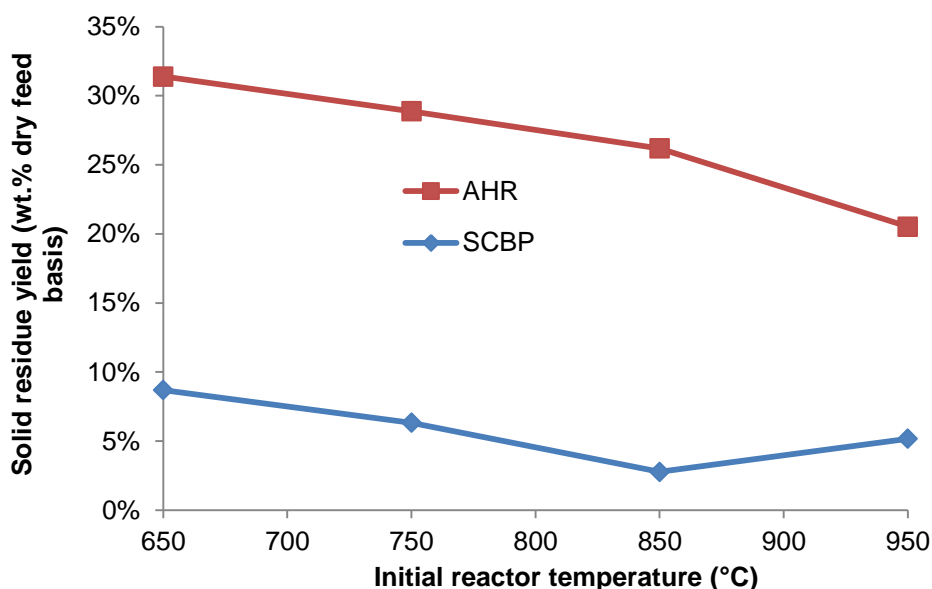
Figure 110: Effect of initial reactor temperature on solid residue yield

Table 62 shows that gasification of SCBP leaves a mixture of black char and grey ash, however gasification of AHR leaves black char. This confirms that AHR is more refractory than SCBP with significant amounts of unreacted carbon remaining after high temperature gasification. Table 62 also shows that the solid residue from SCBP at 850°C was mostly grey ash, but a combination of black char and grey ash for all other temperatures, as there was a delay in stopping air flow and removing the sample from the reactor.

Table 62: Solid residue appearance after gasification

Initial reactor temperature (°C)	Solid residue from SCBP	Solid residue from AHR
650	Black char and grey ash	Black char
750	Black char and grey ash	Black char
850	Mostly grey ash - delay in removing the sample from the reactor	Black char
950	Black char and grey ash	Black char

Figure 111 to Figure 114 shows the samples before and after gasification at 950°C. It can be seen that AHR is more thermally stable leaving a higher carbon content solid product.

Figure 111: SCBP   **Figure 112:**   **Figure 113: AHR**   **Figure 114:**
                         Gasified SCBP at   **Gasified AHR at**
                              950°C   **950°C**

Successful gasification should leave a solid residue consisting of mainly ash. However, due to limitations of this batch system, an increased air flow over the sample could increase carbon conversion, but lead to an increased carbon dioxide concentration and hence lower gas HHV. In typical gasification, CO_2 would be converted to CO so carbon conversion would not be limited. As AHR leaves a significant amount of unreacted carbon after gasification, a recycle system could be used, as those used in fluidised bed gasifiers, to increase the carbon conversion to carbon-bearing gases.

The equations used to calculate cold gas efficiency and carbon conversion efficiency can be found in Appendix 3. Figure 115 shows the effect of temperature on the cold gas efficiency. Generally, cold gas efficiency of AHR gasification increased to 43% with increasing temperature i.e. the energy available in the product gas as a ratio of the energy in the original feed increased as the initial reactor temperature increased. Cold gas efficiency was considerably low due to energy loss in the form of recoverable sensible heat, heat loss and energy remaining in tars and unreacted solids. Figure 115 also shows increasing carbon conversion efficiency with increasing temperatures as heat transfer increases with increasing temperature, therefore, more of the carbon is gasified [198].
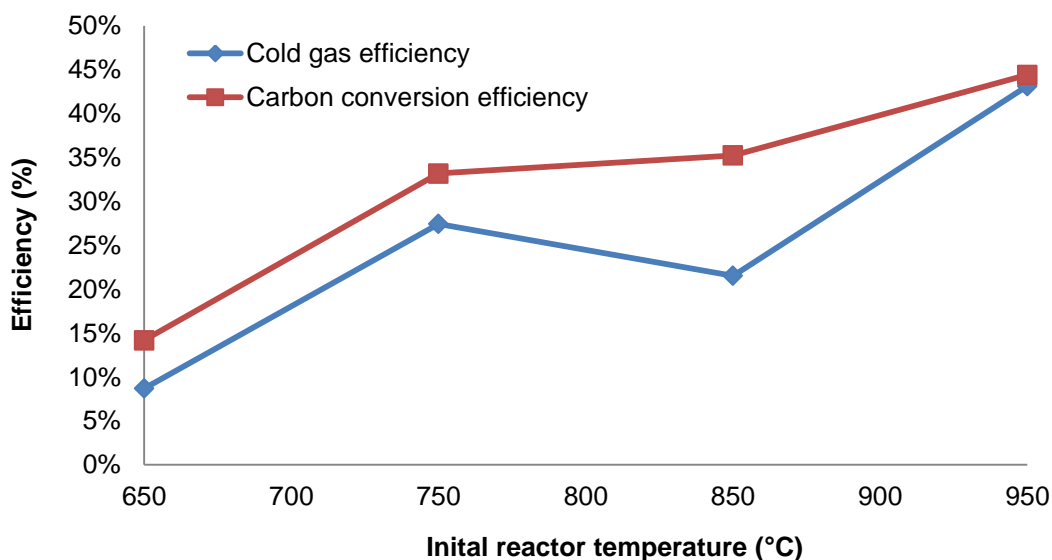
Figure 115: Effect of temperature on cold gas efficiency and carbon conversion efficiency of AHR gasification

Although conversion is expected to be high, gasification in a fluidised bed is limited as once char particles continue to shrink into fine dust, the dust is entrained into the gas stream [67]. Also, as AHR is more refractory than biomass, it is likely that longer residence times and higher temperatures are required to increase the carbon conversion efficiency of AHR. The bed depth of a fluidised bed gasifier is an important design parameter. An increased bed depth in a fluidised bed gasifier would allow for longer solid and gas residence times which would be necessary to improve carbon conversion of refractory AHR, but this is reported to have a cost penalty [156]. Alternatively, fluidised bed gasifiers can use recycle systems to utilise the entrained char and increase the carbon conversion efficiency.

Catalytic gasification was not carried out in this work, but for this, compositional analysis of tars would be necessary to identify the suitable cracking catalysts. The liquid product consisting of tars and water were fractionated and collected in various parts of the glassware collection system such as the piping, iso-propanol and silica gel bottles. Careful washing of these glassware collection components would be required for tar analysis. However, some tars are usually thermally cracked or partially oxidised in typical gasification and tars produced in these batch experiments would not be representative of those produced in commercial gasifiers. Therefore, the tar composition was not analysed in this work.

Figure 116 shows clean iso-propanol before tar collection. Figure 117 and Figure 118 show the tars collected in the iso-propanol after a run with SCBP and AHR respectively. Although fewer tars were produced from AHR, it can be seen that the tars collected from AHR are much darker than those collected from SCBP.

Figure 116: Iso-propanol before run   **Figure 117: Iso-propanol after SCBP run**   **Figure 118: Iso-propanol after AHR run**

For the purposes of this work, the mass of tar was of more importance to compare tar yield (wt.%) from SCBP and AHR. It was assumed that there was no tar in the reactor as it was glowing orange at the end of experiments. Figure 119 shows the effect of temperature on tar yields from SCBP and AHR. An increase in temperature reduces the tar yield from 33.37 wt.% to 13.98 wt.% for SCBP and from 15.41 wt.% to 5.27 wt.% for AHR. In commercial gasification, these tars would be further reduced by thermal cracking or partial oxidation inside the gasifier. However, as AHR produce less tars, the product gas from AHR is expected to be cleaner than that from SCBP which requires less cleaning and tar removal from the product gas.
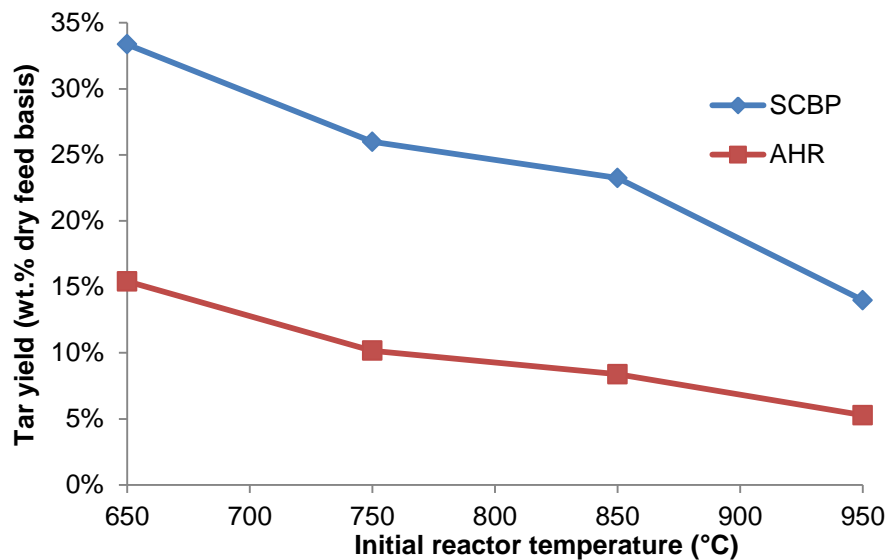
Figure 119: Effect of initial reactor temperature on tar yield

The gas yields from SCBP are expected to be higher than from AHR as SCBP has a higher volatile content and biomass is more reactive than AHR. Figure 120 shows a distinct trend where increasing temperature increases the gas yield.
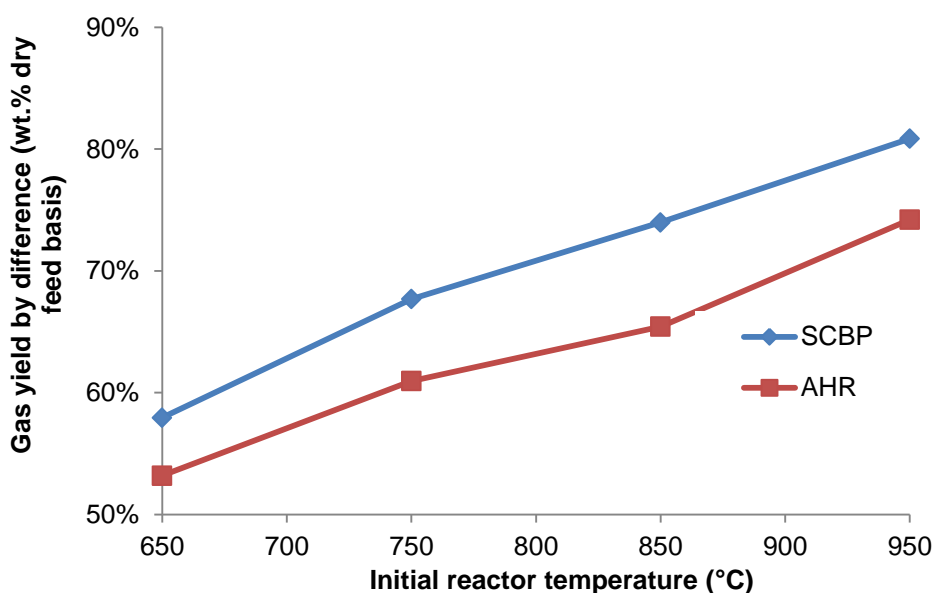
Figure 120: Effect of initial reactor temperature on gas yield

Table 63 summarises the mass balance for air-blown batch gasification of AHR and SCBP at 650-950°C.

Table 63: Mass balance from air-blown batch gasification

Initial reactor T (°C)	650°C	750°C	850°C	950°C
Solid (unreacted carbon & ash) from SCBP	8.68	6.32	2.77	5.16
Solid (unreacted carbon & ash) from AHR	31.39	28.88	26.20	20.52
Liquid (water & tars) from SCBP	33.37	25.99	23.24	13.98
Liquid (water & tars) from AHR	15.41	10.16	8.38	5.27
Gas (by difference) from SCBP	57.95	67.69	73.98	80.85
Gas (by difference) from AHR	53.20	60.96	65.42	74.21

9.3 Interim conclusions

9.3.1 Pyrolytic gasification

- AHR is a powder which is difficult to screw feed, handle and process in a reactor such as the 300g/h fluidised bed reactor used in this work.

- Although pyrolytic gasification is suitable for high volatile content feedstocks, pyrolytic gasification is not suitable for AHR and high lignin content feedstocks as char yields stabilise between 550-650°C without the addition of oxygen. For this reason, char yields from AHR would stabilise at approximately 40 wt.% char yield at temperatures higher than 650°C.

- The batch system at Cardiff University resembles slow pyrolysis using nitrogen due to longer reaction times compared to the 300g/h continuous system. More solids and fewer tars were produced with increased reaction times. The solid yield increased from 36.58 wt.% to 50.40 wt.% and the tar yields decreased from 43.34 wt.% to 26.64 wt.% for AHR. The gas yields were marginally higher using the batch system for both feedstocks.

166

9.3.2 Batch air-blown gasification

- Increasing reactor temperature reduced solid and tar yields, but increased gas yield from both SCBP and AHR. AHR gave relatively low gas yields (74.21 wt.%), low tar yields (5.27 wt.%) and high solid yields (20.52 wt.%) at 950°C.

- Air-blown gasification produces high yields of a low energy content gas as the product gas is diluted with nitrogen. When compared to pyrolytic gasification, oxygen increases carbon conversion and reduces the remaining solid yield from AHR to 20.52 wt.% (dry feed basis) at 950°C.

- Efficiency of AHR gasification was defined by cold gas efficiency and carbon conversion efficiency. Cold gas efficiency of approximately 44% was achieved from AHR gasification in the batch system. These efficiencies are considerably low when compared to those obtained commercially and reported in the literature due to the heat loss from the reactor and the energy remaining in the unreacted carbon and tars.

- The maximum carbon conversion efficiency of AHR at 950°C was 43%. Typical carbon conversion efficiencies of >95% are expected, but AHR gasification was limited by the use of a batch system as the completion of gasification was defined at the point where CO level started to fall. If more oxygen was added, CO_2 would be produced at the expense of CO which lowered the gas HHV. This point was also the maximum H_2 concentration which was obtained from this batch system and this is reported to be the optimum point for process efficiency [178]. However, in continuous gasification, the reaction would not be stopped at this point.

- More unreacted carbon remained from AHR compared to SCBP in the batch system due to the refractory nature of the lignin and humins in AHR and so rate of reaction was slower. Increasing the initial reactor temperature reduced the time taken for CO to peak, but AHR took longer for CO to peak compared to SCBP.

- The low volatile content AHR yielded less tars than biomass which is beneficial as gas cleaning is likely to be less problematic.

- In this system, higher temperatures favoured the production of CO which increased the gas HHV.

- Air-blown gasification of high lignin and humin content AHR produces a lower energy content gas (5.78MJ/Nm^3) compared to standard biomass (7.28MJ/Nm^3). Both are suitable for boiler and engine applications [196]. However, a higher energy content gas is required for the production of biofuels.

- Significant amounts of useful carbon remain in the solid product after AHR gasification, therefore, modifications to exiting biomass gasifiers would be required to increase carbon conversion e.g. longer reaction times by increased

bed height, higher reaction temperatures by increasing equivalence ratio or extensive solid recycling as in fluidised bed gasifiers.

- Nitrogen content of the product gas from SCBP and AHR at 950°C in the batch gasifier is comparable with the nitrogen content of the product gas in commercial fluidised bed gasification. The product gas from SCBP consists of approximately 50vol% of gasification products and the product gas from AHR consists of approximately 35vol% of gasification products. The remainder of the gas is nitrogen which requires larger downstream equipment.

10 IMPROVING FEEDING AND HANDLING PROPERTIES OF POWDERED ACID HYDROLYSIS RESIDUES

The objective of this chapter is to improve feeding and handling properties of acid hydrolysis residues (AHR). AHR have a high lignin and humin content that represent a considerable proportion of the original energy in the biomass and crumble into a powder when touched. Tests detailed in Chapter 9 have shown that feeding a powder into a fluidised bed reactor can be problematic as the powder can be blown out of the reactor before it has been thermally processed. Paste feeding an AHR and methanol mixture are attempted. Producing pellets from AHR and fast pyrolysis bio-oil is also presented as a more promising technique to improve feeding and handling properties of AHR. Comparison with commercial pelletisation methods are made in this work.

10.1 Background

10.1.1 Paste feeding

Aston is currently patenting a pressurised (3 bar) paste feeding system to feed high lignin content residues into the top of a fluidised bed reactor. Previous work was carried out at Aston University where a paste was produced by mixing lignin and methanol (2:1 mass ratio). Methanol is cheap and hydrogen rich which can act as a hydrogen transferring agent potentially reducing char formation [59]. Methanol is reported to thermally decompose into carbon monoxide and hydrogen where hydrogen reacts with pyrolysis products to produce aromatic hydrocarbons from lignin.

The paste feeding procedure was repeated with AHR as these AHR have higher lignin content compared to whole lignocellulosic biomass. AHR was mixed with methanol to produce a paste which would then be directly fed into the top of the 100g/h reactor. Large quantities of AHR were not available so could not be tested on larger systems.

10.1.1 Pelletisation

The powder nature of AHR posed a challenge in screw feeding and hence needed to be addressed in order to process the AHR powder in laboratory equipment. Densification of the powder was required and pelletisation of AHR was tested as an alternative approach.

Biomass has a low energy density and therefore, using biomass close to the source would be the most economically feasible option. However, if biomass is to be transported to remote locations, the cost of transportation can be reduced by densification. Densification technologies can also help overcome feeding problems

associated with fine powders. Therefore, pelletisation not only increases bulk and energy densities, but can also improve material strength and create a more uniform feedstock for improved handling, storage and screw feeding to conversion processes such as boilers and gasifiers. The pellets produced can then be used in biomass-based thermal conversion processes such as combustion, pyrolysis or gasification more effectively.

A fact sheet published by Ciolkosz provides details on the biomass pellet production process. The fact sheet states that a fuel pellet is usually cylindrical in shape with a diameter of 6-8mm and a maximum length of 38mm [199]. Furthermore, an ideal fuel pellet has a high heating value, is dry, hard, durable and has a low ash content. The pelletising process involves forcing ground biomass through a die using pressure. A roller compresses the biomass against a heated metal plate. The biomass is then forced through small holes at approximately 150°C and a blade subsequently slices the pellet to the desired length. This process is commonly known as extrusion. The pellets are finally cooled and dried by blowing air over them.

Pressure, heat and binders are conventionally used to strengthen inter-particle bonding and promote adhesion. Some biomass materials, such as wood and bagasse, fuse together naturally. It is reported that naturally occurring lignin can help hold a pellet together [199]. Kaliyan and Morey report that steam conditioning or pre-heating is necessary as the heat and moisture activate the natural constituents of biomass to act as binders or additives [200]. In order to avoid excessive biomass volatilisation the recommended limit for the pre-heating temperature is 300°C [200].

The fracture strength of the sugarcane bagasse pellets (SCBP) provided was considered to be acceptable for commercial thermal processing, allowing for transportation, handling and storage with minimal loss of fines. Sugarcane bagasse (Figure 121) was dried in a flash drier at approximately 280°C with a contact time of 3-4 seconds until the moisture content was around 11-12%. The dried bagasse was then ground and mechanically pelletised (shown in Figure 122) at Cane Technology Centre (CTC). The heat applied in the pelletising process was sufficient and so additional binders were not required.

Figure 121: SCB   **Figure 122: SCBP**

Some biomass materials require commercially available binders to produce more robust feedstocks. The most commonly used binders are lignosulphonates or sulphonate salts from lignin [201]. Other binders such as clay, mud, starch, vegetable oil or wax have also been used.

Pellets were made with the addition of water using an agricultural pelletiser as mentioned in Chapter 9. These pellets were ground and screw fed into a fluidised bed reaction system. The ground pellets crumbled into a powder before entering the reactor and so were entrained out the reactor before being thermally processed. Some temporary adjustments were made to the operating procedure and the ground pellets were eventually fed into the reactor. However, alternative binders were required in order to produce a more robust sample and improve feeding into larger scale gasifiers such as fluidised beds.

The refractory nature of AHR limits successful pelletisation with additives and most conventional additives are costly or have a deleterious effect on the properties. A new approach of using fast pyrolysis bio-oil as a binder was therefore considered in this work. Bio-oil polymerises and solidifies on curing at temperatures above above 100ºC producing a solid residue. 50 wt.% of the bio-oil is vapourised into a by-product consisting of water and light organic volatiles (aldehydes, organic carboxylic acid and alcohols) [202, 203]. Therefore, if bio-oil was added to AHR and cured in the oven above 100°C, the bio-oil was expected to solidify and help fuse the AHR powder into a robust feedstock.

The primary aim of this work was to determine whether bio-oil could be added to AHR to densify and strengthen the material for screw feeding into thermal processing units, such as a gasifier. The second objective was to determine the minimum amount of bio-oil required for pelletisation. The third objective was to devise a processing method to produce suitable pellets for thermal processing. As the acid

hydrolysis process produces an AHR with a high moisture content (approximately 70 wt.%), it was also necessary to investigate the effect of the addition of water.

10.2 Methodology

10.2.1 Paste feeding AHR

Modifications were made to the paste feeding system to measure pressure and avoid overpressure. The pressure of nitrogen in the feeder could be controlled on the nitrogen cylinder. However, a safety relief valve was required on the nitrogen line in case of an error in controlling the valve on the cylinder. Figure 123 shows the paste feeder with a compression fitting added to measure the pressure in the paste feeder. A pressure relief valve could be added in case the vessel over pressures. Several feeding tests were carried out to determine conditions required to allow the paste to flow from the hopper into the reactor without phase separating or blocking the feeding tube. Also, although a 2:1 mass ratio of lignin and methanol was used, the consistency and viscosity of the paste was important.
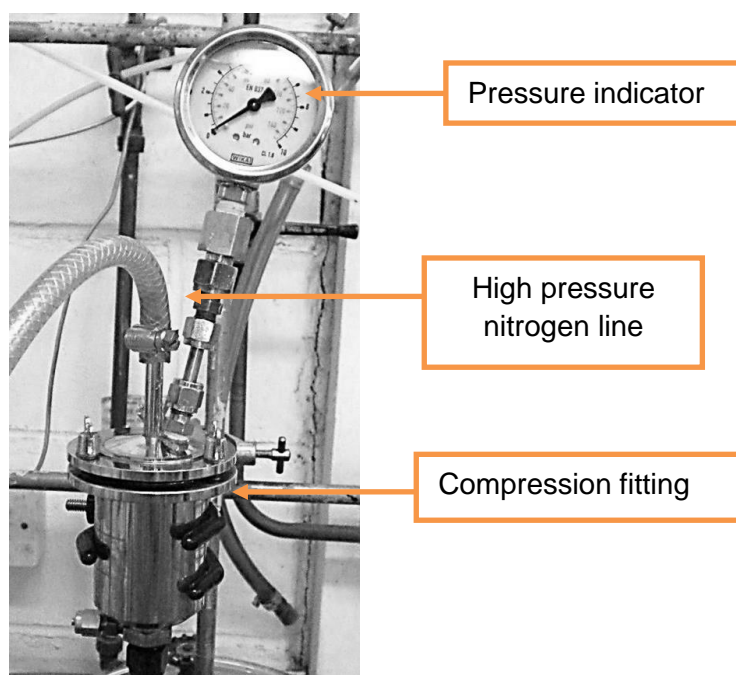
Figure 123: Modified paste feeding system

10.2.2 Pelletisation of AHR and SCB

Bio-oil produced from the BTG fast pyrolysis process [204] was purchased and used as a binder in this work. Four methods for producing pellets were tested on both SCB and AHR, which included the following:

- Method A – Addition of water to SCB or AHR
- Method B – Addition of bio-oil to SCB or AHR
- Method C – Addition of water to SCB or AHR, followed by bio-oil
- Method D – Addition of bio-oil to SCB or AHR, followed by water

Pellets produced from SCB using the preparation techniques detailed above were compared to mechanically pressed SCB pellets provided by CTC. This procedure also helped indicate the improvement in pellet fracture strength that could potentially be achieved as a result of mechanical pressing.

A pestle and mortar was used to thoroughly mix and distribute the binder (water and/or bio-oil) over the SCB or AHR particles. 1g of each mixture was then manually pressed in an 8mm or 12.5mm diameter glass vial. Pellets are industrially extruded at 150°C [199] and at this temperature bio-oil polymerises forming a solid that acts as the pellet binder. Hence, the glass vials containing each mixture were placed in an oven and cured at 150°C for 1 hour until there was no further mass loss. 1g of bio-oil was also cured in the oven at 150°C to determine the mass loss profile of bio-oil at this temperature.

All pellets prepared are identified using a reference to their component proportions:

Material (wt.% Material, wt.% BTG bio-oil, wt.% water)

where the first word indicates the type of material used (SCB or AHR), followed by the wt.% BTG bio-oil and wt.% water. For example, SCB (75/0/25) represents a pellet composed of 75 wt.% SCB, 0 wt.% BTG bio-oil and 25 wt.% water. Table 64 summarises the methods used and the composition of the pellets prepared in this work.

Table 64: Preparation methods and composition of pellets

Sample ID	Preparation method	SCB or AHR (wt.%)	Bio-oil (wt.%)	Water (wt.%)
SCB				
SCB (100/0/0)	A	100	0	0
SCB (75/0/25)	A	75	0	25
SCB (75/25/0)	B	75	25	0
AHR				
AHR (75/0/25)	A (mechanical pressing)	75	0	25
AHR (75/0/25)	A (manual pressing)	75	0	25
AHR (100/0/0)	B	100	0	0
AHR (90/10/0)	B	90	10	0
AHR (80/20/0)	B	80	20	0
AHR (75/25/0)	B	75	25	0
AHR (70/30/0)	B	70	30	0
AHR (60/40/0)	B	60	40	0
AHR (50/50/0)	B	50	50	0
AHR (60/20/20)	C (8mm pellet diameter)	60	20	20
AHR (60/20/20)	C (12.5mm pellet diameter)	60	20	20
AHR (60/20/20)	D	60	20	20

Fresh pellets were analysed i.e. as soon as they were prepared. The fracture strength of the pellets produced was tested using a pellet fracture strength tester, purchased from AMANDUS KAHL, Germany. Each pellet was placed between the two bars in this device as shown in Figure 124 and the force (measured in kg) required to crack the pellet was determined by manually increasing static pressure. This device was used to determine whether the addition of bio-oil could increase the fracture strength of the feedstock. These tests were carried out in triplicates.
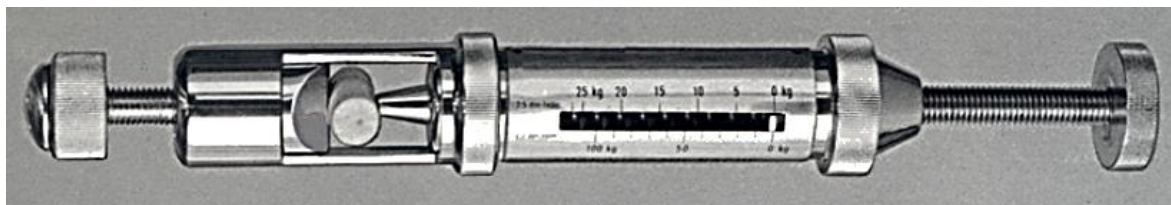
Figure 124: KAHL Pellet Fracture Strength Tester

10.3 Results and discussion

This section details and discusses the results from the paste feeding and pelletisation tests of AHR.

10.3.1 Paste feeding AHR

AHR crumbles into a fine powder when touched, but there is still some needle-like residue which was less hydrolysed and did not crumble. This can cause blockages in the outlet of the paste feeder. Therefore, the sample was sieved (<0.25mm) to leave a homogeneous powder before being mixed with methanol to form a paste (see Figure 125).

Figure 125: Needle-like AHR on the left and homogenous powder AHR on the right

Unpublished work carried out within the Bioenergy Research Group showed a 2:1 ratio of lignin (Alcell) to methanol could be successfully fed into the reactor [59]. This Alcell lignin and methanol mixture was reproduced and is shown in Figure 126.

This mixture was a sticky, tar-like mixture which did not phase separate even under pressure.

Figure 126: Alcell lignin with methanol (2:1) paste

A 1:1 (AHR to methanol) produced a mixture which did not flow. A 2:1 (AHR to methanol) ratio produced a mud-like mixture rather than a sticky paste. The mixture did not phase separate at standard room temperature and pressure. However, the methanol was squeezed out when pressure was applied to the mixture leaving an AHR filter cake in the feeder (see Figure 127) and methanol filtrate (see Figure 128).

Figure 127: AHR acts as a filter cake for methanol

Figure 128: Methanol filtrate is forced through the solid AHR

When additional methanol was added to improve feeding of the AHR paste, the mud-like paste on top of the feeder outlet was forced out as shown in Figure 129. The nitrogen flows straight through the outlet which meant the pressure in the feeder could not be maintained.

Figure 129: Mud-like paste in the bottom of feeder

Figure 130: Rubber bung to act as a press on the paste and avoid nitrogen leaving the feeder

A rubber bung was used like in a syringe as shown in Figure 130 to maintain nitrogen pressure in the feeder. The nitrogen applies pressure to the bung pushing the paste out of the feeder. When an excessive amount of methanol was used, the methanol acted as a carrier for the AHR, but there was little or no control over the flow of the mixture. There were immediate blockages with narrow pipes so a larger diameter pipe was used. Figure 131 shows the paste being pushed out like a thread at only 1 bar. However, there was no control of flow of paste and the paste was exiting the feeder too quickly.

Rapid feeding like a thread

Figure 131: Thread-like feeding which could not be controlled and feeding too fast

It was concluded that the AHR could not be fed using this high pressure paste feeding system as with Alcell lignin. This work indicated that the miscibility properties of AHR and Alcell lignin with methanol were dissimilar likely to be due to the presence of humins in AHR. Also, lignin properties are dependent on how it was recovered. For example, Alcell lignin is solubilised in organic solvents in the Organosolve process, whereas AHR are insoluble residues as a result of acid hydrolysis.

10.3.2 Pelletisation of AHR

Pelletisation was investigated as an alternative method to improve feeding and handling properties of AHR. AHR and bio-oil properties are shown in Table 65. The HHV of AHR (24.94 MJ/kg) is greater than the HHV of bio-oil (17 MJ/kg). The HHV of bio-oil is comparable to the HHV of biomass. AHR has significantly higher lignin and humin content than biomass and so the HHV is expected to be greater than that of bio-oil.

Table 65: AHR and BTG bio-oil ultimate analysis

Sample	C (wt.%)	H (wt.%)	N (wt.%)	O* (wt.%)	S (wt.%)	Ash (wt.%)	HHV (MJ/kg)
AHR	62.61	5.00	0.15	26.07	0.18	6.00	24.94
Bio-oil [16]	56	6	<0. 1	38	Nm	Nm	17

*Oxygen by difference

Bio-oil polymerises above 100°C and pellets are produced at 150°C in commercial pelletisers. Therefore 1 g of bio-oil was cured in an oven at 150°C for one hour until there was no further mass loss. Figure 132 and Figure 133 show 1 g of bio-oil before and after curing in the oven at 150°C for one hour. 44.3 wt.% of the bio-oil was vapourised leaving a solid residue which is expected to strengthen the bonds between the AHR particles.

Figure 132: 1g of bio-oil

Figure 133: Bio-oil after curing in the oven at 150°C for 1 hour

As expected, the addition of bio-oil to AHR increased the volatile content of the AHR as shown in Figure 134. Increasing the bio-oil concentration from 0 to 50 wt.% increased the volatile content from 36.60 to 46.17 wt.%. As a result, the char content

decreased from 63.40 to 53.83 wt.% There is an unexpected trend with a 20% bio-oil concentration. Volatile content was measured in duplicates and char was calculated by difference (on a dry feed basis), The volatile and char content for 20% is expected to fall in between the results for 10% and 30%.
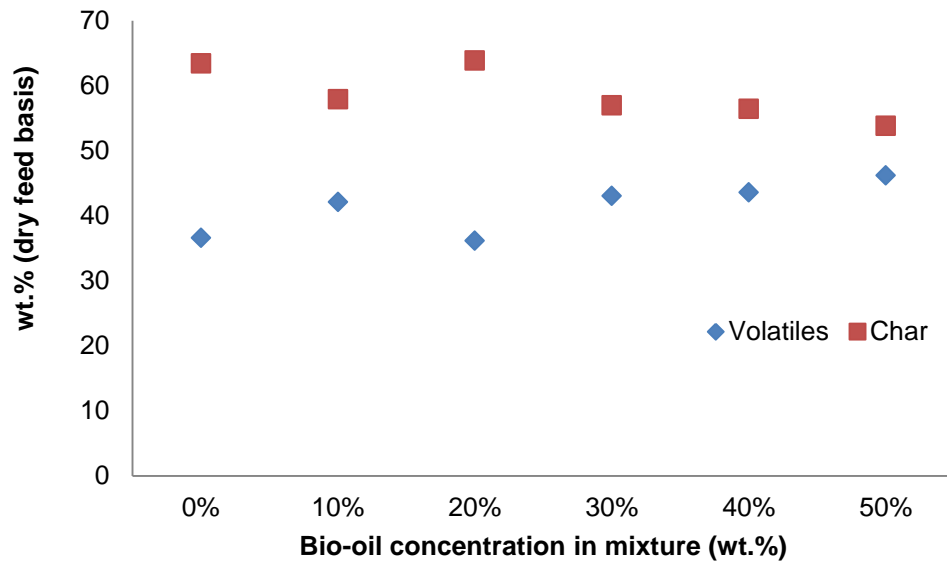
Figure 134: Effect of bio-oil addition on volatile and char content

Figure 135 shows the DTG profiles of the pellets from Method B with increasing bio-oil concentration from 0 wt.% to 50 wt.%. The increase in bio-oil concentration showed a distinct enhancement of the first shoulder which can be attributed to the volatiles present in bio-oil.
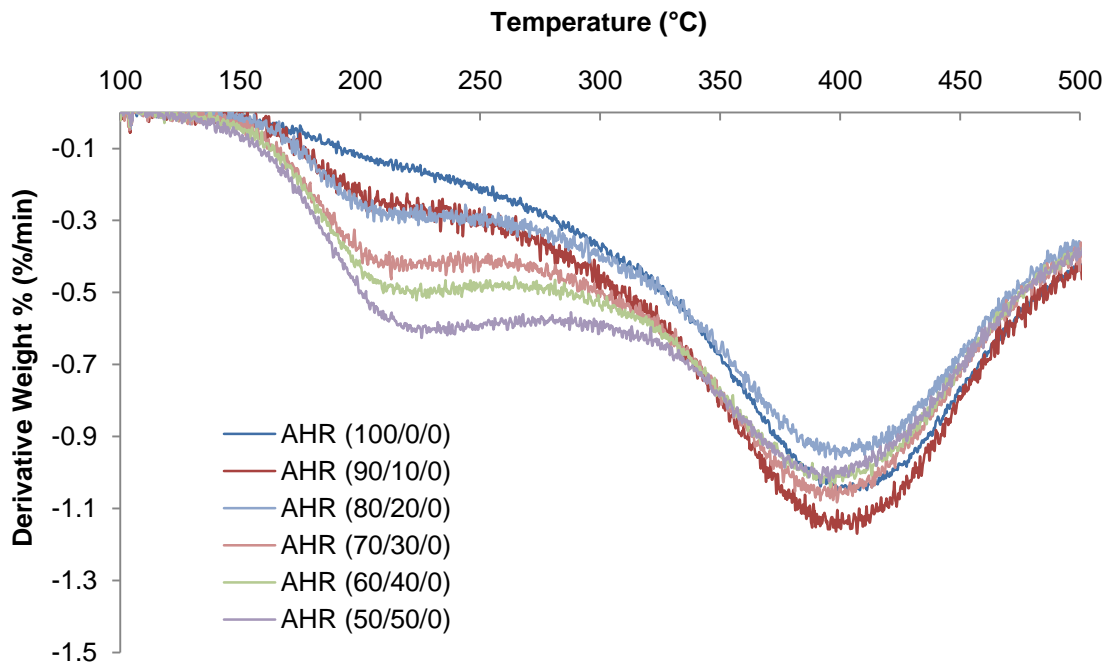
Figure 135: DTG profiles of ground cured pellets

Table 66 shows the ultimate analysis of the pellets produced using Method B with increasing bio-oil concentrations. The composition of the pellets does not vary

significantly and as a result, neither does the HHV. However, the AHR produced with 10 wt.% bio-oil (90/10/0) is low due to the low carbon and hydrogen content which is likely to be a result of experimental error in preparing the pellet.

Table 66: Ultimate analysis of pellets produced after curing AHR and bio-oil mixtures in the oven at 150°C for 1 hour

Dry basis	C (wt.%)	H (wt.%)	N (wt.%)	O* (wt.%)	S (wt.%)	Ash (wt.%)	HHV (MJ/kg)
AHR (100/0/0)	64.77	4.64	0.15	30.41	Nm	0.07	24.92
AHR (90/10/0)	60.59	4.41	0.15	34.83	Nm	0.06	22.74
AHR (80/20/0)	63.59	4.70	0.13	31.56	Nm	0.05	24.46
AHR (75/25/0)	64.48	4.78	0.14	30.58	Nm	0.05	24.98
AHR (70/30/0)	62.28	4.67	0.12	32.40	Nm	0.04	24.46
AHR (60/40/0)	63.48	4.86	0.10	31.54	Nm	0.04	24.62

*Oxygen by difference

The physical appearance and fracture strength of the SCB and AHR pellets results follow. Mechanically pressed SCB pellets provided by CTC (Figure 136) with an 8mm diameter are considered to be of sufficient strength to withstand crumbling that can occur during screw feeding. Pellet fracture strength tests showed that these mechanically pressed pellets can withstand up to 23kg of force before cracking. This pellet fracture strength value was used for comparison with other pellets made manually in this work.

Figure 136: Mechanically pressed SCB pellet (as received)

SCB was manually pressed into an 8mm glass vial and cured in an oven using the methods outlined earlier. This was carried out in order to indicate the extent to which pellet fracture strength could potentially be improved by mechanical pressing as opposed to manual pressing. Both mechanically and manually pressed pellets were of 8mm diameter for comparison. The first sample (Figure 137) was pressed and cured in an oven without the addition of a binder to use as a standard. The second sample (Figure 138) contained 25 wt.% water and the third sample (Figure 139) contained 25 wt.% bio-oil.

| **Figure 137: SCB (100/0/0)** | **Figure 138: SCB (75/0/25)** | **Figure 139: SCB (75/25/0)** |

Figure 140 shows that the presence of 25 wt.% water increased the force required to crack the pellet from 1.4kg to 7.2kg, therefore increasing the pellet fracture strength. Feedstocks such as sugarcane bagasse can be adequately pelletised using water. Mechanically pressed SCB pellets, produced with the presence of water, required 23kg of force to crack, whereas manually pressed SCB pellets, with the addition of water only, required 7.2kg. Therefore, this indicates that mechanical pressing, in an industrial scale pelletiser, is expected to significantly increase the fracture strength of a pellet.

Replacing the 25 wt.% water with 25 wt.% bio-oil further increased the force required to crack the pellet from 7.2kg to 8kg. Therefore, bio-oil does not significantly increase pellet fracture strength of sugarcane bagasse.
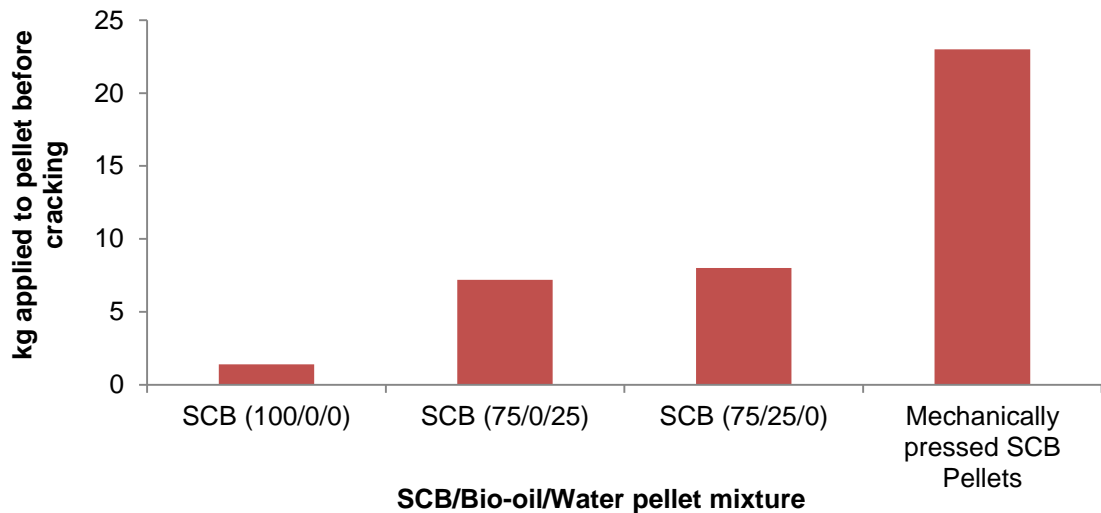
Figure 140: Effect of adding water and bio-oil to SCB in comparison with mechanically pressed SCB pellets

An AHR pellet made with 25 wt.% water using Method A is shown in Figure 141. These pellets were brittle and crumbled very easily requiring only 1kg to crack. Another test using Method B was carried out to investigate the effect of replacing water with bio-oil (Figure 142).
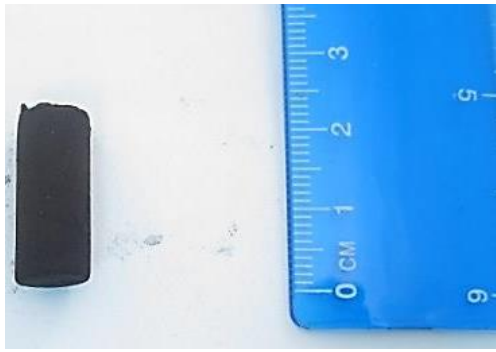
Figure 141: AHR (75/0/25)
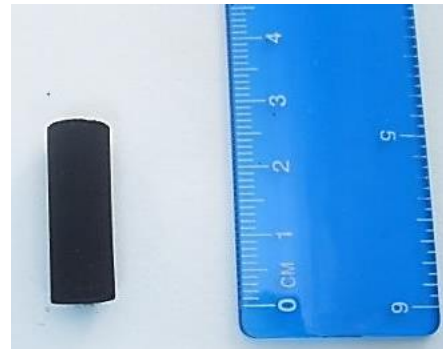
Figure 142: AHR (75/25/0)

Although bio-oil does not significantly increase fracture strength of sugarcane bagasse pellets, the results in Figure 143 indicate that adding bio-oil to AHR can significantly increase the force required to crack the pellet from 1kg to 7.4kg.
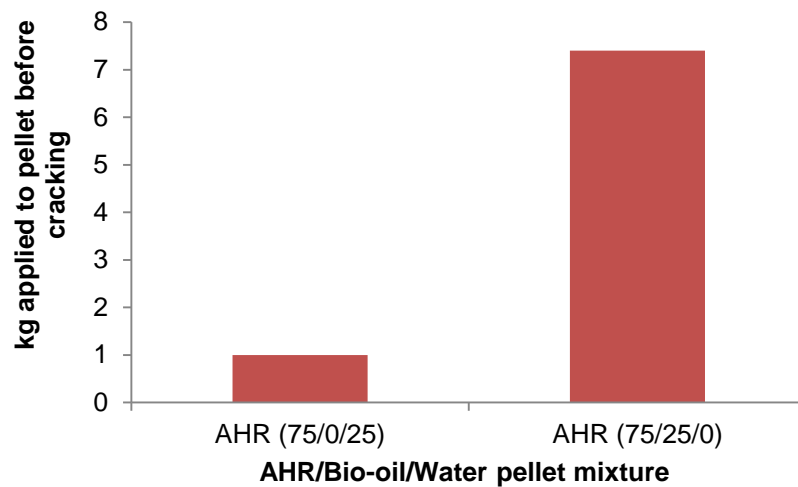
Figure 143: Effect of adding bio-oil to AHR for pelletisation compared with adding water on pellet fracture strength

The minimum amount of bio-oil required for pelletisation of AHR using the manual pressing technique was investigated. Figure 144 to Figure 149 show the pellets made using Method B with increasing bio-oil concentrations from 0 to 50 wt.%. When using the manual pressing technique, bio-oil concentrations lower than 20 wt.% were insufficient as the pellets still crumbled into a powder. Using bio-oil concentrations as high as 50 wt.% had undesirable effects on the structure of the pellet. Figure 149 shows the pellet to have split.
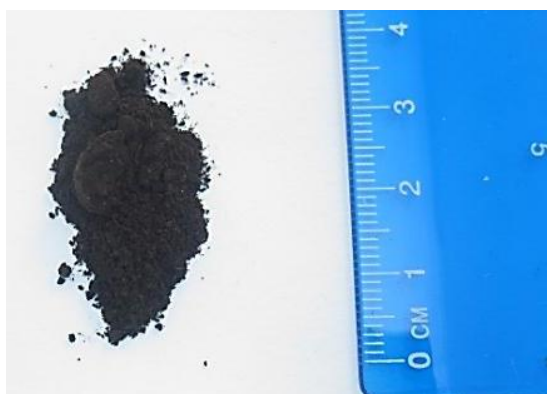
Figure 144: AHR (100/0/0)

Figure 145: AHR (90/10/0)
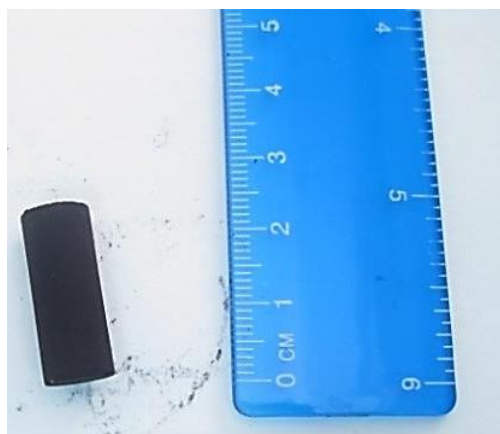
Figure 146: AHR (80/20/0)
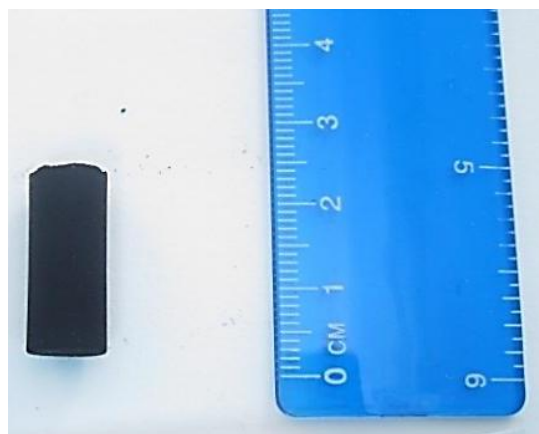
Figure 147: AHR (70/30/0)
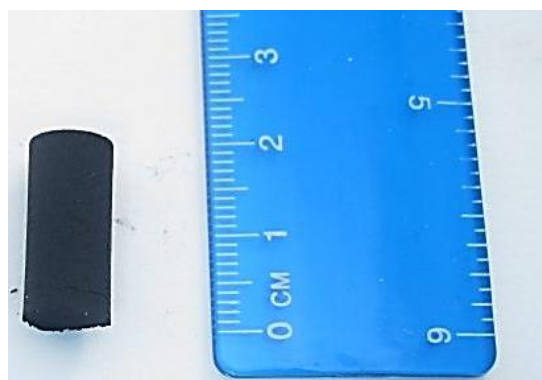
Figure 148: AHR (60/40/0)
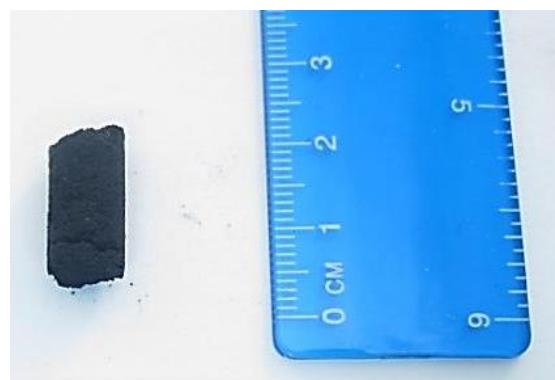
Figure 149: AHR (50/50/0)

Figure 150 indicated that increasing the bio-oil concentration increased the force required to crack the pellet from 0kg to a maximum of 23kg, leaving a more robust pellet. However, using concentrations as high as 50 wt.% reduced the force required to crack the pellet to 16.8kg. Therefore, bio-oil can be added to AHR in the range of 20-40 wt.% for improved pellet fracture strength.
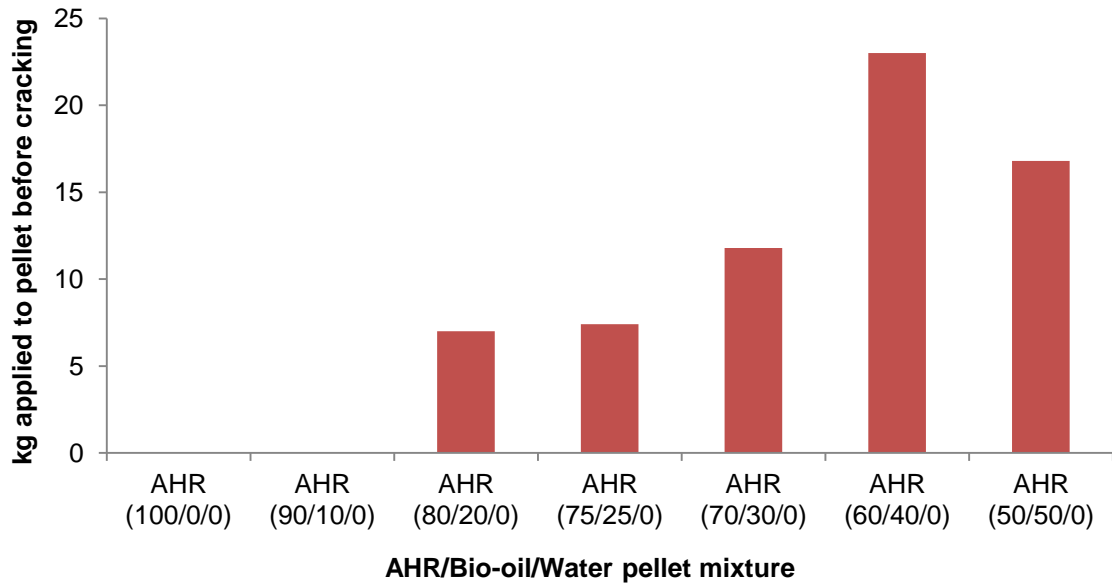
Figure 150: Effect of bio-oil concentration on AHR pellet fracture strength

As previously stated, 44.3 wt.% of bio-oil vapourised when it was cured in the oven at 150°C. Similar results were also reflected when AHR and bio-oil mixtures were cured at 150°C in the oven.

As the ash content of bio-oil is less than 0.02 wt.% [79], the ash content of the AHR (6 wt.%) was used to calculate the ash content of the cured pellet. Figure 151 shows that the ash content decreases from 6.52 to 3.80 wt.% when increasing the bio-oil concentration from 0 to 50 wt.%. This is as expected and beneficial for biomass thermal conversion processes such as combustion and gasification where low ash feeds are required.
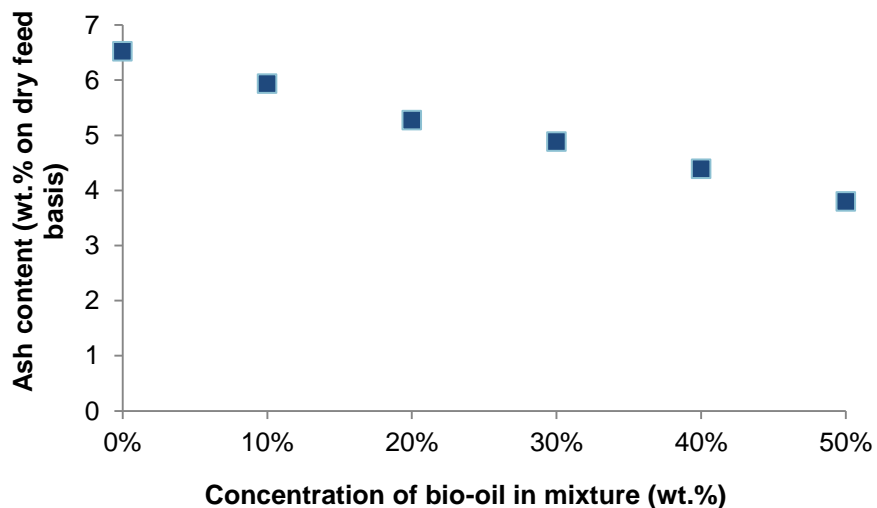
Figure 151: Ash content of cured AHR pellet with increasing concentration of bio-oil

The effect of the binder addition procedure on the pellet fracture strength was investigated. It is known that adding significant amounts of water to bio-oil leads to

phase separation [8]. This is confirmed and shown in Figure 152 where a 1:1 bio-oil to water ratio (mass ratio) is used.

Figure 152: Phase separation when water is added to bio-oil at a 1:1 mass ratio

Therefore, the bio-oil or water should be directly added to the AHR as mixing bio-oil with water prior to adding to AHR will lead to phase separation. As AHR produced from the acid hydrolysis process contains 70 wt.% moisture, bio-oil should be added to wet AHR to avoid unnecessary drying. Figure 153, Figure 154 and Figure 155 shows the pellets produced using method C and D and the larger diameter pellet respectively.
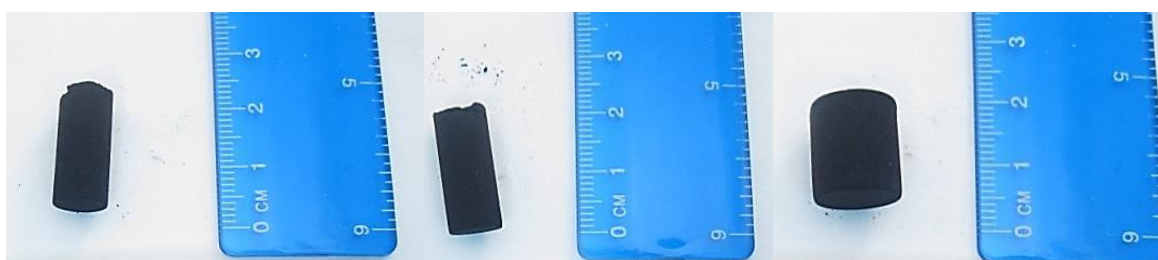
| **Figure 153: AHR (60/20/20) Method C - 8mm** | **Figure 154: AHR (60/20/20) Method D - 8mm** | **Figure 155: AHR (60/20/20) Method C - 12.5mm** |

Figure 156 shows that the pellets produced using Method D required less force to crack the pellet (6.8kg) compared to pellets produced using Method C (8kg). The addition of water before bio-oil produced a harder pellet suggesting that the bio-oil was distributed more effectively and uniformly covering more AHR particles when water was already present in AHR. On the other hand, the bio-oil may have phase separated on contact with the water leading to a polymerised material which further improved fracture strength of the cured pellet. Bio-oil would probably be added to wet AHR in a commercial process subsequent to an acid hydrolysis process. Increasing the pellet diameter from 8mm to 12.5mm increased the force required to crack the pellet from 8kg to 22.4kg. However, gasification of large particles can lead to significant amounts of unreacted carbon in the solid product.
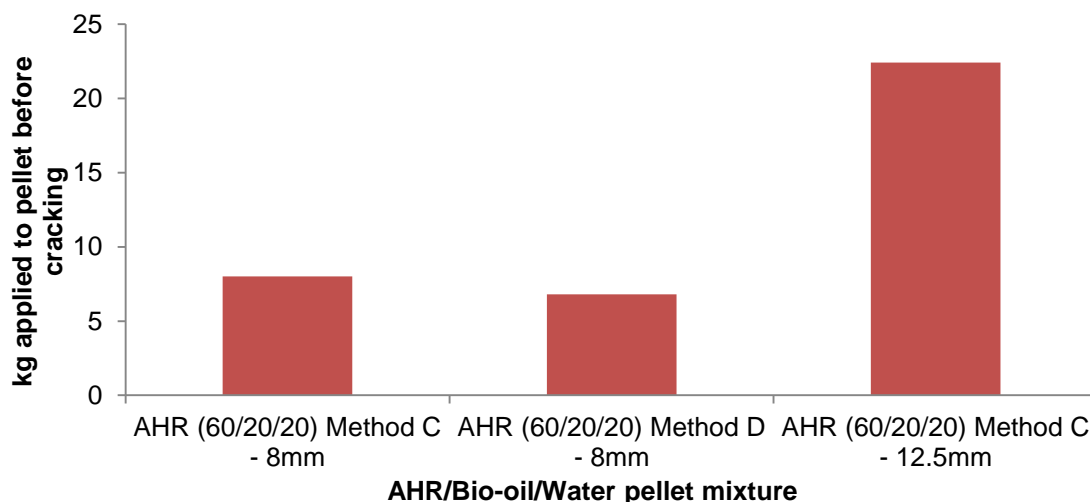
Figure 156: Pellets formed using bio-oil compared with using bio-oil and water

AHR pellets consisting of 60 wt.% AHR, 20 wt.% water then later with 20 wt.% bio-oil with a 12.5mm diameter were comparable in fracture strength (22.4kg) with mechanically pressed SCB pellets (23kg). However, as the AHR pellets were made using a manual pressing technique, a mechanical pellet press is likely to further compress the pellets and increase the fracture strength as previously shown in Figure 140, thus requiring less bio-oil.

10.4 Interim conclusions

- Paste feeding of AHR and methanol in a pressurised feeding system was unsuccessful as the paste was easily phase separated under pressure and the flow of paste could not be controlled.

- In order to process the AHR powder in fluidised bed gasifier, pelletisation is believed to be required. Pelletisation of AHR can reduce loss of fines during handling and improve screw feeding into a gasifier.

- A binder is required for successful pelletisation. Water is commonly used for pelletising biomass such as sugarcane bagasse.

- AHR is hydrophobic and AHR pellets produced with the addition of water only, are too weak to be successfully handled.

- Bio-oil was tested as a binding agent as this was a new approach. The extent of mixing, pressing, concentration of water and bio-oil, curing time and temperature influence pellet fracture strength.

- Tests show that more robust pellets can be made with the addition of bio-oil. 20 wt.% bio-oil of the total mixture is the minimum amount of bio-oil required to produce a pellet of suitable fracture strength which does not crumble and could potentially be screw fed as whole pellets into a gasifier. 40 wt.% of bio-oil of the total mixture is the maximum amount of bio-oil that can be added to AHR. Any further addition of bio-oil results in a decline in pellet robustness.

- Bio-oil should be added to wet AHR to avoid unnecessary drying subsequent to an acid hydrolysis process. At least a 1:1 ratio of bio-oil to water should be used to spread the bio-oil uniformly over all AHR particles.

- Increasing pellet diameter effectively increases pellet fracture strength.

- Mechanical pressing of an AHR, water and bio-oil mixture is likely to further enhance pellet fracture strength thus requiring less bio-oil.

11 CONCLUSIONS

The objective of this chapter is to recap the interim conclusions that were drawn at the end of each chapter and matched to the original aims and objectives of this work. Biomass and residues could play an important role in meeting the future world energy demands. The overall objective of this research was to derive useful products by pyrolysis and gasification of the acid hydrolysis residues (AHR) formed from the production of levulinic acid with the objective of creating energetically self-sufficient processes to minimise use of fossil fuels for the production of energy and fuels. Table 67 indicates how the work presented in this thesis has met the aims and objectives set at the beginning of the project.

Table 67: Conclusions match to the aims and objectives of this work

Aims and Objectives	Conclusion
To evaluate the composition and properties of biomass and AHR. To compare AHR with other lignin materials and investigate the effect of humins	• Lignin is more refractory than hemicellulose and cellulose and so AHR is more refractory than whole lignocellulosic biomass. • AHR mainly consists of humins (derived from cellulose) and lignin which makes AHR more refractory than biomass. • AHR is refractory and reacts more slowly than biomass. AHR is shown to decompose at even higher temperatures than lignin suggesting that the presence of humins makes AHR even more refractory. AHR decomposes slowly over a wide range of temperatures as with lignin. Therefore, humins are expected to be refractory like lignin. • Feeding of powdered AHR into a thermal processing unit is likely to be problematic. • The volatile content of miscanthus and sugarcane bagasse is between 73-83 wt.% suggesting fast pyrolysis of these feedstocks would give a high liquid yield. • Sugarcane bagasse shows the highest volatile content of 82.40 wt.% so expected to give the highest organic liquid yields from fast pyrolysis. • The low volatile content (36-40 wt.%) of the AHR from miscanthus and sugarcane bagasse indicates AHR would give low liquid yields and high char yields from fast pyrolysis. • AHR from sugarcane bagasse (5% H_2SO_4, 1h, 175°C) has the highest HHV of 24.94MJ/kg which is an indication that it has the highest lignin and humin content. • AHR yield from biomass is 62% dry feed basis when the optimum acid hydrolysis conditions reported by UL are used. • AHR represents approximately 80% of the original energy in the biomass. • AHR, as received from University of Limerick, contains ash (6 wt.%), moisture (5.6 wt.%), lignin (33.9 wt.% estimated by calculation) and humins (54.53 wt.% by difference). The humin content of the AHR is greater (54.5 wt.%) than the lignin content (33.9 wt.%). • Lignin has a low melting point (<180°C). The melting point of humins is unknown. AHR does not melt at temperatures as high as 600°C and is more refractory compared to other high lignin materials due to the presence of humins. Therefore, AHR is not likely to melt in the pipework leading to the reactor thus avoiding blockages.
Investigate fast pyrolysis of biomass and AHR in order to produce liquid bio-oil	• Low liquid yields and high char yields are expected from fast pyrolysis of AHR. AHR has a higher carbon content (62.6 wt.%) than biomass (47.6 wt.%) which is responsible for the high char yields from fast pyrolysis. Therefore, the focus for value added products from AHR is product gas using gasification. • Fast pyrolysis of lignin will produce an inhomogeneous and unstable liquid and a high char yield (approximately 30–50 wt.%). • Fast pyrolysis of humins has not been reported in literature. • Fast pyrolysis of AHR produces a lower organic liquid yield and higher char yield compared to whole lignocellulosic biomass. • Liquid yields from fast pyrolysis can be maximised with a reaction temperature of 500°C and hot vapour residence time of less than 2 seconds. • Biomass with less than 10 wt.% moisture is recommended to limit the water collected in the liquid product and reduce the

188

	- potential of phase separation.
	- Removal of small particle sizes can lower feed ash content to reduce the catalytic activity and maximise liquid yields and optimise liquid quality.
	- Maximum particle sizes of 2-3mm should be used to achieve high heating rates and short residence times.
	- Fast pyrolysis of high bulk density feedstocks gives higher char yields than lower bulk density feedstocks.
	- Total liquid yield yields of approximately 60 wt.% (dry feed basis) can be expected from miscanthus.
	- Successful pyrolysis of sugarcane bagasse, sugarcane trash or ground SCBP have not been reported using a laboratory-scale continuous fluidised bed reaction system.
	- Higher organic liquid yields can be achieved from fast pyrolysis of higher holocellulosic content feedstocks.
	- Currently bio-oils do not meet the requirements of a transportation fuel and so require deoxygenation before being accepted commercially.
	- Catalytic pyrolysis of pyrolysis vapours seems a promising approach as long as catalyst deactivation can be overcome.
	- Integrated catalytic pyrolysis using molybdenum carbide has been not been reported in the literature and the effect of this catalyst on pyrolysis products is interesting.
	- The most promising catalytic upgrading technique would involve condensing the vapours after catalysis in order to avoid the need to re-vapourise the bio-oil. It is likely that catalytic pyrolysis will need to be carried out in multiple steps in order to satisfactorily upgrade the bio-oil.
	- The 100g/h rig can be used to screen feedstocks when there is limited availability of feedstocks. The 100g/h rig pneumatic feeding system cannot be used to feed fibrous feedstocks such as sugarcane bagasse and fine powder feedstocks such as AHR into the top of the fluidised bed reactor due to blockages in the feeder tube and the fluidised bed.
	- Screw feeding biomass through a water cooled screw into the side of the reactor is more versatile and reliable than feeding into the top of a fluidised bed reactor. Therefore, the 300g/h rig with a screw feeding system is a suitable size system which can be used to screen feedstocks without the need for significant amounts of sample preparation or rig cleaning.
	- Ground SCBP was the most promising feedstock producing 60.45 wt.% organic liquid on a dry feed basis from fast pyrolysis on the 300g/h rig with the glassware collection system. The bio-oil oxygen content from ground SCBP was one of the lowest (40.76 wt.%) which is more suited for catalytic upgrading to further deoxygenate the bio-oil. The bio-oil HHV was also the highest (22.48MJ/kg). There were no problems with screw feeding ground sugarcane bagasse pellets. Densified material such as ground sugarcane bagasse pellets is preferred to loose sugarcane bagasse for more reliable feeding and improved biomass throughputs (207.72g/h).
	- Using the glassware collection system ensures a good mass balance closure of approximately 95%. Ethanol washing of the quench system on the 300g/h rig, after an experiment, has been demonstrated to improve the mass balance using the quench column.
	- The mass balance closure on the 1kg/h rig was improved by around 5% with the addition of silica gel which recovers more light tars and moisture.
	- The quench column is easy to scale up and produces a more representative whole bio-oil compared to the glassware

	collection system.
	• The 1kg/h rig is more representative of a commercial fast pyrolysis unit as it produces a whole bio-oil with reduced viscosity and improved flow properties. However, the smaller scale 300g/h rig can be used with the glassware collection system to approximate the product yields expected from larger scale fast pyrolysis processing.
	• The 300g/h rig with glassware collection system is the most suitable for catalytic pyrolysis tests as there are no issues of miscibility or contamination of upgraded liquid products with quench liquids.
Compare miscanthus, miscanthus pellets, sugarcane bagasse, sugarcane bagasse pellets sugarcane trash. Test most promising feedstock on fast pyrolysis rigs at Aston University. Suggest methods to improve mass balances and compare product yields using different liquid collection systems.	• The components in fuel gas from air-blown gasification are diluted with nitrogen which significantly lowers the gas HHV (4-7 MJ/Nm3). Fuel gas is suitable for boilers, engines and turbine operation to ultimately produce heat or electricity. Syngas (synthesis gas) is a better quality medium energy content gas (10-18 MJ/Nm3) from oxygen blown or steam gasification. However, air gasification is the simplest and avoids high costs associated with oxygen and steam production.
	• Pyrolytic gasification, without an oxidant, can also produce a lower gas yield with medium heating value (17-19 MJ/Nm3).
	• Fluidised beds are preferred to fixed beds due to the scalability and feed properties requirement. Entrained flow gasifiers may be suitable for processing fine AHR powder, but there are high costs associated with the high oxygen requirements and high temperature resistant materials of construction.
	• Pressurised gasification is suitable for refractory feeds such as coal, but the higher equipment and construction costs associated with pressurised gasification makes it unattractive.
	• The optimum water content of biomass for gasification is reported to be between 10% and 30%. High moisture in feedstocks can aid steam gasification.
	• A feedstock with less than 5% ash is recommended for gasification, but ash is beneficial for gasification as they crack tars.
	• High char yielding feedstocks are expected to require longer reaction times in order to reduce the unconverted carbon in the residual ash.
	• Densified sugarcane bagasse will help overcome feeding problems and increase biomass throughput, but the remaining solid yield is likely to be marginally higher.
	• Refractory biomass components such as lignin are reported to be difficult to gasify and require gasification temperatures of approximately 900°C similar to that of coal. Humins are refractory like lignin, so AHR are also expected to require gasification temperatures of approximately 900°C.
	• There is no literature reporting the gasification of AHR in a single gasification step.
	• Gasification is a well-established technology where tar removal seems critical to enable this technology to be commercialised. Thermal cracking could be used, but the use of catalyst could reduce the process operating temperature and the need for downstream physical gas cleaning. Combining existing catalysts seems a promising approach to combat tars from the gas stream in gasification e.g. dolomite as a catalyst support for nickel or nickel impregnated olivine.
Investigate the effect of molybdenum carbide on pyrolysis	• Py-GC-MS can be used to investigate catalyst effect on product composition to a certain extent. However, Py-GC-MS is of limited value in this work as the results cannot give estimations on product yields produced from fast pyrolysis. Also, the product distribution obtained from Py-GC-MS cannot be used to predict the products and quantities expected on large scale

	systems as the liquid collection system has shown to have a significant effect on the liquid product composition. It should also be noted that using peak areas to quantify products is not ideal as only small sample is analysed so not all compounds are identifiable. • The 300g/h rig is a suitable size system which can be used to screen feedstocks and catalysts to give acceptable mass balance closures of approximately 95% and realistic product yields believed to be representative of those achievable on a larger and/or commercial scale. The glassware collection system is more suited for catalytic pyrolysis as there are no problems of miscibility with hydrocarbons in upgraded bio-oil. • Direct addition of Mo_2C/ Al_2O_3 into a fast pyrolysis fluidised bed reactor does not deoxygenate bio-oil, but reduces the organic content and increases the water content of the liquid product. Mo_2C/ Al_2O_3 improves the viscosity and homogeneity of bio-oil which is important if liquid bio-oil is to be further upgraded as the lower viscosity can facilitate the flow in a hydrotreater operated in trickle-bed regime. • An increased concentration of molybdenum carbide reduces the concentration of sugars (levoglucosan) and increases the concentration of furanics and phenolics for production of speciality chemicals.
Understand the effect of process and feedstock variables on fast pyrolysis and gasification	• The components in fuel gas from air-blown gasification are diluted with nitrogen which significantly lowers the gas HHV (4-7 MJ/Nm3). Fuel gas is suitable for boilers, engines and turbine operation to ultimately produce heat or electricity. Syngas (synthesis gas) is a better quality medium energy content gas (10-18 MJ/Nm3) from oxygen blown or steam gasification. However, air gasification is the simplest and avoids high costs associated with oxygen and steam production. • Pyrolytic gasification, without an oxidant, can also produce a lower gas yield with medium heating value (17-19 MJ/Nm3). • Fluidised beds are preferred to fixed beds due to the scalability and feed properties requirement. Entrained flow gasifiers may be suitable for processing fine AHR powder, but there are high costs associated with the high oxygen requirements and high temperature resistant materials of construction. • Pressurised gasification is suitable for refractory feeds such as coal, but the higher equipment and construction costs associated with pressurised gasification makes it unattractive. • The optimum water content of biomass for gasification is reported to be between 10% and 30%. High moisture in feedstocks can aid steam gasification. • A feedstock with less than 5% ash is recommended for gasification, but ash is beneficial for gasification as they crack tars. • High char yielding feedstocks are expected to require longer reaction times in order to reduce the unconverted carbon in the residual ash. • Densified sugarcane bagasse will help overcome feeding problems and increase biomass throughput, but the remaining solid yield is likely to be marginally higher. • Refractory biomass components such as lignin are reported to be difficult to gasify and require gasification temperatures of approximately 900°C similar to that of coal. Humins are refractory like lignin, so AHR are also expected to require gasification temperatures of approximately 900°C. • There is no literature reporting the gasification of AHR in a single gasification step.

	• Gasification is a well-established technology where tar removal seems critical to enable this technology to be commercialised. Thermal cracking could be used, but the use of catalyst could reduce the process operating temperature and the need for downstream physical gas cleaning. Combining existing catalysts seems a promising approach to combat tars from the gas stream in gasification e.g. dolomite as a catalyst support for nickel or nickel impregnated olivine.
Investigate gasification of AHR with biomass in order to produce a usable gas for heat and power or potentially synfuels	• AHR is a powder which is difficult to screw feed, handle and process in a reactor such as the 300g/h fluidised bed reactor used in this work. • Although pyrolytic gasification is suitable for high volatile content feedstocks, pyrolytic gasification is not suitable for AHR and high lignin content feedstocks as char yields stabilise between 550-650°C without the addition of oxygen. For this reason, char yields from AHR would stabilise at approximately 40 wt.% char yield at temperatures higher than 650°C. • Increasing reactor temperature reduced solid and tar yields, but increased gas yield from both SCBP and AHR. AHR gave relatively low gas yields (74.21 wt.%), low tar yields (5.27 wt.%) and high solid yields (20.52 wt.%) at 950°C. • Air-blown gasification produces high yields of a low energy content gas as the product gas is diluted with nitrogen. When compared to pyrolytic gasification, oxygen increases carbon conversion and reduces the remaining solid yield from AHR to 20.52 wt.% (dry feed basis) at 950°C. • Efficiency of AHR gasification was defined by cold gas efficiency and carbon conversion efficiency. Cold gas efficiency of approximately 44% were achieved from AHR gasification in the batch system. These efficiencies are considerably low when compared to those obtained commercially and reported in the literature due to the heat loss from the reactor and the energy remaining in the unreacted carbon and tars. • The maximum carbon conversion efficiency of AHR at 950°C was 43%. Typical carbon conversion efficiencies of >95% are expected, but AHR gasification was limited by the use of a batch system as the completion of gasification was defined at the point where CO level started to fall. If more oxygen was added, CO_2 would be produced at the expense of CO which lowered the gas HHV. This point was also the maximum H_2 concentration which was obtained from this batch system and this is reported to be the optimum point for process efficiency [177]. However, in continuous gasification, the reaction would not be stopped at this point. • More unreacted carbon remained from AHR compared to SCBP in the batch system due to the refractory nature of the lignin and humin in AHR and so rate of reaction was slower. Increasing the initial reactor temperature reduced the time taken for CO to peak, but AHR took longer for CO to peak compared to SCBP. • The low volatile content AHR yielded less tars than biomass which is beneficial as gas cleaning is likely to be less problematic. • In this system, higher temperatures favoured the production of CO which increased the gas HHV. • Air-blown gasification of high lignin and humin content AHR produces a lower energy content gas (5.78MJ/Nm3) compared to standard biomass (7.28MJ/Nm3). Both are suitable for boiler and engine applications [195]. However, a higher energy content gas is required for the production of biofuels. • Significant amounts of useful carbon remain in the solid product after AHR gasification; therefore, modifications to exiting

	biomass gasifiers would be required to increase carbon conversion e.g. longer reaction times by increased bed height, higher reaction temperatures by increasing equivalence ratio or extensive solid recycling as in fluidised bed gasifiers. • Nitrogen content of the product gas from SCBP and AHR at 950°C in the batch gasifier is comparable with the nitrogen content of the product gas in commercial fluidised bed gasification. The product gas from SCBP consists of approximately 50vol% of gasification products and the product gas from AHR consists of approximately 35vol% of gasification products. The remainder of the gas is nitrogen which requires larger downstream equipment.
Improve feeding and handling properties of AHR. Evaluate screw feeding, paste feeding and pelletisation of AHR. Investigate whether bio-oil can be used as a binder in pelletisation of AHR. If so, determine the minimum about of bio-oil required for successful pelletisation.	• Paste feeding of AHR and methanol in a pressurised feeding system was unsuccessful as the paste was easily phase separated under pressure and the flow of paste could not be controlled. • In order to process the AHR powder in fluidised bed gasifier, pelletisation is believed to be required. Pelletisation of AHR can reduce loss of fines during handling and improved screw feeding into a gasifier. • A binder is required for successful pelletisation. Water is commonly used for pelletising biomass such as sugarcane bagasse. • AHR is hydrophobic and AHR pellets produced with the addition of water only, are too weak to be successfully handled. • Bio-oil was tested as a binding agent as this was a new approach. The extent of mixing, pressing, concentration of water and bio-oil, curing time and temperature influence pellet fracture strength. • Tests show that more robust pellets can be made with the addition of bio-oil. 20 wt.% bio-oil of the total mixture is the minimum amount of bio-oil required to produce a pellet of suitable fracture strength which does not crumble and could potentially be screw fed as whole pellets into a gasifier. 40 wt.% of bio-oil of the total mixture is the maximum amount of bio-oil that can be added to AHR. Any further addition of bio-oil results in a decline in pellet robustness. • Bio-oil should be added to wet AHR to avoid unnecessary drying subsequent to an acid hydrolysis process. At least a 1:1 ratio of bio-oil to water should be used to spread the bio-oil uniformly over all AHR particles. • Increasing pellet diameter effectively increases pellet fracture strength. • Mechanical pressing of an AHR, water and bio-oil mixture is likely to further enhance pellet fracture strength thus requiring less bio-oil.

12 RECOMMENDATIONS

The objective of this chapter is to make recommendations for pyrolysis and gasification of biomass and acid hydrolysis residues. The areas discussed in this work which require further investigation are reported in this chapter.

12.1 Fast pyrolysis of biomass

- Silica gel should be added after the cotton wool filters on both collection systems (glassware and quench) to absorb moisture and light tars and further improve liquid recovery and mass balances on the 300g/h fluidised bed fast pyrolysis rig.

- A flange should be added to the bottom of the quench column on the quench system on the 300g/h rig so that the quench column can be detached and physically weighed with increased accuracy for improved mass balances.

- A wet walled ESP on the 1kg/h rig has shown to improve the liquid recovery and collect a more representative and whole bio-oil so should replace the dry walled ESP on the 300g/h quench system.

- Fast pyrolysis of ground SCBP has shown to give comparable results to beech and promising organic liquid yields (up to 63.9 wt.% organic liquid on a dry feed basis) so should be considered for catalytic upgrading.

- Catalytic pyrolysis of ground sugarcane bagasse pellets using cracking catalysts such as ZMS-5, which are susceptible to coking, should be tested with in a secondary fixed bed reactor on the 300g/h rig.

- A valve should be added to the glassware collection system on the 300g/h rig so that liquid samples can be regularly collected (every minute) and analysed for water content throughout each catalytic experiment. The water content of the liquid collected will test catalyst resistance to rapid deactivation or alteration. The water content of the liquid is expected to decrease as the cracking catalyst deactivates.

12.2 Gasification of biomass and AHR

- AHR pellets should be made with bio-oil using a mechanical pelletiser to investigate whether the increasing pressure can reduce bio-oil requirements for AHR pellet production i.e. less than 20 wt.% bio-oil.

- The application of gas needs to be defined in order to recommend a suitable gasification agent. If a low energy fuel gas (4-7MJ/Nm^3) is acceptable and required for use in boilers and engines then the focus should be on air-blown gasification. However, if a medium energy content syngas (10-18MJ/Nm^3) is required for the production of biofuels then oxygen or steam should be used as the gasification agent.

- Gasification of whole sugarcane bagasse pellets should be compared to gasification of AHR pellets (produced with bio-oil) on a larger scale continuous air-blown gasification system such as a 10kg/h fluidised bed gasifier. Gasifying whole pellets will reduce the need for grinding and increase biomass throughputs. These tests should be repeated with ground pellets and compared to whole pellets to investigate the influence of particle size on gasification.

- Catalytic gasification of SCBP and AHR should be explored using catalysts such as dolomite or nickel to crack tars and increase gas yields. These catalysts should be tested in both a fluidised bed and in a secondary tar cracker where the equipment configuration permits. Combining existing catalysts and testing them in the fluidised bed gasifier seems a promising approach to combat tars from the gas stream in gasification e.g. dolomite as a catalyst support for nickel and vice versa, therefore, these should be tested. Dolomite and nickel should also be tested in sequence i.e. one catalyst in the fluidised bed and the other in a sequential tar cracker.

- Higher pressures may be required to gasify AHR as they are less reactive than biomass and are more similar to coal. Therefore, whole AHR pellets should be gasified in a pressurised fluidised bed and compared to atmospheric fluidised bed gasification using air, oxygen and steam.

- If sufficient quantities of AHR are available, then AHR and water (as produced from an acid hydrolysis process) should be directly fed as slurry into an entrained flow gasifier and the results compared with fluidised bed gasification results.

- If the energy demand for the overall Dibanet process cannot be solely met by gasification of the AHR, energy from pyrolysis or gasification of SCBP could supplement the energy demands. Gasification of whole pellets would avoid grinding costs; however, whole pellets are not suitable for fast pyrolysis. Larger scale fluidised bed air-blown gasification of whole SCBP should be compared with fluidised bed fast pyrolysis of ground SCBP.

- An economic evaluation is necessary to compare all of the stated process scenarios before a recommendation can be made as to which process is preferred for thermal conversion of SCBP.

REFERENCES

1. Deutmeyer, M., Large Scale BTL production in Germany - current technological approach, feedstock sourcing and handling concepts. 2008, Choren.

2. Melligan, F., et al., Characterisation of the products from pyrolysis of residues after acid hydrolysis of Miscanthus. Bioresource technology, 2012. **108**: p. 258-263.

3. Girisuta, B., *Levulinic Acid from Lignocellulosic Biomass*, in *Chemical Engineering*. 2007, PhD Thesis. University of Groningen: Indonesia.

4. Dibanet, The Production of Sustainable Diesel-Miscible-Biofuels from the Residues and Wastes of Europe and Latin America. 2008, European Commission funded FP7 CP-SICA Collaborative project: Europe and Latin America.

5. van Paasen, S.V.B., M.K. Cieplik, and N.P. Phokawat, *Gasification of non-woody biomass: Economic and Technical Perspectives of Chlorine and Sulphur Removal from Product Gas*. 2006, Energy Research Centre of the Netherlands (ECN), Petten: Netherlands.

6. Goyal, H.B., D. Seal, and R.C. Saxena, *Bio-fuels from thermochemical conversion of renewable resources: A review.* Renewable and Sustainable Energy Reviews, 2008. **12**(2): p. 504-517.

7. Mohan, D., C. Pittman, and P. Steele, *Pyrolysis of Wood/Biomass for Bio-oil A Critical Review.* Energy and Fuels, 2006. **20**(3): p. 848-889.

8. Bridgwater, A.V., *Upgrading biomass fast pyrolysis liquids.* Environmental Progress & Sustainable Energy, 2012. **31**(2): p. 261-268.

9. Butler, E., et al., A review of recent laboratory research and commercial developments in fast pyrolysis and upgrading. Renewable & Sustainable Energy Reviews, 2011. **15**(8): p. 4171-4186.

10. Hendriks, A.T.W.M. and G. Zeeman, *Pretreatments to enhance the digestibility of lignocellulosic biomass.* Bioresource Technology, 2009. **100**(1): p. 10-18.

11. Kumar, V., Pyrolysis and gasification of lignin and effect of alkali addition, in School of Chemical & Biomolecular Engineering. 2009, PhD Thesis. Georgia Institute of Technology: Georgia.

12. Shen, D.K., et al., *The pyrolytic degradation of wood-derived lignin from pulping process.* Bioresource Technology, 2010. **101**(15): p. 6136-6146.

13. Jiang, G., D.J. Nowakowski, and A.V. Bridgwater, *A systematic study of the kinetics of lignin pyrolysis.* Thermochimica Acta, 2010. **498**(1-2): p. 61-66.

14. Biagini, E., F. Barontini, and L. Tognotti, *Devolatilization of Biomass Fuels and Biomass Components Studied by TG/FTIR Technique.* Industrial & Engineering Chemistry Research, 2006. **45**(13): p. 4486-4493.

15. Brosse, N., et al., Miscanthus: a fast growing crop for biofuels and chemicals production. Biofuels, Bioproducts and Biorefining, 2012.

16. Kallis, K.X., G.A. Pellegrini Susini, and J.E. Oakey, A comparison between Miscanthus and bioethanol waste pellets and their performance in a downdraft gasifier. Applied Energy, 2013. **101**: p. 333-340.

17. Waldheim, L., M. Morris, and M. Verde, Biomass power generation: Sugar cane bagasse and trash, in Progress in thermochemical biomass conversion, Bridgwater A.V, Editor. 2001, Wiley. p. 509-523.

18. Hayes, D.J., Analysis of Lignocellulosic Feedstocks for Biorefineries with a Focus on The Development of Near Infrared Spectroscopy as a Primary

Analytical Tool in Science and Engineering. 2011, PhD Thesis. University of Limerick: Limerick.

19. Bergman, P.C.A., et al. Torrefaction for entrained-flow gasification of biomass. in The 2nd World Conference and Technology Exhibition on Biomass for Energy, Industry and Climate Protection. 2004. Rome, Italy.

20. Larson, E.D., R.H. Williams, and M.R.L.V. Leal, A review of biomass integrated-gasifier/gas turbine combined cycle technology and its application in sugarcane industries, with an analysis for Cuba. Energy for sustainable development, 2001. **5**(1): p. 54-76.

21. Valchev, I., et al., *Use of Enzymes in Hydrolysis of Maize Stalks.* Bioresources, 2009. **4**(1): p. 285-291.

22. Fahmi, R., et al., Prediction of Klason lignin and lignin thermal degradation products by Py-GC/MS in a collection of Lolium and Festuca grasses. Journal of Analytical and Applied Pyrolysis, 2007. **80**(1): p. 16-23.

23. Sun, Y. and J. Cheng, Hydrolysis of lignocellulosic materials for ethanol production: a review. Bioresource Technology, 2002. **83**(1): p. 1-11.

24. Kim, S.B. and Y.Y. Lee, Diffusion of sulfuric acid within lignocellulosic biomass particles and its impact on dilute-acid pretreatment. Bioresource Technology, 2002. **83**(2): p. 165-171.

25. Lloyd, T.A. and C.E. Wyman, Combined sugar yields for dilute sulfuric acid pretreatment of corn stover followed by enzymatic hydrolysis of the remaining solids. Bioresource Technology, 2005. **96**(18): p. 1967-1977.

26. Bower, S., et al., Modeling sucrose hydrolysis in dilute sulfuric acid solutions at pretreatment conditions for lignocellulosic biomass. Bioresource Technology, 2008. **99**(15): p. 7354-7362.

27. Bose, S.K., et al., An improved method for the hydrolysis of hardwood carbohydrates to monomers. Carbohydrate Polymers, 2009. **78**(3): p. 396-401.

28. Mansilla, H.D., et al., *Acid-catalysed hydrolysis of rice hull: Evaluation of furfural production.* Bioresource Technology, 1998. **66**(3): p. 189-193.

29. Mosier, N., et al., Features of promising technologies for pretreatment of lignocellulosic biomass. Bioresource Technology, 2005. **96**(6): p. 673-686.

30. Lee, Y., P. Iyer, and R. Torget, *Dilute-acid hydrolysis of lignocellulosic biomass.* Advances in Biochemical Engineering Biotechnology, 1999. **65**: p. 93-116.

31. Hayes, D., An examination of biorefining processes, catalysts and challenges. Catalysis Today, 2009. **145**(1-2): p. 138-151.

32. Gámez, S., et al., *Study of the hydrolysis of sugar cane bagasse using phosphoric acid.* Journal of Food Engineering, 2006. **74**(1): p. 78-88.

33. Vázquez, M., et al., Hydrolysis of sorghum straw using phosphoric acid: Evaluation of furfural production. Bioresource Technology, 2007. **98**(16): p. 3053-3060.

34. Rodríguez-Chong, A., et al., *Hydrolysis of sugar cane bagasse using nitric acid: a kinetic assessment.* Journal of Food Engineering, 2004. **61**(2): p. 143-152.

35. Patil, S.K.R. and C.R.F. Lund, Formation and Growth of Humins via Aldol Addition and Condensation during Acid-Catalyzed Conversion of 5-Hydroxymethylfurfural. Energy & Fuels, 2011. **25**(10): p. 4745-4755.

36. Girisuta, B., L.P.B.M. Janssen, and H.J. Heeres, *Green Chemicals: A Kinetic Study on the Conversion of Glucose to Levulinic Acid.* Chemical Engineering Research and Design, 2006. **84**(5): p. 339-349.

37.   Nowakowski, D. and A.V. Bridgwater, *Unpublished work at the Bioenery Research Group*. 2010, Aston University.

38.   Nowakowski, D.J., Influence of potassium and phosphorus on the thermochemical conversion of the cell wall components of biomass. 2008, PhD Thesis. Leeds University: Leeds. p. 75.

39.   Girisuta, B., et al., An integrated process for the production of platform chemicals and diesel miscible fuels by acid-catalyzed hydrolysis and downstream upgrading of the acid hydrolysis residues with thermal and catalytic pyrolysis. Bioresource technology, 2012. **126**: p. 92-100.

40.   Dapía, S., V. Santos, and J.C. Parajó, *Study of formic acid as an agent for biomass fractionation.* Biomass and Bioenergy, 2002. **22**(3): p. 213-221.

41.   Košíková, B., M. Hricovini, and C. Cosentino, *Interaction of lignin and polysaccharides in beech wood (Fagus sylvatica) during drying processes.* Wood Science and Technology, 1999. **33**(5): p. 373-380.

42.   De Vrije, T., et al., *Pretreatment of Miscanthus for hydrogen production by Thermotoga elfii.* International Journal of Hydrogen Energy, 2002. **27**(11-12): p. 1381-1390.

43.   Michel, R., et al., Catalytic steam gasification of Miscanthus X giganteus in fluidised bed reactor on olivine based catalysts. Fuel Processing Technology, 2011. **92**(6): p. 1169-1177.

44.   Boussarsar, H., B. Rogé, and M. Mathlouthi, *Optimization of sugarcane bagasse conversion by hydrothermal treatment for the recovery of xylose.* Bioresource technology, 2009. **100**(24): p. 6537-6542.

45.   Chen, W.-H., Y.-J. Tu, and H.-K. Sheen, Disruption of sugarcane bagasse lignocellulosic structure by means of dilute sulfuric acid pretreatment with microwave-assisted heating. Applied Energy, 2011. **88**(8): p. 2726-2734.

46.   Das, P., A. Ganesh, and P. Wangikar, *Influence of pretreatment for deashing of sugarcane bagasse on pyrolysis products.* Biomass and Bioenergy, 2004. **27**(5): p. 445-457.

47.   Fortes, C., P.C.O. Trivelin, and A.C. Vitti, *Long-term decomposition of sugarcane harvest residues in Sao Paulo state, Brazil.* Biomass and Bioenergy, 2012. **42**(0): p. 189-198.

48.   Grinins, J., et al., Analytical pyrolysis as an instrument to study the chemical transformations of hydrothermally modified wood. Journal of Analytical and Applied Pyrolysis, 2012.

49.   ECN. *Phyllis 2: Database for biomass and waste* 2013; Available from: http://www.ecn.nl/phyllis2/Home/About/ECN-Phyllis.

50.   Channiwala, S.A. and P.P. Parikh, A unified correlation for estimating HHV of solid, liquid and gaseous fuels. Fuel, 2002. **81**(8): p. 1051-1063.

51.   Bridgwater, A.V., S. Czernik, and J. Piskorz, *Progress in thermochemical biomass conversion*. 2001: Wiley Online Library.

52.   Nowakowski, D.J., et al., *Lignin fast pyrolysis: Results from an international collaboration.* Journal of Analytical and Applied Pyrolysis, 2010. **88**(1): p. 53-72.

53.   Demirbas, A., *Biorefineries: For Biomass Upgrading Facilities*. Green Energy and Technology. 2009: Springer Verlag.

54.   Nowakowski, D.J., et al., Potassium catalysis in the pyrolysis behaviour of short rotation willow coppice. Fuel, 2007. **86**(15): p. 2389-2402.

55. Yang, H., et al., Characteristics of hemicellulose, cellulose and lignin pyrolysis. Fuel, 2007. **86**(12-13): p. 1781-1788.

56. Alcala, A., Internal communication within the Bioenergy Research Group. 2012.

57. Bridgeman, T., et al., Influence of particle size on the analytical and chemical properties of two energy crops. Fuel, 2007. **86**(1): p. 60-72.

58. Milligan, J.B., Downdraft gasification of biomass. 1994.

59. Jiang, G. and A.V. Bridgwater, *Unpublished work at the Bioenery Research Group.* 2010, Aston University.

60. Demirbas, F.M., *Biorefineries for biofuel upgrading: A critical review.* Applied Energy, 2009. **86**(Supplement 1): p. S151-S161.

61. Roos, C., Clean Heat and Power Using Biomass Gasification for Industrial and Agricultural Projects. 2008, Northwest CHP Application Centre.

62. Pieratti, E., Biomass gasification in small scale plants: experimental and modelling analysis, in School in Environmental Engineering. 2011, PhD Thesis. University of Trento: Trento, Italy. p. 159.

63. Balat, M., et al., Main routes for the thermo-conversion of biomass into fuels and chemicals. Part 1: Pyrolysis systems. Energy Conversion and Management, 2009. **50**(12): p. 3147-3157.

64. International Energy Agency, *IEA Bioenergy 27th update.* Biomass and Bioenergy, 2007.

65. Barrio, M., *Experimental investigation of small-scale gasification of woody biomass.* 2002, PhD Thesis. Norwegian University of Science and Technology.

66. Bridgwater, A., *Renewable fuels and chemicals by thermal processing of biomass.* Chemical Engineering Journal, 2003. **91**(2): p. 87-102.

67. Earp, D.M., *Gasification of biomass in a downdraft reactor.* 1988, PhD Thesis. Aston University.

68. Roos, C.J., Clean Heat and Power Using Biomass Gasification for Industrial and Agricultural Projects. 2010: Northwest CHP Application Center.

69. Dutta, A. and B. Acharya, Production of bio-syngas and biohydrogen via gasification, in Handbook of Biofuels Production - Processes and Technologies, R. Luque, J. Campelo, and J. Clark, Editors. 2011, Woodhead Publishing.

70. Lu, Q., W.-Z. Li, and X.-F. Zhu, *Overview of fuel properties of biomass fast pyrolysis oils.* Energy Conversion and Management, 2009. **50**(5): p. 1376-1383.

71. Piskorz, J., et al., *Fast pyrolysis of sweet sorghum and sweet sorghum bagasse.* Journal of Analytical and Applied Pyrolysis, 1998. **46**(1): p. 15-29.

72. Bridgwater, A.V., *Review of fast pyrolysis of biomass and product upgrading.* Biomass and Bioenergy, 2012. **38**: p. 68-94.

73. Bridgwater, A.V., Upgrading biomass fast pyrolysis liquids, in Thermochemical Processing of Biomass: Conversion into Fuels, Chemicals and Power, R.C. Brown, Editor. 2012, Wiley-Blackwell: UK. p. 157-199.

74. Demirbas, A., Partly chemical analysis of liquid fraction of flash pyrolysis products from biomass in the presence of sodium carbonate. Energy Conversion and Management, 2002. **43**(14): p. 1801-1809.

75. Bridgwater, A., Progress in thermochemical biomass conversion. 2001: Wiley-Blackwell.

76. Bridgwater, A.v., *Biomass Fast Pyrolysis Review Paper.* Thermal Science, 2004. **8**(2): p. 21-49.

77. Song, C. and D.C. Elliott, *Thrust 2: Utilization of Petroleum Refinery Technology for Biofuel Production.* 2007, Pacific Northwest National Laboratory.

78. Zhang, Q., et al., *Review of biomass pyrolysis oil properties and upgrading research.* Energy Conversion and Management, 2007. **48**(1): p. 87-92.

79. Bridgwater, A.V., Production of high grade fuels and chemicals from catalytic pyrolysis of biomass. Catalysis Today, 1996. **29**(1-4): p. 285-295.

80. Brownsort, P., Biomass pyrolysis processes: performance parameters and their influence on biochar system benefits. 2009, Masters Thesis. The University of Edinburgh.

81. Sannita, E., et al., *Medium-temperature conversion of biomass and wastes into liquid products, a review.* Renewable and Sustainable Energy Reviews, 2012. **16**(8): p. 6455-6475.

82. Nguyen, T.S., et al., Catalytic upgrading of biomass pyrolysis vapours using faujasite zeolite catalysts. Biomass and Bioenergy, 2013. **48**(0): p. 100-110.

83. Brown, R.C. and J. Holmgren. *Fast Pyrolysis and Bio-Oil Upgrading.* [Presentation] 2006 [cited 2012; Available from: http://www.ascension-publishing.com/BIZ/HD50.pdf.

84. Ullmann, Ullmann's processes and process engineering: Processes under Special Conditions. Vol. 3. 2004: Weinheim : Wiley-VCH.

85. Coulson, J., et al., Chemical engineering. Volume 2: Particle technology and separation processes. Pergamon, 1991.

86. Salter, E., Catalytic pyrolysis of biomass for improved liquid fuel quality, in Chemical Engineering. 2001, PhD Thesis. Aston University: Birmingham.

87. Kunii, D. and O. Levenspiel, *Fluidization engineering.* 1991, USA: Butterworth-Heinemann.

88. Howard, J., *Fluidized bed technology: principles and applications.* 1989: Institute of Physics Publishing.

89. Sinnige, M.A. and C.R. Seco, Design and Fluid Dynamic Investigation of a Bench-scale Pressurized Chemical Looping Combustor. 2005.

90. Yang, W.-C., Handbook of fluidization and fluid-particle systems. Vol. 91. 2003: CRC Press.

91. Geldart, D., *Types of gas fluidization.* Powder technology, 1973. **7**(5): p. 285-292.

92. Kalgo, A.S., The development and optimisation of a fast pyrolysis process for bio-oil production, in Chemical Engineering and Applied Chemistry. 2011, PhD Thesis. Aston University: Birmingham.

93. Rautenbach, C., *An Experimental and Theoretical Study of Dense Fluidized Bed Fluid Dynamics.* 2012, PhD thesis, Telemark University College, Porsgrunn, Norway.

94. Bridgwater, A.V., *Principles and practice of biomass fast pyrolysis processes for liquids.* Journal of Analytical and Applied Pyrolysis, 1999. **51**(1-2): p. 3-22.

95. Isahak, W., et al., *A review on bio-oil production from biomass by using pyrolysis method.* Renewable and Sustainable Energy Reviews, 2012. **16**(8): p. 5910-5923.

96. Akhtar, J. and N. Saidina Amin, *A review on operating parameters for optimum liquid oil yield in biomass pyrolysis.* Renewable and Sustainable Energy Reviews, 2012. **16**(7): p. 5101-5109.

97.   Bridgwater, A., D. Meier, and D. Radlein, *An overview of fast pyrolysis of biomass.* Organic Geochemistry, 1999. **30**(12): p. 1479-1493.

98.   Scott, D.S., et al., *The role of temperature in the fast pyrolysis of cellulose and wood.* Industrial & Engineering Chemistry Research, 1988. **27**(1): p. 8-15.

99.   Scott, D.S., et al., *A second look at fast pyrolysis of biomass--the RTI process.* Journal of Analytical and Applied Pyrolysis, 1999. **51**(1-2): p. 23-37.

100.   Oasmaa, A. and S. Czernik, Fuel Oil Quality of Biomass Pyrolysis Oils State of the Art for the End Users. Energy & Fuels, 1999. **13**(4): p. 914-921.

101.   Abdullah, N. and H. Gerhauser, *Bio-oil derived from empty fruit bunches.* Fuel, 2008. **87**(12): p. 2606-2613.

102.   Scott, D.S. and J. Piskorz, *The flash pyrolysis of aspen-poplar wood.* The Canadian Journal of Chemical Engineering, 1982. **60**(5): p. 666-674.

103.   Bridgwater, A. and G. Peacocke, *Fast pyrolysis processes for biomass.* Renewable and Sustainable Energy Reviews, 2000. **4**(1): p. 1-73.

104.   Erlich, C., et al., Pyrolysis and gasification of pellets from sugar cane bagasse and wood. Fuel, 2006. **85**(10-11): p. 1535-1540.

105.   Jong, W.d., A. Pirone, and M.A. Wójtowicz, Pyrolysis of Miscanthus Giganteus and wood pellets: TG-FTIR analysis and reaction kinetics[small star, filled]. Fuel, 2003. **82**(9): p. 1139-1147.

106.   Jeguirim, M., S. Dorge, and G. Trouvé, Thermogravimetric analysis and emission characteristics of two energy crops in air atmosphere: Arundo donax and Miscanthus giganthus. Bioresource technology, 2010. **101**(2): p. 788-793.

107.   Yorgun, S., *Fixed-bed pyrolysis of miscanthus x giganteus: Product yields and bio-oil characterization.* Energy Sources, Part A: Recovery, Utilization, and Environmental Effects, 2003. **25**(8): p. 779-790.

108.   Hodgson, E.M., et al., Miscanthus as a feedstock for fast-pyrolysis: Does agronomic treatment affect quality? Bioresource Technology, 2010. **101**(15): p. 6185-6191.

109.   Drummond, A.R.F. and I.W. Drummond, *Pyrolysis of sugar cane bagasse in a wire-mesh reactor.* Industrial & Engineering Chemistry Research, 1996. **35**(4): p. 1263-1268.

110.   Keown, D.M., et al., Volatilisation of alkali and alkaline earth metallic species during the pyrolysis of biomass: differences between sugar cane bagasse and cane trash. Bioresource technology, 2005. **96**(14): p. 1570-1577.

111.   Lanças, F.M., et al., *Chromatographic characterization of thermally upgraded products from alternative fuels.* Journal of High Resolution Chromatography, 1994. **17**(4): p. 237-244.

112.   Stubington, J. and S. Aiman, *Pyrolysis kinetics of bagasse at high heating rates.* Energy & Fuels, 1994. **8**(1): p. 194-203.

113.   Ounas, A., et al., Pyrolysis of olive residue and sugar cane bagasse: Non-isothermal thermogravimetric kinetic analysis. Bioresource technology, 2011. **102**(24): p. 11234-11238.

114.   Asadullah, M., et al., *Production of bio-oil from fixed bed pyrolysis of bagasse.* Fuel, 2007. **86**(16): p. 2514-2520.

115.   Tsai, W.T., M.K. Lee, and Y.M. Chang, *Fast pyrolysis of rice straw, sugarcane bagasse and coconut shell in an induction-heating reactor.* Journal of Analytical and Applied Pyrolysis, 2006. **76**(1-2): p. 230-237.

116.   Ghetti, P., L. Ricca, and L. Angelini, *Thermal analysis of biomass and corresponding pyrolysis products.* Fuel, 1996. **75**(5): p. 565-573.

117.   Jiang, G., D.J. Nowakowski, and A.V. Bridgwater, *Effect of the Temperature on the Composition of Lignin Pyrolysis Products.* Energy & Fuels, 2010: p. 127-130.

118.   de Wild, P.J., W.J.J. Huijgen, and H.J. Heeres, *Pyrolysis of wheat straw-derived organosolv lignin.* Journal of Analytical and Applied Pyrolysis, 2012. **93**: p. 95-103.

119.   Huang, Y., et al., Pyrolytic characteristics of biomass acid hydrolysis residue rich in lignin. Bioresource technology, 2012. **103**(1): p. 470-476.

120.   Agarwal, A.K., *Biofuels (alcohols and biodiesel) applications as fuels for internal combustion engines.* Progress in Energy and Combustion Science, 2007. **33**(3): p. 233-271.

121.   Candeia, R.A., et al., Influence of soybean biodiesel content on basic properties of biodiesel-diesel blends. Fuel, 2009. **88**(4): p. 738-743.

122.   Bulushev, D.A. and J.R.H. Ross, Catalysis for conversion of biomass to fuels via pyrolysis and gasification: A review. Catalysis Today, 2011. **171**(1): p. 1-13.

123.   Jones, D.S.J. and P.R. Pujadó, *Handbook of petroleum processing.* 2006: Springer.

124.   Mahfud, F., et al., Biomass to Fuels Upgrading of Flash Pyrolysis Oil by Reactive Distillation Using a High Boiling Alcohol and Acid Catalysts. Process Safety and Environmental Protection, 2007. **85**(5): p. 466-472.

125.   Junming, X., et al., Bio-oil upgrading by means of ethyl ester production in reactive distillation to remove water and to improve storage and fuel characteristics. Biomass and Bioenergy, 2008. **32**(11): p. 1056-1061.

126.   Vitolo, S., et al., Catalytic upgrading of pyrolytic oils to fuel over different zeolites. Fuel, 1999. **78**(10): p. 1147-1159.

127.   Pütün, E., B.a.B. Uzun, and A.e.E. Pütün, Rapid Pyrolysis of Olive Residue. 2. Effect of Catalytic Upgrading of Pyrolysis Vapors in a Two-Stage Fixed-Bed Reactor. Energy & Fuels, 2009. **23**(4): p. 2248-2258.

128.   Lappas, A.A., et al., Biomass pyrolysis in a circulating fluid bed reactor for the production of fuels and chemicals. Fuel, 2002. **81**(16): p. 2087-2095.

129.   Corma, A., et al., Processing biomass-derived oxygenates in the oil refinery: Catalytic cracking (FCC) reaction pathways and role of catalyst. Journal of Catalysis, 2007. **247**(2): p. 307-327.

130.   Winterbottom, J.M. and M.B. King, *Reactor design for chemical engineers.* 1999: CRC.

131.   Li, H.-y., Y.-j. Yan, and Z.-w. Ren, *Online upgrading of organic vapors from the fast pyrolysis of biomass.* Journal of Fuel Chemistry and Technology, 2008. **36**(6): p. 666-671.

132.   Vitolo, S., et al., Catalytic upgrading of pyrolytic oils over HZSM-5 zeolite: behaviour of the catalyst when used in repeated upgrading–regenerating cycles. Fuel, 2001. **80**(1): p. 17-26.

133.   Cooke, L.A., The effect of a ZSM-5 containing catalyst on the fluidised bed fast pyrolysis of pine wood, in Chemical Engineering. 1999, PhD Thesis. Aston University: Birmingham, UK.

134. Adjaye, J., S. Katikaneni, and N. Bakhshi, Catalytic conversion of a biofuel to hydrocarbons: Effect of mixtures of HZSM-5 and silica-alumina catalysts on product distribution. Fuel Processing Technology, 1996. **48**(2): p. 115-143.

135. Horne, P. and P. Williams, Upgrading of biomass-derived pyrolytic vapours over zeolite ZSM-5 catalyst: effect of catalyst dilution on product yields. Fuel, 1996. **75**(9): p. 1043-1050.

136. Triantafyllidis, K., et al., Hydrothermally stable mesoporous aluminosilicates (MSU-S) assembled from zeolite seeds as catalysts for biomass pyrolysis. Microporous and Mesoporous Materials, 2007. **99**(1-2): p. 132-139.

137. Nokkosmäki, M.I., et al., *Catalytic conversion of biomass pyrolysis vapours with zinc oxide.* Journal of Analytical and Applied Pyrolysis, 2000. **55**(1): p. 119-131.

138. Fisk, C., et al., *Bio-oil upgrading over platinum catalysts using in situ generated hydrogen.* Applied Catalysis A, General, 2009. **358**(2): p. 150-156.

139. Adam, J., et al., Pyrolysis of biomass in the presence of Al-MCM-41 type catalysts. Fuel, 2005. **84**(12-13): p. 1494-1502.

140. Zhang, Q., et al., *Upgrading bio-oil over different solid catalysts.* Energy Fuels, 2006. **20**(6): p. 2717-2720.

141. Gopakumar, S.T., Bio-oil Production through Fast Pyrolysis and Upgrading to "Green" Transportation Fuels. 2012, PhD Thesis. Auburn University: Auburn, Alabama.

142. Fivga, A., Comparison of the effect of pre-treatment and catalysts on liquid quality from fast pyrolysis of biomass, in Chemical Engineering and Applied Chemistry. 2012, PhD Thesis. Aston University: Birmingham, UK.

143. Xiu, S. and A. Shahbazi, *Bio-oil production and upgrading research: A review.* Renewable and Sustainable Energy Reviews, 2012. **16**(7): p. 4406-4414.

144. Gayubo, A., et al., Transformation of oxygenate components of biomass pyrolysis oil on a HZSM-5 zeolite. II. Aldehydes, ketones, and acids. Ind. Eng. Chem. Res, 2004. **43**(11): p. 2619-2626.

145. Valle, B., et al., *Integration of Thermal Treatment and Catalytic Transformation for Upgrading Biomass Pyrolysis Oil.* International Journal of Chemical Reactor Engineering, 2007. **5**(1): p. 1559.

146. Adjaye, J. and N. Bakhshi, Production of hydrocarbons by catalytic upgrading of a fast pyrolysis bio-oil. Part I: Conversion over various catalysts. Fuel Processing Technology, 1995. **45**(3): p. 161-183.

147. Czernik, S. and A.V. Bridgwater, *Overview of Applications of Biomass Fast Pyrolysis Oil.* Energy & Fuels, 2004. **18**(2): p. 590-598.

148. Pattiya, A., Catalytic pyrolysis of agricultural residues for bio-oil production, in Chemical ngineering and Applied Chemistry. 2007, PhD Thesis. Aston University.

149. Bridgwater, A.V., *Internal communication.* 2009.

150. Li, X., et al. Experimental Study of the Effect of Spray Medium on the Collection of Bio-Oil Produced from Biomass Fast Pyrolysis. 2009: IEEE.

151. Sadaka, S. and A.A. Boateng, *Pyrolysis and Bio-oil.* 2009, Cooperative Extension Service, University of Arkansas, US Department of Agriculture and county governments cooperating.

152. Oyama, S.T., Novel catalysts for advanced hydroprocessing: transition metal phosphides. Journal of Catalysis, 2003. **216**(1–2): p. 343-352.

153. Dhandapani, B., T. St. Clair, and S.T. Oyama, *Simultaneous hydrodesulfurization, hydrodeoxygenation, and hydrogenation with molybdenum carbide.* Applied Catalysis A: General, 1998. **168**(2): p. 219-228.

154. Iliopoulou, E.F., et al., Catalytic upgrading of biomass pyrolysis vapours using transition metal-modified ZSM-5 zeolite. Applied Catalysis B: Environmental, 2012. **127**(1): p. 281-290.

155. Qiang, L., et al., Analytical pyrolysis–gas chromatography/mass spectrometry (Py–GC/MS) of sawdust with Al/SBA-15 catalysts. Journal of Analytical and Applied Pyrolysis, 2009. **84**(2): p. 131-138.

156. Basu, P., Design of Biomass Gasifiers, in Biomass Gasification and Pyrolysis: Practical Design and Theory. 2010, Elsevier.

157. Song, T., et al., Experimental investigation on hydrogen production from biomass gasification in interconnected fluidized beds. Biomass and Bioenergy, 2012. **36**(0): p. 258-267.

158. Bridgwater, A.V., The technical and economic feasibility of biomass gasification for power generation. Fuel, 1995. **74**(5): p. 631-653.

159. Double, J., The design, evaluation and costing of biomass gasifiers. 1988, PhD Thesis. Aston University.

160. Higman, C. and M. Van der Burgt, *Chapter 5: Gasification Processes*, in *Gasification*. 2011, Gulf professional publishing.

161. Zainal, Z.A., et al., *Experimental investigation of a downdraft biomass gasifier.* Biomass and Bioenergy, 2002. **23**(4): p. 283-289.

162. Cao, Y., et al., A novel biomass air gasification process for producing tar-free higher heating value fuel gas. Fuel Processing Technology, 2006. **87**(4): p. 343-353.

163. Pereira, E.G., et al., *Sustainable energy: A review of gasification technologies.* Renewable and Sustainable Energy Reviews, 2012. **16**(7): p. 4753-4762.

164. Bridgwater, A., H. Hofbauer, and S. van Loo, *Thermal biomass conversion.* 2009, Newbury: CPL Press. 445.

165. Rajvanshi, A.K., *Biomass gasification.* Alternative energy in agriculture, 1986. **2**: p. 83-102.

166. Peter, M., Energy production from biomass (part 3): gasification technologies. Bioresource technology, 2002. **83**(1): p. 55-63.

167. Kurkela, E., et al., Development of simplified IGCC-processes for biofuels: Supporting gasification research at VTT. Bioresource technology, 1993. **46**(1–2): p. 37-47.

168. Bang-Møller, C., et al., Design and Optimization of an Integrated Biomass Gasification and Solid Oxide Fuel Cell System. 2010, PhD thesis, Technical University of Denmark.

169. Kurkela, E., *Thermal gasification for power and fuels.* 2010, VTT Gasification team.

170. Maniatis, K., *Progress in biomass gasification: an overview*, in *Progress in thermochemical biomass conversion*, A.V. Bridgwater, Editor. 2001, Blackwell Scientific Publications: Oxford, UK. p. 1-32.

171. Anis, S. and Z.A. Zainal, *Tar reduction in biomass producer gas via mechanical, catalytic and thermal methods: A review.* Renewable and Sustainable Energy Reviews, 2011. **15**(5): p. 2355-2377.

172. Latif, A., A study of the design of fluidized bed reactors for biomass gasification, in Chemical Engineering. 1999, PhD Thesis. University of London: London.

173. Senelwa, K., The air gasification of woody biomass from short rotation forests, in Agricultural Engineering. 1997, PhD Thesis. Massey University: New Zealand.

174. Ahmed, I.I. and A.K. Gupta, Sugarcane bagasse gasification: Global reaction mechanism of syngas evolution. Applied Energy, 2012. **91**(1): p. 75-81.

175. Maniatis, K., *Fluidized bed gasification of biomass.* 1986, PhD Thesis. Aston University: Birmingham.

176. Prins, M.J., *Thermodynamic analysis of biomass gasification and torrefaction.* 2005, PhD Thesis. Technische Universiteit Eindhoven: Netherlands.

177. Dudgeon, R.J., An exergy-based analysis of gasification and oxyburn processes, in Mechanical Engineering. 2009, Masters Thesis. University of Iowa: Iowa. p. 232.

178. Pellegrini, L.F. and S. de Oliveira Jr, *Exergy analysis of sugarcane bagasse gasification.* Energy, 2007. **32**(4): p. 314-327.

179. Prins, M.J., K.J. Ptasinski, and F.J.J.G. Janssen, *From coal to biomass gasification: Comparison of thermodynamic efficiency.* Energy, 2007. **32**(7): p. 1248-1259.

180. Brammer, J.G. and A.V. Bridgwater, The influence of feedstock drying on the performance and economics of a biomass gasifier–engine CHP system. Biomass and Bioenergy, 2002. **22**(4): p. 271-281.

181. Lisy, M., et al., Research into Biomass and Waste Gasification in Atmospheric Fluidized Bed. 2009.

182. Basu, P., Gasification Theory and Modeling of Gasifiers, in Biomass Gasification and Pyrolysis: Practical Design and Theory. 2010, Elsevier.

183. Gómez, E.O., et al., *Preliminary tests with a sugarcane bagasse fueled fluidized-bed air gasifier.* Energy Conversion and Management, 1999. **40**(2): p. 205-214.

184. De Filippis, P., et al., *Gasification process of Cuban bagasse in a two-stage reactor.* Biomass and Bioenergy, 2004. **27**(3): p. 247-252.

185. Erlich, C., Comparative study of residue pellets from cane sugar and palm-oil industries with commercial wood pellets, applied in downdraft gasification, in Department of Energy Technology. 2009, PhD Thesis. KTH: Stockholm, Sweden.

186. Gabra, M., et al., Evaluation of cyclone gasifier performance for gasification of sugar cane residue—Part 1: gasification of bagasse. Biomass and Bioenergy, 2001. **21**(5): p. 351-369.

187. Jorapur, R. and A.K. Rajvanshi, *Sugarcane leaf-bagasse gasifiers for industrial heating applications.* Biomass and Bioenergy, 1997. **13**(3): p. 141-146.

188. Higman, C. and M. Van der Burgt, *Gasification.* Vol. 10. 2008: Gulf Professional Publishing.

189. Bridgwater, A., The technical and economic feasibility of biomass gasification for power generation. Fuel, 1995. **74**(5): p. 631-653.

190. Sun, S., et al., *Experimental research on air staged cyclone gasification of rice husk.* Fuel Processing Technology, 2009. **90**(4): p. 465-471.

191. Min, Z., et al., Catalytic reforming of tar during gasification. Part I. Steam reforming of biomass tar using ilmenite as a catalyst. Fuel, 2011. **90**(5): p. 1847-1854.

192. Meng, X., et al., Biomass gasification in a 100 kWth steam-oxygen blown circulating fluidized bed gasifier: Effects of operational conditions on product gas distribution and tar formation. Biomass and Bioenergy, 2011. **35**(7): p. 2910-2924.

193. Striūgas, N., et al., Comparison of steam reforming and partial oxidation of biomass pyrolysis tars over activated carbon derived from waste tire. Catalysis Today, 2012. **196**(1): p. 67-74.

194. Huang, B.-S., et al., Catalytic upgrading of syngas from fluidized bed air gasification of sawdust. Bioresource technology, 2012. **110**: p. 670-675.

195. Xu, C., et al., Recent advances in catalysts for hot-gas removal of tar and NH3 from biomass gasification. Fuel, 2010. **89**(8): p. 1784-1795.

196. Sadaka, S., Gasification, in Center for Sustainable Environmental Technologies. 2008, Iowa State University: Nevada.

197. Stassen, H. and H. Knoef, *Small-scale gasification systems.* The Netherlands: Biomass Technology Group, University of Twente, 1993.

198. Salleh, M., et al., Gasification of biochar from empty fruit bunch in a fluidized bed reactor. Energies, 2010. **3**(7): p. 1344-1352.

199. Ciolkosz, D., *Renewable and Alternative Energy fact sheet*, in *Manufacturing Fuel Pellets from Biomass*. 2009, Pennsylvania State University Biomass Energy Center and Department of Agricultural and Biological Engineering: Pennsylvania State University.

200. Kaliyan, N. and R. Vance Morey, *Factors affecting strength and durability of densified biomass products.* Biomass and Bioenergy, 2009. **33**(3): p. 337-359.

201. Tumuluru, J.S., et al., *A review on biomass densification technologies for energy applications.* 2010, Report prepared for U.S. Department of Energy. Idaho National Laboratory, Biofuels and Renewable Energy Technologies Department, Energy Systems and Technologies Division: Idaho Falls, Idaho, USA.

202. Sadaka, S., *Pyrolysis*, in *Center for Sustainable Environmental Technologies*. 2008, Iowa State University: Nevada.

203. Zhang, M., et al., *Experimental Study on Bio-oil Pyrolysis/Gasification.* Bioresources, 2010. **5**(1): p. 135-146.

204. BTG. *Biomass Technology Group Fast Pyrolysis*. 2012 [cited 2012 02-09-2012]; Available from: http://www.btgworld.com/en/rtd/technologies/fast-pyrolysis.

APPENDIX 1: GC-MS ANALYSIS OF BIO-OIL FROM CONTINUOUS REACTORS

Table 68 shows 24 compounds identified in the bio-oil by GC-MS analysis. As expected, the bio-oil contains oxygenates with high molecular weight compounds consisting of acids, alcohols, phenolics, esters and ketones.

Table 68: Liquid composition of bio-oil from beech

Retention time	Name	Structure	Molecular Weight
12.10	Acetic acid	$C_2H_4O_2$	60
13.88	Acetic acid, methyl ester	$C_3H_6O_2$	74
18.76	1,2-ethanediol, momoacetate	$C_4H_8O_3$	104
20.98	2-acetate-1,2-propanediol	$C_5H_{10}O_3$	118
23.90	Cyclopropyl carbinol	C_4H_8O	72
24.40	1-(acetylocy)-2-propanone	$C_5H_8O_3$	116
24.85	1,3-butanediol	$C_4H_{10}O_2$	90
27.30	2-hydroxy-2-cyclopenten-1-one	$C_5H_6O_2$	98
30.42	2(5H)-furanone	$C_4H_4O_2$	84
31.15	Methoxy-cyclobutane	$C_5H_{10}O$	86
32.24	2-hydroxy-3methyl-2-cyclopenten-1-one	$C_6H_8O_2$	112
33.78	Phenol	C_6H_6O	94
34.67	2-methoxy-phenol	$C_7H_8O_2$	124
39.42	2-methoxy-4-methyl-phenol	$C_8H_{10}O_2$	138
45.58	2-methoxy-4-vinyl-phenol	$C_9H_{10}O_2$	150
46.57	2-methyoxy-4-(1-propenyl)-phenol	$C_{10}H_{12}O_2$	164
47.75	2,6-dimethoxy-phenol	$C_8H_{10}O_3$	154
50.96	Eugenol	$C_{10}H_{12}O_2$	164
51.44	1,2,4-trimethoxybenzene	$C_9H_{12}O_3$	168
54.31	1,2,3-trimethoxy-5-methyl-benzene	$C_{10}H_{14}O_3$	182
56.53	3'-5'-dimethoxyacetophenone	$C_{10}H_{12}O_3$	180
57.19	2,6-dimethoxy-4-(2-propenyl)-phenol	$C_{11}H_{14}O_3$	194
61.27	1,6-anhydro-β-glucopyranone (levoglucosan)	$C_6H_{10}O_5$	162

Figure 157 and Table 69 show the compounds identified in the bio-oil produced from miscanthus and miscanthus pellets. As expected, similar compounds were identified in both feedstocks. Degradation of hemicellulose, cellulose and lignin produce a liquid bio-oil consisting of acids, aldehydes, alcohols, sugars, esters, ketones, furans, phenolics, oxygenates and hydrocarbons. GC-MS analysis shows the presence of acids, furans and phenolics. The presence of organic acids such as acetic acid contributes to the low pH of bio-oil.
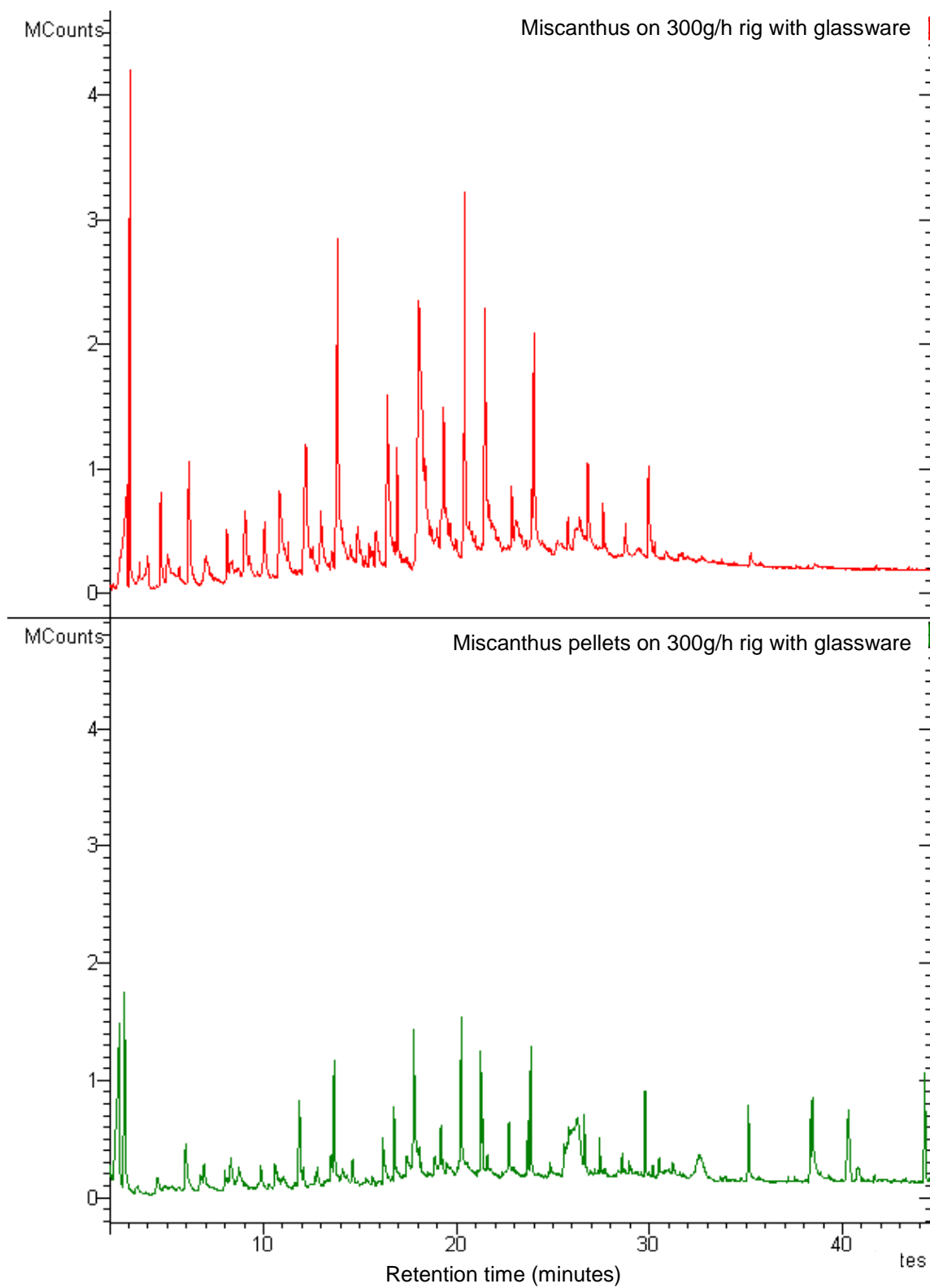
Figure 157: GC-MS chromatograms of bio-oil from miscanthus and miscanthus pellets

Table 69: Liquid composition of bio-oil from miscanthus and miscanthus pellets

Miscanthus	Miscanthus pellets	Compound
-	2.565	Ethyl acetate
-	5.979	2-methyl-Furan
7.003	6.726	2-Furanmethanol
8.11	7.999	2,4-dimethyl-Furan
10.82	10.595	Phenol
12.976	12.791	3-methyl-Phenol
13.835	13.656	2-methoxy-Phenol
16.411	16.19	4-ethyl-Phenol
16.92	16.765	2-methoxy-4-methyl-Phenol
18.062	17.8	1,2-Benzenedimethanol
-	19.192	4-ethyl-2-methoxy-phenol
30.261 and 35.242	35.121	Oleic acid
20.421	20.258	2-Methoxy-4-vinylphenol
21.473	21.257	2,6-dimethoxy-Phenol
22.869 and 24.003	21.337	Eugenol
23.889	23.707	4-hydroxy-3-methoxy-Benzoic acid (vanillic acid)
26.376	26.247	1,6-Anhydro-á-D-glucopyranose (levoglucosan)
27.578 and 28.754 and 29.948	27.426	2,6-dimethoxy-4-(2-propenyl)- Phenol
-	28.942	4-hydroxy-3,5-dimethoxy-Benzaldehyde
30.86	30.509	3,4,5-trimethoxy-Benzaldehyde

Figure 158 and Table 70 shows the compounds identified in the bio-oil from sugarcane bagasse, sugarcane bagasse pellets and sugarcane trash.
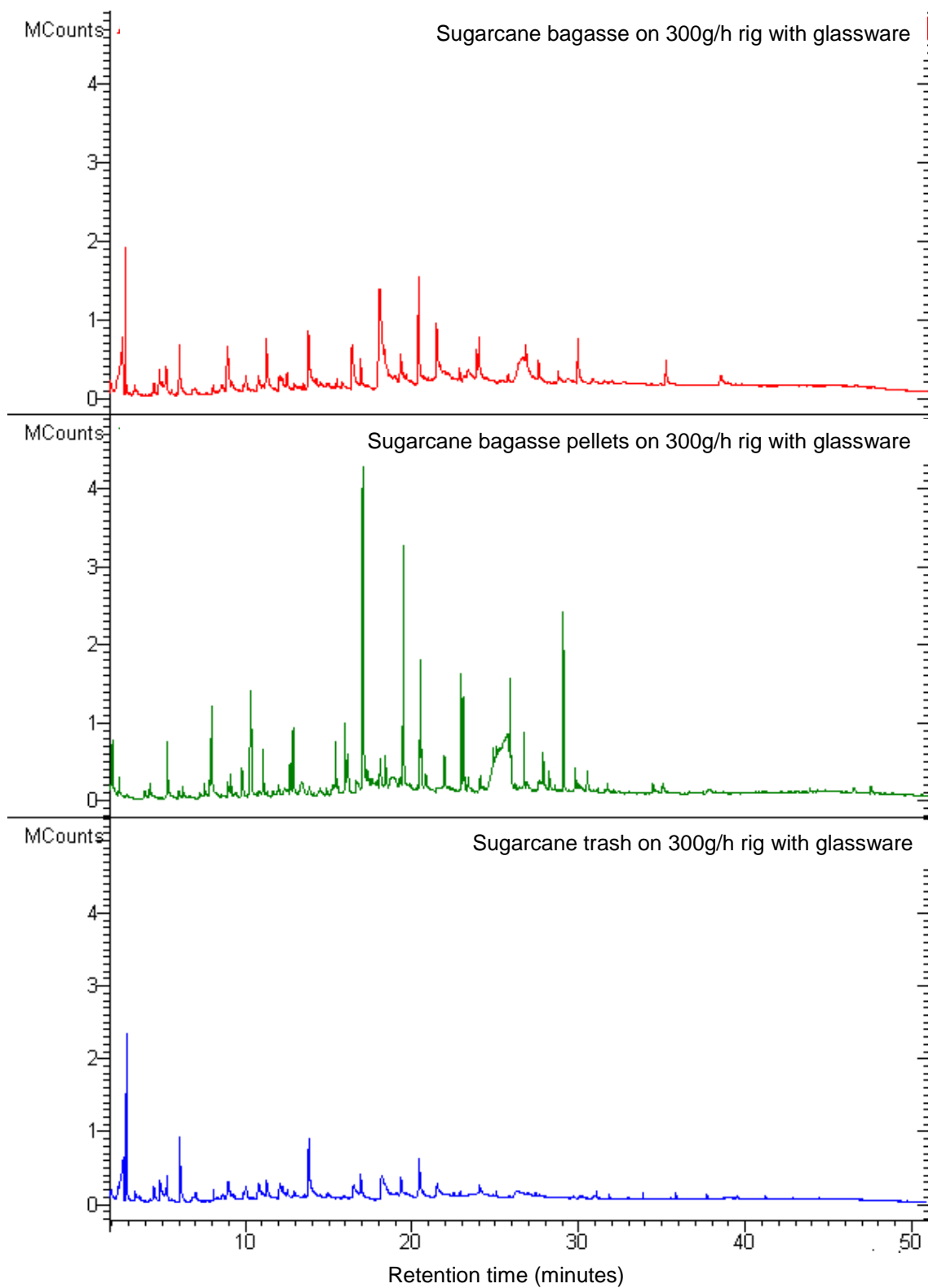
Figure 158: GC-MS chromatograms of bio-oil from sugarcane bagasse, sugarcane bagasse pellets and trash

Table 70: Liquid composition of bio-oil from sugarcane bagasse, sugarcane bagasse pellets and trash

Sugarcane bagasse	Sugarcane bagasse pellets	Sugarcane trash	Compound
-	1.818	-	Ethyl acetate
-	2.013	-	Acetic acid
6.02	-	-	2,5-dimethyl-Furan
-	5.31	6.131	Furfural
8.949	5.991 and 7.839 and 7.987	8.953	2-Furanmethanol
8.07	-	8.078	2,4-dimethyl-Furan
-	-	-	5-methyl-2-Furancarboxaldehyde
10.787	9.772	10.841	Phenol
-	10.287	-	dimethyl ester Butanedioic acid
-	12.766	12.946	3-methyl-Phenol
-	12.685	-	4-methyl-Phenol
12.935	12.865	13.792	2-methoxy-Phenol
16.394	15.4	16.491	4-ethyl-Phenol
16.922	15.969	16.92	2-methoxy-4-methyl-Phenol
18.05	17.045	18.171	1,2-Benzenedimethanol
-	18.078	-	3-methoxy-1,2-Benzenediol
19.32	18.406	19.339	4-ethyl-2-methoxy-phenol
35.235	17.747	22.493	Oleic acid
20.395	19.491	20.417	2-Methoxy-4-vinylphenol
-	20.496	-	2,6-dimethoxy-Phenol
-	-	-	3-hydroxy-5-methoxy-Benzenemethanol
21.474	21.962	21.51	Eugenol
-	21.897	-	Vanillin
-	22.965	-	4-hydroxy-3-methoxy-Benzoic acid (vanillic acid)
-	23.356	-	2-methoxy-4-propyl-Phenol
27.138	25.659	-	1,6-Anhydro-á-D-glucopyranose (levoglucosan)
27.601	26.711 and 27.879 and 29.078	-	2,6-dimethoxy-4-(2-propenyl)-Phenol
-	28.233	-	4-hydroxy-3,5-dimethoxy-Benzaldehyde
-	29.799	-	3,4,5-trimethoxy-Benzaldehyde

These chromatograms are shown in Figure 159. The identified compounds are compared in Table 71. As expected, the identified compounds from the three rig configurations are similar.
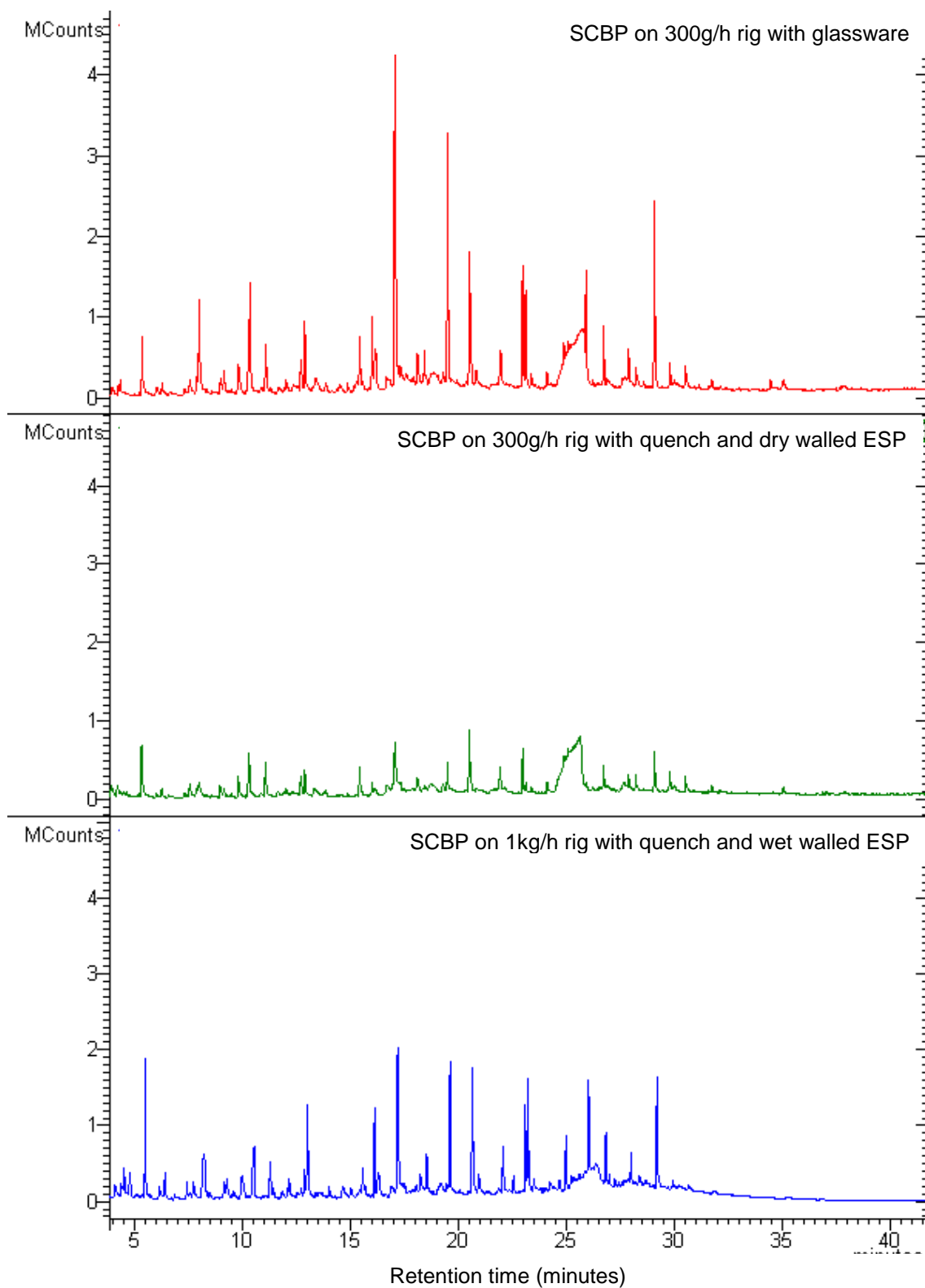
Figure 159: GC-MS chromatograms of bio-oil from sugarcane bagasse pellets using three rig configurations

Table 71: Liquid composition of bio-oil from sugarcane bagasse pellets using three rig configurations

Retention times of compounds in bio-oil from three different set ups			Compound
300g/h with glassware	300g/h with quench and dry walled ESP	1kg/h with quench and wet walled ESP	
1.818	2.047	2.284	Ethyl acetate
2.013	2.523	-	Acetic acid
5.31	5.304	-	Furfural
5.991 and 7.839 and 7.987	7.994	6.125 and 8.194	2-Furanmethanol
-	-	7.391	2,4-dimethyl-Furan
-	-	9.125	5-methyl-2-Furancarboxaldehyde
9.772	9.76	9.953	Phenol
10.287	-	10.514	dimethyl ester Butanedioic acid
12.766	11.985	12.125	3-methyl-Phenol
12.685	12.671	12.836	4-methyl-Phenol
12.865	12.866	12.982	2-methoxy-Phenol
15.4	15.406	15.54	4-ethyl-Phenol
15.969	15.978	16.091	2-methoxy-4-methyl-Phenol
17.045	17.027	17.167	1,2-Benzenedimethanol
18.078	18.073	18.233	3-methoxy-1,2-Benzenediol
18.406	18.402	18.513	4-ethyl-2-methoxy-phenol
17.747	27.16	19.151 ad 29.758	Oleic acid
19.491	19.472	19.596	2-Methoxy-4-vinylphenol
20.496	20.498	20.629	2,6-dimethoxy-Phenol
-	20.824	20.938	3-hydroxy-5-methoxy-Benzenemethanol
21.962	23.101	22.053 and 23.220	Eugenol
21.897	21.898	-	Vanillin
22.965	22.954	23.074	4-hydroxy-3-methoxy-Benzoic acid (vanillic acid)
23.356	23.36	23.483	2-methoxy-4-propyl-Phenol
25.659	25.617	26.42	1,6-Anhydro-á-D-glucopyranose (levoglucosan)
26.711 and 27.879 and 29.078	26.715	26.828 and 27.979 and 29.197	2,6-dimethoxy-4-(2-propenyl)- Phenol
28.233	28.211	28.356	4-hydroxy-3,5-dimethoxy-Benzaldehyde
29.799	29.792	29.925	3,4,5-trimethoxy-Benzaldehyde

Quantification of these compounds is important and has been carried out by peak area as a fraction of the total peak area as shown in Table 72.

Table 72: Compound peak area % of total peak area

300g/h with glassware	300g/h with quench	1kg/h with quench	Compound	Group
0.65	3.77	1.84	Ethyl acetate	ester
0.99	0.04	0	Acetic acid	Acid
1.00	1.57	0	Furfural	Aldehyde
2.37	1.10	2.35	2-Furanmethanol	Furan
0	0	0.21	2,4-dimethyl-Furan	Furan
0	0	0.28	5-methyl-2-Furancarboxaldehyde	Furan
0.87	1.04	0.66	Phenol	Phenol
2.33	0	1.55	dimethyl ester Butanedioic acid	ester
0.00	0.18	0.28	3-methyl-Phenol	Phenol
0.52	0.66	0.54	4-methyl-Phenol	Phenol
1.01	0.68	1.54	2-methoxy-Phenol	Phenol
0.65	0.98	0.42	4-ethyl-Phenol	Phenol
0.73	0.94	1.24	2-methoxy-4-methyl-Phenol	Phenol
6.22	3.11	3.72	1,2-Benzenedimethanol	
0.70	0.71	0.56	3-methoxy-1,2-Benzenediol	
0.32	0.31	0.63	4-ethyl-2-methoxy-phenol	Phenol
0.06	0.07	0.81	Oleic acid	Acid
2.95	0.92	1.89	2-Methoxy-4-vinylphenol	Phenol
1.37	1.93	1.25	2,6-dimethoxy-Phenol	Phenol
0	0.19	0.41	3-hydroxy-5-methoxy-Benzenemethanol	
0.35	0.29	2.45	Eugenol	Phenol
0.44	0.82	0	Vanillin	Phenolic aldehyde
1.27	1.00	1.23	4-hydroxy-3-methoxy-Benzoic acid (vanillic acid)	Phenol
0.21	0.19	0.20	2-methoxy-4-propyl-Phenol	Phenol
13.32	18.99	11.26	1,6-Anhydro-á-D-glucopyranose (levoglucosan)	Carbohydrate
3.24	0.82	3.34	2,6-dimethoxy-4-(2-propenyl)- Phenol	Phenol
0.22	0.54	0.37	4-hydroxy-3,5-dimethoxy-Benzaldehyde	Phenolic aldehyde
0.36	0.55	0.17	3,4,5-trimethoxy-Benzaldehyde	Phenolic aldehyde

APPENDIX 2: GC-MS ANALYSIS FROM PY-GC-MS

Figure 160 shows the chromatograms from the Py-GC-MS experiments which indicate that the catalyst has significant effect on the product composition at 500°C. Table 73 shows the peak area % of product groups obtained from fast pyrolysis of SCBP with and without catalyst. It can be seen that acids, ketones, furanics and carbohydrates decrease while phenolics increase.
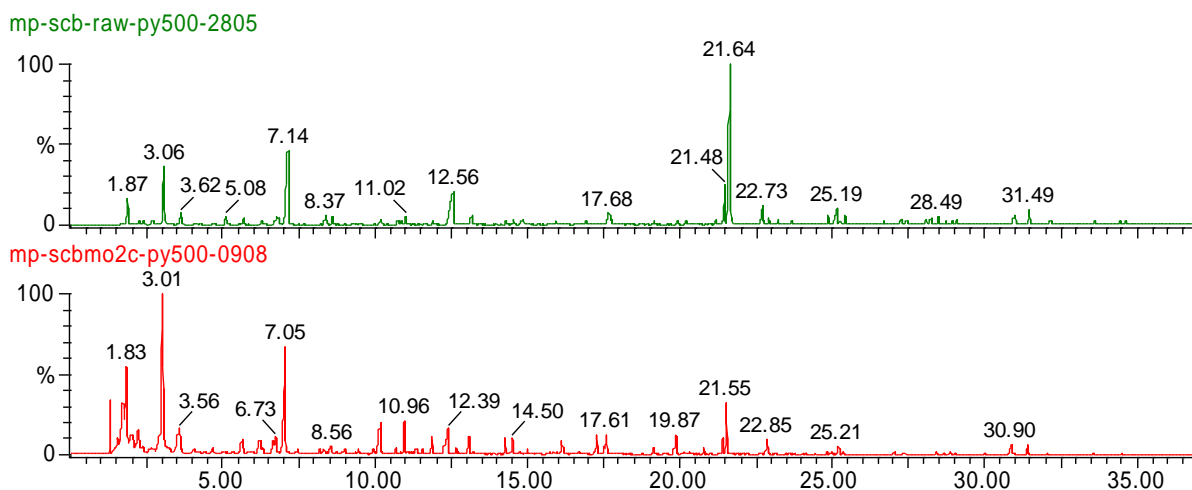
Figure 160: Comparative chromatograms from Py-GC-MS of SCBP with and without molybdenum carbide

Table 73: Quantification of product groups using peak area %

Product group	Peak area % from SCBP	Peak area % from SCBP with Mo2C
Acids	9.48	20.29
Ketones	3.66	12.43
Enones	3.12	1.33
Esters	3.44	6.32
Furanics	4.66	7.28
Phenolics	15.88	10.17
Phenolic aldehydes	21.83	3.62
Carbohydrate	5.57	1.42
Aldehydes	11.48	12.03
Total peak area identified	79.12%	74.88%

Table 74 summarises the compounds identified and calculated peak areas.

Table 74: Compound identification and quantification

Peak RT (mins)	Compound	Formula	Group	SCBP Peak area	SCBP Peak Area (%)	SCBP with Mo2C Peak area	SCBP with Mo2C Peak Area (%)
1.3	?	?	?	0	0.00	4710243	1.38
1.87	Propan-2-one	C_3H_6O	Ketone	46006820	3.01	31867844	9.32
	2,methylfuran	C_5H_6O	Furan	0	0.00	10632337	3.11
3.047	Acetic acid	$C_2H_4O_2$	Acid	120280096	7.86	69405864	20.29
3.62	Methyl acetate	$C_3H_6O_2$	Ester	29019716	1.90	13657524	3.99
5.081	1,2-cyclopentanediol	$C_5H_{10}O_2$	Enone	22550192	1.47	0	0.00
5.674	2-oxo-propanoic acid methyl ester	$C_4H_6O_3$	Ester	11819510	0.77	5355351	1.57
6.254	2- hydroxy-2-cyclopenten-1-one	$C_6H_8O_2$	Enone	7945671	0.52	0	0.00
6.795	Ethanethioic acid	C_2H_4OS	Acid	24772820	1.62	0	0.00
7.121	Furfural	$C_5H_4O_2$	Aldehyde	175605104	11.48	41136380	12.03
	2-propyl-furan	$C_7H_{10}O$	Furan	0	0.00	985920.81	0.29
8.368	2-Furanmethanol	$C_5H_6O_2$	Furan	15520457	1.01	1303994.25	0.38
8.608	1-(acetyloxy)-2-propanone	$C_5H_8O_3$	Ester	11804799	0.77	2608014.75	0.76
10.169	1,2-cyclopentanedione	$C_5H_6O_2$	Ketone	10017844	0.65	10628788	3.11
	5-methyl-2-furancarboxaldehyde	$C_6H_6O_2$	Furan	0	0.00	7813260	2.28
11.009	3-methyl-Phenol (m-cresol)	C_7H_8O	Phenol	12638477	0.83	1169238.13	0.34
11.909	2(5H)-Furanone	$C_4H_4O_2$	Furan	5056964	0.33	4061858.5	1.19
12.556	4-methyl-Phenol (p-cresol)	C_7H_8O	Phenol	115752888	7.57	12225163	3.57
13.156	2-hydroxy-3-methylcyclopent-2-en-1-one (cyclotene)	$C_6H_8O_2$	Enone	17212994	1.13	4534404.5	1.33
14.304	Phenol	C_6H_6O	Phenol	611108	0.04	3358066.25	0.98
14.554	2-methoxy-Phenol (guaiacol)	$C_7H_8O_2$	Phenol	14535937	0.95	4510494.5	1.32
16.924	trans-2-furanmethanol, tetrahydro-5-methyl	-	Furan	9904287	0.65	85018	0.02
17.678	?	?	?	27414412	1.79	4039641.25	1.18
19.185	3-ethyl-Phenol	$C_8H_{10}O$	Phenol	3057546	0.20	1326602.63	0.39
21.206 and 25.173	Sucrose?	$C_{12}H_{22}O_{11}$	Carbohydrate	55383323	3.62	676988	0.20

21.426	2-Methoxy-4-vinylphenol	$C_9H_{10}O_2$	Phenol	57636404	3.77	3601465.25	1.05
21.646	4-methylbenzaldehyde	C_8H_8O	Phenolic aldehyde	294388864	19.24	10394091	3.04
22.719	3-Furanmethanol	$C_5H_6O_2$	Furan	40863720	2.67	0	0.00
22.906	2,6-dimethoxy-Phenol (syringol)	$C_8H_{10}O_3$	Phenol	4684070	0.31	3575558.25	1.05
23.226	2,3-anyhydro-D-galactosan	-	Carbohydrate	5129410	0.34	0	0.00
24.266	3,4-anyhydro-D-galactosan	-	Carbohydrate	2941657	0.19	0	0.00
24.88	Eugenol	$C_{10}H_{12}O_2$	Phenol	11483693	0.75	673445.69	0.20
25.44	Vanillin	$C_8H_8O_3$	Phenolic aldehyde	12393844	0.81	671455.94	0.20
	4-hydroxy-3-methoxy-Benzoic acid (vanillic acid)	$C_8H_8O_4$	Phenol	0	0.00	1867460	0.55
28.248	4-hydroxybenzaldehyde	$C_7H_6O_2$	Phenolic aldehyde	9026038	0.59	0	0.00
28.494	4-methyl-2,5-dimethoxybenzaldehyde	$C_{10}H_{12}O_3$	phenolic aldehyde	7582114	0.50	784570.188	0.23
30.989	1,6-Anhydro-á-D-glucopyranose (levoglucosan)	$C_6H_{10}O_5$	Carbohydrate	21800196	1.42	4166981.75	1.22
28.921 and 31.482	2,6-dimethoxy-4-(2-propenyl)- Phenol	$C_{11}H_{14}O_3$	Phenol	22534870	1.47	2486422.88	0.73
32.142	4-hydroxy-3,5-dimethoxybenzaldehyde (syringaldehyde)	$C_9H_{10}O_4$	Phenolic aldehyde	5636042	0.37	259269	0.08
33.629	3,4,5-trimethoxybenzaldehyde	$C_{10}H_{12}O_4$	Phenolic aldehyde	4994322	0.33	277080.84	0.08
			Total	1529996719	80.92	342012604.9	77.44

APPENDIX 3: EQUATIONS FOR GASIFICATION

The performance parameters of the gasifier used in this work were measured by gas yields, gas HHV, carbon conversion efficiency and cold gas efficiency. Gas yields were calculated as in respective sections. Equation 3 was used to calculate the HHV of the oxygen-free product gas using the HHV of the combustible gases H_2, CH_4 and CO.

Equation 3: Calculating HHV of a gas

$$\text{HHV (MJ/Nm}^3) = (\text{vol.\% } H_2) \times 12.75 + (\text{vol.\% } CH_4) \times 39.82 + (\text{vol.\% CO}) \times 12.63$$

Equation 4 shows the equation used to calculate equivalence ratio of these batch gasification tests.

Equation 4: Calculating equivalence ratio

$$ER = \frac{\text{Actual oxygen to fuel ratio}}{\text{Stoichiometric oxygen to fuel ratio}} = \frac{\left(n_{O2}/n_{biomass}\right)}{\left(n_{O2}/n_{biomass}\right)_{stoich}}$$

Equation 5 and Equation 6 show the complete combustion of SCBP and AHR neglecting the small amount of nitrogen, sulphur and ash in the sample. If air is present, the ratio of oxygen to biomass is typically around 0.3 suggesting that the oxygen to fuel ratio for complete combustion on a molar basis is approximately 1 (1.035 and 1.070) which is confirmed in Equation 5 and Equation 6.

Equation 5: Stoichiometric combustion of SCBP with air

$$CH_{1.48}O_{0.67} + 1.035(O_2 + 3.76N_2) = 0.74H_2O + CO_2 + 3.8916N_2$$
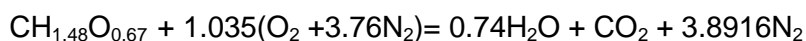
- RMM of SCBP = 24.2
- Mass of oxygen per mole of SCBP = 1.035x32 = 33.12g
- Mass of nitrogen per mole of SCBP = 3.8916 x 28 = 108.9648
- Mass of air per mole of SCBP = 142.0848
- Mass of oxygen for complete combustion of 1g of SCBP = 33.12/24.2 = 1.369g
- Mass of air for complete combustion of 1g of SCBP = 142.0848/24.2 = 5.871g

Equation 6: Stoichiometric combustion of AHR with air

$$CH_{0.84}O_{0.28} + 1.070(O_2 + 3.76N_2) = 0.42H_2O + CO_2 + 4.0232N_2$$
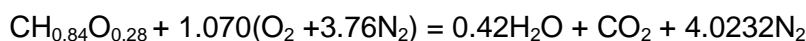
- RMM of AHR = 17.32
- Mass of oxygen per mole of AHR = 1.07x32 = 34.24g
- Mass of nitrogen per mole of SCBP = 4.0232 x 28 = 112.6496g
- Mass of air per mole of SCBP = 146.8896g
- Mass of oxygen for complete combustion of 1g of AHR = 34.24/17.32 = 1.977g
- Mass of air for complete combustion of 1g of AHR = 146.8896/17.32 = 8.481g

The mass of oxygen required to combust one gram of AHR (1.977g) was higher than that required for SCBP (1.369g) due to the higher carbon content of AHR.

Carbon conversion efficiency indicates the amount of carbon in the feed that was successfully converted into a carbon bearing gas such as CO, CO_2 and CH_4. Equation 7 was used to calculate the carbon conversion efficiency.

Equation 7: Calculating carbon conversion efficiency

$$CCE = \frac{\text{wt.\% carbon in product gas (CO,CO2 and CH4)}}{\text{wt.\% carbon content of dry feed}} \; x \; 100$$

Cold gas efficiency was used to determine the energy available in the product gas as a ratio of the energy in the original feed and calculated using Equation 8.

Equation 8: Cold gas efficiency [4]

$$CGE = a\frac{\text{wt.\% gas yield on dry feed basis x HHV of gas } (\frac{MJ}{kg})}{\text{HHV of biomass}} \; x \; 100$$

APPENDIX 4: PUBLICATIONS

Publications

Patel M and Bridgwater AV, 'Influence of acid hydrolysis on pyrolysis behaviour of biomass residues', in Proc. Bioten, Bridgwater AV (Ed.) CPL Press 2011

Patel, M., et al., *In situ catalytic upgrading of bio-oil using supported molybdenum carbide.* Applied Catalysis A: General, 2013. **458**: p. 48-54.

Submitted and Awaiting Review

Patel, M. and A.V. Bridgwater, *Pyrolysis and Gasification of Residues from Levulinic Acid Production from Biomass.* Catalysis Today.